CHARACTERISATION OF SHAPE OF FINE RECYCLED CRUSHED COLOURED GLASS AND THE EFFECT ON THE PROPERTIES OF STRUCTURAL CONCRETE WHEN USED AS A FINE AGGREGATE REPLACEMENT

CHON JIN KOH T.I.Struct.E

A thesis submitted in partial fulfilment of the
requirement of the University of Wolverhampton
for the degree of Doctor of Philosophy

December 2014

Signature……Chon Jin Koh ....……....

Date……29th May 2015..……

ABSTRACT

In order to reduce the use of landfilling within waste management great emphasis is being placed on waste reduction and recycling. Each year in the UK approximately 2.5 Mt of waste glass is produced and approximately half of this waste is not recyclable. Therefore alternative ways need to be found for using waste glass and one possibility is to use it within concrete as a replacement for cement and/ or aggregate.

In the research programme concrete mixes were tested which had 0%, 25%, 50% and 100% of the fine aggregate replaced by crushed waste glass. All glass was originally in bottle form and was crushed to produce 'sand' which had a grading curve more-or-less identical to fine aggregate obtained from a commercial supplier. Three colours of glass were studied, i.e. flint (clear), amber and green. Concretes were also made which contained a mixture of colours (in proportion according to the weight of each type of waste glass produced annually within the UK) and also a mixture of unwashed waste glasses. The overall concrete mix adopted for investigation, i.e. 1:2:4, was selected because of its wide use within industry, and all concrete was made with a water:cement content of 0.6 without the addition of plasticiser or ASR-retarding agents. The suite of laboratory tests included; slump, flow, initial and final setting time, ultrasonic pulse velocity, water absorption by immersion and capillarity rise, ASR measurement (volumetric and linear), compression strength at ages from 7 days to 365 days.

Techniques of developed digital imaging and processing have been applied to the glass aggregate to quantify various particle shape factors, i.e. aspect ratio, percentage concavity, Riley inscribed sphericity and surface texture index. Statistical analysis has been used to compare the distribution of particle forms present within the fine aggregate materials used in the experimental work. Dimensional changes (in three orthogonal directions) were measured as concrete cubes hardened over a period up to 365 days. The length changes of concrete prisms were also measured over the same period of time. The resultant data indicated that a fine aggregate which comprised 25% glass and 75% sand would be categorised as "non-expansive", i.e. the same as the sand on its own. As the proportion of glass in the fine aggregate became greater than the aggregate became more expansive but it did not exceed recommended limits.

CONTENTS **PAGE**

NOTATION

AR	Aspect Ratio
ASR	Alkali silica reaction
BS	British Standard
ºC	Celsius
C	Coulombs
CCD	Charge coupled device
CSH	Calcium-silicate-hydrate
CH	Calcium hydroxide
CRT	Cathode ray tube
FA	Fly ash
GGBS	Ground granulated blastfurnace slag
GFG	Granulated foam glass
GWS	Ground waste glass
ITZ	Interfacial transition zone
LC	Liquid crystal
LCD	Liquid crystal display
MK	Metakaolin
OPC	Ordinary Portland cement
PC	Percentage Concavity
PGP	Pozzolanic glass powder
PFA	Pulverised fuel ash
RCG	Recycled crushed glass
RFA	Recycled fine aggregate
RG	Recycled glass
$Ø_R$	Riley Sphericity
SCC	Self-compacting concrete
SCGC	Self-compacting glass concrete
SEM	Scanning electron microscopy
SF	Silica fume
STI	Surface Texture Index
UPV	Ultrasonic pulse velocity
W/C	Water cement ratio
WG	Waste glass
WGS	Washed glass sand

PUBLICATIONS RESULTING FROM THIS RESEARCH

Koh, C.J., Sarsby, R.W. and Ben Said, A.A.M (2010) Use waste glass as fine aggregate in structural concrete. Construction for a Sustainable Environment - Sarsby & Meggyes (eds), Taylor and Francis Group, London. pp. 355-359.

ACKNOWLEDGEMENTS

I extend my thanks to my advisor (and former supervisor) Professor Robert Sarsby and to my current Director of Studies Dr. David Searle. They have provided invaluable guidance and support throughout my research and study. They have given a lot of time, effort and attention to my research work and without their support I would not have achieved my goal and professional development.

The support of Professor Jamal Khatib (second supervisor at University of Wolverhampton) is also acknowledged. I would also like to thank Dr. Graham True for stimulating technical assistance with glass shape factor investigations.

The contributions of the following are also deeply appreciated:
Geoff Copper and Raymond Bradley for laboratory technical assistance and coordination of the trials.
Hanson Aggregates UK and Tony Dennison (Manager) for their supplies of fine natural aggregates.
Staffordshire County Council and Mark Parkinson (Group Manager of Recycling and Waste Management) for supplies of waste glass.

In addition, I want to thank my lovely girl friend Zhe Qiu for her love. Ever since I started doing my research she always gave support, encouragement, and understanding. Also I give many thanks to my dear family (parents, brother and sisters) because they were always there for me and kept on supporting me, even though we were not living in the same country.

CHAPTER 1 - INTRODUCTION

1.1 Structural Concrete

Each year around 25 billion tonnes (Europe 10% and China 50%) of concrete are used to construct buildings, road, dams, pavement, and even artworks (European Federation of Precast Concrete, 2010). Concrete is the world's most important construction material and is extensively used as a structural material in foundations, columns inside building, beams and slabs in bridges, drainage systems, roads, harbour works and etc. The concrete industry, due to its sheer size, has a considerable impact on the environment. Concrete is composed mainly of cement, coarse aggregate, fine aggregate and water. Typically around 75% to 90% of the volume of structural concrete consists of raw materials extracted from the ground. Conventional structural concrete is thus a conspicuous consumer of primary resources and this is a major concern in the drive to achieve sustainability within construction.

1.2 Waste glass

One of the problems arising from continuous technological, industrial development and increasing population is the disposal of waste materials that are produced. These waste materials include iron, glass, ceramics, and concrete. Demand to reduce waste has created the need to find a use for waste products instead of disposing of the materials in landfills. Many outside of the concrete industry regard concrete as a suitable host for waste materials, rendering the waste materials innocuous and solving a pollution problem. Use of waste materials in concrete is not only a partial solution to environmental and ecological problems; it has the potential to improve the microstructure and consequently the properties of concrete.

It has been estimated that over 2.5 million tonnes of waste glass is generated in the UK every year of which only 59% is recycled and the rest goes to landfill (Wrap, 2013). Glass is a particularly troublesome component of waste because it will not burn, rust, or decay and even after incineration of refuse a considerable amount of glass remains to be disposed of. In terms of glass colour; 63% of the waste is clear,

25% is amber, 10% is green and 2% is blue or other colours. Mixed waste glass generally cannot be reused by the glass industry. Waste glass cullet needs several processes or treatments to be successfully recycled in the production of new glass, and these treatments generate their own waste stream (Bignozzi and Sandrolini, 2004).

Potential means of disposal of glass include landfill (which is strongly discouraged) and salvage and reclamation operations. For instance, waste glass could be returned to a glass manufacturer for melting and reuse. However, transportation costs and the expense of sorting the glass into different categories by colour, type, and so forth, are likely to be prohibitive. In order to maximize potential benefits from salvage and reclamation operations, it is necessary to minimize processing and transportation costs while ensuring a steady market for the salvaged refuse. An alternate method of disposal is to reuse the glass in a different way. For example, the economic benefits from the reuse of recycled waste glasses in cement and concrete production could be very significant. The UK government is committed to sustainable development and around 65 million tonnes of aggregate are derived annually from recycled sources representing approximately one quarter of the total of 275 million tonnes used annually in the UK (Wrap 2011). The government introduced the Aggregate Levy in April 2002 (HMRC, 2011). This is an environmental tax on the commercial exploitation of aggregate to address the environmental costs associated with quarrying that are not already covered by regulation, including noise, dust, visual intrusion, loss of amenity and damage to biodiversity. Many other countries, particularly those in the EU, make increasing use of "green taxes" and have introduced similar taxes to pursue environmental aims. The overall cost of landfill, particularly the Landfill Tax is increasing. The tax is chargeable by weight and there are two rates: lower rate applies to those inactive (or inert) wastes; standard rate applies to all other taxable waste. The lower rate tax that applies to inert materials was set at £2 per tonne in 1996 then at £2.50 per tonne on 1 April 2007; no increase was made in 2008 and 2012. The current standard rate is £80 per tonne (Table 1.1) and this will not fall in future years (HMRC, 2014).

Table 1.1 Increase of standard rate of landfill tax (HMRC, 2014)

Date of change	Standard rate (£ per tonne)
1st October 1996	£7
1st April 1999	£10
1st April 2000	£11
1st April 2001	£12
1st April 2002	£13
1st April 2003	£14
1st April 2004	£15
1st April 2005	£18
1st April 2006	£21
1st April 2007	£24
1st April 2008	£32
1st April 2009	£40
1st April 2010	£48
1st April 2011	£56
1st April 2012	£64
1st April 2013	£72
1st April 2014	£80

However, processing of waste glass may cost from £9 to £19/ tonne depending on the production scale (Shi and Zheng, 2007). According to Limbachiya (2009) the scope for using washed glass sand in various types of construction can be increased considerably, provided there is encouragement for the industry to do so and its use could become more economically viable if taxes were raised for waste disposal and quarrying of natural material.

1.3 Use of waste glass in concrete

Waste glass is likely to be available in significant quantities for the foreseeable future and will therefore pose a disposal problem accentuated by the increasing tendency to restrict landfilling. One outlet for these waste materials, which is attractive from the environmental point of view and technically feasible under certain conditions, is as aggregate in concrete. Moreover, the utilization of glass (and fly ash) as an additive to concrete may introduce some benefits from technical and environmental points of view (Tuncan *et al*., 2001) and this approach is receiving more and more interest worldwide. Being amorphous and containing relatively large quantities of silicon and calcium, glass is, in theory, pozzolanic or even cementitious in nature when it is finely ground. Thus, it could possibly be used as a cement replacement in Portland cement concrete. However, use of crushed glasses as aggregates for Portland cement concrete may have some negative effects on the properties of the concrete. The main concern is the expansion and cracking caused by chemical reactions (Shi and Zheng, 2007).

There has been a general perception in the concrete industry that glass aggregates should be precluded from use in concrete because of the potential for Alkali Silica Reaction (ASR) (Byars *et al.,* 2004). Early studies of ASR due to glass aggregate did not produce definitive conclusions. Whilst recent publications have not specifically supported the use of glass in concrete they have led to a greater understanding of ASR and relevant parameters and methods by which it can be suppressed. Major research in the USA and UK has made it possible for recycled glass to be viewed as a potentially "fit-for-purpose" concrete construction material (Shao *et al*., 2000, Byars *et al.*, 2003, and Byars *et al*., 2004).

Recycled glass can be considered as an amorphous crystalline structure and thus be classified as highly reactive siliceous aggregate when used in concrete (Taha and Nounu, 2008). Furthermore, contamination residues and organic content in waste recycled glass are disadvantageous as they may degrade with time and create voids in the micro-structure of the concrete. Also the cracks inherent in the recycled glass sand particles (due to the crushing to produce suitable grading) are potential source of weakness and can reduce the strength of the concrete. However, as an impervious material, the recycled glass can reduce the permeability of the concrete mix and may

enhance its durability and restrict the migration of the water and ions inside the concrete matrix.

Glasses can be classified into categories such as vitreous silica, soda-lime glasses, lead glasses, etc. The composition of these glasses is very similar, except for small amounts of additives, which are used for colour purposes or to improve specific properties. Soda-lime glasses are most widely used to manufacture containers, sheets, and account for over 80% (by weight) of waste glass. The typical composition of different types of glass are given in Table 1.2. Soda-lime glasses consist of approximately 73% SiO_2, 13–13% Na_2O and 10% CaO, and on the basis of their chemical composition, soda-lime glasses will be pozzolanic-cementitious materials. The second major type of waste is lead glass, (from televisions, neon tubes, etc). A serious concern relating to the use of this type of glass in concrete is its high lead content, which could be leached into the environment.

Table 1.2 Chemical compositions of typical commercial glasses (McLellan and Shand, 1984)

Glass and uses	SiO_2	Al_2O_3	B_2O_3	Na_2O	K_2O	MgO	CaO	BaO	PbO	Other
Soda-lime glasses										
Containers	66-75	0.7-7		12-16	0.1-3	0.1-5	6-12			
Float	73-74			13.5-15	0.2	3.6-3.8	8.7-8.9			
Sheet	71-73	0.5-1.5		12.15		1.5-3.5	8-10			
Light bulbs	73	1		17		4	5			
Tempered ovenware	75	1.5		14			9.5			
Borosilicate										
Chemical apparatus	81	2	13	4						
Pharmaccutical	72	6	11	7	1					
Tungsten sealing	74	1	15	4						
Lead glass										
Colour TV funnel	54	2		4	9				23	
Neon tubing	63	1		8	6				22	
Electronic pars	56	2		4	9				29	
Optical dense flint	32			1	2				65	
Barrium glasses										
Colour TV panel	65	2		7	9	2	2	2	2	10% SrO
Optical dense barium crown	36	4	10						41	9% ZaO
Aluminosilicate glasses										
Combustion tubes	62	17	5	1		7	8			
Fibreglass	64.5	24.5		0.5		10.5				
Resistor substrates	57	16	4			7	10	6		

The structure of glass can be described as a two-dimensional framework of Silica tetrahedra as shown schematically in Figure 1.1.

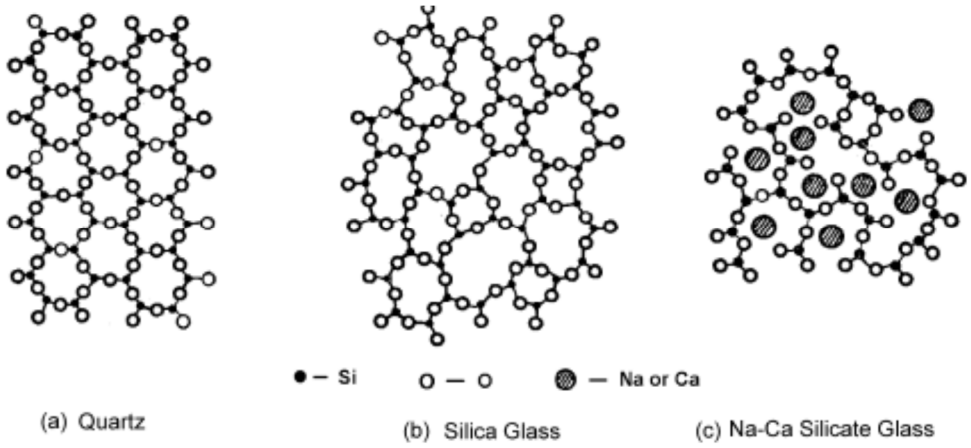

Fig. 1.1 Structure of glass (Din, 1979)

1.4 Aims and objectives

The research project reported herein was an experimental investigation of the effects of replacing conventional, commercially-available fine aggregate (sand) by waste glass (crushed to give a comparable particle size distribution) in structural concrete. A schematic view of the research work is given in Figure 1.2. Attention focussed on the effect of the replacement on flow characteristics of fresh concrete, the compressive strength of cured concrete and its long-term performance. The flow characteristics were quantified in terms of slump and flow value and compressive strength was determined using cube tests. Changes in the dimensions of concrete cubes and prisms as they cured were measured directly. Durability was inferred from assessment of the porosity and internal structure of the hardened concrete. The specifies objectives of the research were to quantify effects in term of:

- Determine the proportion of the sand which is replaced by crushed glass.
- The colour of the waste glass aggregate used in concrete.
- Use of a waste glass stream which contains a variety of colours.
- Preparation and cleaning of the waste glass prior to its use, i.e. waste crushed glass with washed and unwashed.

- Investigate the change in compressive strength with curing time and rate of gain of strength.
- Determine dimensional changes of concrete as it cures and variation of volume with time.
- Explore differences in internal structure as indicated by ultrasonic pulse transmission, bulk density, water absorption and porosity.
- Explore the effect of glass on the Alkali Silica Reaction and Capillary water absorption of concrete.
- Determine the effect on physical properties of concrete compressive strength.
- Classify the particle shape factors (i.e. Aspect ratio, Percentage concavity, Riley inscribed circle sphericity and Surface texture index), using image analysis of two-dimensional images.

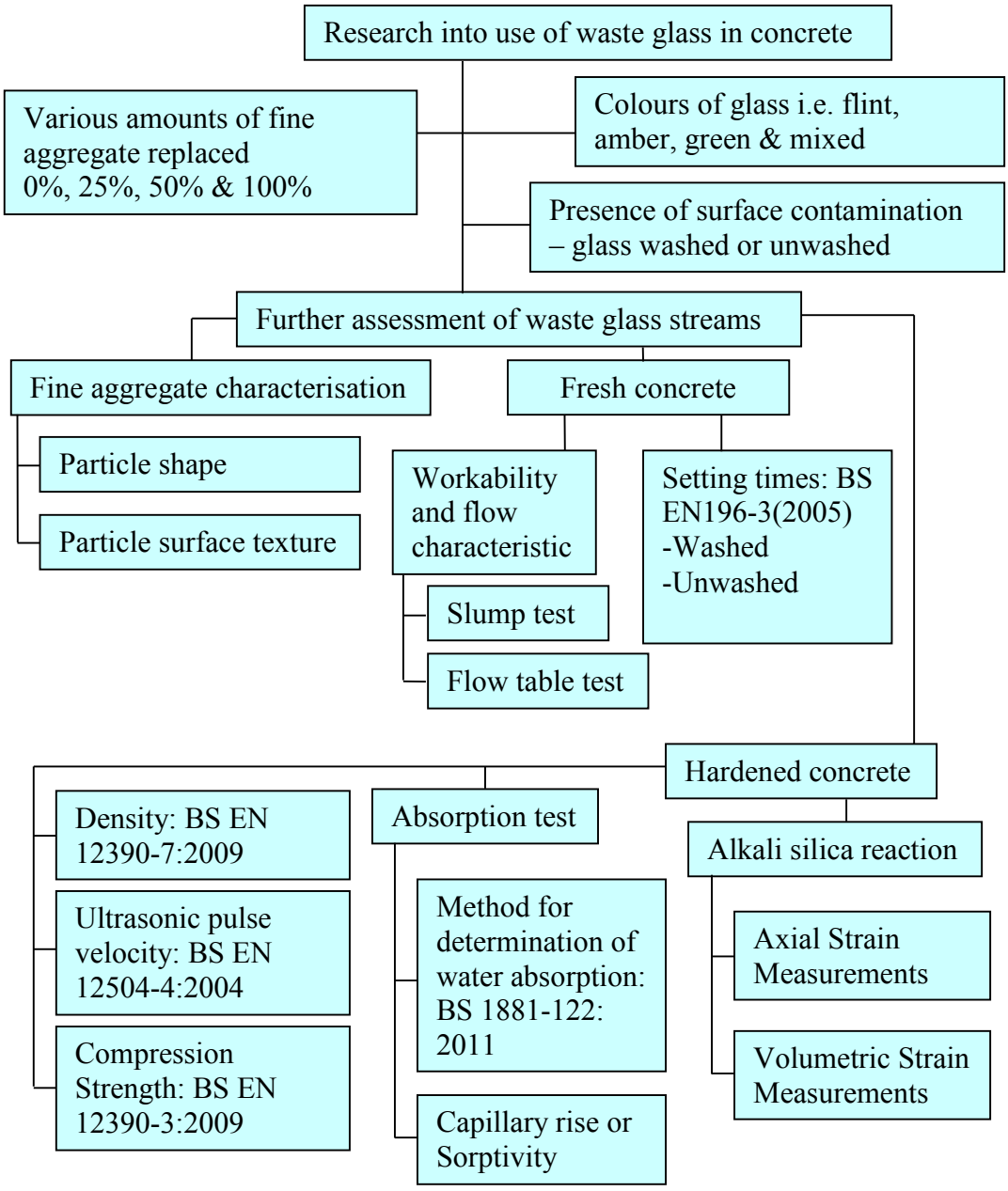

Fig. 1.2 Overview of research project

CHAPTER 2 - LITERATURE REVIEW

2.1 Use of waste glass in concrete

One way for the construction industry to improve its performance with regard to sustainable development would be to use concrete with reduced Portland cement content. There is a variety of products of industrial processes which have some cementitious properties e.g. fly ash, ground granulated blast furnace slag, condensed silica fume, and consideration has been given to substituting some of them for cement. Another strategy to improve the environmental 'considerateness' of the construction industry is to use waste products as substitutes for conventional fine and coarse aggregates - suitable wastes include construction debris, waste glass, dredged material, quarry spoil and mining spoil. The key to successful usage of these wastes lies in the identification and exploitation of the properties inherent in the waste material which can improve the properties of concrete and thereby increase their value (Dhir *et al*., 2005), combined with elimination or suppression of any harmful effects from using a specific waste material.

The use of waste glass in concrete has been tried in the past but deleterious Alkali-Silica Reaction (ASR) between cement paste and glass aggregates may occur. Studies on the expansive reactions between natural aggregates containing amorphous silica and Portland cement containing alkalis (Na^+ and K^+), have indicated that the direct substitution of glass for natural aggregate could have detrimental effects on concrete properties (Phillips *et al*., 1972). Glasses of a wide range of compositions are capable of reacting expansively with Portland cement. The most reactive glasses have a high boron content and/or alkali metal content or have a relatively porous or phase-separated structure (Figg, 1981). Other problems associated with the use of reclaimed glass in concrete are; the probable need to wash and remove sugars which would otherwise retard the hydration of the cement, the glass must be crushed and graded to provide similar engineering properties to natural sand and rock, the cost must suit the market (Phillips *et al.,* 1972).

Aggregates containing naturally-occurring siliceous materials, such as chert and opal cause excessive expansion within concrete. Various studies of the expansive reactions

between natural aggregates containing amorphous silica and Portland cement containing alkalis have indicated that direct substitution of glass for natural aggregate could detrimentally affect concrete strength (Phillips *et al.,* 1972). However, pozzolana, which is a processed siliceous material, is often considered an ideal additive to concrete for replacement of cement. The glass particles tend to be shaped like flakes and interlocking of the flakes causes concrete made with coarse aggregate to have poor workability. Consequently the use of glass as a concrete aggregate has tended to be limited to applications where it is used at the surface of concrete for decorative effect (Dhir *et al*., 2005). On the other hand recycled crushed glass is able to reduce the water absorption and drying shrinkage in concrete products due to its near zero water absorption characteristics, (Lam *et al*., 2007).

The reuse of waste glass in cement and concrete production has many potential benefits:

- Reduces waste disposal costs, which are likely to rise due to landfill tax and pressures to minimise landfilling.
- Conserves the environment by saving large amounts of primary raw materials each year.
- Extends the life of landfill sites, thereby helping to conserve the countryside.
- Saves a significant amount of energy and reduces the amount of CO_2, NOx, and other air pollutants emitted from the manufacturer of cement clinker (when ground glass powder is used as a cement replacement).
- Offers alternative uses for recycled glass based products, without compromising on either cost or quality (Shi and Zheng, 2007).

2.1.1 Cement replacement

When cement is mixed with water, chemical reactions begin between the various compounds and the water. These reactions result in the formation of various compounds; Tricalcium aluminate (which causes the initial stiffening but contributes least to the ultimate strength), Tricalcium silicate (has a marked effect on the strength of concrete at early ages), Dicalcium silicate (mainly responsible for the progressive

increase in strength). The chemical reactions result in the formation of a mixture of gels and crystals from the solution of cement and water, which, by their adherence and physical attraction to one another and the aggregate present, gradually set and harden to produce concrete (Murdock, 1991).

The compressive strength of concrete depends on aggregate-cement interactions and the interface bonding mechanism. It has long been know that silica in glass can be highly reactive with the alkalis present in cement paste. As early as 1973, Pattengill and Shutt used a variety of Standard ASTM tests to demonstrate that ground glass has significant potential as a Type S pozzolan additive in Portland cement concrete.

Nishikawa *et al*. (1995) reported that the strength of cement paste (at 90 days) increased with glass content (up to 25% by weight). The glass was crushed to a powder with similar grading to cement – unfortunately no chemical analysis of the glass powder was given by the authors. Dyer and Dhir (2001) found that the development of compressive strength for cement pastes containing finely-ground glass powder was dependant on the colour of the glass cullet; clear and green glass (at replacement levels of around 10%) produced a slight increase in 28-day compressive strengths relative to the glass-free control whereas amber ground glass cullet merely achieved similar strengths to the control. The rate of strength gain in mortars containing finely-ground glass cullet was noticeably higher between 7 and 28 days compared to the control. This behaviour implied that a pozzolanic reaction was occurring.

Shao *et al*. (2000) used the strength of lime–glass mixtures as an index of pozzolanic activity for three different ground glass powders, i.e. 150μm to 75μm, 75μm to 38 μm and less than 38μm. All particles were significantly coarser than cement powder. The strength results indicated that the less than 38μm glass powder satisfied the strength requirement at 7 days whereas the strength of the mixture with 150μm to 75μm glass was well below the strength target because the size of the glass was too coarse to serve as a pozzolan (according to Shao *et al.,* 2000). The 75μm to 38μm glass performed marginally better in that its 7-day strength was slightly lower than the required value but after additional curing its strength satisfied the 28-day requirement.

Dyer and Dhir (2001) found that the maximum rate of heat evolution in setting concrete drops as the Portland cement content is reduced by substitution of glass powder. It was reported that this was to be expected because any pozzolanic reaction that glass undergoes occurs late in the setting process and generates only minor quantities of heat. It was apparent that the presence of glass cullet had no influence on the normal early Portland Cement hydration reactions. The measurement of free $Ca(OH)_2$ in hardened cement pastes indicated that the presence of ground glass has little influence on the kinetics of Portland Cement hydration, however, calcium silicate hydrate levels were found to be higher in the pastes containing glass.

Unlike the work of Shao *et al.* (2000), a field trial conducted by Shayan and Xu (2006), using a 40MPa concrete mixture which incorporated various proportions of glass powder as cement replacement (20% and 30% by weight), showed that such concrete was initially slower to gain strength. Although this was true at 28 days by 404 days all mixtures exceeded the target strength and achieved about 55MPa compressive strength. In general, the test results demonstrated that glass powder could be incorporated into a concrete at dosage rates of 20–30% to replace cement, without harmful effects. No deleterious expansion was noted in the concrete and it was suggested that this may have been because the pozzolanic reaction of glass powder with cement enhanced the binding of excess alkali thereby making it unavailable for reaction with reactive aggregate. A similar suggestion was made by Al-Otaibi (2008) who experimented with ground granulated blast furnace slag as a partial replacement to cement and also as the sole binder in the form of alkali-activated slag.

Cassar and Camilleri (2012) used an implosion technique to convert waste glass because it was claimed to give fine particles which were not highly abrasive and because contaminants were not reduced in size and therefore could be easily removed. The replacement of 10-20% of the cement by the imploded glass gave a concrete which had a high resistance to chloride-ion penetration and Cassar and Camilleri said that such concrete would be ideal for use in structures built close to / at the sea where. It was also reported that up to 40% of the cement could be replaced by the imploded glass and still obtain a concrete which was suitable for use in structure.

Nassar and Soroushian (2012) used milled waste glass, with particle size of about 13 microns, as partial cement replacement in concrete containing aggregates made from recycled concrete. This substitution resulted in enhancement of durability characteristics, i.e. lower sorption and chloride permeability, and greater resistance to freeze-thaw deterioration. The enhancement was reported to be due to an improvement in the pore structure with the glass particles promoting infilling of the pores through conversion of calcium silicate, which was present in the old mortar/ cement paste attached to the recycled aggregate, into calcium silicate hydrate (C–S–H). The resultant denser, less permeable microstructure led to an increase in the long-term strength of the concrete. The strength increase during a 56 curing period gave an indirect measure of the pozzolanic activity of the fine waste glass.

Cement replacement with added plasticisers

Tuncan *et al.* (2001) investigated the suitability of glass and fly ash for use in concrete. The idea was that fly ash would infill the pores in the concrete and glass would improve the mechanical properties of concrete through pozzolanic reactions. Mixes were made with fly ash proportions between 0% and 30% and glass between 0% to 15% by weight. In all cases the concrete had water/cement ratio of 0.45 and Portland cement was used. It was found that all additions increased the compressive strength of the concrete. Freeze/ thaw tests indicated that addition of glass and fly ash increased the durability of concrete specimens. Concrete with 15% glass and 30% fly ash substitution had the best results with respect to compressive strength, indirect tensile stress and the coefficient of capillary permeability.

Shao *et al*. (2000) also examined the pozzolanic activity of ground glass and its effect on compressive strength by making concrete wherein 30% of the cement was replaced by ground glass. The results showed that ground glass having a particle size finer than 38μm did exhibit pozzolanic behaviour and the finely ground glass helped reduce concrete expansion by up to 50%. This agreed with the findings of Topcu and Canbaz (2004) that waste glass contains a high amount of silica and if it is finely ground (and thus amorphous) it would be expected to show pozzolanic activity. Compared to fly ash concrete, concrete containing only ground glass exhibited a higher strength at both early and late ages. The high early strength gain was possibly attributable to the high alkali content glass (soda-lime lamp material) that was used. Despite the high alkali

content of the waste glass there was no deterioration of strength of the concrete at a late age, in fact a continuous gradual increase in strength was observed. The concrete with glass showed a 120% increase in strength as the curing time progressed from 3 to 90 days- the corresponding increase for fly ash concrete was 102%.

Shi and Wu (2005) reported on the addition of glass powder and fly ash to concrete to increase the 'flow ability' and segregation resistance of self-compacting lightweight concrete. The use of ground glass powder was found to decrease setting time and increase chloride migration resistance, strength and drying shrinkage of the concrete. The finer the glass powder the higher the pozzolanic reactivity. Byars *et al*. (2004) also reported that the high silica content of finely ground grass reacts with alkali in cement (pozzolanic reaction) to form cementitious products. Even when expanded shale or clay was used as coarse aggregate the concrete containing glass powder did not exhibit deleterious expansion, even if alkali-reactive sand was used. Bignozzi and Sandrolini (2004) used milled glass cullet as fine filler in mortars and compared their mechanical and physical properties with those prepared with traditional calcareous filler. There was a clear increase in compressive strength of mortar when calcareous filler was substituted by the same amount of milled waste. This increase became more and more evident with long curing times (up to 34% for 60 and 90 days) thus confirming the pozzolanic behaviour of the milled waste glass.

Schwarz *et al.* (2008) claimed that fine glass powder has the potential to improve the durability of concrete. The optimal replacement level of cement by glass powder as determined from 28-day compression strength and hydration tests was 10%. It was shown that the glass powder facilitated an enhancement in cement hydration at early ages owing to the powder's very low water absorption. The 90-day compressive strengths of glass powder and fly ash modified concretes differed by only 5%. This very small strength difference suggested that concretes with 10% of cement replaced (either by glass powder or fly ash) will behave in a similar manner as far as mechanical properties are concerned- at least for a water: cement ratio of 0.42 as used by Schwarz *et al*. (2008). The durability characteristics were ascertained using tests for rapid chloride permeability, alkali–silica reactivity and moisture transport parameters.

2.1.2 Coarse aggregate replacement

Studies conducted in the 1960s using crushed waste glasses as aggregates in concrete found that the resultant material cracked (Pike *et al.,* 1960; Schmidt and Saia, 1963; Phillips *et al*., 1972). On the other hand, glasses containing lithium and lead were not expansive under similar testing conditions (Pike *et al.,* 1960).

A subsequent key study by Johnston (1974) investigated the performance of 34 different concrete mixes containing glass crushed to 19mm maximum size as coarse aggregate. Reference mixes were made with gravel of the same size and mixtures containing fly ash as partial cement replacement were also tested. Two cements, which were classified as low and high alkali content (according to ASTMC 150-72) were used in combination with glass - both with the fines removed and in the as-crushed condition. Partial cement replacement with fly ash and mixing of glass with gravel aggregate was included in an attempt to find a suitable method of overcoming the expected adverse effects of the reaction between glass and cement alkalis. Measurements of compressive strength, flexural strength, expansion, and visible surface deterioration were made for up to one year. The conditions under which performance of mixtures was satisfactory appeared to relate to limiting values of cement content and alkali equivalent. Using fly ash to replace 25% to 30% (by weight) of the cement, whether it was of low or high alkali variety, appeared to be an effective and widely applicable method of ensuring good long-term concrete performance. The results showed that in many cases the direct combination of glass with Portland cement yielded concrete which exhibited marked strength regression and excessive expansion due to alkali-aggregate reaction. However, mixing of glass with inert gravel aggregate did not appear to be an effective means of suppressing the Alkali-Silica Reaction (ASR) completely. Even with only 20% glass, expansions were noticeably larger than for conventional concrete and surface cracking was visible. It appeared that gravel acted merely as a dilutant of the ASR reaction rather than as a suppressant. In term of concrete strength behaviour, there was little difference between the performance of glass aggregate as-crushed and with the fines smaller than 2.36mm removed. However, the expansions for the as-crushed material were somewhat greater, indicating that a small amount of reactive fines can be tolerated but

that larger amounts are not desirable. The use of low alkali Portland cement did not seen to reduce the expansion of concrete made with crushed mixed waste glass.

Meyer and Baxter (1997) conducted extensive laboratory studies on the use of crushed glasses as coarse aggregate. They found that a feasible concrete mixture could be produced by using 100% crushed glasses as aggregate (using various proportions of clear and amber glasses), Portland cement and 20% metakaolin as partial cement replacement. The size of the glass aggregate had some effect on expansion rate and value. For aggregate made from clear soda-lime glass, Pyrex glass and fused silica the optimum particle size seemed to be smaller then 1.18 mm, 150μm and 75μm respectively. Zhu and Byan (2004) subsequently investigated different size ranges of glass aggregate up to 12mm and found that the expansion increased with the glass aggregate size.

Polley *et al*. (1998) found that concrete with glass aggregates required a higher content of water than conventional aggregates to reach the same workability. Concretes made with fine waste glass aggregates had higher compressive strengths than those made with coarse waste glass and combinations of fine and coarse waste glass at ambient and elevated temperatures. Freeze-thaw tests indicated that concrete with glass aggregates exhibited a slightly poorer durability index than the control conventional concrete, but the main concern for the use of waste glasses as concrete as aggregates was expansion and cracking.

Topcu and Canbaz (2004) used waste glass as coarse aggregates in concrete - the glass size was to 4–16 mm and was used to replace between 0 and 60% of the coarse aggregate. While waste glass addition decreased the slump, air content and fresh unit weight, it increased flow and VeBe flow values. When hardened concrete specimen properties were tested it was found that compressive, flexural and indirect tensile strengths and Schmidt hardness decreased in proportion to the increase in waste glass percentage. The compressive strength decreased by as much as 49% with a 60% substitution of aggregate.

Zhu (2004) reported a major study of Alkali-Silica Reaction (ASR) between glass aggregates and concrete. Materials tested included glass cullet directly from ‘Pub &

Club' and 'Bottle Bank' collections used as coarse and fine aggregate. Concrete containing glass from each source exhibited expansion due to ASR, as determined by test methods ASTM C1260 (Standard Test Method for Potential Alkali Reactivity of Aggregates) and BS 812-123 (Testing aggregates-Method for determination of alkali-silica reactivity). The results showed that the ASR reactivity of waste glass cullet varies with particle size but that, with appropriate use of pozzolanic materials, glass could be viewed as a potentially 'fit-for-purpose' material for precast concrete products.

The effect on strength of glass colour was also investigated by Zhu (2004). The green glass cullet which was used was matched identically to the particle size distribution of the 10mm all-in natural aggregate. Concrete containing cullet replacement was found to be stronger throughout the replacement range (10-60%) studied. The strength benefit due to the use of cullet was attributed to better bonding achieved with the surrounding cement matrix. Strength gains between 28 days and two years for concrete with 60% cullet replacement were double than that for the control concrete, for both compressive and tensile strengths. The performance of glass cullet was equally good with either Portland cement or cement containing ground granulated blast furnace slag. The strength gain was slightly better in tension than in compression. A strength benefit obtained by using glass cullet has also been observed for both air-cured and water-cured concretes (Sangha *et al.*, 2004).

Collins and Bareham (1987) suggested that processing of questionable aggregates might mitigate the expansion caused by alkali–aggregate reactions. It was subsequently reported by Ducman *et al*. (2002) that concrete specimens do not expand when porous glass is used as concrete aggregates. However, expanded glass aggregate is generally regarded as having relatively low strength and high water absorption that can make concrete placing difficult. Nevertheless Nemes and Jozsa (2006) reported that with special surface treatment expanded glass aggregate could be produced with relatively high crushing resistance and low water absorption (similar to conventional lightweight aggregates). A series of experiments, using 18 different expanded glass aggregates and two different expanded clay products in the same cement mortar matrix, demonstrated that it was possible to have aggregate substitution up to 50% by volume, with the ratio of density of concrete to compressive strength being favourable

for making structural concrete. In another study, it was found that when the volume of expanded shale was more than 60% of the total aggregate volume, the expansion of the specimens was greatly reduced and far below the deleterious expansion limit (Shi and Wu, 2005).

Terro (2006) investigated the effect of replacement of fine and coarse aggregates with recycled glass on the fresh and hardened properties of Portland cement concrete at ambient and elevated temperatures. The results indicated that the compressive strength of concrete made with a large proportion of recycled glasses decreased by up to 20% of its original value with increasing temperatures up to 700 °C. However, replacement of up to 10% fine and coarse aggregates with recycled glass had no effect on fresh and hardened properties of concrete at ambient and elevated temperatures.

Poutos *et al.* (2008) reported that significantly higher temperatures are generated during hydration of concrete made with glass aggregates than with natural aggregates. This trend was more marked with green glass than concrete made with amber or clear glass. The findings suggested that concrete made with recycled glass could have two important applications, namely, cold temperature concreting and in buildings to maintain greater temperature stability.

Castro and Brito (2013) found that the size of waste glass aggregate had a significant effect on concrete workability. If waste glass was used as fine aggregate the water-cement ratio needed to be increased to compensate for the loss of workability. However the replacement of up to 20% of conventional aggregate by crushed glass showed, within the limits of experimental error, an increase in compressive strength up to 13.6%. In addition the inclusion of glass aggregate reduced water absorption (capillarity was lowed by 10.1%, immersion fell by 3.8%), reduced carbonation (by 21.7%) and lowered shrinkage (by 7.4%).

2.1.3 Fine Aggregate Replacement

In work reported by Kou and Poon (2009) recycled glass was used to replace river sand (in proportions of 10%, 20% and 30%), and 10 mm granite aggregate (amounts of 5%, 10% and 15%) to make self-compacting concrete mixes. Fly ash was used in the concrete mixes to suppress the potential alkali-silica reaction. It was found that the slump and air content of the mixes increased with increasing recycled glass content. The initial slump flows of all the mixes prepared were at least 750 mm. In addition, the resistance to chloride ion penetration increased and the drying shrinkage of the recycled glass self-compacting concrete mixes decreased when the recycled glass content increased. The compressive strength, tensile splitting strength and static modulus of elasticity of the waste glass concrete mixes decreased with an increase in recycled glass content. The ASR expansion of all the specimens was significantly reduced by the use of fly ash.

Subsequent work by Figg (1981) indicated that glass aggregates were very expansive even in mortars made with high alumina cement and gypsum plaster of very low alkali content. The expansion was dependent on the colour of the glass. Clear soda-lime glass was most reactive, followed by amber glass, with green glass causing least expansion. Park and Lee (2004) also found that brown waste glass showed a greater expansion rate than green glass. Meyer and Baxter (1997) and Jin *et al*. (2000) proposed later that the Chromium within green glass could actually inhibit the expansion of concrete containing glass aggregate. However, Zhu and Byars (2004) found that there was essentially no difference in the behaviour of green, amber and flint glasses. In laboratory tests Dhir *et al*. (2003) found that cullet colour can have significant influence on the ASR expansion of concrete. When 50% of the fine aggregate was replaced by glass all of the mixes showed very similar expansion (only slightly greater than normal concrete) after 52 weeks curing. For 100% replacement the green glass gave expansion much greater than the conventional concrete and mixes with amber (twice as much) and flint (8 times as much) glasses. With regard to the opposite trend being reported by other researchers, Dhir *et al*. (2003) commented that a possible explanation was that elements other than chromium may play a role in controlling ASR expansion. However it must be noted that the grading of the green glass used Dhir *et al*. (2003) was much coarser (most of it was between 0.5 and

2.5mm) than the natural sand it replaced. Grading curves for the other glass colours were not given by Dhir *et al*.

Zammit *et al*. (2004) investigated the use of glass fines to replace different proportions of the fine aggregate in concrete. All mixtures containing glass achieved values similar to, or higher than, the compressive strength values of the control mixes at different time intervals, e.g. a glass sand replacement of 50% achieved compressive strength values 10% higher than that developed by the control mixes. This foregoing mix also showed the highest slump. It was concluded that 50% glass sand replacement would be the best proportion for optimal mechanical properties. Camilleri *et al*. (2004) also found that incorporation of glass fines in concrete reduced the water required by the mix to achieve a specified slump. Compressive strength values of the mixes were comparable to the control concrete. The glass used, which was produced by crushing white glass bottles (a soda lime glass) was completely amorphous. Furthermore, the addition of glass to concrete containing PFA as cement replacement increased both the fresh and hardened density and the compressive strength of the concrete.

On the other hand, Topcu and Canbaz (2004) found that using waste glasses as aggregates did not have a marked effect on the workability of concrete, but decreased the slump, air content and fresh unit weight. Furthermore, they reported that the compressive, flexural and indirect tensile strengths as well as Schmidt hardness decreased in proportion to the increase in waste glass content. The strength decreased noticeably when the glass content was more than 20% - as has been reported previously for brown waste glass by Park and Lee (2004). These comments are in conflict with the findings of Tuncan *et al*. (2004) who found that indirect tensile strength was increased by incorporation of glass aggregate. Specimens with 15% glass gave better results than 10% glass substitution in terms of compressive strength, indirect tensile strength, water absorption and capillary permeability. However, this latter result may be due to the composition of the glass i.e. 40% SiO_2, 14% ZrO_2, 20% Mg0 and 11% Fe_20_3 as opposed to the more usually 65-75% of silica.

Dhir *et al.* (2005) examined the influence of the grading of fine aggregate (made from glass) on the long-term strength (360 days) of concrete. The long curing time was

chosen to allow effects from any alkali silica reaction to develop fully. The results were compared against concrete containing natural sand as fine aggregate of identical grading. It was evident that as the material became finer, performance was enhanced in the concrete containing glass as a result of the pozzolanic reaction that the material undergoes. The dynamic modulus of concrete was less strongly influenced by grading, although in concrete containing glass aggregate, the Young's modulus was consistently higher than equivalent controls. The shrinkage of concrete containing fine glass aggregate was extremely low for coarse grading, due to its low water absorption characteristics. At finer grading, shrinkage was higher, (the result of pozzolanic reaction, converting the non-absorbent glass into absorbent calcium silicate hydrate gel) but was unlikely to present problems as shown in Figure 2.1. Similarly, Corinaldesi *et al*. (2005) found that replacement of fine sand with ground glass particle sizes up to 100μm caused no deleterious effect and in fact at a macroscopic level there was marked improvement in mortar mechanical performance. However a practical concern with the use of glass is that the smooth and plane surface of glass particles may significantly weaken the bond between the cement paste and the aggregate (Taha and Nounu, 2008a).

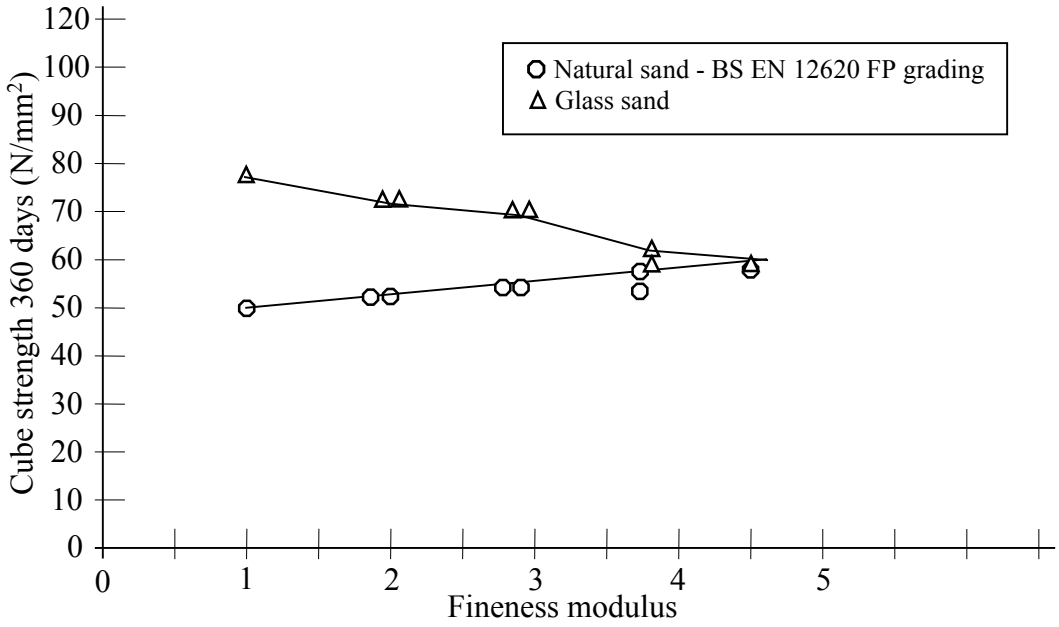

Fig. 2.1 Effect of fineness modulus on 360-day compressive strength of concrete for the range of gradings defined in BS EN 12620. (Dhir *et al.,* 2005)

Topcu *et al*. (2008) investigated the use of a combination of glass colour, mineral material and chemical additives as a way to incorporate glass as fine aggregate in concrete without having detrimental expansion. Mortar bars with a size of 25×25×285mm containing 31% cement and 69% sand with 0.47 water/ cement ratio, were produced using three different colours of glass in four different quantities as fine aggregate by weight. In order to reduce the expansions of mortars, 10% and 20% fly ash and 1% and 2% Lithium Carbonate (Li_2CO_3) were incorporated as mineral or chemical admixtures, respectively. It was observed that in terms of white, green and brown glass aggregates, the white glass caused the greatest expansion. In addition, expansion increased with increase in amount of glass. Over 20% fly ash and 2% Li_2CO_3 was required to produce mortars which had volumetric expansion values below the 0.2% critical value – with these additions it was possible to use up to 25% glass replacement, irrespective of colour. Green glass aggregate showed the best performance for 25% glass content with regard to ASR resistance.

Saccani and Bignozzi (2010) investigated the expansion of mortar bars (40×40×160mm) with a cement-to-sand ratio of 1:3 and water/ cement ratio of 0.5 containing different amounts of glass as fine aggregate and looked at effects of alkalinity and colour. Soda–lime glass showed negligible expansion whilst lead–silicate glass always showed expansive trends and always gave critical expansion

conditions for the relevant mortar samples. The behaviour of Boro-silicate glass depended on its colour. ASR gel composition, as determined by energy dispersive x-ray spectroscopy, was found to depend on chemical composition of the original glass used as aggregate.

If waste Liquid Crystal Display (LCD) glass is used as sand in concrete then the dead weight load of a structure can be reduced because this waste glass sand has a lower density than conventional fine aggregates. Consequently Wang and Huang (2010a) tested concrete mixes with four kinds of sand replaced by different amounts of LCD glass (proportion of 10%, 20%, and 30% by volume) at water-to-binder ratios of 0.28, 0.32, and 0.36. Fly ash, blast furnace slag and super-plasticizer were also added to create a self-compacting concrete mix i.e. a mix which tends to collapse under its own self weight. The slump and flow table values increased according to the amount of glass present and they peaked when the waste glass amounted to 30% of the total volume of fine aggregate. According to Wang and Huang (2010a) the LCD glass was "hydrophobic" with a water absorption rate one-third of the fine aggregate it replaced. Thus the use of waste glass increased the amount of 'free' water in the voids in the fresh concrete. Replacing 20% of the aggregates yielded the highest compressive and flexural strengths. When the proportion of glass was increased to 30% the amount of chloride ion penetration was reduced (the chloride ion penetration for concrete aged for 180 days was less than 100 coulombs (C), which is an insignificant amount) so that the durability of the self-compacting glass concrete improved. According to Wang and Huang (2010a), the glass sand can fill in internal pores and reduce the ability of ions to penetrate. After eight cycles of sulfate infusion, the weight loss as a result of sulfate corrosion ranged from 2.4% to 2.9% indicating that waste LCD glass sand can effectively reduce sulfate corrosion and thereby enhance the durability of the concrete. The volume change of self-compacting concrete containing waste LCD glass was in the range of $540–840\times10^{-6}$ when the concrete was cured for 90 days. A consequence of the proportion of cementious materials in self-compacting concrete is that the shrinkage is larger than that of conventional concrete, but using waste glass as fine aggregate can reduce this shrinkage (Wang and Huang, 2010a).

Limbachiya (2009) undertook an experimental investigation of the performance of Portland-cement concrete containing washed glass sand as substitute for natural sand.

The glass was washed to minimise chemical impurities and other contaminations. Although the crushed glass satisfied British Standard requirements for fine aggregate it was somewhat sharper with irregular texture. Overall the results showed that the glass waste could be crushed to provide fine aggregate with physical properties that satisfy the current requirements in concrete standards for natural sand. For fresh concrete an increase in waste content beyond 20% to 30% produced a measurable reduction in workability of concrete, although slump measurements remained within the allowable margin of ±25 mm. Studies of hardened concrete properties, (compressive cube and cylinder strength, flexural strength, modulus of elasticity, drying shrinkage) and durability (near surface absorption, alkali silica reaction) showed similar performance for conventional concrete and concrete with up to 15% of fine aggregate being waste glass.

Ismail and Al-Hashmi (2009) investigated strength and ASR expansion of concretes containing waste glass as fine aggregate with 10%, 15%, and 20% replacement of sand. The results proved 80% pozzolanic strength activity was given by waste glass after 28 days and the flexural and compressive strengths of specimens with 20% waste glass content were 11% and 4.23% higher, respectively, than those of the control specimen at 28 days. Mortar bar tests demonstrated that the finely crushed waste glass helped reduce expansion by 66% as compared with the control mix.

The use of ground glass (0 to 0.6mm with 60% retained on a 0.12mm sieve) as a partial replacement for both cement and fine aggregate in Self-Compacting Concrete (SCC) was investigated by Liu (2011). Results showed that to keep the filling ability constant, the inclusion of ground glass would require an increase in water/powder ratio and a reduction in superplasticizer dosage. However, these changes lowered the hardened strength, but not to a prohibitive extent. ASR tests that were performed on mortar bars (50×50×150mm in size) over a period of 6 weeks gave practically identical volume changes for conventional SCC and mixes with up to 10% cement and 10% fine aggregate replaced by glass powder. The research concluded that concrete with satisfactory fresh properties can be produced with replacement of about 10% cement and 10% sand.

Chen *et al*. (2011) used waste Liquid Crystal Display glass sand to replace part of the fine aggregate in concrete. Fresh properties were examined, including slump, flow slump and unit weight, and hardened properties were also examined, i.e. compressive strength, elastic modulus, impact-echo, ultrasonic pulse velocity and surface resistance. The results demonstrated that the ultrasonic pulse velocity and surface resistance of concrete with glass were marginally higher than those of the control group with the highest value being obtained at a replacement ratio of 30%. Slump and flow values were not detrimentally affected, in agreement with the findings of Wang and Huang (2010a), and since the concrete containing glass achieved a compressive strength which was 90% of the control group it was concluded that concrete in which natural sand is replaced with waste glass can meet common compressive strength requirements.

Ali and Al-Tersawy (2012) used recycled glass in self-compacting concrete (SCC) with partial replacement (0%, 10%, 20%, 30%, 40%, and 50%) of fine aggregate with cement contents of 350, 400, and 450 kg/m^3 and a water-cement ratio of 0.4. Experimental results showed that the slump flow increased as the glass content increased. On the other hand, compressive strength, tensile splitting strength, bending strength and modulus of elasticity decreased with glass content. From SEM micrographs it was evident that there was reduced contact between the cement matrix and the surface of the glass used as fine aggregate replacement. The smoothness of the surface of the glass aggregate led to weak adhesion between the cement paste and the glass aggregate, thereby promoting cracking and a loss of strength. Nevertheless, the experimental result overall indicated that recycled glass aggregate could be used to make acceptable self-compacting concrete.

Lee *et al*. (2013) claimed that for dry mix concrete blocks the replacement of sand by fine glass caused an increase in water absorption, the magnitude of which was in proportion to the amount of glass within the concrete mix. In addition, the water absorption increased inversely with the particle size of the glass aggregate. As a result, even when the glass aggregate was finer than 600μm, the water absorption of the concrete was increased significantly (by from 4.68% to 6.43%) when glass was used to replace 25% and 100% of the conventional aggregate. It was concluded that the higher water absorption indicated an enhanced void ratio in the concrete block containing glass (by comparison with those made from conventional concrete) and this caused a reduction in compressive strength. Lee *et al*. (2013) also stated that because the fine glass aggregate originated from crushed glass bottles there could be micro-cracks within the particles which gave rise to the observed increase in water absorption. On the other hand Kou and Poon (2009) found that chloride ion penetration decreased with the incorporation of crushed glass into concrete and claimed that normal, recycled waste glass had lower porosity than river sand and natural granite. Similarly Ling and Poon (2012) observed that the water absorption capacity of mortar was reduced when conventional sand was replaced by crushed glass originating from Cathode Ray Tube (CRT) because of the crack-free, impermeable nature of such glass.

Kou and Poon (2009) made a polymer 'concrete' using recycled glass for both coarse and fine aggregate and epoxy resin as the binder. It was claimed that the key characteristic of such 'concrete' was low water absorption which would prevent corrosion of reinforcement when it was used in the construction of sewage works, chemical plants, septic tanks, etc.

A further advantage of polymer 'concrete' was its rapid gain strength (about 85% of final strength was reacted within only 4 days) with a high final compression strength of 55 MPa.

Kou and Poon (2009) then made 'concrete' mixes where up to 15% of the fine glass aggregate was replaced by fly ash or metakaolin. These substitutions increased the workability of the 'concrete' by reducing internal friction and increased final compressive strength because of better adhesion between binder and fly ash and metakaolin.

2.2 Alkali silica reaction (ASR)

2.2.1 Mechanism

Early in 1938, a section of concrete pavement in Monterey County, California, failed because of excessive expansion (Stanton, 1940). The distress was manifested in the form of expansion, which caused buckling at the expansion joints and a severe cracking throughout the length of certain slabs. A close inspection of all sections disclosed that excessive expansion had occurred only in those sections in which the local fine aggregate (Oro Fino) had been used, and it was obvious, therefore, that aggregates from this area contained at least one of the sources of trouble.

The first concrete structure in which distress due to Alkali-Silica Reaction (ASR) developed to such an extent as to attract attention was King City Bridge (built in 1919-1920) - Stanton (1940). This bridge consisted of an all-concrete trestle approach to a series of concrete piers and steel trusses over the main channel of a river. The fine aggregate for the concrete was taken from the bed of the Salinas River and, within three years of construction, cracks developed in the caps of the piers and extended into the columns of the piers. Several subsequent concrete trestles and road pavements built using fine aggregate from the Salinas River also developed serious distress. The aggregates were all of the same general type, containing from 4% to 15% total of shale, cherty shale, and chert.

Following an extensive field and laboratory investigation Stanton (1940) concluded that certain mineral constituents, if present in concrete aggregates, could cause expansion of the concrete and develop stresses of such magnitude as to cause failure. Some shales expand excessively when saturated with water or when they are alternately wetted and dried and, therefore, the presence of such material should be kept to a practical minimum. The chemical reaction which produced excessive expansion apparently occurs only when the Portland cement component contains an appreciable percentage of alkali in the form of sodium and potassium oxides. The reaction is of an intensity proportional to the percentage of such oxides, apparently being of such low order as to be negligible when the alkali content is less than 0.6%. (Stanton, 1940)

Pike *et al*. (1960) pointed out that the reaction between high alkali cements and reactive aggregates, which frequently causes expansion, was affected by numerous factors. These included; the relative amounts of reactive and inert aggregates, the alkali content of the cement, the amount and quality of the mixing water and the nature of the water to which the hardened concrete is exposed, the minor constituents of the cement other than alkalis, the permeability of the cement paste, the particle size of the reactive particles.

According to Figg (1981), the mode of generation of swelling pressure due to ASR within a concrete appears to be due to the alternation and softening of the aggregate grains by inward diffusion of alkali metals and hydroxyl ions. This is followed by intake of water with the development of considerable osmotic pressure and eventual tensile failure and cracking of the surrounding matrix. Reaction rims on the periphery of aggregate grains have been observed with the residues of altered aggregate particles and copius amounts of isotropic alkali silicate gel and gel secondary reaction products Figg (1981). Amorphous silica can be corroded easily when the pH of the environment is greater than 12.

Suwito *et al*. (2002) developed a mathematical model to characterize the effects of various parameters on ASR and to predict ASR expansion. The model encompasses chemo-mechanical coupling of the expansion process, the size distribution of aggregates and micro-structural features of the cement paste. The chemical part of the model includes two opposing diffusion processes, i.e. diffusion of chemical ions from pore solution into the aggregate and permeation of ASR gel from the surface of the aggregate out into the surrounding porous cement paste matrix. The total ASR gel formed is considered to comprise two parts, i.e. gel directly deposited in the interface pores which is not governed by diffusion and does not cause expansion and gel which permeates into the surrounding pores in the cement paste and generates interface pressure and expansion. The amount of the first type of gel and the rate of the permeation of the second type of gel depend on the aggregate size and the porosity of the cement paste. For a fixed volume of aggregate, a decrease of aggregate size results in an increase of ASR expansion (due to increased surface area) and this is a diffusion-dominant process. When the aggregates are small enough that the amount of ASR gel formed around each aggregate is comparable to the pore space available in

the surrounding cement paste the gel pressure is released and the ASR expansion is reduced - this is a permeation-dominant process. In the limiting case, the aggregate size is sufficiently small that the interstitial pore space can hold all ASR gel even if the entire aggregate turns into gel and there will be no ASR expansion at all. The size for which the two diffusion processes are balanced is the pessimum aggregate size. The pessimum size depends on the pore space in the interfacial zone and the cement paste porosity. The higher the porosity the larger the pessimum size. Although Suwito *et al*. (2002) claimed that the foregoing model was capable of simulating the development of ASR expansion and predicting the pessimistic size of reactive aggregates, no actual analysis was subsequently presented and it was stated that experiments were needed to validate the model.

Bazant *et al*. (2000) subsequently proposed a micro-mechanical fracture theory to explain the effect of particle size on ASR expansion in terms two opposing mechanisms, i.e. the extent of chemical reaction (as a function of surface area) which causes the strength to decrease with a decreasing particle size and the size effect of the cracks produced by expansion of the ASR gel. Analyses employing fracture mechanics were undertaken by considering a repetitive cubical cell of mortar with one spherical glass particle embedded in it. Expansion was assumed to cause a ring crack. The situation was assumed to be approximately equivalent to an edge crack in an elastic half-space in the initial stage and to small circular uncracked ligaments in the terminal stage. A stress intensity factor was defined to represent the pressure from the gel and externally applied stress and was expressed in terms of a damage parameter representing the crack area fraction. Calculation of the pressure was based on the condition of compatibility of the volume expansion of the ASR, the change of volume of the crack and spherical void containing the particle, and the volume of the gel that gets squeezed into the adjacent capillary pores. Numerical solution of the problem was then fitted to observed volume expansions as a function of the particle size. The analysis predicted that there exists a certain worst (pessimum) size below which any further decrease of particle size improves the strength and expansion damage becomes virtually nonexistent if the particles are small enough. This pessimum size was reported to be about 1.5 mm and for particles smaller than 0.15mm, no adverse effects were reported as detectable.

Mechanism to the sizes and surface area

Meyer and Baxter (1997) and Jin *et al*. (2000) found that the pessimum sizes for clear (flint) soda-lime glass, Pyrex glass and fused silica appear to be 1.18 mm, 150μm and 75μm respectively. Zhu and Byars (2004) tested different size ranges of glass aggregate up to 12mm and found that the expansion always increased with increase of glass aggregate size, but they did not give a particle size below which expansion was negligible.

The interaction of cement and municipal solid waste incinerator bottom ash (when utilized as an aggregate in concrete) was investigated by Muller and Rubner (2006). The most prominent reaction observed in laboratory and field concrete was the formation of aluminium hydroxide and the release of hydrogen gas from aluminium grains reacting in the alkaline environment and the expansive reaction was identified as a main cause of extensive spalling on the concrete surface. Due to the high content of bottle glass as part of the ash, products of an alkali-silica reaction were also observed in all samples. However, damage due to ASR was less severe than that caused by the aluminium reaction. The expansion rates were low and only a few of the laboratory samples showed cracking. Microstructural analysis of the samples indicated clearly that a large quantity of the alkali-silica gel which was formed was accommodated in the pores and voids formed by release of Hydrogen gas from the aluminium reaction in the cement paste matrix so that no strain was created within the material.

It would appear that milling/ grinding of waste glass to a fine powder (about 13μm particle size) is the key to developing its pozzolanic potential. Cassar and Camilleri (2012) reported that finely ground glass could be used to replace cement to produce a good quality concrete that did not exhibit ASR. The high surface area of the milled/ ground waste glass changes the kinetics of the pozzolanic reaction so that alkaline material is utilised advantageously (in forming bonds) before production of a detrimental ASR gel (Nassar and Soroushian, 2012).

2.2.2 Prevention of ASR

By the 1950s there was a general consensus that there were just two possible remedial measures when reactive aggregates were to be used in concrete i.e., low alkali cement or substitution of a pozzolanic material for 20 to 30% of the Portland cement. However, McCoy and Caldwell (1951) reported a new approach to inhibiting alkali aggregate expansion through the addition of small amounts of specific materials, i.e. lithium salts or an air-entraining agent. Meyer and Baxter (1997) subsequently reported that the introduction of an air-entraining agent could reduce concrete expansion by up to 50%. It was believed that such concrete contained pores which permit the expansive reaction products to permeate into these pores and thereby relieve the expansive pressure and reduce or eliminate the expansion (as reported in section 2.2.1). According to McCoy and Caldwell (1951) the addition of that small amounts (0.2% or less) of certain proteins to cement appeared to have a greater inhibiting effect on the expansive reaction than that obtained by conventional air-entraining agents.

Pike *et al*. (1960) combined various glasses with high and low alkali cements and with high alumina, cement and pressure-calcined gypsum plaster and found that whilst sodium and potassium silicate glasses acted as reactive aggregates the lithium and lead silicate glasses did not. This demonstrated the effect of differing ions on the alkali-aggregate reaction and the necessity for the presence of sodium or potassium (or both) for the reaction to occur. The non-expansion of the mixes with potassium compounds could be expected because these silicates are insoluble and therefore would be non-reactive. The expansive reaction of the sodium silicate glass could be inhibited by substituting pozzolan for a relatively large portion of the cement. This potential expansion was reduced to 0.2% by the substitution of 4% of pozzolan and to 0.02% by the substitution of around 20% of pozzolan (Pike *et al*., 1960)

Turanli *et al.* (2003) undertook an experimental study of the potential of ground clay brick as a pozzolanic material to minimize ASR expansion. Two different types of clay bricks were finely ground and accelerated mortar bar tests were performed. The microstructure of the mortar was investigated using scanning electron microscopy. The mortars met strength activity requirements and the ground brick was apparently

effective in suppressing the alkali silica reaction expansion which decreased in magnitude as the amount of ground brick in the mortar increased.

Supplementary cementing materials such as ground blast furnace slag, fly ash, silica fume and metakaolin have also been tried to reduce or eliminate the alkali–aggregate reactions. Turanli *et al*. (2003) reported that when both the alkali and fly ash content are very high it is possible to have considerable ASR without large expansion of the concrete. Laboratory studies have indicated that the use of the foregoing materials can reduce the expansion of concrete containing glass aggregates (Jin *et al*., 2000; Dhir *et al*., 2003; Zhu and Byars, 2004).

The effectiveness of suppressants is dependent upon the chemical and physical characteristics of the material. To date, metakaolin is claimed to be most effective material (Jin *et al*., 2000; Zhu and Byars, 2004). Concrete systems modified with metakaolin have been reported to profit from a superior Portlandite-free microstructure, which explains its excellent durability, low shrinkage and substantially lowered creep deformation (Sabir *et al*., 2001). Zhu (2004) reported that for concrete blocks incorporating post-consumer cullet aggregate the replacement of 20% cement by super-classified pulverized fuel ash and metakaolin could totally mitigate ASR expansion.

Khatib (1998) claimed that Metakaolin used as a partial cement replacement in concrete gave increased resistance to Alkali-Silica Reaction, prevented efflorescence and increased resistance to acid attack. Increasing the levels of Metakaolin in Portland cement mortars exposed to Na_2SO_4 solution reduced levels of expansion and increased resistance to cracking. It was suggested that at low Metakaolin contents (0 - 10%), there is excess calcium hydroxide available, therefore, the onset and magnitude of expansion is controlled by the amount of C_3A available to react to form an expansive product. Hence, the high C_3A-content Portland cement mortars show early and rapid expansion, whereas the intermediate C_3A-content Portland cement mortars show much later expansion and slower expansion rates. At high Metakaolin contents (15-25%) calcium hydroxide availability becomes restricted, and the magnitude and rate of expansion is very much smaller and less sensitive to C_3A content.

The effect of ASR on concrete paving blocks produced with partial replacement of natural fine aggregates by crushed glass cullet was investigated by Lam *et al*., 2007. The approach used was to quantify the extent of the ASR expansion and then determine the amount of mineral admixtures needed to eliminate the expansion. Concrete blocks containing different recycled crushed glass contents were subjected to accelerated mortar bar testing (ASTM test C 1260). It was found that incorporation of 25% or less of waste glass induced negligible ASR expansion after a testing period of 28 days. For mixes with a glass content greater than 25% the incorporation of admixtures such as pulverized fuel ash and metakaolin suppressed the ASR expansion within the stipulated limit. It was concluded that the optimal mix for utilizing crushed waste glass in concrete blocks would contain at least 10% PFA by weight of the total aggregates used.

Taha and Nounu (2008) studied the influence of two different mineral admixtures, lithium nitrate and Pozzolanic Glass Powder on the expansion induced by ASR. Concrete prisms were produced for each concrete to measure the expansion and chemical analysis was performed using X-ray spectrometry. Test results confirmed that the lithium compound and glass powder significantly reduce expansion due to ASR. A lower calcium to silica ratio was found in concrete mixes containing glass powder because of the high amorphous reactive silica and low calcium content in the powder compared to ordinary Portland cement. The low calcium content caused the ASR gel produced to be thinner than the ASR gel of normal Portland cement concrete so that it was able to permeate and dissimulate into the concrete microstructure thereby reducing the risk from ASR expansion. The presence of glass powder as cement replacement led to changes in the concentration of hydroxide ions in the pore solution and this was also considered to directly reduce the ASR expansion risk. The lithium nitrate was believed to lower the ASR risk by; i) reducing the dissolution ability of the reactive silica by applying a coating action to the surface of the particles, ii) reducing the opportunities for the dissolved reactive silica to re-polymerise and form ASR gel, iii) increasing the repulsive force between the particles of the ASR gel.

2.3 Influence of aggregate profile

2.3.1 Classification and quantification of particle shape

Wentworth (1919) developed an apparatus (a tumbling barrel) to study the abrasion of cobbles resulting from movement along a river bed. It was believed that quantitative determination of the change of cobble shape and size, as a function of the distance of travel, would be a valuable parameter for the study of the geological properties of transported materials. Wentworth stated that in order to study the change of shape of the cobbles it was necessary to recognize varying degrees of roundness and he identified three possible measure of roundness, namely; 1) the ratio of surface area to volume; 2) the average deviation of diameters from a mean diameter; 3) the average deviation of convexities from a mean convexity. For practical applications Wentworth proposed a coefficient of roundness (R) which was the ratio of the radius of curvature of the most convex part of the particle surface to half of the longest diameter through that point. Wentworth (1919)

Cox (1927), Pentland (1927) and Tickell (1931) subsequently produced definitions of 'roundness' which took account of the overall shape of a particle by including the total area of the grain within their definition. In Cox's definition the surface area was divided by the area of the circle which had the same perimeter. In Pentland's definition the surface area was divided by the area of a circle with a diameter equal to the longest diameter of the particle. In Tickle's definition the surface area was divided by the area of the smallest circumscribing circle.

Wadell (1932) investigated the deposition of particles within geological sediments and stated that the spherical form was a determinant factor in sorting particles in traction by rolling whereas surface area of a grain players the major part in sorting particles as they settle from suspension. Hence particle properties that were of particular importance were volume, shape and roundness. However, particles may have the same size value, as defined in terms of the arithmetic or geometric mean of their diameters, yet they may differ distinctly in respect to both shape and volume. Therefore a distinction needed to the made between the two properties. Wadell

advanced expressions for the determination of ‘true sphericity’ and ‘degree of roundness’ for particles whereby.

$$\Psi = \text{True sphericity} = \left(\frac{\text{surface area of a sphere with the same volume as a particle}}{\text{Actual surface area of the particle}} \right)$$

Equ. 2.1

$$P = \text{degree of roundness (in one plane)} = \text{arithmetic mean of the roundness of the individual corners in the plane}$$

Equ. 2.2

According to Wadell (1932) the roundness of the roundness of a corner was equal to

$$\frac{\text{radius of curvature of a corner}}{\text{radius of the maximum inscribed circle in the plane of measurement}}$$

Equ. 2.3

Thus Wadell’s degree of roundness had some similarity to the coefficient of roundness defined earlier by Wentworth (1919).

Zingg (1935) developed a system of classification of pebble shapes which had some general correspondence with Wadell’s true sphericity parameter. However, the parameters used in Zingg’s system are easier to assess than Wadell’s true sphericity. In Zingg’s system three mutually-orthogonal particle dimensions (a, b and c) are used to define an Elongation ratio (b/a) and a Flatness ratio (c/b) i.e. 'aspect ratios' in mutually-perpendicular directions. Dimension a is the maximum length of the particle, dimension b is the maximum width perpendicular to the axis of dimension a. The value of c is the maximum dimension perpendicular to both the a and b axes. The 'aspect ratios' (for defining elongation and flatness) may be assessed by formal measurement of a, b and c or by visual inspection. The values of the ratios are then used to assign the particle shape to one of the four categories shown in Table 2.1. Alternatively the ratios may be used to define a portion within the particle shape regions shown in Figure 2.2.

Table 2.1 Zingg's (1935) classification of particle shape

Class	Elongation ratio – (b/a)	Flatness ratio – (c/b)	Shape
I	> 2/3	< 2/3	Flat/ disks
II	> 2/3	> 2/3	Spherical
III	< 2/3	< 2/3	Flat blades
IV	< 2/3	> 2/3	Rod-like

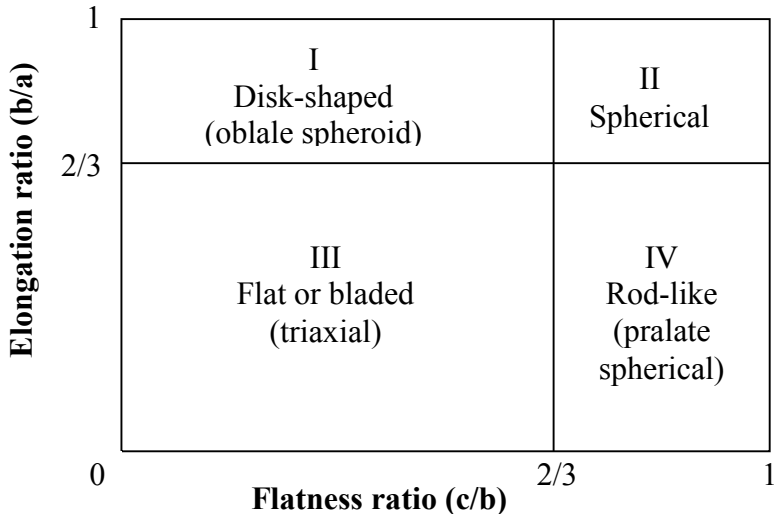

Fig. 2.2 Zingg's (1935) classification of particle shape

Whilst there is a general correspondence between Zingg's classification system and Wadell's sphericity it should be noted that a cube or a short length of circular bar would have Elongation and Flatness ratios of unity but their resistance to rolling motion would be very different to that of a sphere. These differences could be accounted for by incorporation of a roundness parameter such as Wadell's.

Russell and Taylor (1937) made measurements of numerous samples of river bed sand taken at intervals along a 1000-mile strength of the Mississippi River to investigate the then perception that stream transportation of sands and pebbles characteristically rounded the grains. Russell and Taylor observed that in most studies of the shape characteristics of river sands no systematic attempt had been made to define carefully 'roundness' and that classification systems (such as these of Cox (1927) and Tickell (1931)) had been set up without full realization of the difference between shape and roundness. The sphericity and roundness proposed by Wadell (1932) were recognised

as being the most appropriate for qualifying the shape and wear of sand particle during sedimentation and were adapted by Russell and Taylor for their study. However became of the difficultly of making numerous measurements of true spehericity (Ψ) Russell and Taylor used an approximation for sphericity, namely

$$\phi = \text{sphericity} = \frac{d_C}{D_C} \qquad \text{Equ. 2.4}$$

d_C = Diameter of a circle equal to the area of the grain when it rests on one of its larger faces more-or-less parallel to the plane of the longest and intermediate diameters

D_C = Diameter of the smallest circle circumscribing the grain

For most geometrical shape the ϕ value closely approaches the Ψ value with the chief deviation occurring in the case of very flat shapes.

Because of the large number of samples of sand to be tested, and the objective of their study, Russell and Taylor undertook the majority of assessments of particle shape using a qualitative method. In this method the grains were classified into groups (angular, subangular, subrounded, rounded) and well-rounded) based upon degree of wear-the criteria given in Table 2.2.

Table 2.2 Russell and Taylor (1937) Sand grains in various degree of rounding

Class	Criteria	Photograph
Angular	Very little/ no evidence of wear, edges and corner are sharp	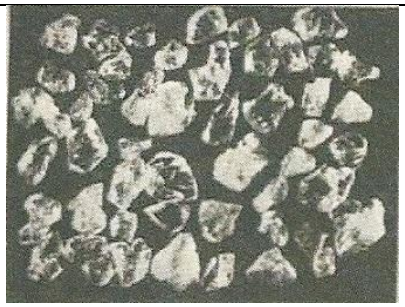
Sub-angular	Definite signs of wear. Grains still have original form, faces are practically untouched but the edges and corners have been rounded off.	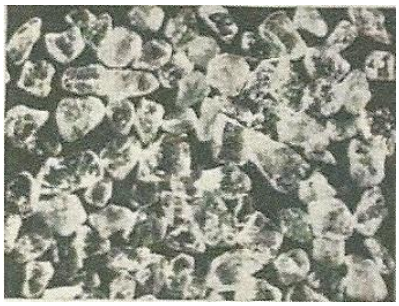
Sub-rounded	Considerable wear. Edges and corners are rounded off to smooth curves, area of the original faces are considerably reduced. Original faces are considerably reduced. Original shape of the grain is still evident.	
Rounded	Original faces almost completely destroyed, some comparatively flat surfaces may be present. All edges and corners have been smoothed off to rather broad curves.	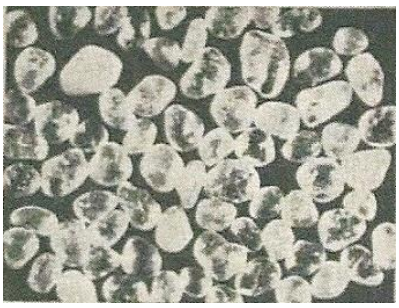
Well-rounded	No original faces, edges or corners left. The entire surface consists of broad curves.	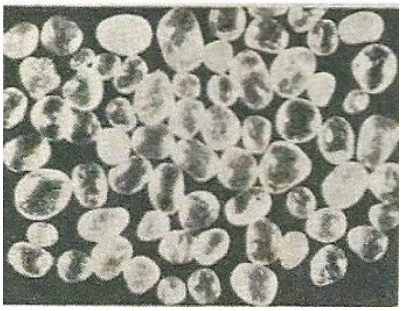

With regard to progressive changes in roundness and sphericity with distance along the river bed Russell and Taylor (1937) commented that for the two methods employed (their visual inspection and Wadell's quantitative measures) the results showed workable similarity, especially in the mean values for the samples. The mean values were calculated using weighting of parametric values according to their frequency (based on particles 'size') within each sand sample. On the basic of their analysis Russell and Taylor proposed a correspondence between their usual clarification categories and Wadell's roundness parameter (*P*) as shown in Table 2.3.

Table 2.3 Russell and Taylor (1937) roundness classification schemes

Particle class	***P* values**
Angular	0 – 0.15
Sub angular	0.15 – 0.30
Sub rounded	0.30 – 0.50
Rounded	0.50 – 0.70
Well rounded	0.70 – 1.00

Furthermore it was concluded that for the river sand studied there was a general relationship between roundness and sphericity – Figure 2.3. Rounded grains were generally found to possess higher sphericity values – this was especially true of grains ranging from angular to sub-rounded.

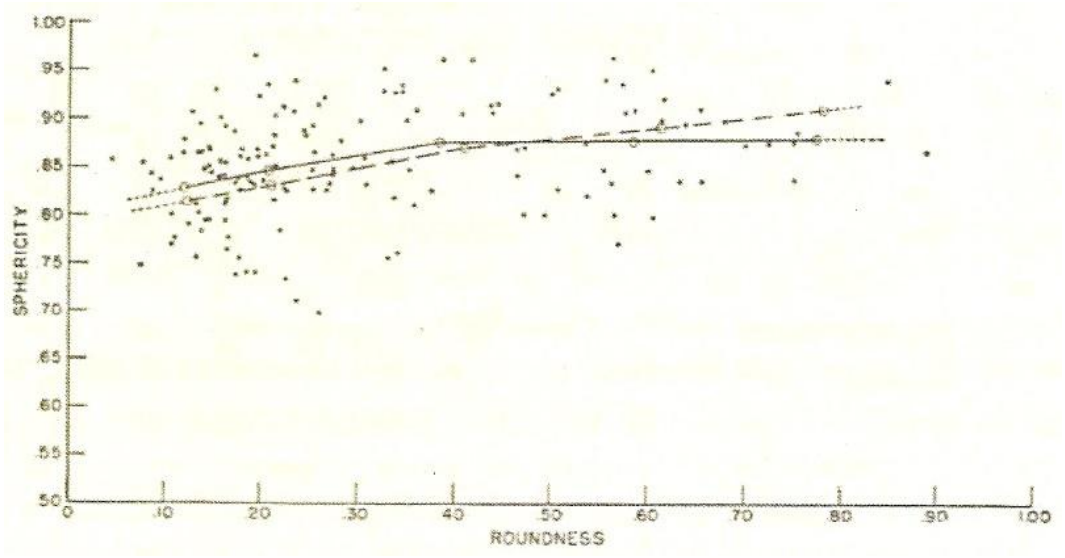

Fig. 2.3 Relationship between roundness (*P*) and sphericity (ϕ), from Russell and Taylor (1937)

Krumbein (1941) presented a method for the measurement of shape and roundness which was claimed to drastically reduce the time needed to assess a sample of pebbles. Like Zingg's (1935) approach, Krumbein's method required only the long, intermediate and short diameters of a pebble to be measured and the sphericity was then read directly from a chart by means of ratios between pairs of the diameters, i.e. b/a and c/b. Krumbein claimed that by superimposing the zones defined by Zingg for pebble classification on his sphericity chart (Figure 2.4) there was direct reconciliation of Zingg's and Wadell's shape concepts because a pair of b/a and c/b values defined a point which gave a sphericity value and a shape classification.

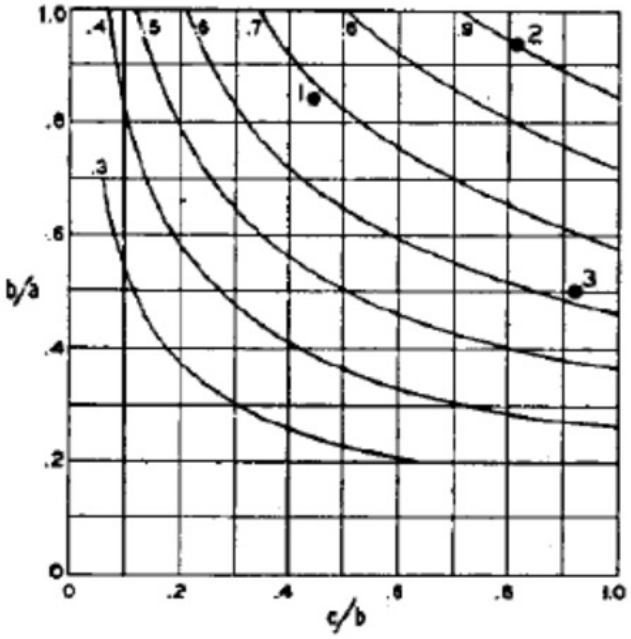

Fig. 2.4 Chart for determining sphericity, the curves represent lines of equal sphericity (Krumbein, 1941)

Krumbein (1941) also presented a visual roundness method in which the silhouette of a pebble was compared with standard images of known roundness in order to assign a roundness value to it. The images used for comparison were redrawn from pebbles which were measured by Wadell's method and it was claimed that statistical studies showed that average values (but not necessary individual values) agreed well with Wadell's values. Krumbein (1941) recommended that a set of pebbles (preferably around 50 but at least 25) should be used and that each pebble should be assigned a value. The average roundness value for the set was the arithmetic mean roundness, i.e. (the total sum of products of roundness value and number of particles with this value) divided by (total number of particles). Roundness measurements on a large number of

pebble sets indicated that the usual method had an average error of only about 1% compared to Wadell's method unless broken pebbles were present in a sample. For the latter case an empirical correction was derived whereby the roundness of the unbroken half of a pebble is divided by 2.

According to Riley (1941) all sphericity measurements could be divided into two general classes, namely those depending on individual particle measurements and those depending on grain aggregate measurements. However, grain aggregate measurements (such as those of Krumbein (1941)) give only a mean sphericity without any information about the sphericity distribution and therefore their use for investigating sedimentary deposits was limited. Riley stated that the study of sedimentary particles was handicapped by the great number of shape measures advanced by different people. Furthermore he claimed that calculation of sphericity by the foregoing methods was very time consuming and Riley proposed a method involving only the square root of the ratio of the inscribed and circumscribed circles. This value was termed the inscribed circle sphericity, where

$$Ø_{Riley} = \sqrt{\frac{2 \times \text{minimum Radius}}{2 \times \text{maximum Radius}}} \qquad \text{Equ. 2.5}$$

Riley then measured Wadell's sphericity and the inscribed circle shphericity for particles within large sets of beach pebbles, crushed quartz grains and glacial outwash pebbles. Although the histograms (percentage occurrence against sphericity value) for Wadell's and Riley's sphericity were quite dissimilar the average coefficient of correlation for the those sets was 0.94. Riley claimed that this meant that the Riley sphericity values was very similar to the Wadell sphericity value (which indicates how easy it is for a particle to more by rolling/ flowing and thus the effect of aggregate shape on the workability of a concrete), i.e.

$$Ø_{Riley} \cong Ø_{Wadell} \qquad \text{Equ. 2.6}$$

Sneed and Folk (1958) considered Zingg's diagram to be inadequate in that it contained only four shape classes which divided the field of particle form variation very unequally. They suggested that rods were under-represented and blades were

over-represented. Sneed and Folk (1958) considered that only three end-members limit the system of dimensional variation, namely; a prelate spheroid with one long axis and two short ones (a>b=c), an oblate spheroid with two long axes and one short one (a=b>c) and a sphere with all axes equal (a=b=c). They concluded that for analysing particle shape the most satisfactory device was a triangular plot (as shown in Figure 2.5).

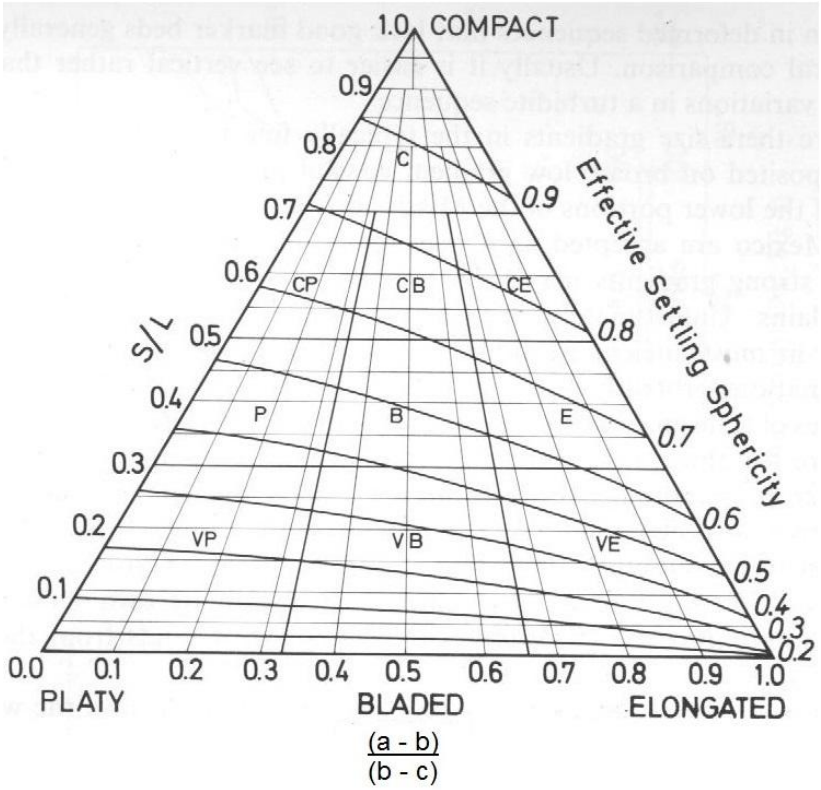

Fig. 2.5 Chart based on work of Sneed and Folk (1958)

Complete characterisation of three-dimensional particle morphology is a complex task which may be necessary for production of the likely transport and sedimentation behaviour of particle. However, for many practical purposes, including object description and comparison, relatively simple characterisation of particle form, involving quantification of the degree of particle flattening or particle elongation may be all that is required. According to Lees (1964) assessment of the engineering behaviour of particles of different shape for use as concrete aggregate or road dressing can be undertaken using relatively simple description of form, sphericity and roundness/ angularity. A similar approach was shown by BS812 (1975) with its six general classification categories of particle shape – Table 2.4 and Figure 2.6. The

particle descriptions within this table seem to be amalgum of those classifications and observations given by Zingg (1935), Russell and Taylor (1937), and Riley (1941). BS812 (1990) concerns the testing of aggregates with Part 105 dealing specifically with particle shape. The particular parameters defined in Part 105 are Flakiness index and Elongation index, but the respective tests for this indices are stated to be not applicable to material passing a 6.3mm BS test sieve. However, if the size limitation is ignored then a piece of aggregate which is neither flaky or elongated according to BS812 would:

a) have a Riley inscribed circle sphericity of slightly greater than 0.7 and would be defined as having moderate circularity / sphericity,
b) be more-or-less located within Zone II / spherical of the Zingg diagram
c) be classified as rounded or irregular or angular according to BS 812 (1975).

Table 2.4 Particle shape classification of (BS 812: Part 1: 1975 in Table 2)

Classification	Description	Examples
Rounded	Fully water-worn or completely shaped by attrition	River or seashore gravel; desert, seashore and wind-blown sand
Irregular	Naturally irregular, or partly shaped by attrition and having rounded edges	Other gravels; land or dug flint
Flaky	Material of which the thickness is small relative to the other dimensions	Laminated rock
Angular	Possessing well-defined edges formed at the intersection of roughly planar faces	Crushed rocks of all types; talus; crushed slag
Elongated	Materials, usually angular, in which the length is considerably larger than the other two dimensions.	-
Flaky and elongated	Material having the length considerably larger than the width, and the width considerably larger than the thickness	-

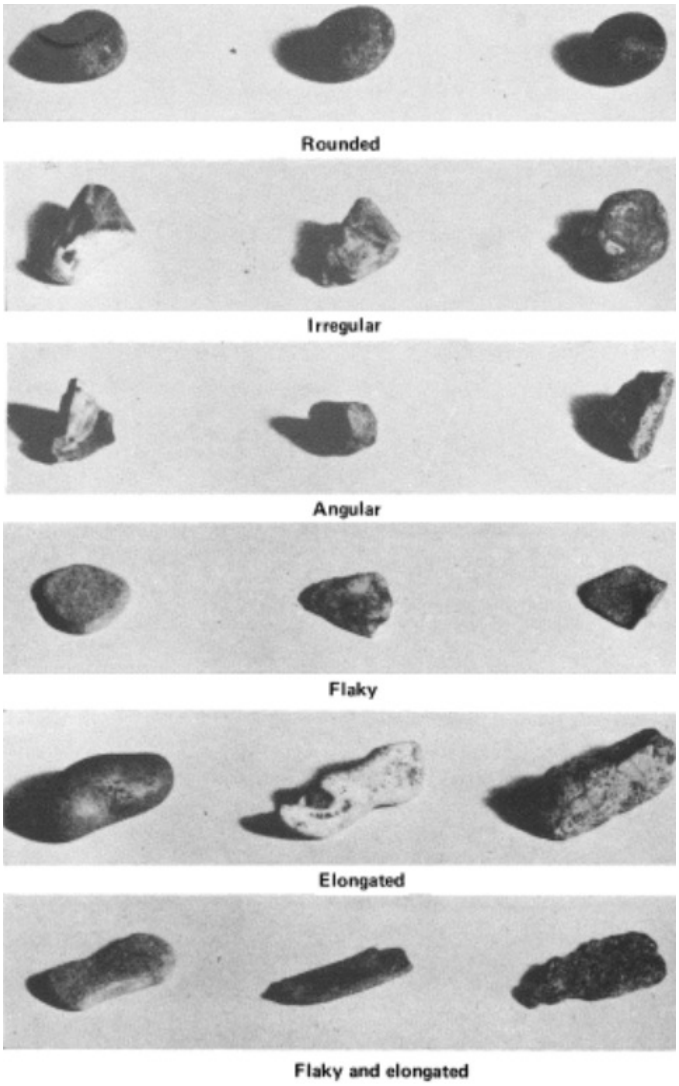

Fig. 2.6 Typical particle shapes (BS 812-1 1975)

Blott and Pye (2008) undertook a thorough and detailed review of methods of characterisation and classification of the shape sedimentary particles. They concluded that the most important aspects of particle form could be characterised and classified on the basic of measurements in two or three dimensions which are used to calculate a number of simple indices representing the form, roundness sphericity and irregularity. They noted that the Sneed and Folk (1958) and Zingg (1935) type diagrams (both of which use combinations of orthogonal particle dimensions a, b and c) have advantages and disadvantages for usual data representation and suggested that particle form data should be plotted on both types of diagram. In addition Blott and Pye (2008) proposed a new form diagram, based on elongation ratio (b/a) and flakiness ratio, which was an extension of Zingg's diagram with 25 form classes instead of the original four. The new form diagram allowed the relative frequency of particles of each form class

within a batch of particles to be easily seen and calculated. With regard to estimation of sphericity Blott and Pye (2008) concluded that Riley's inscribed circle parameter could be determined easily and quickly using photographic digital images and simple image processing software.

Particle measurements using image analysis are undertaken many times faster, more accurately and with far better repeatability than by manual techniques. Moore (1968) developed an approach to image analysis by computer and laid the basis for rapid methods of automated measurement. In the early stages of development, it was not possible to save or freeze the image and measurements have to be made "semi-manually" directly on the monitor. Today data for the image is stored in memory and measured immediately. This technology also allows the measurement and collection of a very large of dataset. Examples of image analysis processes include:

- A high resolution digital camera for image production and a program macro to measure longest and shortest diameter, the area and aspect ratio of each particle (Persson, 1998), Sukumaran and Ashmawy (2001) for sand samples. Grain sizes between 2mm and 0.25mm were illuminated by light from various directions and viewed through a light microscope. For sand particles between 0.25mm and 63μm images were captured using a microscope with polarization options and UV light. Particles finer than 63μm were 'viewed' by Scanning Electron Microscope.
- X-ray microcomputer tomography (μCT) and laser diffraction to measure particle sizes and their distribution within microfine aggregate, i.e. aggregates formed in a crushing process to make them pass a number 200 sieve, (Erdogan *et al*., 2007). Laser diffraction works by collecting the light scattered when it strikes a collection of particles and focusing it onto a detector array. The received signal is then converted to a particle size distribution by using a mathematical algorithm, which assumes that the particles are spherical since laser diffraction is sensitive to the volume particle. In the μCT process a particle is subjected to X-rays from many angles and reconstruction algorithms are used to yield 2-D 'slice' images which are then computationally stacked to yield a 3-D view of the specimen.

In 1919 Wentworth proposed a method for classifying geological particles based on roundness. However, this method did not provide a quantifiable measures for

roundness. This is because it only related to one position on the surface of a particle. Furthermore, Wentworth (1919) stated that none of his proposed measures of roundness satisfactory, especially for field use, became of the great difficulty of undertaking multiple, accurate measurements of particle surface areas, diameter and convexities. The current situation is that particle/ aggregate shape can be classified and quantified sufficiently accurately (for practical, construction purposed) by Aspect Ratio, Riley Sphericity and Percentage Concavity (True, 2011) - as proposed by Lees (1964). Modern digital imaging and process techniques enable multiple, and sufficiently accurate, measurements to be made of samples of particles within a relatively short space of time and to a constant degree of accuracy. Hence, by using digital imaging, a more precise and informed shape comparison can be made with respect to the influence on particle packing and interparticle voidage.

2.3.2 Effect of aggregate shape and texture on concrete properties

Neville (1995) claimed that aggregate shape and texture have a significant impact on the strength of concrete. This is because the degree of packing of the aggregates, and hence the voids content of the concrete, is dependent on the actual particle shapes as indicated in Figure 2.7.

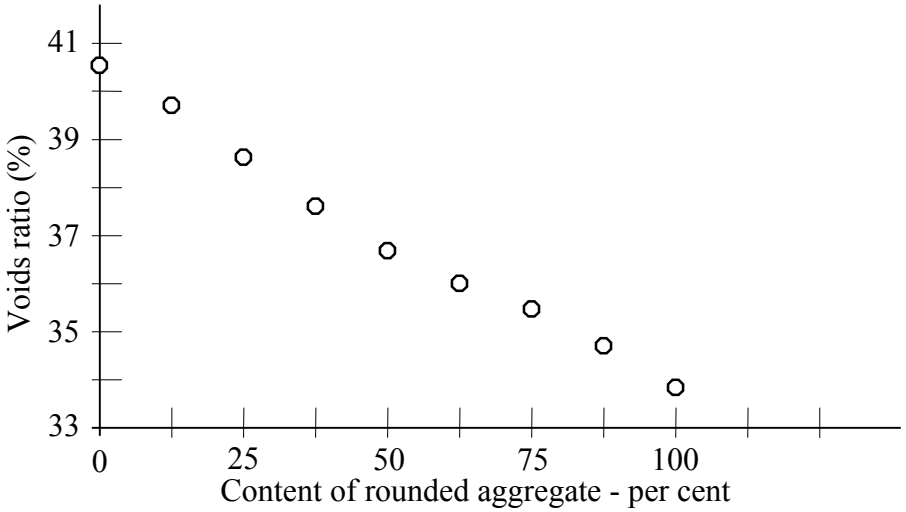

Fig. 2.7 Influence of angularity of aggregate on voids ratio (Neville, 1995)

If an aggregate when compacted has a high voids content then more cement paste is needed to provide the same workability as concrete containing an aggregate that compacts with a low voids content. In general particle angularity increases voids content and well-graded aggregate gives rise to lower voids content than single-size particles. The relative importance of aggregate properties on the strength of concrete was given by Neville (1995) as shown in Table 2.5.

Table 2.5 Average relative importance of the aggregate properties affecting the strength of concrete (Neville, 1995)

Property of concrete	**Relative effect of aggregate properties (%)**		
	Shape	Surface texture	Modulus of elasticity
Flexural strength	31	26	43
Compressive strength	22	44	34

Bonding between the cement paste and the coarse aggregate is an important factor in the strength that a concrete achieves, particularly the bending strength. The bond is due to the interlocking of the aggregate and hydrated cement paste and the surface roughness of the former. Rough surfaces, such as with crushed particles, potentially result in a better mechanical interlock, provided that the cement paste is able to flow into, and occupy, the undulations/ cavities on the surface of a particle.

After undertaking research into the pozzolanic nature of ground glass powders Shao *et al*. (2000) reported that the workability of glass concrete was less (by about 18%) than the conventional concrete. It was stated that the angular shape of the glass particles (Figure 2.8) could be the direct cause of this decrease in workability. However, Shao *et al*. (2000) also stated that only a slightly higher water content was needed to maintain the same concrete consistency.

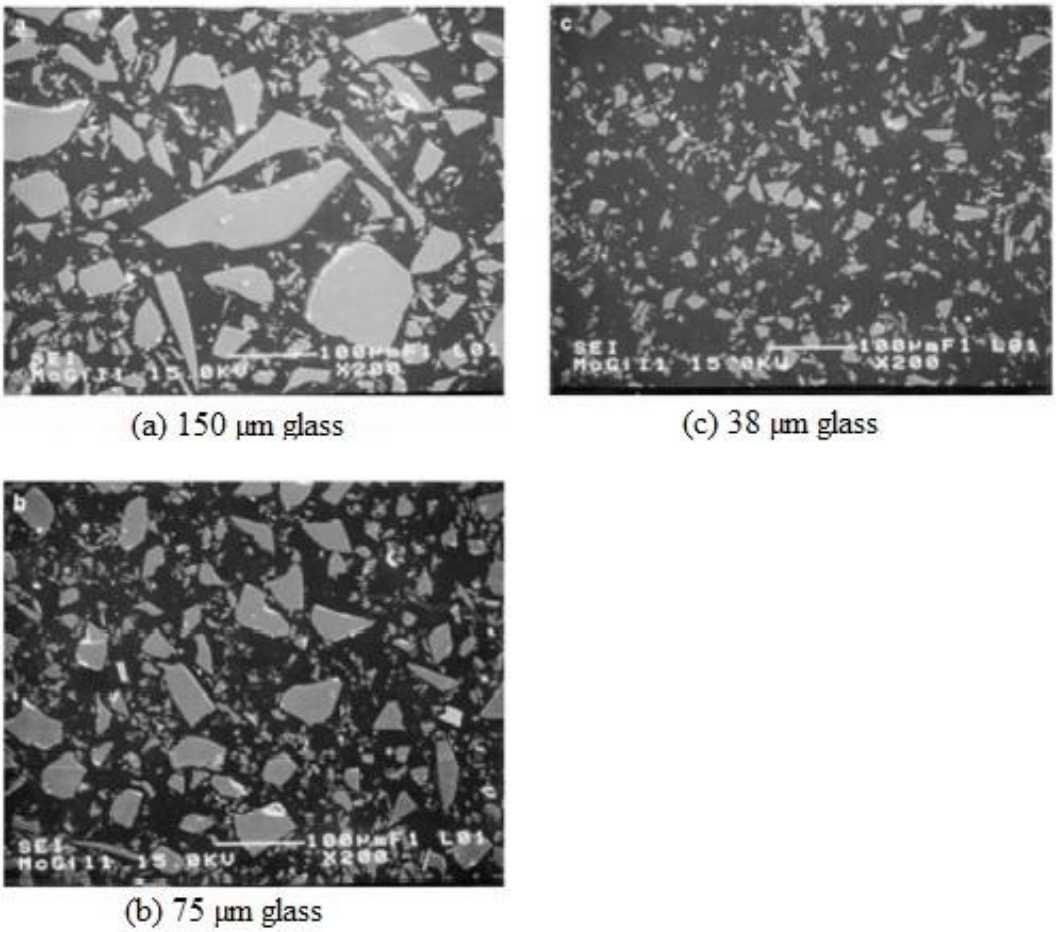

Fig. 2.8 Particle size and shape of ground waste glass (Shao *et al*. 2000)

According to Park *et al*. (2004) the use of crushed glass as aggregate in concrete affected the slump and compaction factor of fresh concrete because of the sharp and angular shape of the glass grains. The prevailing grain shape was claimed to be angular regardless of the colour of the glass. This angularity reduced the fluidity of fresh concrete and there was also a tendency to entrain more air (which affected long-term strength) because the irregular shape of glass aggregate results in a larger relative surface area and entrapment of more air. Similar comments about waste glass grain shape reducing the fluidity and hence slump of fresh concrete were made by Ismail & Al-Hashmi (2009) and Borhan (2012).

As a result of laboratory studies Topcu and Canbaz (2004) concluded that as the amount of waste glass used as aggregate in a concrete increased so did the air content (voids content) as a result of the angular shape of the particles which led to poor compactness. Furthermore, it was stated that there was less bond between cement paste and glass aggregate, as a result of the surface texture of the glass, and there was a corresponding reduction in compressive, tensile and flexural strength. Cassar and Camilleri (2012) made similar comments about the bond between glass aggregate and cement paste and the effect on concrete strength.

Ismail and Al-Hashmi (2009) reported that the slump of waste glass concrete specimens decreased with increase in glass content, although the mixes still had good workability. The reduction in slump was believed to be due to the shape of the waste glass grains.

Liu (2011) also found that when waste glass aggregate was used then the water and superplasticizer contents had to be adjusted. Due to the angular and flaky shape of glass particles concrete mixes required a small increase in water/powder ratio and decrease in superplasticizer dosage with an increase in glass content. Pereira-de-Oliveira *et al.* (2012) stated the ground glass powders consist mainly of elongated and plateshaped particles with a narrow particle size range, as shown in Figure 2.9. Borhan (2012) commented that the sharper edges and harsher texture of glass particles gave rise to more cohesion between the cement paste and the aggregate, which leads to reduced flow of fresh concrete. Lee *et al*. (2013) stated that while natural sand aggregate had a rounded smooth shape fine glass aggregate was generally elongated,

flat and angular, as shown in Figure 2.10. This difference in shape was qualified by Castro and Brito (2013) using a shape index.

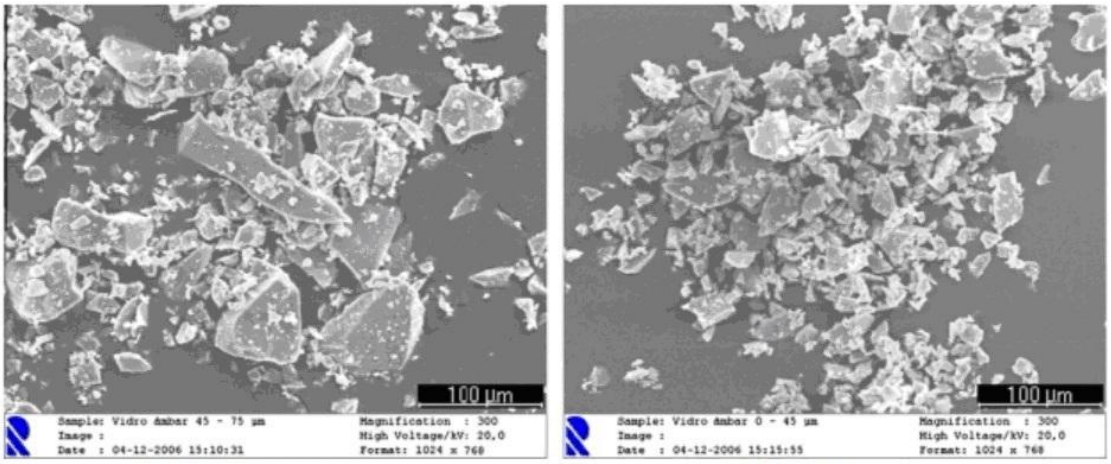

(a) 45–75 µm size (b) 0–45 µm size

Fig. 2.9 Particle size and shape of glass waste after grinding (Pereira-de-Oliveira *et al*. 2012)

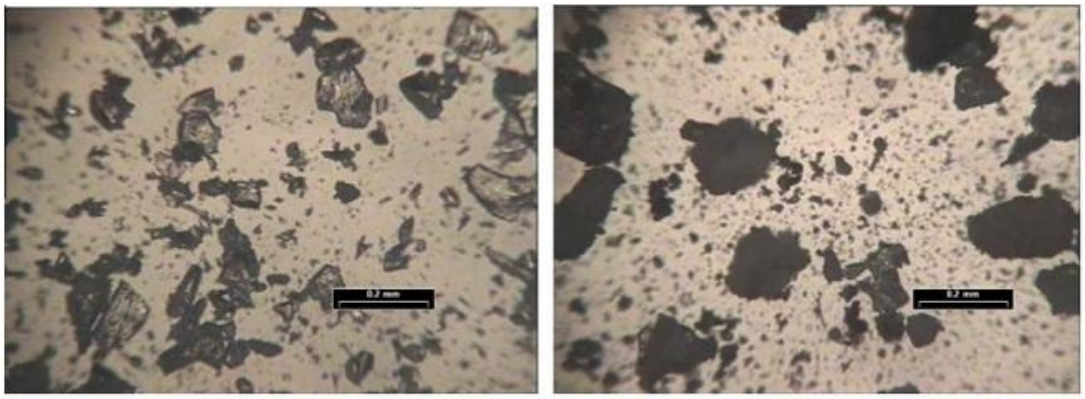

(a) (b)

Fig. 2.10 The shape and surface texture fine glass (a) and sand (b) (Lee *et al*., 2013)

On the other hand CCANZ (2011) found that the shape of crushed glass is a major drawback in using it to replace coarse aggregate in concrete because the glass particles are smooth and elongated. However, the smooth surface texture of the glass aggregate and it being non-absorbent was reported to improve the rheological properties of fresh concrete and workability was not affected. Furthermore the mechanical properties of concrete (compressive strength, flexural strength and splitting strength) actually increased when up to 20% of the fine aggregate was replaced by glass because of the strength and surface texture of the glass particles.

Limbachiya *et al*. (2012) claimed that granulated foam glass (GFG) particles are sharper and have a more angular shape than natural sand which results in less fluidity and less workability in concrete mixes containing fine glass aggregate. However the shape, rough texture of and porosity GFG particles could enhance bonding strength between aggregate and cement matrix leading to higher strength and greater resistance to cracking under tensile stress. Increasing the GFG content in the mixture resulted in a more porous and lightweight concrete material. Therefore, porous foam glass concrete may behave more elastically than natural aggregate concrete and enhance ductility before failure.

Ai *et al*. (2013) stated that aggregate geometric shape has a significant effect on the compressive strength of polyurethane polymer concrete. If an aggregate has a small number of sides its cross-section will contain sharp angles which will cause stress concentrations during loading. Such concentrations will promote the onset of microcraking and lead to a reduction of the compressive strength of the concrete. The images show previously in Figure 2.10 indicate that there is a tendency for fine glass particles to have less sides than sand.

2.4 Conclusions

A number of researchers have investigated the potential for using crushed waste glass as a partial replacement for aggregate (both coarse and fine) in structural concrete. It is apparent that previous research has not shown conclusively whether the use of fine glass aggregate significantly affects the flow characteristics of (slump) of fresh concrete. On balance previous research seems to suggest that some fine aggregate may be replaced by waste glass without any significant detrimental effect on concrete strength. Previous research finding's summary are discussed in Chapter 5.

Previous research on the effect of using waste glass has not been conclusive. To date little work has been done on the effect of particle shape and surface texture of crushed waste glass aggregate on the workability and flow characteristics of fresh concrete and on the strength of hardened concrete. The terms refer to image analysis shape factors from scans processed using ImageJ analysis software. An attempt has been made to relate the effect of shape of fine aggregate natural sand and crushed waste glass on the workability, strength and internal structure of concrete.

CHAPTER 3: MATERIALS AND EXPERIMENTAL METHODS

3.1 Methodology

The research work was undertaken with the overarching aim of contributing to the current state of knowledge about the effects of replacing fine aggregate (sand) in structural concrete with crushed waste glass. It is hoped that the results of the work promote the used of waste glass by the construction industry to create a hybrid structural material ('glascrete') and thereby reduce the industry's current rate of consumption of primary aggregates. However, a concern for industrial usage of 'glascrete' is that the introduction of crushed glass within a structural concrete mix has the potential to promote Alkali Silica Reaction (ASR), which is characterised by abnormal volume increase of the concrete, with detrimental consequences. Previous research on the effect of using waste glass has not been conclusive but it is generally agreed that using fine particles of waste glass in concrete is less likely to create significant ASR reaction than the use of glass as coarse aggregate. Because concrete is not a 'single component or hypothetical material', and because of inherent variation in its components and the desire to make the research relevant to industry, experimentation was considered the appropriate research methodology.

3.1.1 Testing programme

The suitability of a structural concrete obviously depends on it achieving an acceptable compressive strength after a specified curing period. However, it is also vital that when the concrete is in a freshly mixed state (before any setting or hardening occurs) it is workable and stable (Neville, 1995). This initial state affects the ability to transport and pump the concrete (without segregation) and for it to flow to occupy a chosen space and be compacted to give the desired final shape (so bleeding should be minimal when the wet concrete is left to stand). It was intended that, as far as possible, experimentation would be undertaken using standard industrial tests and procedures so that the outcomes would be directly relevant to the needs of industry.

For a particular source of ready-mixed concrete the natural sand aggregate will be from a specific source, which ensures a high degree of consistency of particle shape,

surface texture, aggregate grading and hence concrete properties. Hence, it was desired that waste glass would be crushed and graded to match the particle size distribution of a natural sand provided by a commercial supplier-identifier supplier and source. At the start of the programme, a sufficiently large batch of sand was obtained for the manufacture of all cubes to eliminate variations due to use of different sources and production methods.

Clear (Flint) glass has been chosen as the 'standard' waste glass because it is the most common waste glass. However, it is known that other colours of glass exhibit different amounts of ASR within concrete and so concrete made with green and brown waste glasses was also investigated. Consideration was given to whether the negative effects from ASR could be minimised by combining different proportions of coloured glasses in the fine aggregate for concrete.

A variety of mixes were prepared to find out the effects of different percentages of sand replacement and colour of waste glass. The main characteristics investigated were workability and compressive strength. Physical properties, such as density and specific gravity, were also determined for the various concrete mixes. At the same time Ultrasonic Pulse Velocity was used to test and qualitatively assess the homogeneity and integrity of the different concretes.

Research work to date does not show a clear consensus on how the magnitude of any effects of using glass as aggregate in concrete relates to the amount of glass present. Hence, within the research project concretes were produced which had 0, 25, 50 and 100%, by weight, of the conventional fine aggregate replaced by crushed, waste glass. Furthermore, the compressive strength of concrete is dependant on its curing time. Hence, time-dependent hardening was studied over one year by testing of cubes at 7 days, 28 days (the normal testing time), 112 days and 365 days.
An attempt was made to measure the change in the dimensions of concrete cubes with time. Measurements were made on all faces of the cubes to assess distortional changes, preferred direction for changes, non-uniform changes, and overall volume change. The dimensional changes were expected to be small (even if significant ASR occurs), of the order of 0.001 strain, if the concrete containing glass aggregate was to comply with British Standard requirements and appropriate measurement systems

were selected. Concrete bars were also made and tested in accordance with the relevant British Standard. For these bars only changes in the length of the bars were measured.

The overall system of referencing test specimens is outlined in Table 3.1

Table 3.1 Code and sample number for tests

Mix code	Glass (%)	Colour of glass	Age (days)	Test number
Slump and Flow				
0N0	0	N/A	0	6
25F0	25	Flint	0	6
50F0	50	Flint	0	6
100F0	100	Flint	0	6
25A0	25	Amber	0	6
50A0	50	Amber	0	6
100A0	100	Amber	0	6
25G0	25	Green	0	6
50G0	50	Green	0	6
100G0	100	Green	0	6
25W0	25	Washed mixed	0	6
50W0	50	Washed mixed	0	6
100W0	100	Washed mixed	0	6
25U0	25	Unwashed mixed	0	6
50U0	50	Unwashed mixed	0	6
100U0	100	Unwashed mixed	0	6
			Sub-total	96
Setting times				
0N0a	0	N/A	0	3
25W0a	25	Washed mixed	0	3
50W0a	50	Washed mixed	0	3
100W0a	100	Washed mixed	0	3
25U0a	25	Unwashed mixed	0	3
50U0a	50	Unwashed mixed	0	3
100U0a	100	Unwashed mixed	0	3
			Sub-total	21
Density, UPV, Compression strength and Volumetric strain measurements				
0N(7-365)	0	N/A	7,28,112&	12
25F(7-365)	25	Flint	365	12
50F(7-365)	50	Flint		12
100F(7-365)	100	Flint		12
25A(7-365)	25	Amber		12
50A(7-365)	50	Amber		12
100A(7-365)	100	Amber		12
25G(7-365)	25	Green		12
50G(7-365)	50	Green		12
100G(7-365)	100	Green		12
25W(7-365)	25	Washed mixed		12
50W(7-365)	50	Washed mixed		12
100W(7-365)	100	Washed mixed		12
25U(7-365)	25	Unwashed mixed		12
50U(7-365)	50	Unwashed mixed		12
100U(7-365)	100	Unwashed mixed		12
			Sub-total	192

Table 3.1 (Cont'd) Code and sample number for tests

Mix code	Glass (%)	Colour of glass	Age (days)	Test number
Water absorption by Immersion and Capillary rise				
0N-absorp	0	N/A		6
25F-absorp	25	Flint		6
50F-absorp	50	Flint		6
100F-absorp	100	Flint		6
25A-absorp	25	Amber		6
50A-absorp	50	Amber		6
100A-absorp	100	Amber		6
25G-absorp	25	Green		6
50G-absorp	50	Green		6
100G-absorp	100	Green		6
25W-absorp	25	Washed mixed		6
50W-absorp	50	Washed mixed		6
100W-absorp	100	Washed mixed		6
25U-absorp	25	Unwashed mixed		6
50U-absorp	50	Unwashed mixed		6
100U-absorp	100	Unwashed mixed		6
			Sub-total	96
ASR (axial strain measurements)				
0N-ASR	0	N/A	7,14,28,56,	3
25F-ASR	25	Flint	112,252 &	3
50F-ASR	50	Flint	365	3
100F-ASR	100	Flint		3
25A-ASR	25	Amber		3
50A-ASR	50	Amber		3
100A-ASR	100	Amber		3
25G-ASR	25	Green		3
50G-ASR	50	Green		3
100G-ASR	100	Green		3
25W-ASR	25	Washed mixed		3
50W-ASR	50	Washed mixed		3
100W-ASR	100	Washed mixed		3
25U-ASR	25	Unwashed mixed		3
50U-ASR	50	Unwashed mixed		3
100U-ASR	100	Unwashed mixed		3
			Sub-total	48
Particle shape and surface texture of fine aggregate				
Natural sand		N/A		50
Crushed glass		Flint		50
Crushed glass		Amber		50
Crushed glass		Green		50
			Sub-total	200

3.1.2 Relevance to industrial practice

Fine aggregate particle sizes

Conventional specifications for the fine aggregate which can be used in structural concrete permit a wide range of particle sizes and grading curves as shown in Figure

3.1. A commercially-available sand was chosen and preliminary experiments showed that glass could be crushed to give the same particle sizes as the sand used.

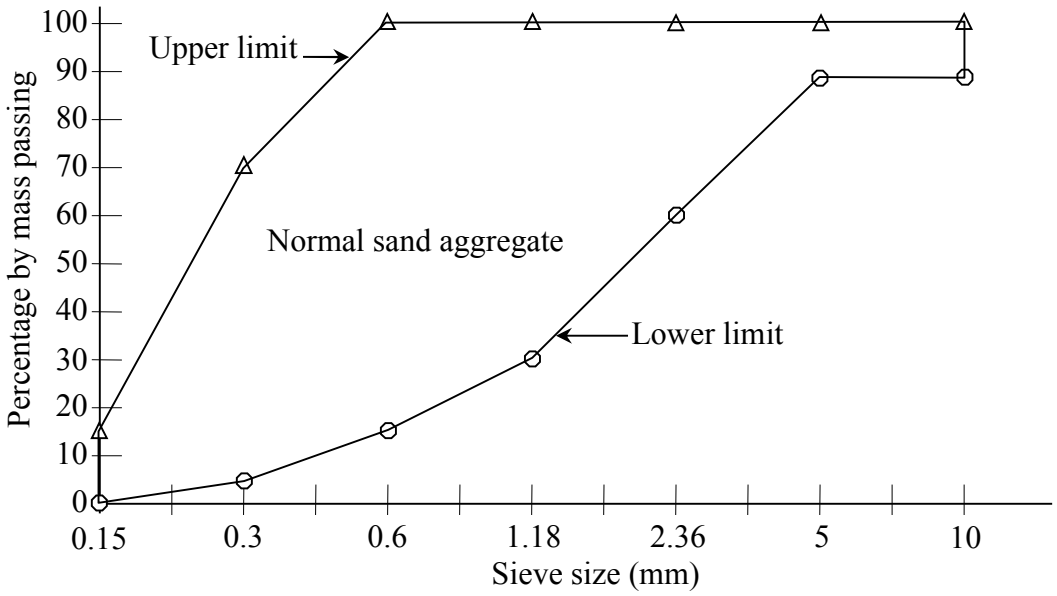

Fig. 3.1 Grading limits for fine aggregate (sand)
(BS882: 1992)

Fresh concrete

In the UK there are well-established tests for categorisation of fresh concrete properties in term of workability or consistency i.e. slump test and flow table. The slump test (BS EN 12350-2:2009) is used extensively in site work all over the world for assessing concrete of normal consistency i.e. with a slump of 10mm to 210mm (BSI, 2009). The test is very useful in detecting variations in the uniformity of a mix of given nominal proportions and is described by ASTM C143-90a and BS 1881: Part 102: 1983 (BSI, 1983) in European classification of ENV 206:1992. The slump test does not strictly measure the workability of concrete and it may be better considered as a measure of consistency in line with document ACI 116R-90 (American Concrete Institute). The flow table test is sensitive to changes in the consistency of concrete, which correspond to flow values between 340mm and 600mm (BSI, 2009). The flow test was developed in Germany (BS EN 12350-5:2000) but it is used in many European countries. The Flow test is covered by BS 1881 (Part 105:1984) and has become more widely used in the UK in recent years as it is appropriate for concrete of

high and very high workability, including self-compacting concrete, which would exhibit a collapsed slump.

Compression strength, UPV and concrete mix

It is normal practice when specifying the compressive strength of a concrete to state a particular curing duration and this is commonly 28 days. However, sometimes a rapid gain of strength of the concrete is needed and so the strength after 7 or 14 days is sometimes specified to enable early removal of formwork on site. On the other hand, concrete is known to continue to gain strength after 28 days (and this provides an enhancement of structural stability or an implicit, additional safety factor). To cover the various aspects of the time-dependant nature of compressive strength it was decided to conduct tests on cubes with curing ages from 7 days to one year.

The concrete mix to be used was selected as 1:2:4 because this is a common structural concrete mix in terms of cement, fine aggregate and coarse aggregate. Other possible mixes such as 1:1:2 (considered the best quality mixture) and 1:3:6 (low quality mixture mostly used for concrete filling) were considered but 1:2:4 was selected became of its widespread use (Buzzle, 2010).

The compressive strength of concrete is obtained from test on cubes (with size either 100mm or 150mm cubes) or cylinders (150mm diameter × 300mm long). Cubes are made on site and are the normally used in the United Kingdom and most European countries, cylinders are used in the United States of America (Murdock, 1991). It is difficult to say which type of specimen, cylinder or cube, is better (Neville, 1995). The strengths of cubes and cylinders made from the same concrete differ from one another because of the restraining effect of loading (Neville, 1995). Cylinders are weaker than cubes (Reynolds *et al*. 2007). According to expressions converting the strength of cores into the strength of equivalent cubes in (BS 1881: Part 120: 1983), the strength of a cylindrical sample is equal to 0.8 of the strength of a cube. European standard ENV 206:1992 recognises the use of both cylinders and cubes (Neville, 1995).

The velocity of an ultrasonic pulse travelling through concrete is influenced by the properties of concrete, e.g. its elastic stiffness and mechanical strength, and hence the

state of the concrete. Voids due to poor compaction or damaged concrete cause a reduction in pulse velocity time (IAEA, 2002). Ultrasonic Pulse Velocity measurements of concrete structures may thus be used for quality control purposes in conjunction with mechanical tests on control samples such as cubes or cylinders. There is no unique relation between ultrasonic pulse velocity and compressive strength, however Figure 3.2 contains indicative data for hardened cement paste, mortar, and concrete.

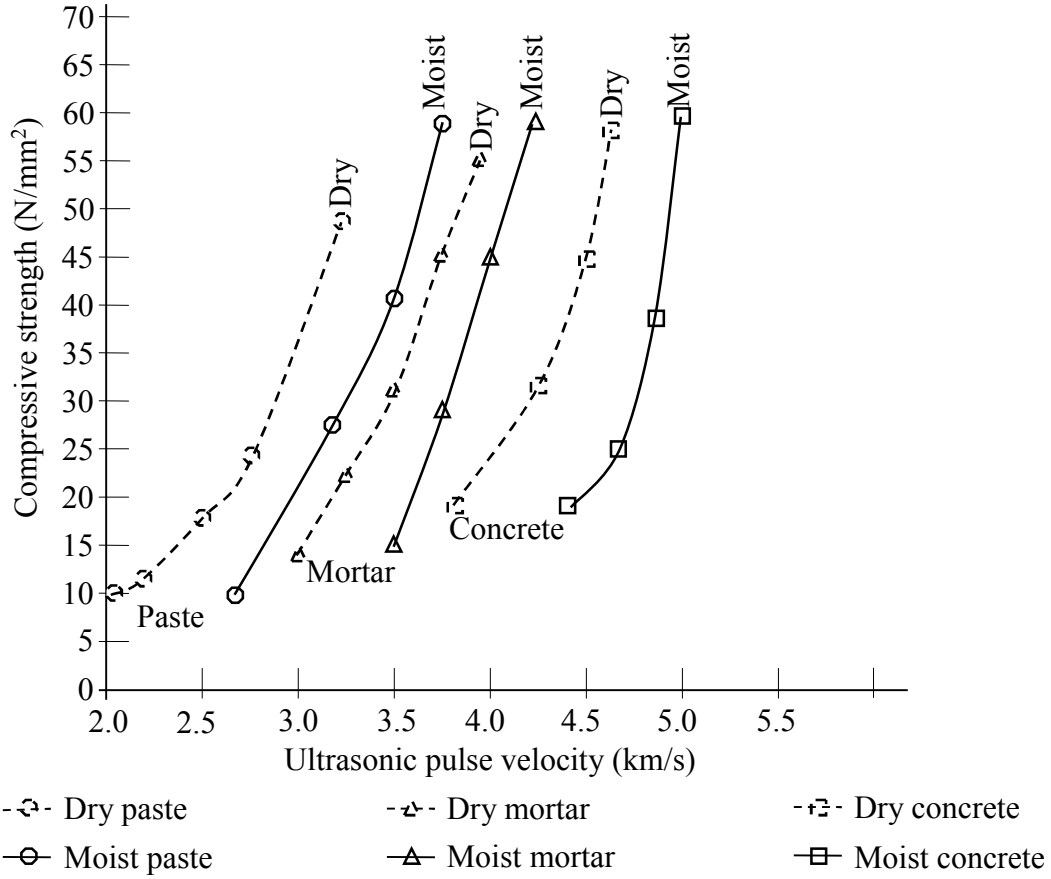

Fig. 3.2 Relation between compressive strength and ultrasonic pulse velocity (Neville, 1995)

Table 3.2 shows the classification of the quality of concrete in terms of ultrasonic pulse velocity ranging between 2 and 4.5 km/s. A number of factors, including age, curing conditions, moisture condition, mix proportions, type of aggregate and type of cement, affect the relationship between ultrasonic pulse velocity and strength. If an estimate of strength is required it is necessary to establish a correlation between strength and velocity for the particular type of concrete under investigation (IAEA, 2002). An UPV value of more than 4.5 km/s is indicative of an excellent quality of

concrete because it has less voids and is more solid with highest strength. However a UPV value of less that 2 km/s indicates that the quality of concrete is very poor because it is cracked, damaged, has high voids content, etc.

Table 3.2 Classification of the quality of concrete on the basis of pulse velocity (IAEA, 2002)

Longitudinal pulse velocity (km/s)	Quality of concrete
> 4.5	Excellent
3.5 – 4.5	Good
3.0 – 3.5	Doubtful
2.0 – 3.0	Poor
< 2.0	Very poor

Figure 3.3 shows the typical gain in strength with time for conventional concrete. It is likely that there will be significant gain of strength beyond 28 days. However, in BS 8110-1 no increase in strength beyond 28 days is permitted in satisfying limit state requirements. A smaller increase in strength will occur with small structural members that are exposed to a dry environment after initial curing.

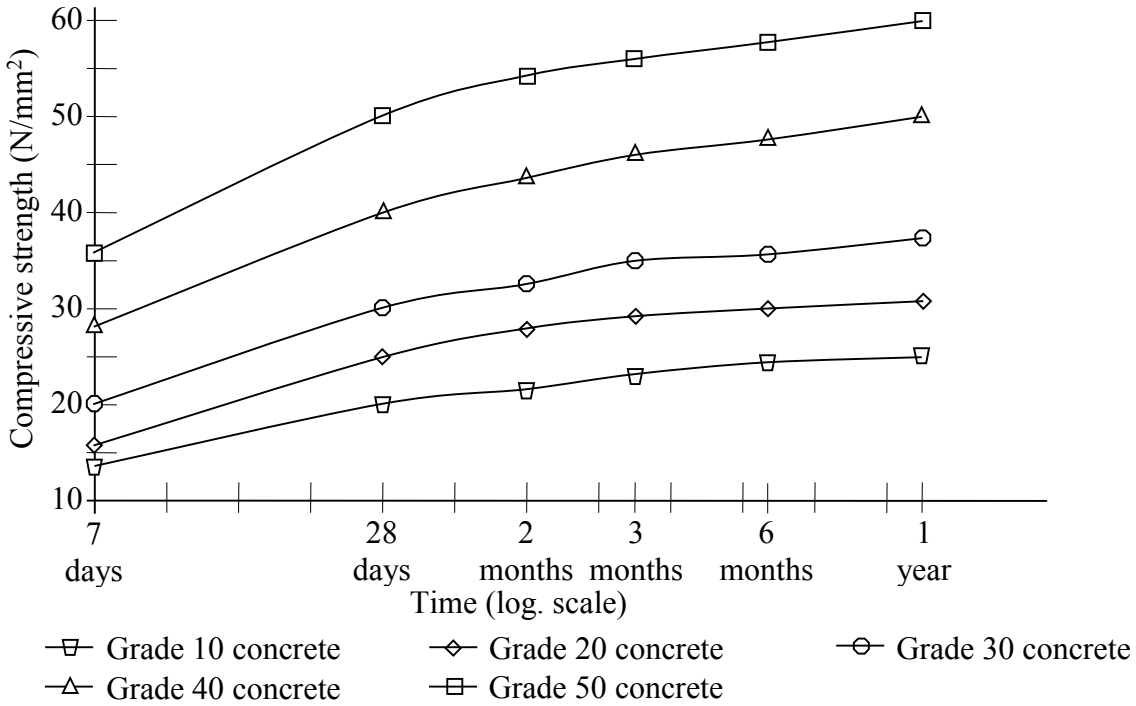

Fig. 3.3 Increase of compressive strength with time (BS 8110-2:1985)

Table 3.3 contains indicative data on suitable water: cement ratios. Table 3.4 shows the consistency of fresh concrete required (according to BS EN 12350-5:2009) for it to be suitable for handling and placing so that after compaction the concrete surrounds all reinforcement and completely fills formwork. Kerb and block works have low water cement ratio (classes S1 or F1), trench fill and in-situ piling have a high water cement ratio (classes S4 or F4). For structural concrete class S3 or F3 is required. Water-cement ratio affects workability and concrete durability. For environments in which reinforced concrete is subjected to mild or moderate exposure during its working life BS 1881-128 (1997) suggests that a water-cement ratio of 0.6 would be appropriate for concrete made with normal weight aggregates of 20 mm nominal maximum size. Hence a water: cement ratio of 0.6 was chosen for this research as it represented a value commonly used in practice for structural concrete.

Table 3.3 Guidance on mix design limits for durability of concrete made with normal weight aggregates of 20 mm nominal maximum size (BS EN 12350-5:2009)

Condition of exposure	**Type of concrete**	**Maximum free w/c ratio**
Mild	Unreinforced non-structural	—
	Unreinforced structural	0.80
	Reinforced	0.65
	Prestressed	0.60
Moderate	Unreinforced non-structural	—
	Unreinforced structural	0.65
	Reinforced and prestressed	0.60
Severe	Unreinforced	0.60
	Reinforced and prestressed	0.55
Very severe	All	0.55
Most severe	Unreinforced	0.50
	Reinforced and prestressed	0.45

Table 3.4 Consistency requirements for different uses of in-situ concrete (BSI 8500-1, 2006)

Use of concrete	Form of compaction	Consistency class		
		Normal weight concrete	Slump test req. (mm)	Flow test req. (mm)
Floors and hand placed pavements	Poker or beam vibration	S2, F2	40-110	330-440
Strip footings	Poker or beam vibration and/or tamping	S3, F3	90-170	400-510
Mass concrete foundations		S3, F3	90-170	400-510
Blinding		S3, F3	90-170	400-510
Normal reinforced concrete in slabs, beams, walls and columns		S3, F3	90-170	400-510
Pumped concrete		S3, F3	90-170	400-510
Sliding formwork construction		S2, F2	40-110	330-440

Guidance on shrinkage and expansiveness

The actual shrinkage of concrete in structures is dependent upon the moisture environment, thickness of the concrete section and its age. Figure 3.4 provides guidance on shrinkage factor as a function of effective thickness for a uniform section. The shrinkage of plain concrete is primarily dependent on the relative humidity of the air surrounding the concrete, the surface area from which moisture can be lost relative to the volume of concrete and on the mix proportions. BS812: Part 120 contains guidance on shrinkage as indicated in Table 3.5. There is no shrinkage restriction on concrete which never dries out and where and resultant cracking and other movements are of minor importance.

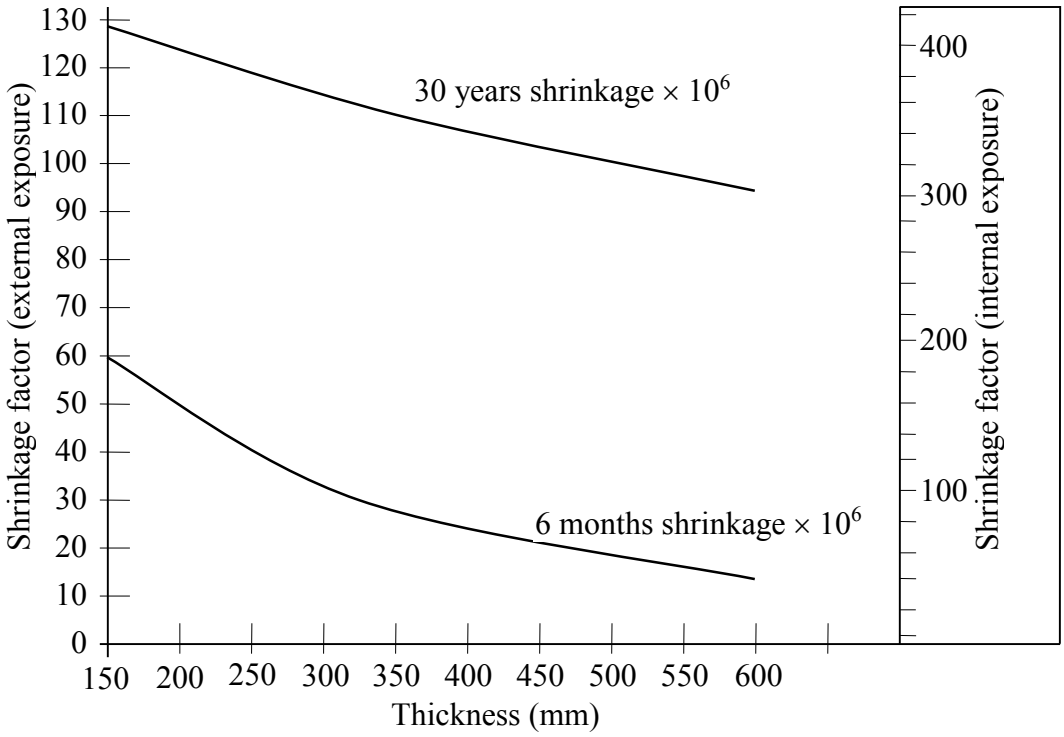

Fig. 3.4 Shrinkage coefficients (Reynolds *et al*. 2007)

Table 3.5 Shrinkage limits (BSI 812-120, 1989)

Category A	Shrinkage not exceeding 0.075% - acceptable for all concreting purposes
Category B	Shrinkage exceeding 0.075% - permissible for positions where complete drying never occurs, mass concrete surfaced with air entrained concrete, and for members symmetrically and heavily reinforced not exposed to the weather.

Table 3.6 contains guidance on the expansiveness of low and normal reactivity aggregates (as recommended by BSI Working Group B/502/6/10). If a low reactivity aggregate is combined with a more reactive type, and there is no information to suggest otherwise, reactivity of the combination is classified on the basis of the higher reactivity aggregate. For example, if a low reactivity aggregate is combined with a normally reactive one, the combination is assumed to be normally reactive.

Table 3.6 Aggregate reactivity based on concrete prism test (BRE, 2004a)

Expan-sion for up to 12 months (%)	Classifica-tion for the aggregate combinati on tested	Aggre-gate type	Notes	Some examples from UK sources
>0.20	Expansive	Normal reactivity	Exhibited by combinations known to have been involved in cases of actual damage to concrete	Chert and flint-bearing sand with non-reactive, low porosity coarse aggregates
0.10 to ≤0.20	Possibly expansive	Normal reactivity	Includes combinations which have sometimes been involved in cases of actual damage to concrete structures, but also includes some widely used combinations with no record of causing damage to concrete	Quartzitic gravels and sands from the English Midlands and some crushed rock containing microcrystalline quartz
>0.05 to ≤0.10	Probably non-expansive	Low reactivity	Combinations in this range have rarely been associated with actual cases of damage to concrete structures. However, these might be considered unsuitable in extreme conditions	Some of the quartzitic gravel sands from the English Midlands
≤0.05	Non-expansive	Low reactivity	Combinations which have no record of causing damage to concrete	Crushed limestone and igneous rock aggregates; chert and flint bearing coarse/fine combinations with > 60% chert and flint contents

3.2. Materials used in the research

3.2.1 Cement

Type 1 ordinary Portland cement was used in this study and was supplied by Castle Cement UK Ltd. All of the cement was obtained at the start of the research as a batch of 3 'identical' 25kg bags to reduce 'natural' variability of the material. The cement was primarily composed of silicon, aluminium, iron and calcium oxides. The chemical and physical properties of the cement were provided by the cement manufacture and are given in Tables 3.7 and 3.8, respectively.

Table 3.7 Chemical composition of Portland cement (from Castle Cement UK)

Chemical composition	Castle cement %	Usual limits % (Neville, 1995)	BS 12: 1996
Silicon oxide, SiO_2	19.81	17-25	20.2
Aluminium oxide, Al_2O_3	6.01	3-8	5.4
Iron oxide, Fe_2O_3	2.58	0.5-6.0	2.6
Calcium oxide, CaO	64.83	60-67	64.5
Magnesium oxide, MgO	1.04	0.5-4.0	1.6
Sulphur trioxide, SO_3	3.26	2.0-3.5	2.8
Sodium oxide, Na_2O	0.18		
Potassium oxide, K_2O	0.91	0.3-1.2	
Chloride, Cl	0.016		

Table 3.8 Physical properties of Portland cement (from Castle Cement UK)

Physical properties	Castle cement	Tarmac	Hanson	Cemex
Specific surface:	331 m^2/kg	430 m^2/kg		400 m^2/kg
Average particle size	5-30 µm	Fine powder	5-30 µm	5-30 µm
Coarse particles	(>45 µm):11.2%			
Specific gravity	3.14	3.12	2.75-3.2	2.8-3.2
Loss on ignition	0.92%			
Colour	steel grey	white to grey	grey/ white	
Melting/ decomposition point		> 1600°C	> 1250°C	

3.2.2 Coarse aggregate

Twenty millimetre maximum size river gravel supplied by Salop Sand & Gravel Supply Co Ltd was used as natural coarse aggregates. Table 3.9 indicates the chemical composition of these aggregates, which had a specific gravity of 2.62 and water absorption of 0.87%. The particle size distribution is shown in Figure 3.5 and it can be seen that the coarse aggregate fits within the middle of the range permitted by BS882:1992 (Specification for aggregates from natural sources for concrete). Figure 3.6 contains an image of typical coarse aggregate, which can be described as a mixture of sub-angular and sub-rounded particles (as defined by Russell and Taylor (1937) Section 2.3.1), or as irregular (BS 812, Section 2.3.1). Figure 3.7 illustrates the surface texture (lightly pitted) of the coarse aggregate.

Table 3.9 Chemical composition of coarse aggregate
(as supplied by Salop Sand & Gravel Supply Co Ltd)

Properties	**Percentage (%)**
Silicon, (SiO_2)	92.560
Titanium, (TiO_2)	0.200
Aluminium, (Al_2O_3)	2.880
Iron, (Fe)	0.990
Lime, (CaO)	0.150
Magnesium, (MgO)	0.310
Potassium, (K_2O)	0.780
Phosphorus, (P)	0.011
Phosphorus Pentoxide, (P_2O_5)	0.025
Manganese, (Mn)	0.018
Manganese oxide, (MnO)	0.023
Sulphur, (S)	0.013
Vanadium, (V_2O_5)	0.002

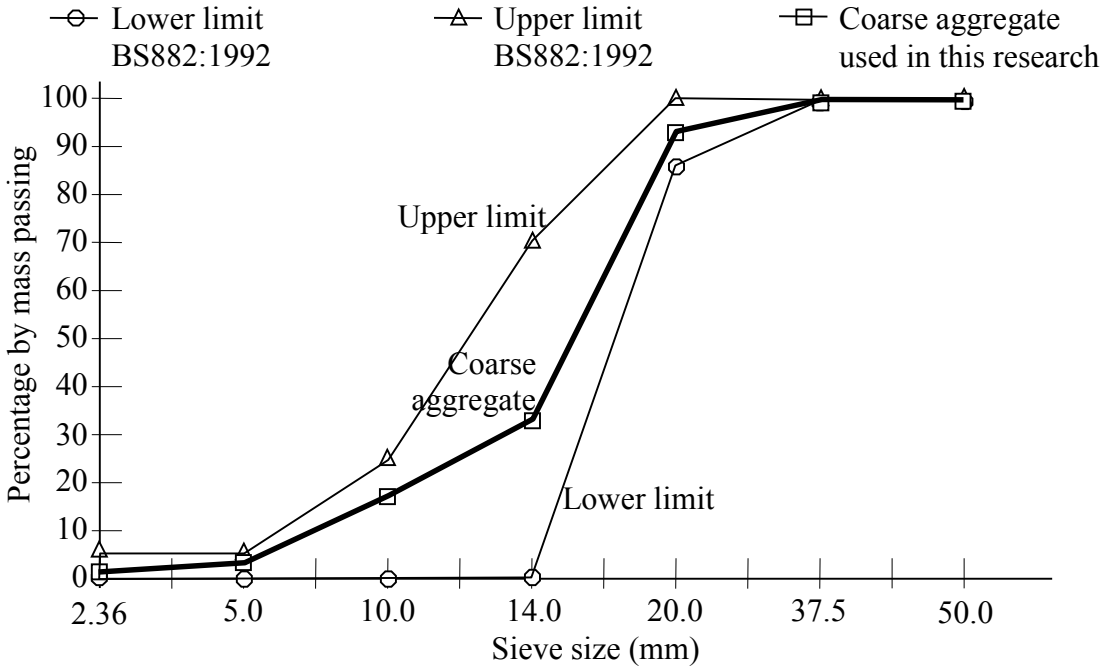

Fig. 3.5 Coarse aggregate grading curve

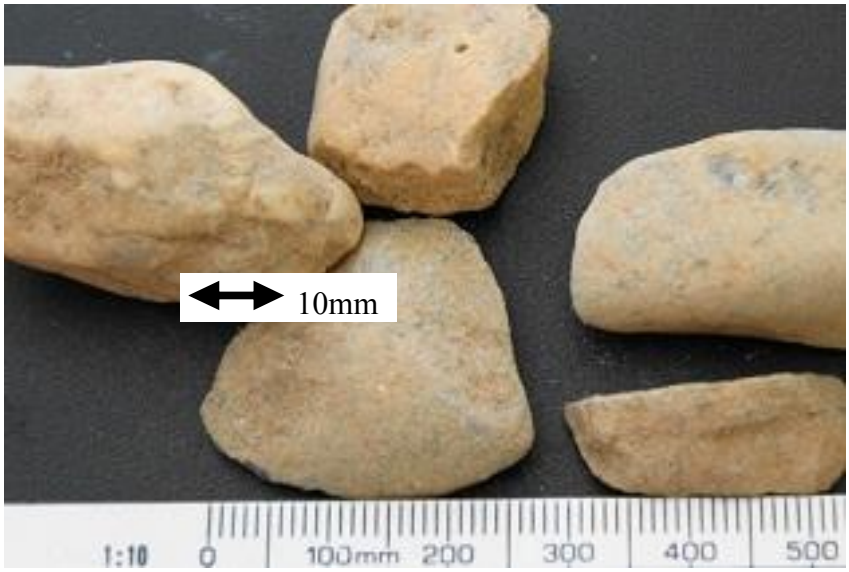

Fig. 3.6 Coarse aggregate shape

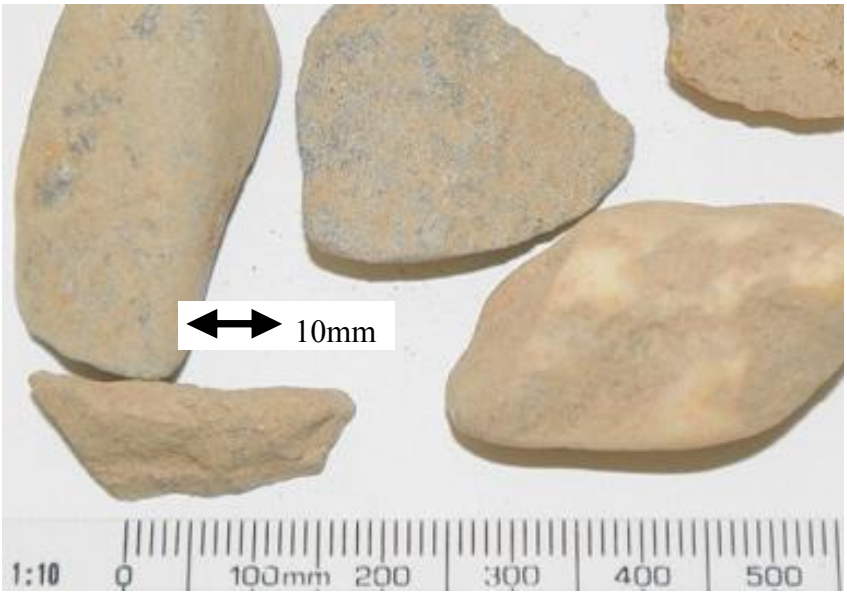

Fig. 3.7 Coarse aggregate surface texture

3.2.3 Fine aggregate

The conventional natural fine aggregate was a sand obtained from Barton quarry, which is located at Barton-under-Needwood (Staffordshire) and was supplied by Hanson Aggregate Ltd. Details of the chemical composition of the fine aggregate are given in Table 3.10 and Figure 3.8 contains the particle distribution curve for the sand which can be seen to lie within the middle of the permitted range.

Table 3.10 Chemical composition of fine aggregate
(as provided by Hanson Aggregate Ltd)

Properties	Percentage (%)
Silicon, (SiO_2)	93.120
Titanium, (TiO_2)	0.130
Aluminium, (Al_2O_3)	2.280
Iron, (Fe)	1.280
Lime, (CaO)	0.130
Magnesium, (MgO)	0.240
Potassium, (K_2O)	0.840
Phosphorus, (P)	0.013
Phosphorus Pentoxide, (P_2O_5)	0.030
Manganese, (Mn)	0.024
Manganese oxide, (MnO)	0.031
Sulphur, (S)	0.010
Vanadium, (V_2O_5)	0.001

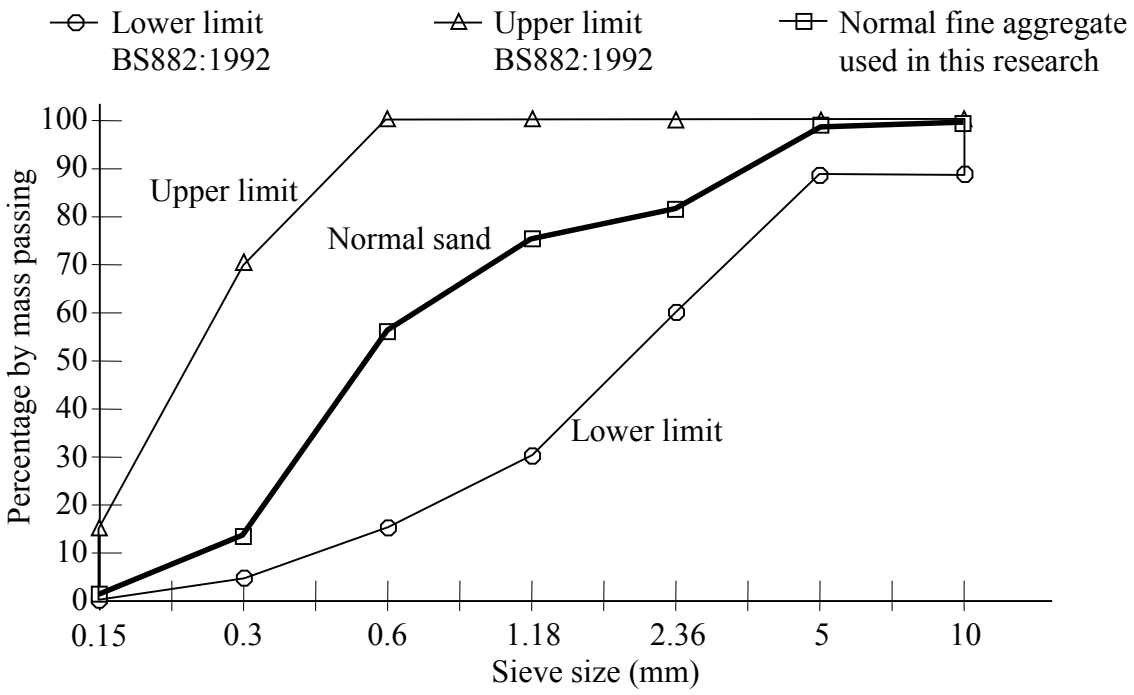

Fig. 3.8 Normal fine aggregate (sand) grading curve

Figure 3.9 contains an image of the conventional fine aggregate (sand) from which it can be seen that the individual particles could be described as sub-angular (Russell and Taylor, 1937) or angular (BS 812). Figure 3.10 illustrates that the surface texture of the sand was fairly rough.

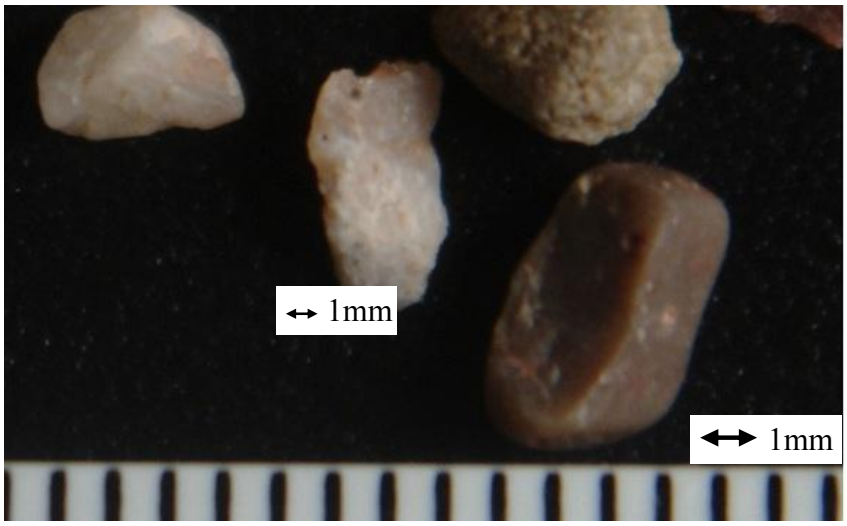

Fig. 3.9 Conventional fine aggregate shape

Fig. 3.10 Conventional fine aggregate surface texture

3.2.4 Waste glass

Flint waste glass was collected from the Millennium Restaurant at the University of Wolverhampton. All of the bottles were from the same manufacturer and were previously used to hold mineral water which was free of alcohol and sugar.

Amber colour glass was collected personally and comprised bottles from one manufacturer and all had contained beer, i.e. the inside of the bottles could be coated with alcohol or sugar.

Green colour glass was collected from a recycling centre. The green bottles were not from one individual source or manufacturer and had held different liquids, primarily mineral water, beer, or wine. The typical chemical compositions of different colours of glass bottle are given in Table 3.11. Figure 3.11 presents the particle grading of the different crushed waste glass used in this research.

Table 3.11 Typical chemical composition of waste glass fine aggregate (as provided by Viridor Resource Management Ltd)

Oxide	**Flint glass**	**Amber glass**	**Green glass**
Silica, (SiO_2)	72.720	72.210	71.880
Sodium, (Na_2O)	12.930	13.750	13.040
Potassium, (K_2O)	0.530	0.200	0.690
Magnesium, (MgO)	1.230	0.460	1.330
Calcium, (CaO)	10.720	11.570	10.590
Barium, (BaO)	0.044	0.020	0.045
Aluminium, (Al_2O_3)	1.460	1.370	1.730
Titnium, (TiO_2)	0.076	0.041	0.339
Iron, (Fe_2O_3)	0.067	0.255	0.294
Chromium, (Cr_2O_3)	0.003	0.129	0.139
Sulphur, (SO_3)	0.166	0.069	0.048

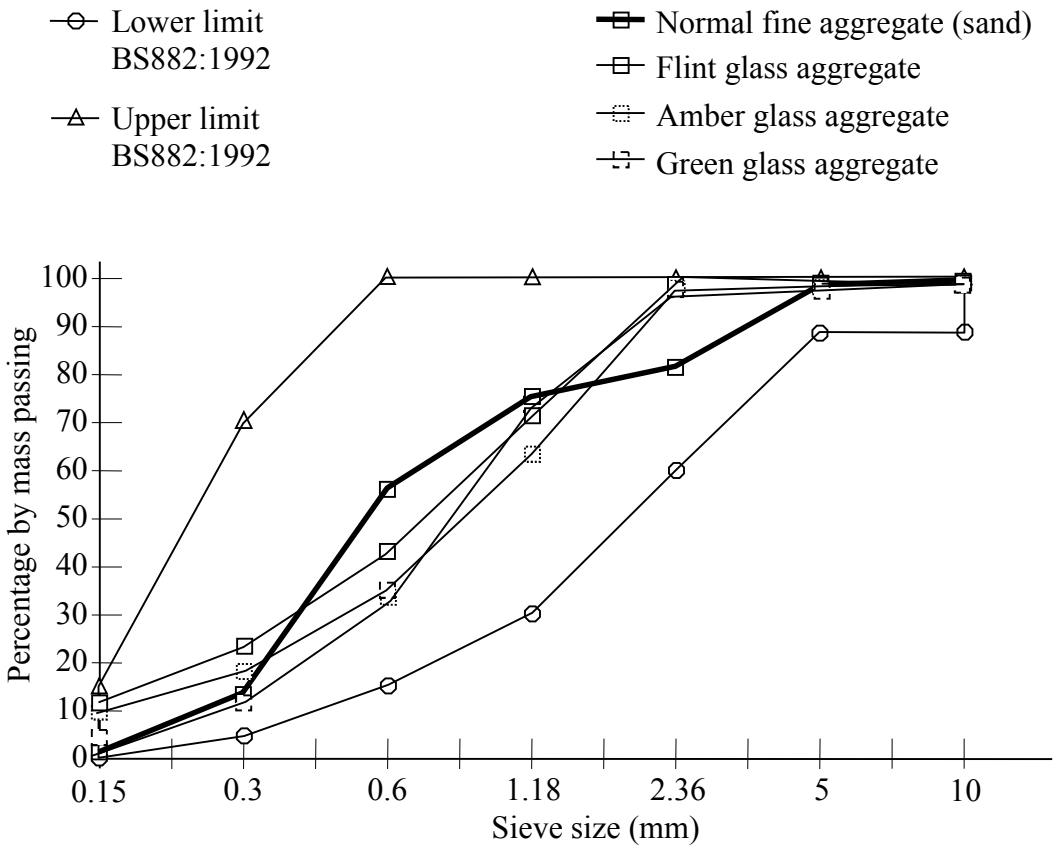

Fig. 3.11 Grading curves for crushed waste glass used as fine aggregate

Photographs of the glass particles used as replacement for the sand in conventional concrete are included in Figures 3.12 to 3.17, inclusive. These photographs show that the glass aggregates can be classed as sub-angular (compare with the photographs and classification given by Russell and Taylor (1937) – Table 2.2) or angular (BS 812 - Figure 2.6). Comparison of Figures 3.12, 3.14 and 3.16 with Figure 3.9 shows that the glass aggregates had slightly different shape to the conventional sand that they replaced, i.e. sharper less-rounded edges, more faces, generally smoother faces (but with striations/ grooves on broken surfaces).

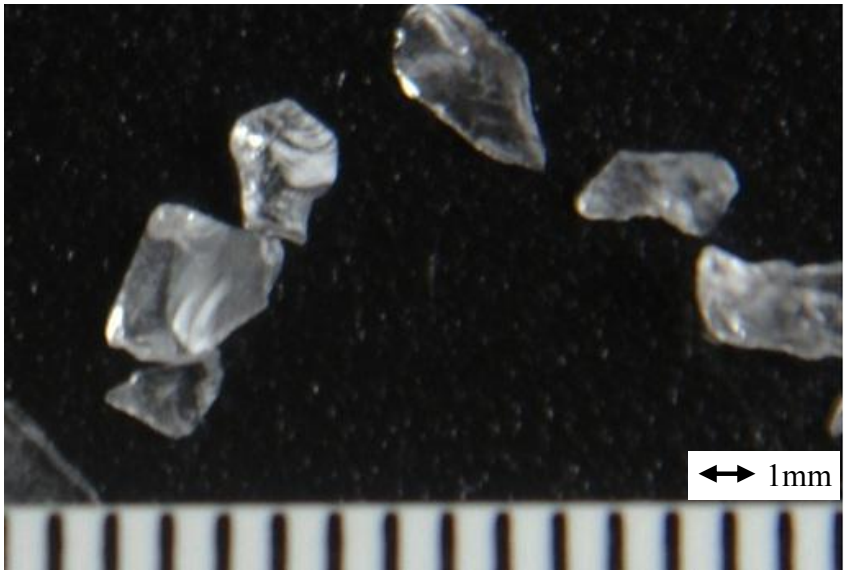

Fig. 3.12 Flint glass aggregate shape

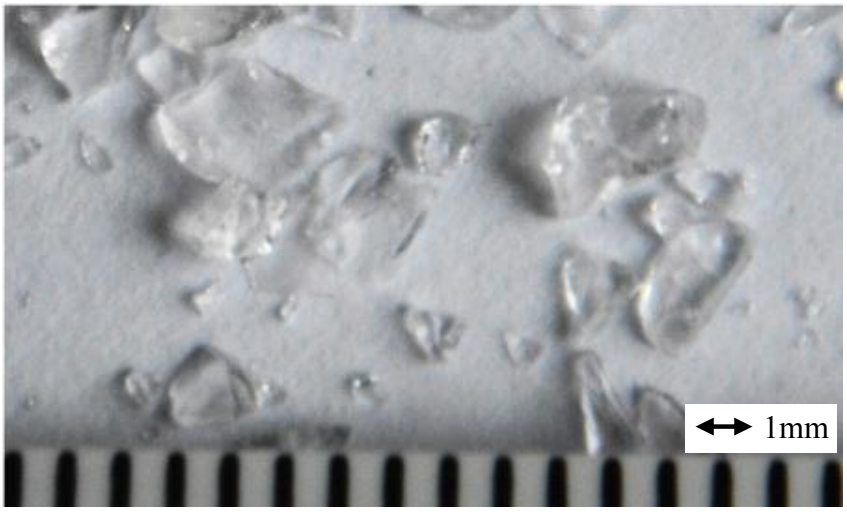

Fig. 3.13 Flint glass aggregate surface texture

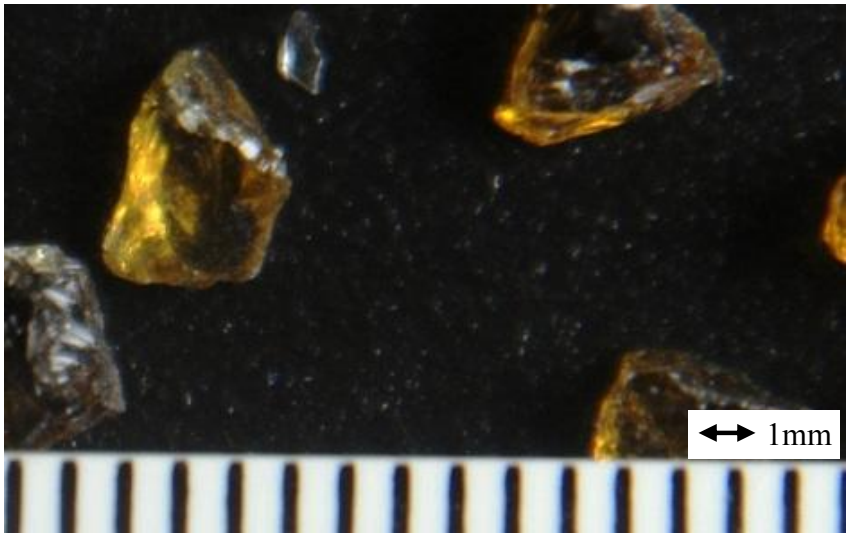

Fig. 3.14 Amber glass aggregate shape

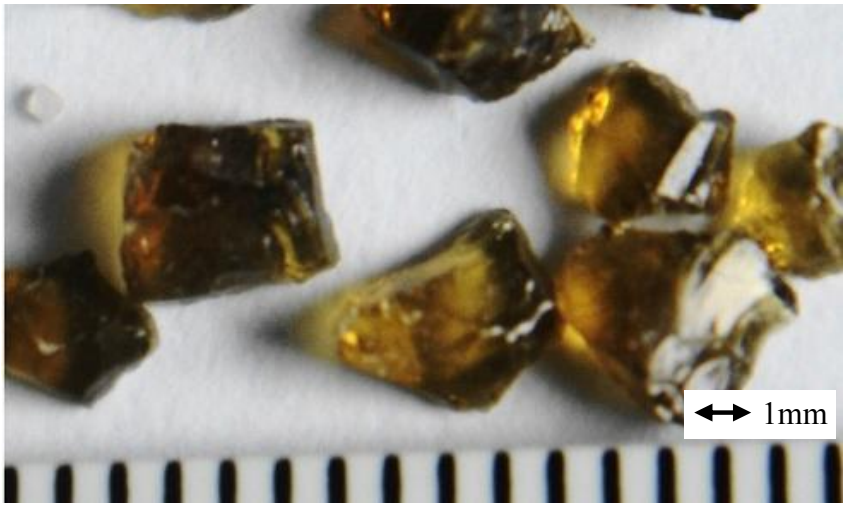

Fig. 3.15 Amber glass aggregate surface texture

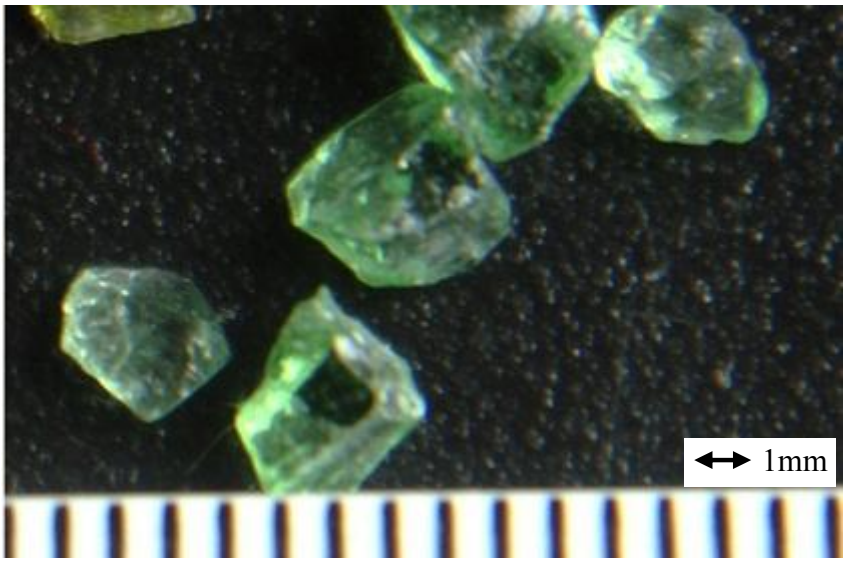

Fig. 3.16 Green glass aggregate shape

Fig. 3.17 Green glass aggregate surface texture

3.2.5 Water

The water used in making concrete was ordinary potable tap water. It was clear and did not contain measureable quantities of organic substances or inorganic constituents. The curing tank was also filled with ordinary tap water.

3.3 Apparatus

3.3.1 Aggregate image scanner and recorder

Image analysis was used to determine simultaneously the axial length of all particles and to give the distribution of particle size and particle shape within a sample of aggregate. The method used image capture of particles in lying positions, as illustrated in Figure 3.18 with all particles in a sample being contained in a single image. The particles are placed so as not to touch or overlap one another and no pre-processing is required which ensures high accuracy of the results. The images are assumed to give the largest projected area of the particles in the plane of the scanner plate. However, this assumption is not entirely correct, because the particles have several stable positions.

Crushed glass or fine aggregate was placed on the glass bed of a scanner (Figure 3.19) and covered by a lid with automatic scan and image, transparencies facilities. The scanner used was Epson perfection 4870 photos with resolutions of 1200 dpi and 2400dpi. Images were produced by back-lit illumination of aggregate samples.

A scanning array was obtained by moving back and forth beneath a glass mirror, a lens and to the image pickup.

The light beam passes through a colour filter to screen out any projections not conforming to the spectrum of the scanned particles. The beam is received by a photomultiplier tube or a charge coupled device (CCD), wherein the light beam is converted to an electrical signal. The resultant data array was stored and then processed using image-analysis software.

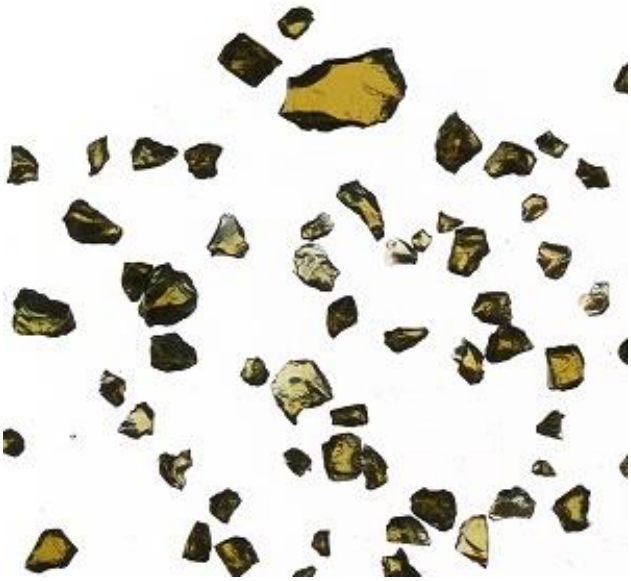

Fig. 3.18 Sample of crushed glass

Fig. 3.19 Scanner and computer laptop

3.3.2 Aggregate image processing software

There are many image analysis software packages available in the commercial market, e.g. Image-Pro, Volocity 3D, etc, and a package was chosen that was, fast, accurate and known to be reliable. Image data was assessed using ImageJ software

because it is well supported (http://rsb.info.nih.gov/), contains advanced statistical tools and is user friendly.

ImageJ is a public domain image processing program which provides a comprehensive range of analytical tools for measuring length, area, circumference and to undertake particle counting and density determination. The program can accept a wide range of data types, covering most of the major sources of images, such as brightfield, fluorescence, confocal and electron microscopy and gel electrophoresis. Versions are available for use with Macintosh, Linux and Windows. It was written by Research Services Branch (RSB) of the National Institute of Mental Health (NIMH) based in Maryland (USA).

ImageJ is based on Java /JavaScript (Sun Micosystems) and can display, edit, analyze, process, save and print 8-bit, 16-bit and 32-bit images. It can read a variety of image formats, including TIFF, GIF, JPEG, BMP, DICOM, FITS and "raw." ImageJ provides filtering standard image processing functions such as contrast manipulation, (sharpening, smoothing), edge detection and median filtering. It is multi-threaded, so it can be executed in parallel with other time-consuming operations such as image file reading. Image J can calculate the area and pixel value statistics, user-defined options and measure the distance and angle. Also it can create density histograms and line profile plots.

ImageJ can undertake geometric transformations such as scaling, rotating, flipping and zooming. Images can be scaled from 32:1 to 1:32. All analysis and processing functions are available at any magnification. The program supports any number of windows (images) at the same time, limited only by available memory. Spatial calibration is used to provide real world dimensional measurement units such as millimeters. Density or gray scale calibration is also available. Plug-ins to Image J are available which provide additional software modules or code to give the ability to perform other specific tasks, e.g. statistical analysis.

3.3.3 Concrete mixer

All concrete was made in the pan mixer shown in Figure 3.20. The mixer head can be lifted clear of the lower, rotating drum into which the concrete components (cement, aggregates and water) are placed. The mixer head supports vertical blades which are rotated by an electric motor. A homogeneous concrete mix is produced by the bottom drum and the upper blades rotating at the same time.

Fig. 3.20 Concrete Mixer (Pan Type)

3.3.4 Slump equipment

The slump equipment conformed to the requirements of standard EN 12350–2 and BS 1881: 102 and consisted of a metal slump cone (300mm high with a top diameter of 100mm and a bottom diameter of 200mm) a 14mm steel tamping rod and metal base plate as shown in Figure 3.21.

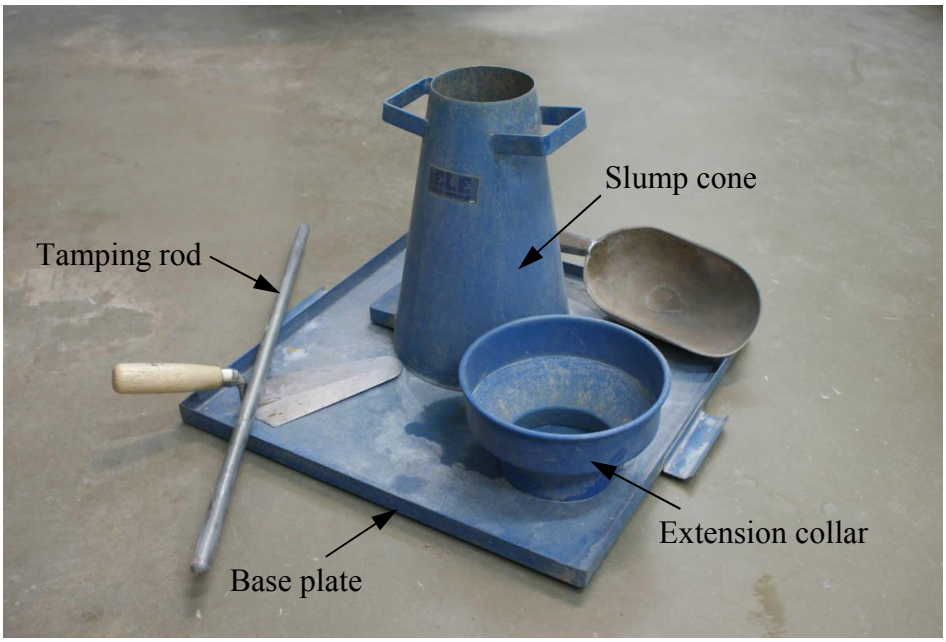

Fig. 3.21 Slump equipment

3.3.5 Flow table test equipment

The flow table equipment conformed with requirements of standard EN 12350-5 and BS 1881-105 and comprised a metal slump cone (200mm high with a top diameter of 130mm and a bottom diameter of 200mm) metal base plate and wooden tamping rod as shown in Figure 3.22. The base plate was 700mm by 700mm with a hinge at one end which connected it to a lower wooden base. A handle was attached to the metal base plate, at the opposite end to the hinge, which allowed the plate to be raised to give a 40mm gap.

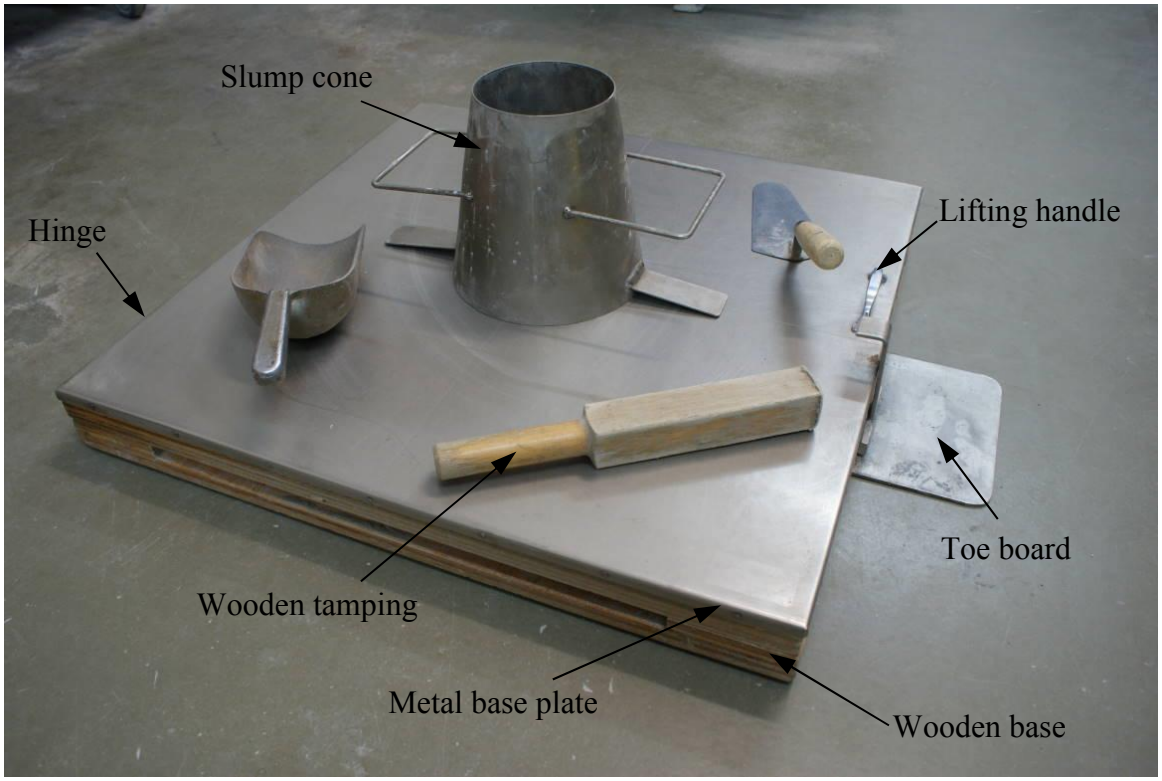

Fig. 3.22 Flow table equipment

3.3.6 Buoyancy balance

This equipment comprised a digital balance sat at on the top of a frame which incorporated a water tank at its base as shown in Figure 3.23. A wire basket (200mm by 200mm) was suspended from the frame by hooks. The water tank could be raised by turning a side handle a so that the wire basket, and its contents, was immersed in water contained in the tank.

Fig. 3.23 Buoyancy balance

3.3.7 Demec Gauge

A Demec gauge was used to measure small changes in length between two specific points i.e. pairs of studs glued onto a face of a concrete cube. The Demec gauge has two prongs which are set about 100mm apart and prongs are inserted into the studs mounted on a concrete cube One prong is mounted rigidly above a horizontal deflection dial gauge as shown in Figure 3.24. The other prong is on a rotating bearing and presses onto the spindle of a dial gauge. The dial gauge can be read to the nearest 0.001mm and was used to measure the difference in distance between two studs at any time and the distance (100mm) between the studs when they were first affixed to a cube using the stud mounting bar.

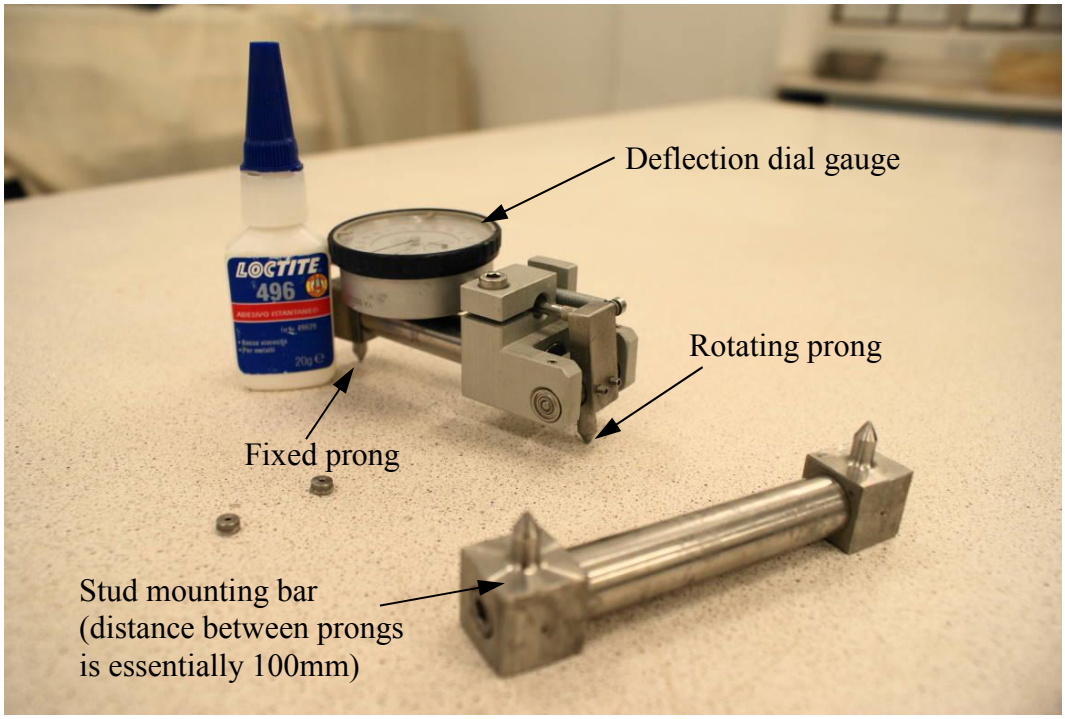

Fig. 3.24 Demec gauge component

3.3.8 Ultrasonic Pulse Velocity

The velocity at which an ultrasonic pulse travels through concrete is used as on indicator of concrete quality because it is influenced by the presence of cavities and cracks and the strength of the concrete. The apparatus consists of a pulse transmitter and receiver, which are connected to transducers as shown in Figure 3.25. The transmitter and receiver are positioned on opposing face of the concrete element under test.

Fig. 3.25 Ultrasonic pulse velocity equipment

3.3.9 Concrete vibrator

The vibrator is used to minimise air holes in concrete and to achieve maximum density and compaction. Hence concrete cubes should have a finished surface which is even, dense, and free from honeycombing and pronounced blowholes. The vibrator has electric motors which provide a constant speed. A poker vibrator driven by an electric motor is shown in Figure 3.26. The poker head is 20mm diameter and its length is 200mm long.

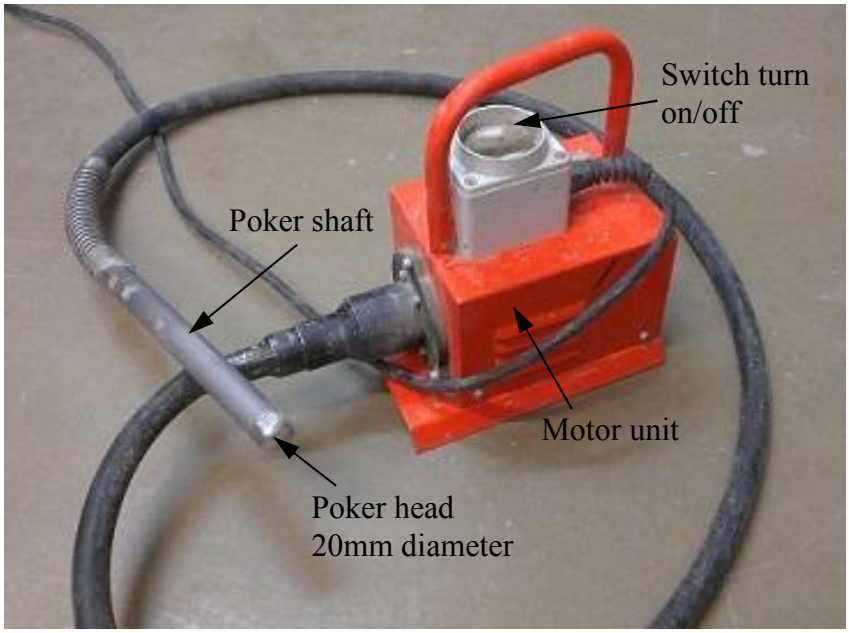

Fig. 3.26 Concrete vibrator

3.3.10 Compression strength tester

This cube crushing machine, which conformed with the requirement of BS EN 12390-4:2000, could be read directly 200kN to and had a load capacity of 3000kN and is shown in Figure 3.27. The concrete cube is located between two heavy metal platens. The lower platen is driven upwards at a constant role of load increase, while the upper platen is fixed in position. There was automatic recording of the maximum load but no measurement of change of dimension of a cube. The loading speed could be set in the range 600N to 60kN per second.

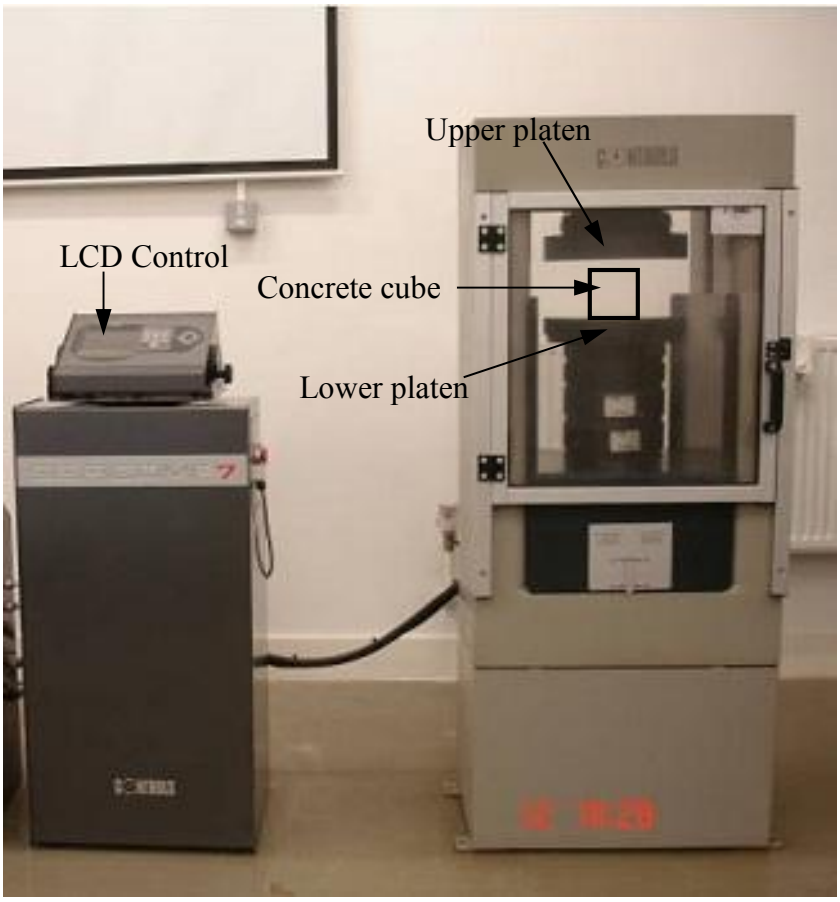

Fig. 3.27 Compression Machine

3.3.11 Glass crushing bin

The glass crushing bin was made from a heavy metal dustbin formed of pre-galvanised metal sheet and is shown in Figure 3.28. Its overall dimensions were 700mm height by 480mm diameter so that it had a volume of 90 litres. The bin was covered by a lid with a 50mm diameter hole at its centre and through which the shaft of the crushing tool passed. This tool was a manual rammer (used commercially to compact tarmac patches) with a heavy metal plate (100mm by 100mm, weighing 4.5kg) welded to the end of a metal shaft (1.35m long). The bin was seated on a composite base of wood and metal sheets to provide additional based rigidity and to reduce noise.

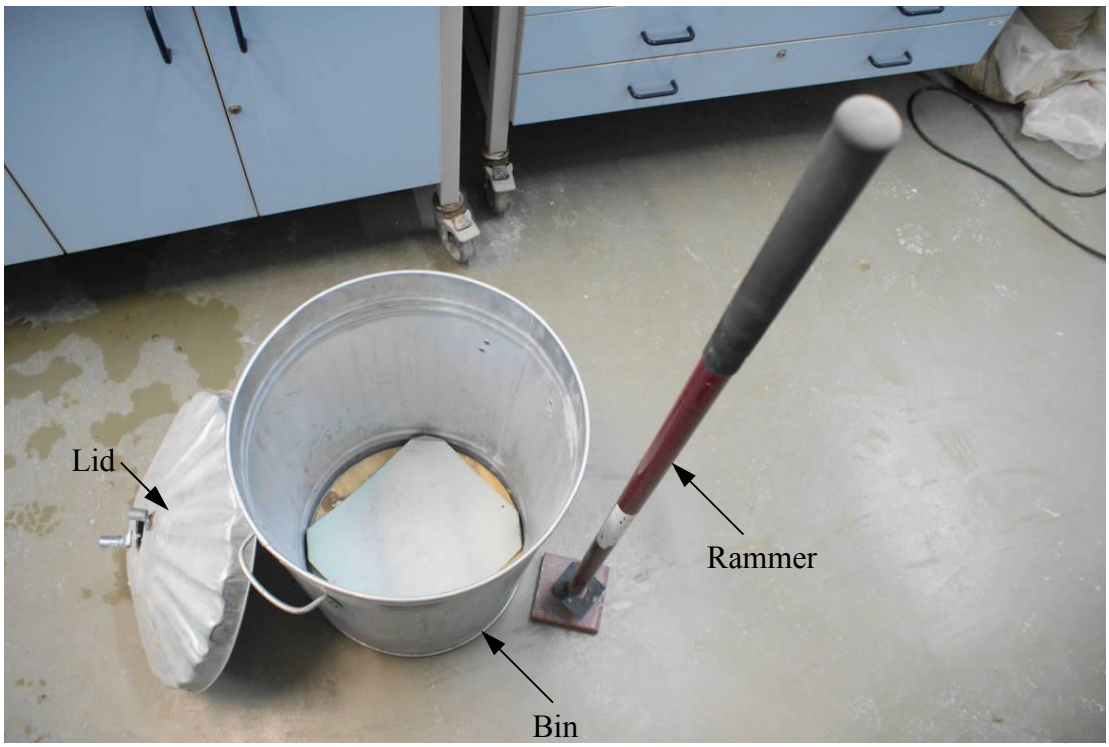

Fig. 3.28 Glass crushing bin

3.3.12 Glass 'grinder'

After the waste glass had been crushed in the crushing bin (section 3.3.11) to fine gravel size particles it was fed into the glass 'grinder'. The glass 'grinder' was originally a manual food mincer with a cast iron body as shown in Figure 3.29. The body contained an Archimedean screw and metal blades, which were rotated manually to force the crushed glass through a stiff perforated plate. Crushed glass was fed into the top of the grinder and was collected in a large tray for sieving.

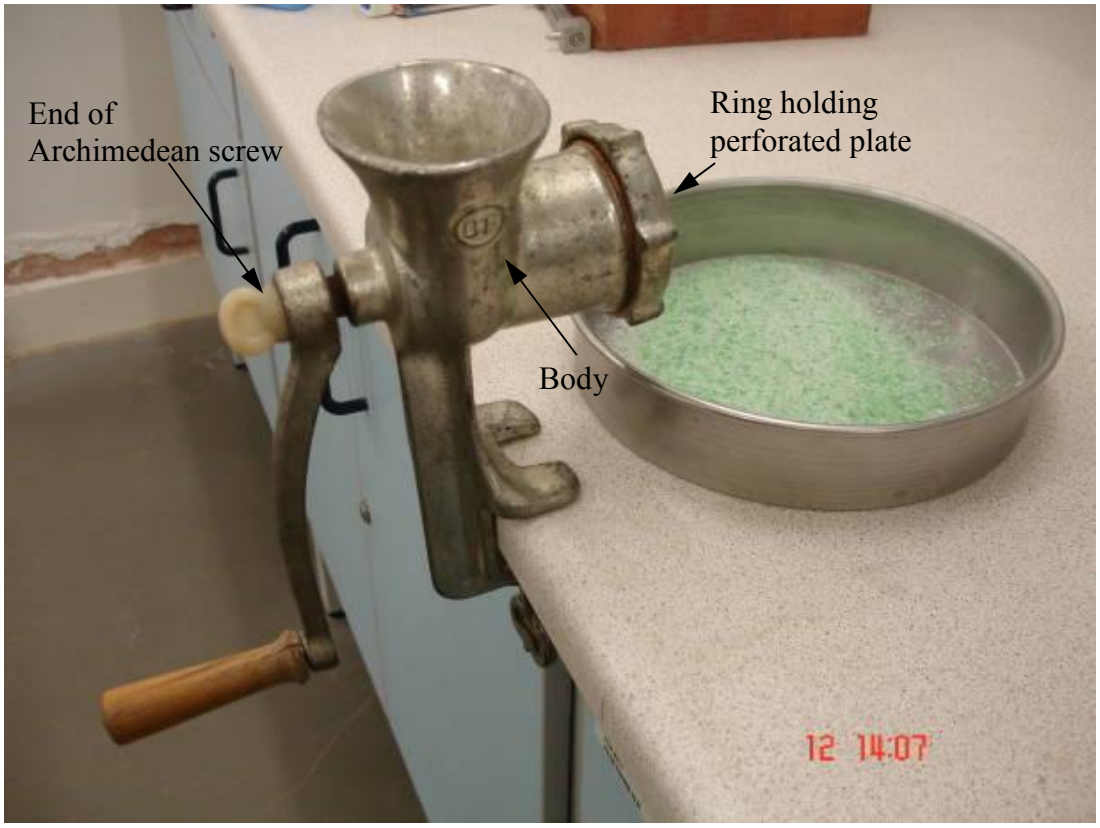

Fig. 3.29 Glass 'grinder'

3.3.13 Vicat apparatus for setting times (BS EN 196-3:2005)

The Vicat apparatus is used to determine the quantity of water necessary to produce a mortar paste of normal consistency and to determine the setting times of mortars. The Manual Vicat apparatus is illustrated in Figure 3.30. The metallic plunger is 45 mm long and 10mm in diameter with a mass of 300g and it can move vertically without significant friction. The Vicat mould is hard rubber in the form of a truncated cone which is 40mm deep and with internal 75mm diameter at bottom and 65mm diameter at top. The base plate is 2.5mm plane glass which is impermeable and resistant to cement paste attack.

Normal consistency is defined as the state at which the Vicat plunger penetrates to within 4mm to 6mm of the bottom of the Vicat mould within 4 ¼ minutes from the moment of adding water to from the cement paste. The initial setting time is the period which elapses between water being added to the cement and the time at which the Vicat needle penetrates 4 to 6mm from the bottom of the mould.

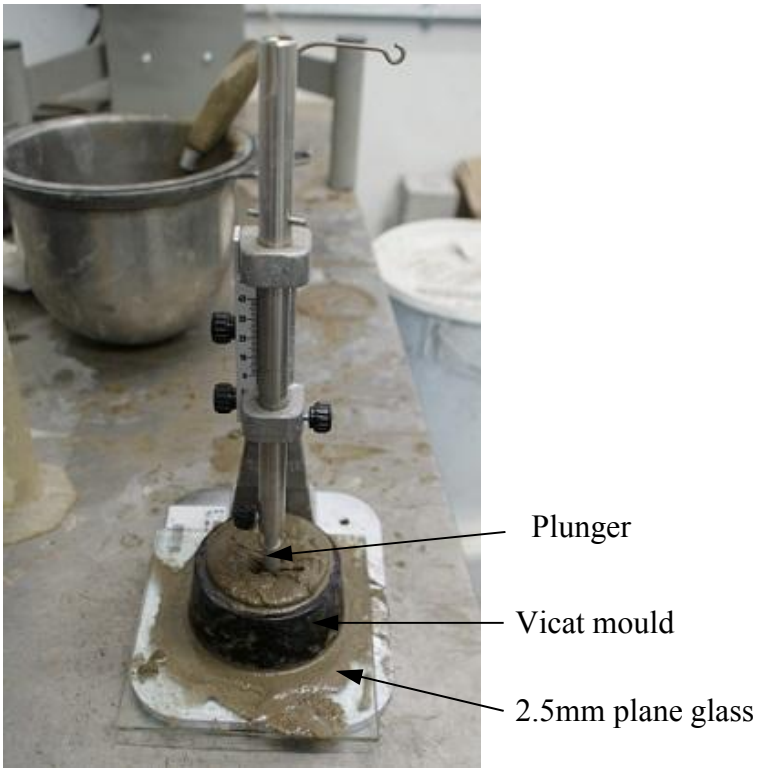

Standard consistency test

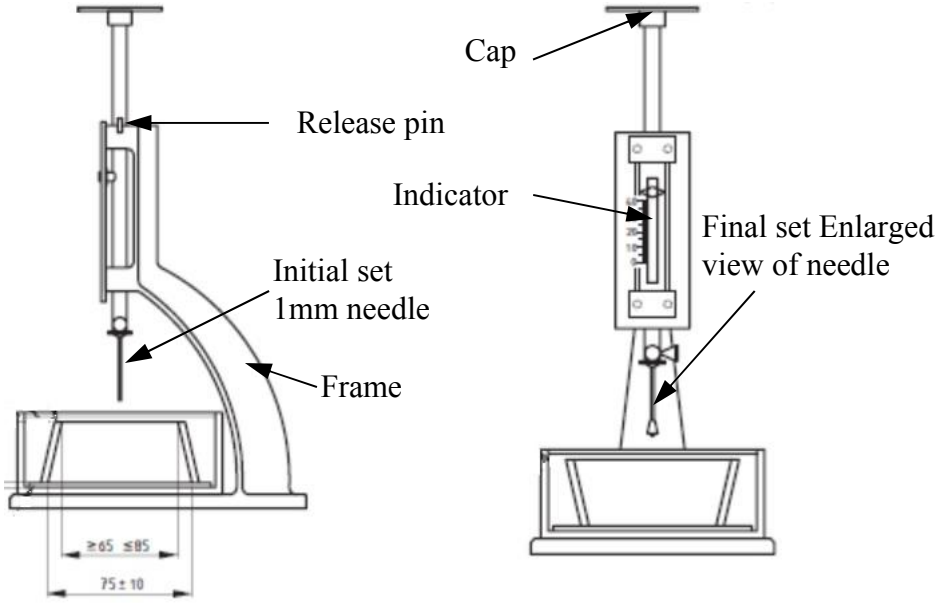

Initial setting time test **Final setting time test**

Fig. 3.30 Vicat apparatus for setting time measurement

3.4. Experimental methods

3.4.1. Aggregate image acquisition

Digital images of aggregate particles (in the size range 1mm to 2mm) were obtained using the Epson scanner described in Section 3.3.1. Particles were randomly placed on sticky transparent tape so that the particles were isolated from one another. The sticky tape then held the aggregate sample in place as it was transferred to the scanner. With the sample in a stable position. It was illuminated by lighting which eliminated object shadows and reflections. The image size was set at 25 mm × 25mm to get a measurement area which was sufficiently large to allow scaling to be carried out at a later stage to relate particle size to shape characteristics. The scanner was adjusted to produce a clear, sharp image for analysis.

The aggregate samples have different sizes and shapes so only one colour glass was scanned at a time. After image capture the data went sent to pre-processing and feature extraction stages by computer. In the feature extraction stage area and perimeter are used to identity of the form to give shape characteristic pattern recognition. A simple moment calculation method reduces the feature extraction processing time, thereby improving the efficiency of the system so that it is suitable for real-time computer vision system.

3.4.2. Crushed glass preparation

The same manufacturing process was used for all the concrete mixes which had the same water-cement ratio and the same ratio of cement: fine aggregate: coarse aggregate. Cement, coarse aggregate and conventional fine aggregate (sand) were all obtained from commercial stockists.

The waste glass fine aggregate was produced in the laboratory:

1. All waste glass was obtained in the form of bottles and, regardless of colour, it was processed in the same way to produce the required fine aggregate.
2. All bottles were submerged in a bucket of hot tap water and left for 15 minutes to soak, after which the were taken out and any labelling was removed and the bottles were air-dried by leaving them upside down in a laboratory for 3 hours.

3. The bottles were crushed, four at a time, in a bin (Figure 3.28). After laying he bottles flat on the bottom of the bin, it was sealed with the lid so that the handle of the heavy protruded through the central hole. The rammer was raised and dropped approximately 30 times to break the bottles and after removing the lid and rammer the broken glass was tipped into the top of a stack of sieves.
4. The sieve stack comprised 7 sieves with aperture sizes of 10mm, 5mm, 2.36mm, 1.18mm, 600µm, 300µm and 150µm. The sieve stack was shaken for 5 minutes and then dismantled. Material retained on the 10mm and 5mm sieves was returned to the bin for further crushing. Glass returned to the bin was subjected to further crushing and sieving until the amount retained on the 2mm sieve was insignificant. Material that was retained on the 2.36mm and 1.18mm sieves was fed into the manual grinder (section 3.3.12) for further processing. Material retained on the 600µm, 300µm and 150µm sieves and also the collection pan at the base of the sieve stack were bagged up.
5. Material was passed though the grinder in small quantities until it was all processed and then it was re-sieved. Anything retained on the 1.18mm sieve was fed through the grinder and glass passing the 1.18mm sieve was placed in the bag containing crushed glass from previous sievings.

3.4.3 Determination of voids content of a dry uncompacted mass of aggregate

The uncompacted voids content of a fine aggregate provides some general measure of its angularity and texture as voids content increases with angularity and decreases for a well-graded material. The voids content affects the concrete mix design and performance. A high voids content of aggregates typically requires more cement paste to provide the same workability for a given mix design.

The voids content was determined according to BS EN 1097-3 1998: (Tests for mechanical and physical properties of aggregates – Part 3). This test uses a sample of dry aggregate which is 1.2 to 1.5 times the mass of aggregate required to fill the test container. This container is filled to overflowing by resting the scoop on top of the rim of the container - this prevents aggregate segregation. Surplus aggregate is then removed from above the top of the container and the aggregate surface is levelled

with a straight edge, taking care not to compact any part of the upper surface. The filled container is weighed and the loose bulk density (ρ_b) is obtained from formula:-

$$\rho_b = (M_2 - M_1) / V \qquad \text{Equ. 3.1}$$

where ρ_b is the loose bulk density (Mg/m³)

M_2 is the mass of the container and test specimen (kg)

M_1 is the mass of the empty container, in kilograms (kg)

V is the capacity of the container (litres)

Three such determinations should be undertaken.

Voids percentage v (which is equivalent to the porosity of a mass of particles) is given by the following formula:-

$$v = \frac{(\rho_p - \rho_b)}{\rho_p} \times 100 \qquad \text{Equ. 3.2}$$

where ρ_p is the particle density (Mg/m³)

3.4.4. Concrete manufacture

The concrete mixing process commenced by weighing out all components using a balance with a capacity of 20kg and reading directly to 10g:

1. Firstly the coarse aggregate was placed in the pan of the mixer (Figure 3.20), then the fine aggregate was added, then the cement and everything (Figure 3.31) was mixed manually before water was added.
2. The materials were then mixed by machine for 5 minutes. The mix was stirred manually to incorporate segregated materials which had collected around the sides of the mixer, this was done until a homogenous concrete was obtained and the concrete was finished off with a further two minutes of mechanical mixing.
3. After the mixing process the concrete was tipped out onto a large metal tray and it was ready for the slump and flow table testing and production of cubes.

Fig. 3.31 Concrete components prior to mixing

The flow characteristics of all concrete mixes were determined immediately after batching of the concrete. After completion of slump and flow table, the concrete was re-mixed in the pan mixer before being used to make cubes.

3.4.5 Slump test: BS EN 12350-2:2009

The slump test was performed according to BS EN 12350-2: 2009 with the internal surface of the cone (Figure 3.21) being thoroughly clean and coved with a light coat of oil. The cone was placed on a metal base plate and was held down by placing the feet on lugs attended to the bottom of the cone. The extension collar was attached to top of the cone.

Fig. 3.32 Measurement of Slump

After filling the cone to approximately one third of its height with concrete the concrete was tamped 25 times using the rounded end of the tamping rod with the blows being distributed evenly over the cross section of the concrete. A further two layers of concrete were placed and tamped in the same way so that top surface of the concrete protruded above the cone. After removing the extension collar, the concrete was struck off level with the top of the cone using a trowel. The cone was the immediately removed from around the concrete by raising it slowly in vertical direction. The cone was then inverted and positioned next to the pile of fresh concrete and a steel bar was placed across the top of the cone as shown in Figure 3.32. The difference in height between the highest point of the subsided concrete and the steel bar was measured using a steel tape-this difference in height (in mm) is the slump of the concrete. After measuring the slump, the concrete was returned to that part of the mix remaining on the metal tray and the whole lot was turned in the pan mixer for one minute before a further slump test was performed. Slump was measured three times for each batch of concrete.

3.4.6 Flow table test: BS EN 12350-5:2009

The flow table test was performed according to BS EN 12350-5:2009. Initial preparation of a test specimen was similar to the slump test procedure (section 3.4.5). After preparing the metal cone (Figure 3.22), it was placed on the centre of the flow table and was held down by putting a foot on each of the lugs. The cone was then filled in two layers, tamping each layer ten times with the wooden tamping rob in a similar way to the slump test. After the tamping, a trowel was used to strike off the concrete level with the top of the cone. Any spilled concrete around the cone and on top of the table was removed and the cone was slowly lifted vertically to leave a free-standing pile as shown in Figure 3.33.

Fig. 3.33 Concrete on flow table prior to testing

A foot was placed on the toe board at the front of the table (Figure 3.33) and the handle was used to slowly lift the tabletop until it reached an upper stop. The lifting handle was then released to allow the table to fall freely to impact the wooden base. This cycle of raising and dropping the table top was repeated to give a total 15 drops with each cycle taking about 4 seconds. The plan dimension of the slumped concrete was then measured in two orthogonal directions parallel to, and at the midpoint of, the table edges as shown in Figure 3.34. These two approximate diameters were recorded to the nearest 5mm.

Fig. 3.34 Flow table test measurement

All the concrete was then and returned to the pan mixer and turned for one minute before repeating the flow table test. A total of three flow table tests was performed on each concrete mix.

3.4.7 Setting times: BS EN196-3:2005

The setting times of the cement mixes were determined according to BS EN 196-3:2005 using a Vicat apparatus at room temperature. The initial setting time occurred when a Vicat needle 1 mm in diameter penetrated the sample to a point 5±1mm from the bottom of the mould (Figure 3.35). The final setting time was defined as when a 5mm cap ring would leave no visible mark when placed on the surface of the sample.

Fig. 3.35 Vicat apparatus for setting

3.4.8 Casting concrete cubes

Before assembling the cube moulds (100×100×100) their inside surfaces were lightly oiled to facilitate removal of a cube from the mould. Each mould was filled with concrete in two stages and an electric vibrator was used to compact the concrete fully after placement of each layer. Surplus concrete was then removed from the surface of the cube which was smoothed over with a trowel. Each filled mould was covered with plastic sheet and stored inside the laboratory with a temperature maintained at 18ºC to 20ºC.

Test cubes were removed from the moulds between 16 and 24 hours after they had been made and were clearly labelled. The cubes were then placed in a curing tank

containing water whose temperature was maintained at 20°C. The cubes were positioned to provide adequate space between them to permit adequate circulation of water. Curing was continued right up to the time of compression testing.

3.4.9 Density of hardened concrete: BS EN 12390-7:2009

Immediately after each cube was removed from its mould it was subjected to a buoyancy test using the apparatus shown in Figure 3.23. A cube was placed in the supporting basket and its weight was recorded using the digital balance. The water tank was then raised and the submerged weight of the cube was measured. The difference between the two foregoing 'weights' was the upthrust on the cube from which the cube volume was obtained. All of the proceeding weights were monitored automatically by the buoyancy apparatus and the bulk density was read directly from the display unit.

3.4.10 Ultrasonic Pulse Velocity: BS EN 12504-4:2004

This testing was conducted on cubes after different hardening periods, e.g. 7 days, 28days, etc after casting. The test was performed between opposite 'smooth faces' i.e. those faces formed by the sides of a mould. Two measurements were made for each direction. Cubes were tested after being removed from the curing tank and so the tests were performed with the cube faces in a damp condition. A special liquid gel (couplant) was spread over the faces of the pulse transmitter receiver and concrete faces. The transmitter and receiver were then pressured against the concrete.

The LCD screen of the monitor was set to maximum accuracy of 0.1 microsecond range for the 100mm path length. The transducers were held against the surface of the concrete cube until a consistent reading appeared on the monitor display - this was the time in microseconds for the ultrasonic pulse to travel 100mm distance. This procedure was then applied to different directions. The whole test procedure was performed twice for each cube.

3.4.11 Dimensional changes of concrete

Immediately after a cube was removed from a mould and had been weighed, demec studs (section 3.3.7) were mounted on each of its faces. Because the concrete cubes had sides of 100mm and the gauge length of the demec gauge was 100mm the studs were positioned near the corners of a cube and the gauge was used to measure

distance changes between diagonally-opposite pairs of studs. The studs were attached to the concrete using an epoxy-resin glue, which hardened in approximately 10 seconds. The stud mounting bar was used to position the pairs of studs at a distance of 100mm from each other. Once the glue had set the prongs of the demec gauge were located in the studs and the reading of the deflection dial gauge was taken-this was taken as the reference reading for a particular pair of studs. Subsequently deflection dial gauge readings were compared to this initial dimension. Measurements were made after curing times of 14 days, 1, 2, 3, 6, 9 and 12 months.

Dimensional changes of set concrete were also monitored by conducting the ASR test defined in BS 812-123. The size of the mortar bars was 160×40×40mm. The bars were made by compacting concrete into a mould and the bars were stored in water which was maintained at a temperature of 38ºC (100ºF) - see Figure 3.36. The bar lengths were measured after 14, 28, 56, 112, 252 and 365 days of curing using Demec gauge.

Fig. 3.36 Mortar bars for measurement of expansion

3.4.12 Compressive strength test: BS EN 12390-3:2009

A cube, while still wet (after being taken from the curing tank), was placed with the cast faces in contact with the platens of the testing machine, i.e. the position of the cube when tested is at right angles to that as-cast. The load on the cube was applied at a constant rate of stress equal to 0.6 MPa per second (BS EN 12390-3: 2009). Because

of the non-linearity of the stress-strain relation of concrete at high stresses, the rate of application of strain must be increased progressively as failure is approached, i.e. the speed of movement of the head of the testing machine has to be increased.

3.4.13 Water absorption by immersion: BS 1881-122:2011

Water absorption by immersion of concrete specimens was determined according to BS 1881-122: 2011 when the concrete had been curing for 28 to 32 days. Each determination used three concrete bars with dimensions of 100×100× 50mm made using cement, fine and coarse aggregate in the ratio 1:2:4. Drying of specimens was started at an age of 24 to 28 days by placing them in an oven maintained at a temperature of 105ºC ± 5ºC. They were kept there for 72 ± 2hours before being removed and cooled to a room temperature of 20ºC ± 2ºC and then weighted.

The immersion test was conducted by placing a specimen in a curing tank containing water maintained at a temperature of 20ºC ± 2ºC. The specimen was positioned so that the water level was within 25mm ± 5mm above the top of the specimen, as illustrated in Figure 3.37. After 10 minutes the specimen was removed from the tank, shaken to remove the bulk of the surface water and dried with tissue paper and weighed as quickly as possible. The specimen was then returned to the tank. Further measurements of weight were made after 30 minute and at various intervals up to a total soaking period of 7 days. The absorption was calculated and expressed as the increase in mass (as a percentage) of the mass of the dry specimen.

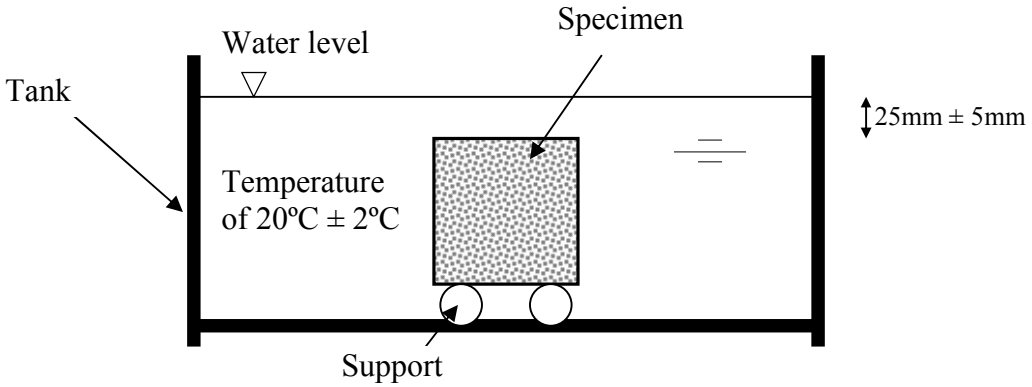

Fig. 3.37 Determination of water absorption

3.4.14 Water absorption by capillary rise (sorptivity testing)

A porous concrete structure results in water being drawn into the body of the concrete by the capillary force of a fluid material. Concrete sorptivity is a measure of unsaturated liquid (water) flow into a volume of concrete.

Specimens were tested after curing for 28 to 32 days. Each determination used three bars with dimensions of 100×100×50mm made from concrete containing cement, fine and coarse aggregate in the ratio 1:2:4. Specimens were dried in an oven maintained at 105 ºC ± 5 ºC until they reached a constant weight. After being allowed to cool to room temperature each specimen was weighed (to the nearest 0.01 gram) and the area of the face to be subjected to immersion was measured to the nearest mm². The specimen was then placed in a metal tray containing water (Figure 3.38) and sat on a PVC mesh (which allowed water to flow freely to the surface of the concrete) so that the immersed face was 2-5 mm below the surface of the water (Figure 3.38). At time intervals of 10, 30, 60 minutes, 2, 4, 8, 24 hours and 3, 7 days after immersion a specimen was removed from the tray, surplus water was wiped off and the specimen was weighed to the nearest 0.01 gram and then returned to the tray.

The sorptivity the concrete is defined by the relationship:

$$i = S\, t^{0.5} \qquad \text{Equ. 3.3}$$

where i = increase in mass (per unit are of wetted face) since the beginning of the testing divided by the density of water.

t = time (minutes) at which the mass is determined.

S = sorptivity (mm/min$^{0.5}$)

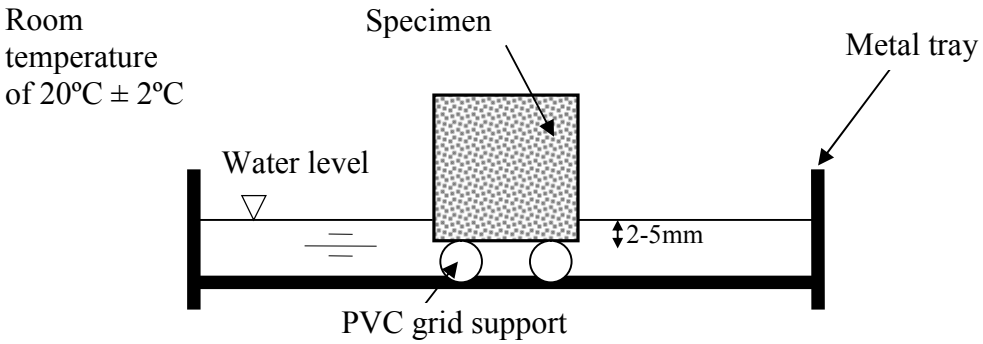

Fig. 3.38 Capillary rise/ Sorptivity test

3.5 Analytical methods for aggregate shape characterisation

For the natural sand and each colour of glass 50 randomly-selected particles were scanned and the images were analysed using ImageJ processing software.

The output data were used to quantity the magnitude and distribution of particle shape functions within each aggregate samples. The results for the samples were then compared using statistical analyses. Determination of the Aspect Ratio (Figure 3.39) shows the circumscribing rectangular prism that is used to define feret values.

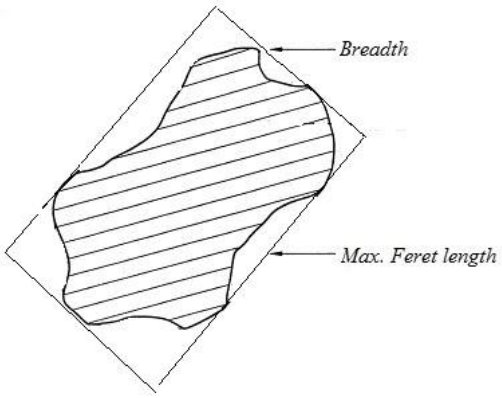

Fig. 3.39 Dimensions used in the determination of Aspect Ratio

3.5.1 Aggregate digital image processing

With processing software ImageJ, original digital images can be converted into binary images which consist of black objects (which will be the aggregate particles) and white background. This binary form of image means that the profile of a particle is well defined with a sharp contrast against the background and this promotes accurate delineation of a particles boundaries for subsequent measurement. The images obtained from the scanner (Section 3.3.1) will be in greyscale form. A threshold value of pixel grey level is specified and the greyscale intensity of any point on the digital image is compared to the threshold value to decide whether the point should be represented as black, i.e. part of a particle, or white, i.e. part of the background. Specific image processes such as 'erode', 'dilate' and 'fill holes' can be used to smooth, and sharpen particles and to facilitate edge detection. 'Erode' is used to remove pixels from the edge of black objects and 'dilate' adds pixels to the edge of objects. Due to illumination effects during the digital image acquisition stage some black objects, i.e. particles, may contain white spots and these may be eliminated by using 'fill holes'. The number of steps of 'erode', 'dilate' and 'fill holes' are decided by the, quality of the

digital images. The number of steps of 'erode' and 'dilate' are maintained equal so that there is no net addition or removal of pixels from the real particles.

After the image processing techniques had been applied the pixel values were converted to values of area and perimeter for each particle. An excel spreadsheet was then used to provide values of aspect ratio, Riley circularity and percentage concavity for the particles within each aggregate sample.

Figure 3.40 gives an overview of the image analysis process and an illustration of how an original image appears in binary form.

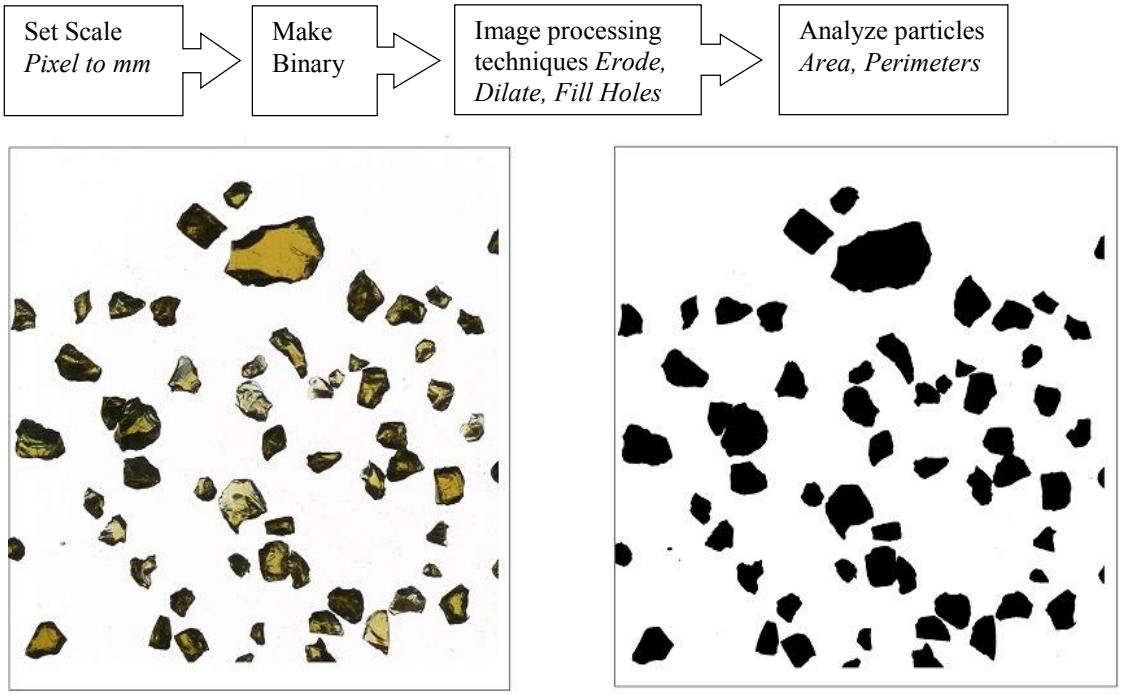

Original image Binary image

Fig. 3.40 Illustration of processing using ImageJ

To determine the pixel and convert to mm, setting measurement scale was drawing a line between two points of known distance from the edge to edge of image frame. That analyze and Set Scale, in the Set Scale window the length of the line, in pixels, will be displayed (Figure 3.41). Type the known distance as 25mm and units of measure in (mm) the appropriate boxes, which scale measurements of 15.321pixel/mm.

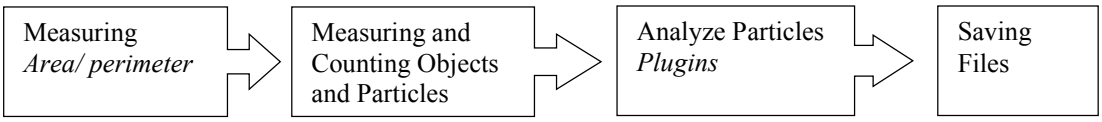

Image analysis process

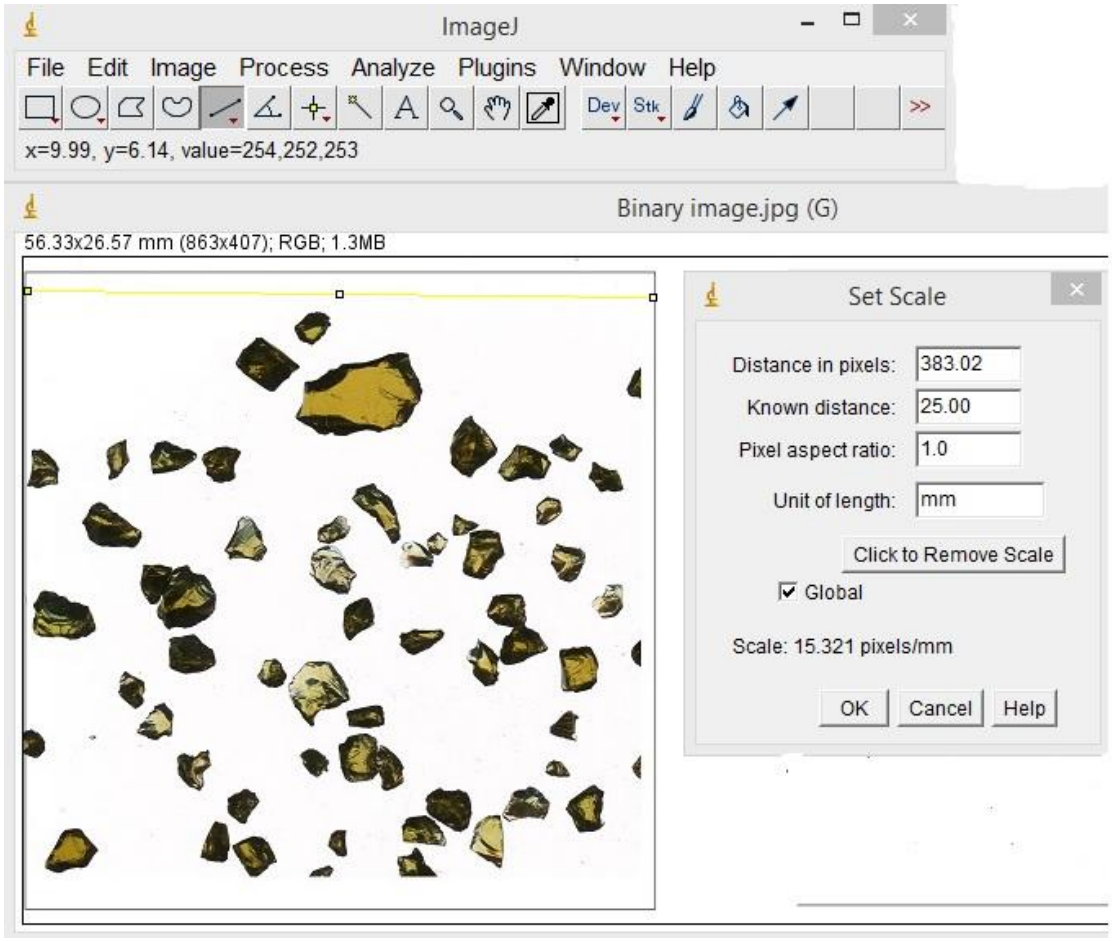

Fig. 3.41 ImageJ of setting scale

Measuring the surround an area with a perimeter, using an area selection tool, the wand (for high contrast images) or with Analyze particles. Analyze Measure and transfers the area measurement to a data window.

Counting Particles, convert the image to 8-bit grayscale and then 'threshold' the image. Analyze Particles, set the upper (999999) and lower limits (5) for the particle size, toggle and each counted particle will be outlined and numbered in Figure 3.41. The data window contains measurements for each particle. Saving the files and images, histograms, measurement results etc Figure 3.42 shows the tabular output obtained using the ImageJ program for image processing and optimisation.

Results

File Edit Font Results

	Label	Slice	Number	XStart	YStart	Perim	Area	Pixels	XM	YM
1	null	1	1	572	34	365.019	5826	5983	520.270	87.233
2	null	1	2	104	42	360.978	6090.500	6249	96.121	112.514
3	null	1	3	910	43	248.936	3238	3344	908.091	79.494
4	null	1	4	660	46	459.144	8742.500	8936	716.645	98.470
5	null	1	5	241	54	307.120	5149.500	5279	239.537	105.203
6	null	1	6	417	59	271.966	4137	4257	386.161	90.424
7	null	1	7	991	59	408.291	9608.500	9789	1011.149	112.443
8	null	1	8	861	141	301.966	5172	5307	874.342	186.882
9	null	1	9	356	176	420.049	7850	8037	387.126	255.247
10	null	1	10	1078	201	252.693	2183.500	2292	1092.806	253.340
11	null	1	11	782	210	325.563	5438	5579	763.648	261.961
12	null	1	12	547	219	483.789	10950	11161	610.166	294.718
13	null	1	13	174	228	462.014	10733	10924	204.161	295.944
14	null	1	14	966	232	289.865	4514.500	4642	972.642	266.253
15	null	1	15	728	321	525.872	7852	8077	767.923	432.425
16	null	1	16	909	346	386.090	8563.500	8730	903.853	404.239
17	null	1	17	361	347	490.475	11923	12138	371.715	400.310
18	null	1	18	1109	353	491.144	10679.500	10889	1074.803	422.435
19	null	1	19	39	383	450.416	9489	9680	99.543	458.435
20	null	1	20	603	416	313.179	5194.500	5332	576.036	450.925

Fig. 3.42 Output from ImageJ processing software

3.5.2 Statistical plots of particle shape data

The particle shape and size data related to a variety of particles within each aggregate sample and therefore could not be represented by single value of any particular, parameter. Hence a number of 'statistical procedures' were applied to the data in order to compare 'populations' of values.

- **Normal probability (normal QQ)** plot for one column of data. A normal distribution will plot as a straight line. For comparison, an RMA (Reduced Major Axis) regression line is given, together with the Probability Plot Correlation Coefficient.

- **Histograms (frequency distributions)** for one or more columns. The number of bins is by default set to an "optimal" number (the zero-stage rule of Wand 1997):

- **A Bubble Plot** of 3D data (three columns) by showing the third axis as size of disks. Negative values are not shown. The "Size" slider scales the bubbles relative to unit radius on the x axis scale.

- **Bar chart** for each sample with the mean value shown by a bar. In addition, “whiskers” can be shown. The whisker interval can represent a one-sigma or a 95% confidence interval (1.96 sigma) for the estimate of the mean (based on the standard error), or a one-sigma or 95% concentration interval (based on the standard deviation).

- **Univariate analysis will provide a variety of data characteristics:**
  N: The number of values *n* in the sample
  Min: The minimum value
  Max: The maximum value
  Sum: The sum
  Mean: The estimate of the mean, calculated as *n*
  Std. error: The standard error of the estimate of the mean, calculated as *n*
  Variance: The sample variance
  Stand. dev.: The sample standard deviation,

Median: The median of the sample. For *n* odd, the given value is such that there are equal number of values above and below. For *n* even, the average of the two central values.
25 prcntil: The 25th percentile, i.e. the given value such that 25% of the sample is below, 75% above. The "interpolation" method is used (see Percentile plot above).
75 prcntil: The 75th percentile, i.e. the given value such that 75% of the sample is below, 25% above. The "interpolation" method is used (see Percentile plot above).
Skewness: The sample skewness, zero for a normal distribution, positive for a tail to the right.
Kurtosis: The sample kurtosis, zero for a normal distribution.
Geom. mean: The geometric mean, calculated as $(x_1 x_2 ... x_n)^{1/n}$.
Coeff.var: Coefficient of variation, or ratio of standard deviation to the mean, in percent

- **Correlation table** consists of a matrix in which is presented the correlations between pairs of columns. Correlation values are given in the lower triangle of the matrix, and the two-tailed probabilities that the columns are uncorrelated are given in the upper. Both parametric (Pearson) and non-parametric (Spearman and Kendall) coefficients and tests are available. Algorithms follow Press *et al*. (1992) except that the significance of Spearman's coefficient is calculated with an exact test for $n<=9$

3.5.3 Statistical tests applied to particle shape data

Statistical tests were applied to investigate whether the data for each aggregate type were directly comparable or whether each population had fundamental differences which could have arisen because of the made of formation of the particles or their internal structure.

Correlation

Means and variances are obtained from the previously mentioned Univariate statistics. The 95% confidence interval for the mean is based on the standard error for the estimate of the mean, and the *t* distribution.

- The *F* test has a null hypothesis that the two samples are taken from populations with equal variance. The *F* statistic is the ratio of the larger

variance to the smaller. The significance is two-tailed, with $n1$ and $n2$ degrees of freedom.

- The t test has a null hypothesis that the two samples are taken from populations with equal means. From the standard error sD of the difference of the means given above.

- The unequal variance t test is also known as the Welch test. It can be used as an alternative to the basic t test when variances are very different, although it can be argued that testing for difference in the means in this case is questionable.

Normality tests

Three statistical tests for normal distribution of one or several samples of univariate data, were applied. The control data were generated by a random number generator with uniform distribution. If the calculated p(normal) is less than 0.05, normal distribution can be rejected. Of the three tests, the Shapiro-Wilk is considered to be the more exact, and the two other tests. (Jarque-Bera and a chi-square test) are given for reference. There is a maximum sample size of n=5000, while the minimum sample size is 3 (the tests will of course have extremely small power for such small n).

- The Shapiro-Wilk test (Shapiro and Wilk, 1965) returns a test statistic W, which is small for non-normal samples, and a p value. The implementation is based on the standard code "AS R94" (Royston, 1995), correcting an inaccuracy in the previous algorithm "AS 181" for large sample sizes.
- The Jarque-Bera test (Jarque & Bera 1987) is based on skewness S and kurtosis K.
- The chi-square test uses an expected normal distribution in four bins, based on the mean and standard deviation estimated from the sample, and constructed to have equal expected frequencies in all bins. The upper limits of all bins, and the observed and expected frequencies, are displayed. A warning message is given if n<20, i.e. expected frequency less than 5 in each bin. There is 1 degree of freedom. This test is both theoretically questionable and has low power, and is not recommended.

ANOVA

One-way ANOVA (analysis of variance) is a statistical procedure for testing the null hypothesis that several univariate samples (in columns) are taken from populations with the same mean. The samples are assumed to be close to normally distributed and have similar variances. If the sample sizes are equal these two assumptions are not critical. If the assumptions are strongly violated the Kruskal-Wallis test should be used instead.

The Kruskal-Wallis test is a non-parametric ANOVA, comparing the medians of several univariate groups (given in columns). It can also be regarded as a multiple-group extension of the Mann-Whitney test (Zar, 1996). It does not assume normal distribution, but does assume equal-shaped distribution for all groups. Kruskal-Wallis does not test the null hypothesis that the samples being compared are taken from populations with equal medians. It is used to determine if two, or more, distribution are similar or from the same source.

CHAPTER 4: RESULTS

4.1 Fresh concrete

The fluid, unset state of concrete only lasts for a short time and so this state is only of limited interest for structural engineering. However it should be noted that concrete strength and durability are seriously impacted by the degree of workability achievable for given mix properties and compaction effort. If concrete is not fully compacted numerous bubbles of air will trapped resulting in a voided and porous structure. It is therefore important, that the consistency of a concrete mix enables it to be transported, placed, compacted, and finished satisfactorily and without segregation. Therefore, the following sections relate to the properties of fresh concrete and observations on slump, flow ability and setting times.

4.1.1 Slump value for conventional concrete

Table 4.1 contains slump data for all concrete mixes, both conventional and those with crushed glass. Three slump tests were conducted on each concrete mix and the slump values are presented in the order of undertaking the tests. The typical slump data in Figure 4.1 do not show any clear effect of order/ sequence of testing each mix even though the third sample to be tested from a batch could be slightly drier and stiffer than the first so there could be an expectation that the first test would always have the greatest slump. Testing was done as rapidly as possible so that the time between first and last test was very short and thus drying and ageing effects in the laboratory would be minimal.

The slump values for conventional concrete would seem to cover quite a range of values but with this test, the upper surface of the slumped mix of the concrete is never smooth or level – see Figure 3.32. The upper surface generally does not remain parallel to the surface on which the concrete rests and a variation of ±5mm for an average slump of 30mm is not unusual (Neville, 1995). All three values for each mix are close and the difference in slump values does not cause significant shift in categorisation of the mixes in term of workability. For the conventional concrete, each of the slump values would mean that the mix would be classified as being of middle slump.

Table 4.1 Slump values for all concrete mixes

Glass replacement sand (%)	Slump (mm) ranged in order of test, i.e. 1st, 2nd & 3rd					
	Natural sand	**Flint glass**	**Amber glass**	**Green glass**	**Mixed washed**	**Mixed unwashed**
0	78, 80, 67					
25		62, 67, 74	78, 56, 70	63, 73, 60	70, 65, 60	58, 70, 65
50		50, 45, 42	58, 35, 43	45, 48, 55	47, 50, 38	40, 35, 45
100		42, 28, 31	30, 45, 27	42, 30, 33	28, 40, 35	25, 42, 30
	Slump (mm) in mean values					
	Natural sand	**Flint glass**	**Amber glass**	**Green glass**	**Mixed washed**	**Mixed unwashed**
0	75					
25		68	68	65	65	64
50		46	45	49	45	40
100		34	34	35	34	32

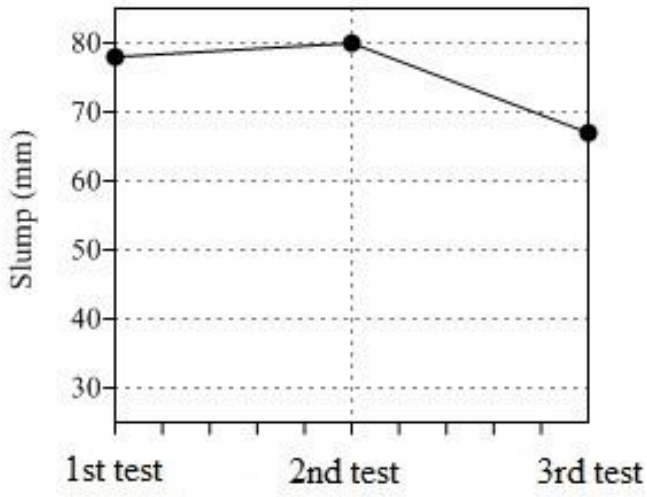

Fig. 4.1 Slump values of conventional fine aggregate – typical slump data

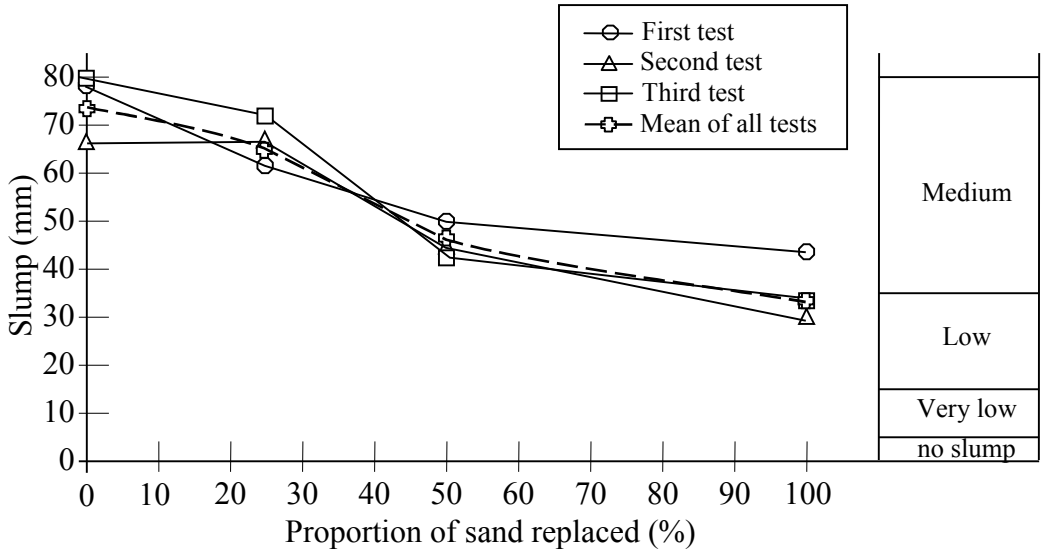

Fig. 4.2 Slump of concrete containing flint glass

Neville (1995) produced a table for determining the amount of water required for a concrete mix to achieve a given slump on the basic of aggregate size. The research reported herein used rounded aggregate with a maximum size of 20mm and a water cement ratio of 0.6 (corresponding to a water content of 186kg/m3). Table 4.2 shows the relevant part of Neville's chart and this predicts a slump value of approximately 50-75mm if the aggregate is classified as rounded. As noted in section 3.2.3 the conventional fine aggregate which was used was intermediate between rounded and angular in shape. The lack of precise agreement between predicted and measured values of frequently-used parameters, such as slump, supports the adoption of an experimental research methodology as stated in section 3.1.

Table 4.2 Approximate water content for different slumps and maximum sizes of aggregate (Neville, 1995)

Max size of aggregate (mm)	**Water content of concrete (kg/m^3)**					
	Slump 25-50mm		**Slump 50-75mm**		**Slump 150-175mm**	
	Rounded aggregate	Angular aggregate	Rounded aggregate	Angular aggregate	Rounded aggregate	Angular aggregate
19.0	165	190	185	205	200	220
25.4	155	175	175	200	195	210

4.1.2 Slump for concrete containing glass

The data in Table 4.1 show that all mixes lay within the 'low and middle workability' category i.e. from 15 to 80mm (Neville, 1995), with slump values ranging from 30 to 70mm. Thus, the substitution of crushed glass for conventional sand has not had a major effect on mix workability. However, there does appear to be a trend for some significant decrease in slump as the percentage of sand replaced by crushed glass becomes high as indicated in Figure 4.2 (for flint glass). For the conventional concrete, the slump ranged from 67 to 80mm whereas for 100% replacement of the sand the slump ranged from 30 to 45mm.

Figure 4.2 also shows that the first test of each concrete batch quite often gave the lowest slump value so drying/hardening of the concrete between tests was not significant (as noted in section 4.1.1 for the conventional concrete).

Figure 4.2 shows that the upper slump value for 100% glass replacement is out-of-step with other values in that it suggests little change in slump as all the sand is replaced (to such an extent that this mix would be categorised as medium workability rather than 'low'). This trend is not supported by findings reported by other researchers. Furthermore, the test records do not indicate any reason for the foregoing anomalous value and hence this result has been discarded. The amended data set is plotted in Figure 4.3, wherein all slump values have been 'relative' by dividing them by the mean slump value for conventional concrete.

Figure 4.3 clearly suggests that up to 25% replacement of sand has no major affect on slump but greater replacement produces a proportional decrease in slump values. Nevertheless for up to 50% replacement of sand by glass the slump values for the concrete with flint glass all lie in the same workability category. As will be noted in section 4.3 the general shape of the crushed glass aggregate was different to that of the conventional fine aggregate. The surface of the crushed glass contained a number of sharp ridges, which could have caused interlocking of this fine aggregate and so increased frictional resistance between the particles thereby reducing movement under a given loading.

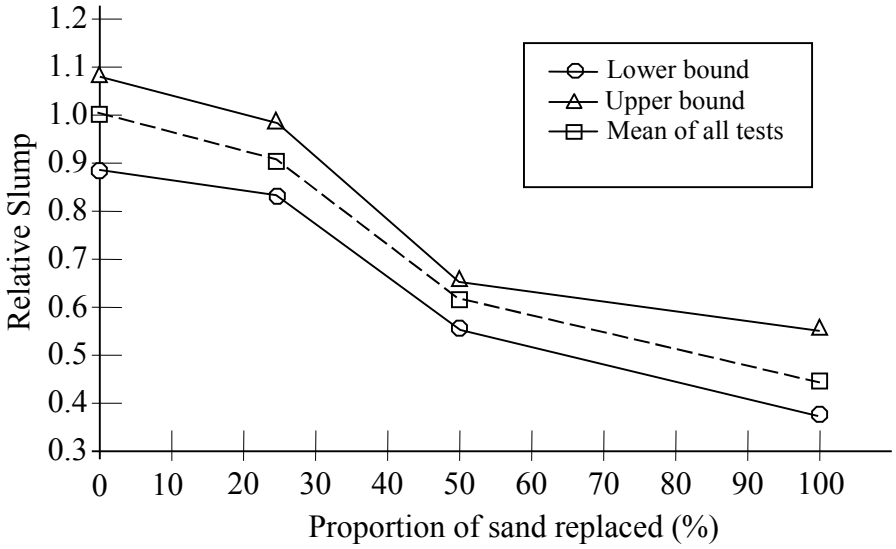

Fig. 4.3 Relative slump for concrete containing flint glass

Figure 4.4 shows slump values for concrete containing amber glass. The figure shows that for up to 50% replacement of conventional fine aggregate the same workability category is exhibited by concrete with flint glass aggregate and conventional concrete. The normalised slump values in Figure 4.5 show similar values for concrete with 25% replacement and conventional concrete with a progressive decrease up to complete replacement of the sand by amber glass with consequential change in workability categorisation for 100% sand substitution by crushed glass.

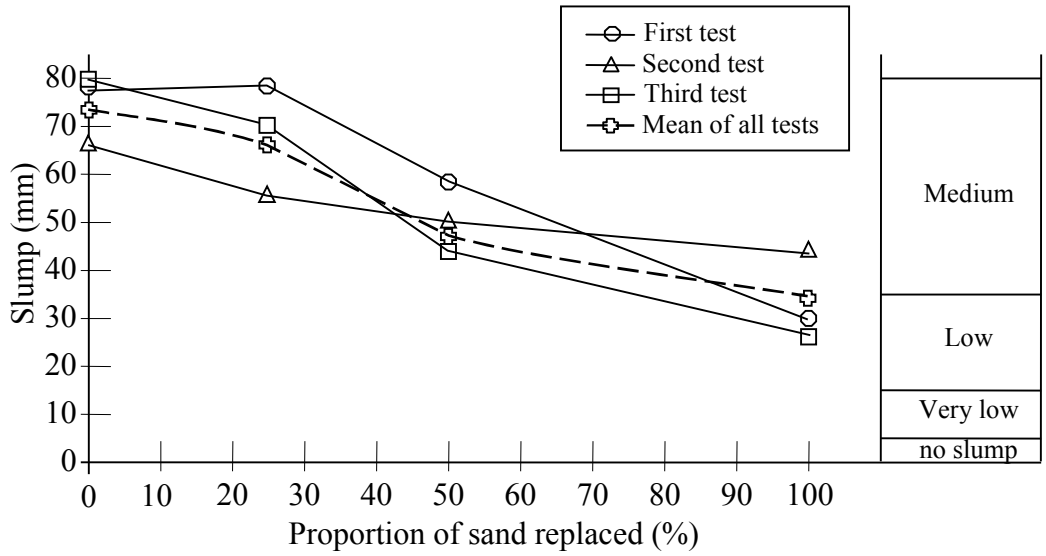

Fig. 4.4 Slump for concrete sand containing amber glass

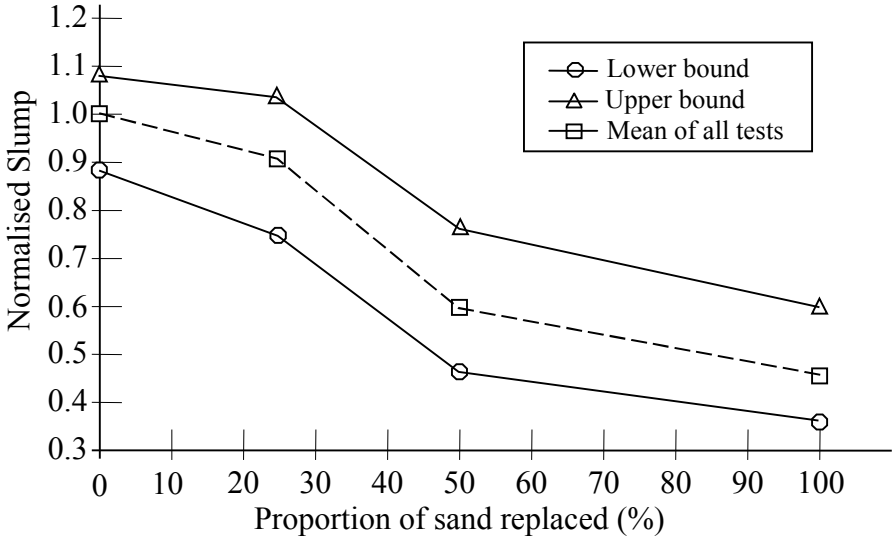

Fig. 4.5 Normalised slump for concrete containing amber glass

Figures 4.6 and 4.7 shows slump data for concrete containing green glass. The data show the same general trends as were noted for flint and amber glass i.e. replacement of approximately one quarter of the sand has negligible effect on concrete workability.

The colour of a glass is determined by the addition of small quantities of different chemical/ elements but the general chemical composition of the glasses is common, i.e. predominantly silica. Furthermore, all waste glasses were washed and crushed in identical ways and so should have similar surface texture and particle shape (as supported by the images in Figures 3.12 to 3.17) so that interspatial fiction resistance and particle interlock should not be affected by colour. Hence, it is expected that glass colour would not be an important factor in determining the workability of a concrete containing waste glass as fine aggregate.

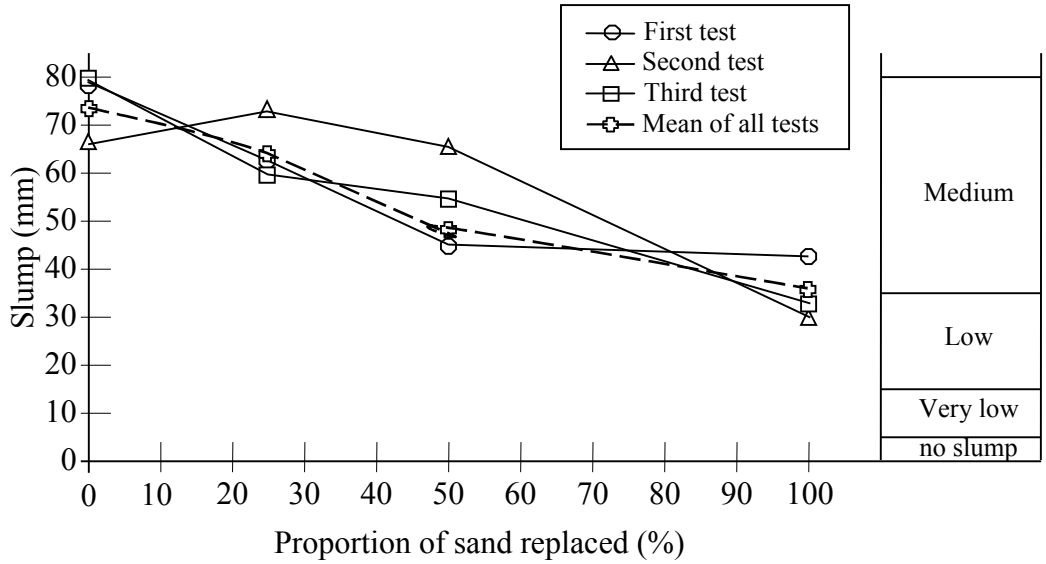

Fig. 4.6 Slump for concrete containing green glass

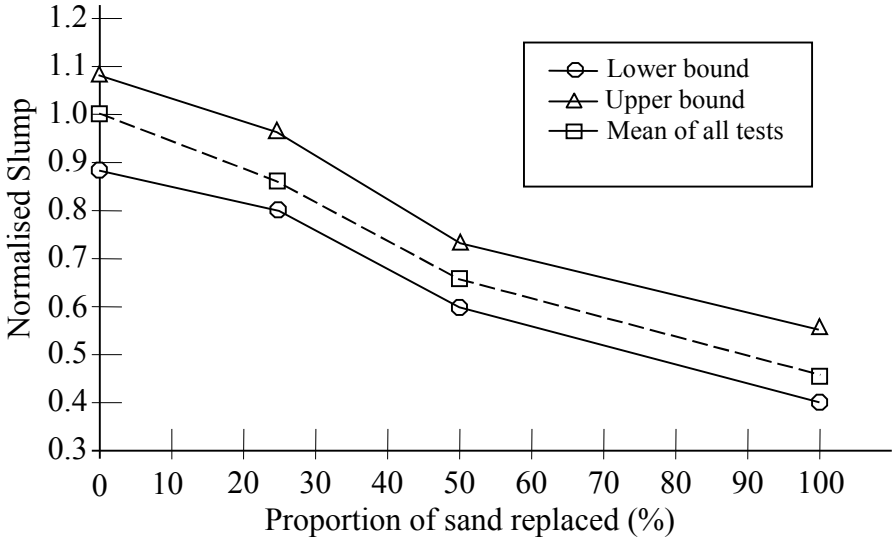

Fig. 4.7 Normalised slump for concrete containing green glass

Figures 4.8 and 4.9 show slump data for concrete containing a mixture of glasses. The mixture comprised a combination of flint, amber and green glasses in the proportions (by weight) that would be typical of mixed glass from a glass recycling source i.e. 65% clear, 25% amber, 10% green (Section 1.2). Tests were conducted using waste glasses which were washed for 30 minutes prior to crushing. Once again, the data exhibit no major change in slump for upto replacement of one quarter of sand aggregate by crushed glass and a subsequent approximately linear decrease up to complete replacement of the fine aggregate.

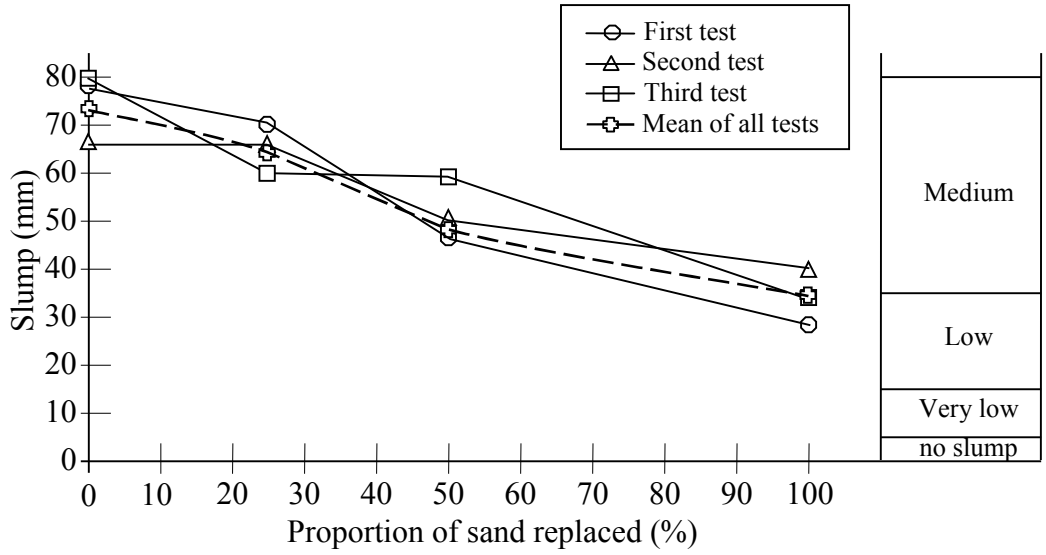

Fig. 4.8 Slump for mixed washed glass concrete containing

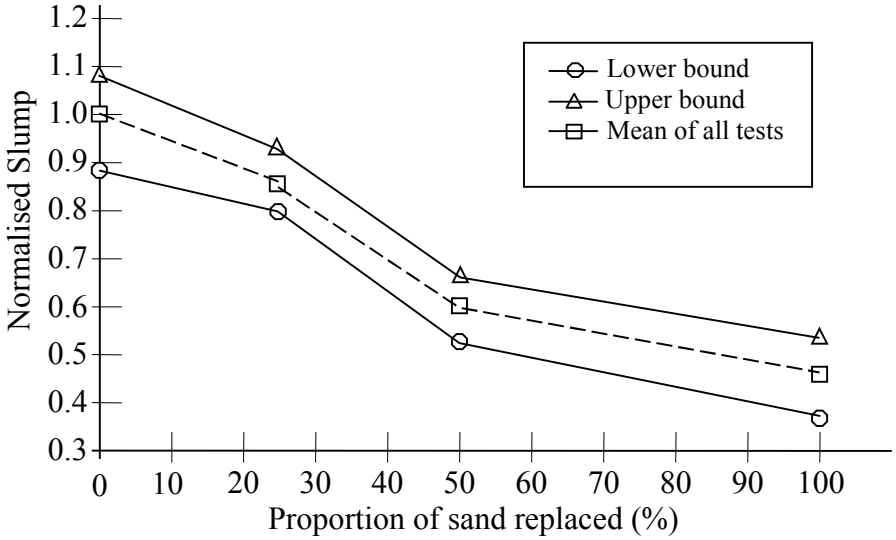

Fig. 4.9 Normalised slump for concrete containing mixed washed glass

Figures 4.10 and 4.11 show slump data for concrete containing a mixture of unwashed glasses which simulates that found in a mixed colour recycling bank. The results are very similar to those obtained for the mixture of washed glasses (Figures 4.8 and 4.9), Since the bottles used in this research had contained only water, soft drinks and low-alcohol drinks, any liquid left in the bottles would represent only a small proportion of the liquid (water) within in the concrete and so it was expected that the washed/ unwashed state of the waste glass would have little, if any, effect on the workability.

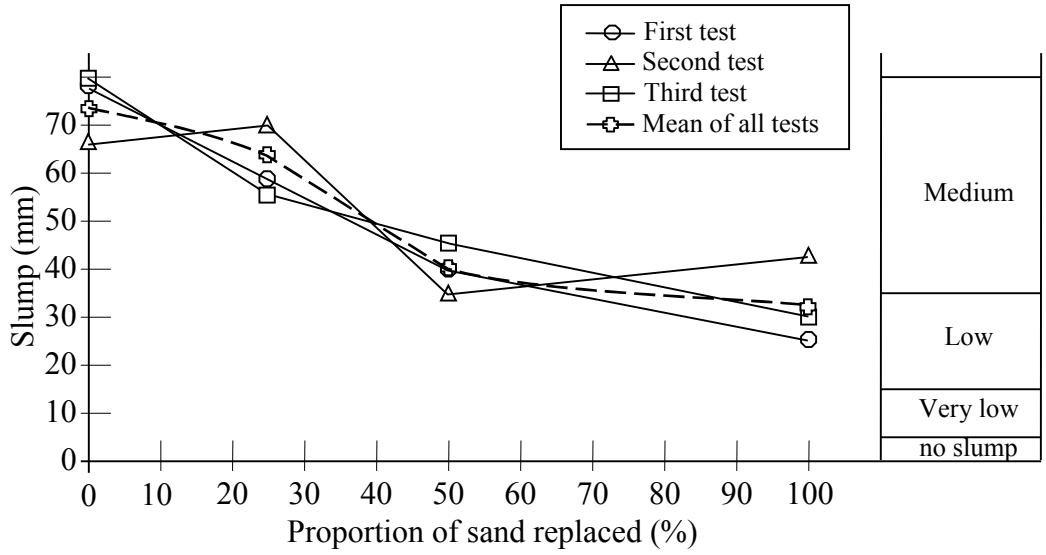

Fig. 4.10 Slump for mixed unwashed glass concrete containing

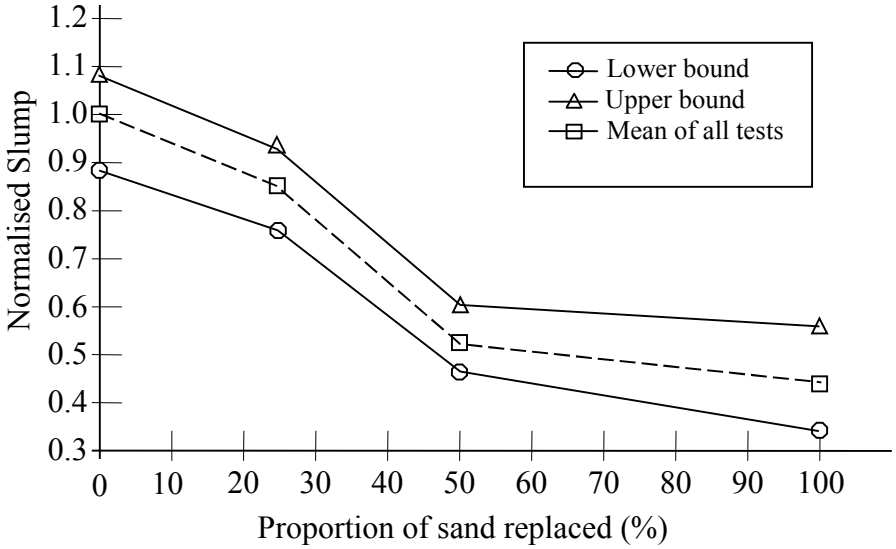

Fig. 4.11 Normalised slump for concrete containing mixed unwashed glass

Figure 4.12 summarises the flow characteristic of slump test for crushed waste glass with different colours and mixing ratios for replacement of fine aggregate in concrete. The results demonstrate that the slump values decrease as the amount of crushed waste glass in the concrete mix increases, regardless of the colour (flint, amber and green).

Mean slump values have decreased by 9-15%, 35-47% and 53-57% due to replacement of 25%, 50% and 100% (respectively) of the conventional fine aggregate by waste glass.

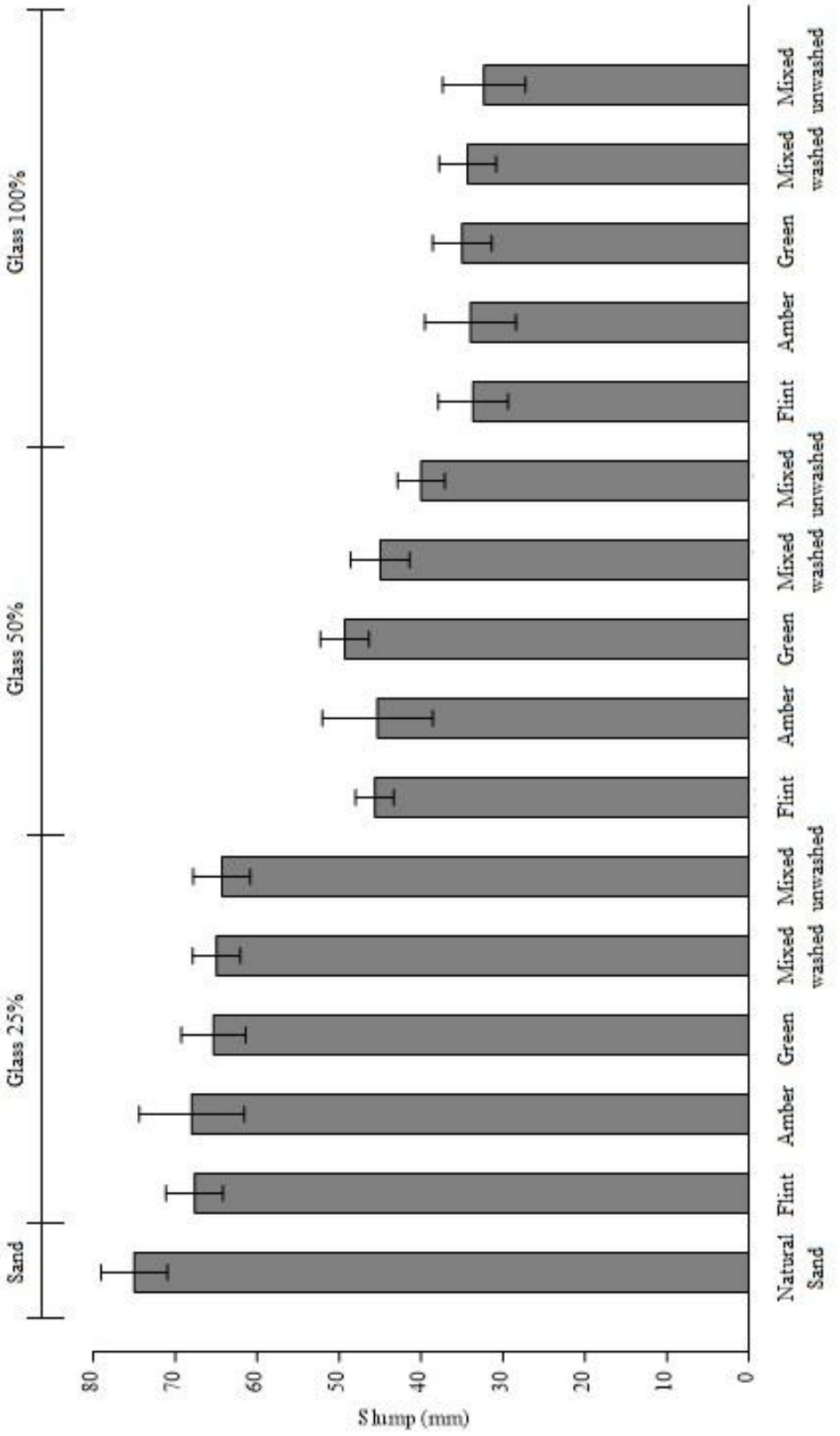

Fig. 4.12 Summary of slump data

4.1.3 Flow table values

Table 4.3 contains all flow table data. The values do not indicate any effects due to hardening or drying of the mix between tests, i.e. there is no consistent trend of decrease in value with repetition of a test. For conventional concrete, the flow table values are very similar to these required for F3 class concrete (BSI 8500-1, 2006) i.e. 400-510mm. This class of concrete would be used for strip footings or normal reinforced concrete in slabs, beams, walls and columns.

Figure 4.13 shows how the flow table value is influenced by proportion of flint glass, which is used as fine aggregate. It is apparent that flow table value decreases as the proportion of glass used as the fine aggregate increases. Figure 4.14 contains Flow table data which have been 'normalised' by dividing actual values by the mean Flow table value for conventional concrete. The data indicate an almost linear relationship between normalised Flow table value and percentage of fine aggregate replaced by glass. However, there is inherent variation of Flow table value for any concrete (as shown in Table 4.3). So there is no strict justification for assuming that a particular batch of concrete which gave the measured upper bound flow value for concrete containing glass would have given the upper bound value for the corresponding conventional concrete if there had been no incorporation of glass aggregate. Hence it is important to consider other combinations of upper and lower bound flow values.

Boundary values to estimate the linear homogenous restrictions on whether its wide or narrower bound, which facilitate sensitivity analysis to be undertaken.

If, FT_{NU} = Upper bound flow value for normal concrete

FT_{NL} = Lower bound flow value for normal concrete

FT_{GU} = Upper bound flow value for concrete containing glass

FT_{GL} = Lower bound flow value for concrete containing glass

Then, for 25% replacement of fine aggregate by clear (Flint) glass

$$\left(\frac{FT_{GU}}{FT_{NL}}\right) = \left(\frac{490}{500}\right) = 0.98 \quad \text{and} \quad \left(\frac{FT_{GL}}{FT_{NU}}\right) = \left(\frac{460}{520}\right) = 0.88$$

These values and those corresponding to sand replacements of 50% and 100% are shown in Figure 4.14 as the "extreme" upper and lower bounds respectively. When the Flow table data are presented in this way (Figure 4.14) then the influence of incorporating fine glass aggregate could be described in two ways, i.e.

a) Up to 25% of conventional fine aggregate can be replaced by glass without any significant effect on flow value. The flow value decreases in direct proportion to the amount of sand replacement in excess of 25%.

Or

b) There is an approximately liner relation between decrease in flow value and percentage of conventional fine aggregate replaced by glass.

The decrease in flow value is such that there can be a significant change in the workability categorisation of the mix – the conventional concrete fell into the 'upper medium' designation whilst at 100% sand replacement the mix had fallen to the bottom of the 'low' category or even into the 'very low' range. The flow table test has indicated a much more severe decrease in workability than the slump test and this may be due to the amounts of energy dissipated in friction in each test (due to the extent of flow in the tests) as mentioned in Section 4.1.2, or the size of the voids/ pores in the concrete containing glass inhibiting liquefaction of the cement paste by acting as a cushion.

Interestingly the decrease in the numerical value obtained from the flow table test is of the order of 30% for complete replacement of the sand aggregate and the same percentage decrease was previously reported for the slump test (section 4.1.2).

Table 4.3 Workability Flow table verses percentage glass in the concrete mixes

Glass replaces sand (%)	Flow table test (mm) ranged in order test, i.e. 1st, 2nd & 3rd					
	Natural sand	**Flint glass**	**Amber glass**	**Green glass**	**Mixed washed**	**Mixed unwashed**
0	520, 510, 500					
25		460, 490, 475	485, 460, 480	480, 490, 470	465, 475, 480	480, 460, 470
50		450, 430, 410	470, 440, 460	460, 460, 430	460, 450, 420	430, 450, 420
100		350, 380, 360	375, 340, 375	350, 370, 350	350, 360, 350	350, 325, 340

	Flow table test (mm) in mean values					
	Natural sand	**Flint glass**	**Amber glass**	**Green glass**	**Mixed washed**	**Mixed unwashed**
0	510					
25		475	475	480	473	470
50		430	457	450	443	433
100		363	363	357	353	338

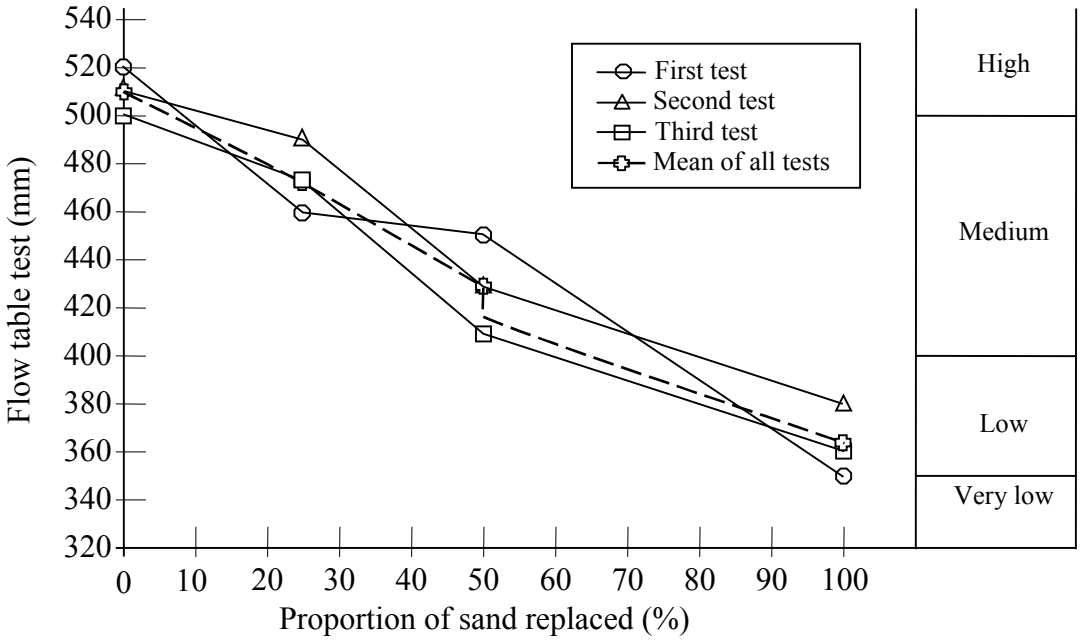

Fig. 4.13 Flow table test of concrete containing flint glass

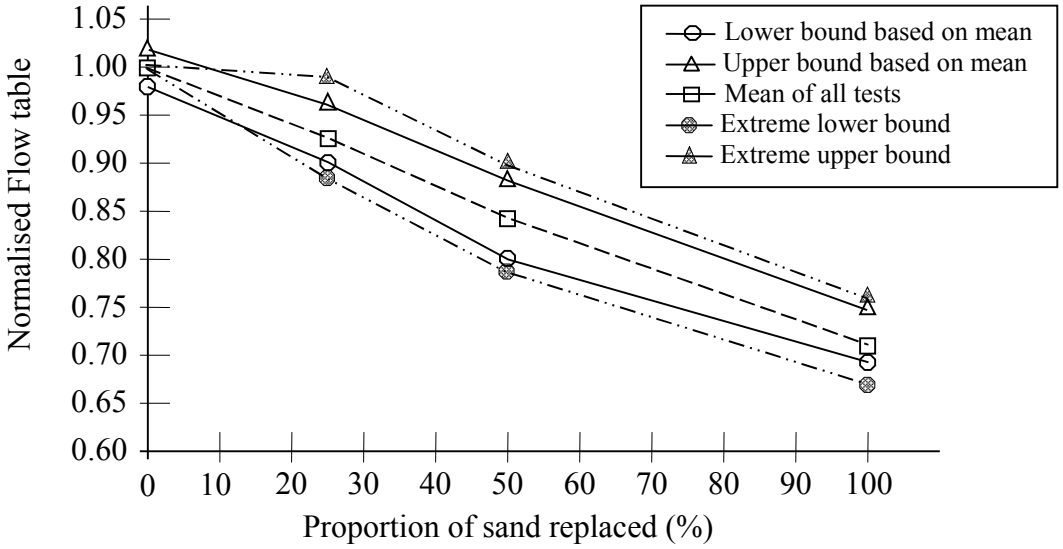

Fig. 4.14 Normalised flow table for concrete containing flint glass

The concrete containing amber glass showed the same general trends as for the flint glass (Figure 4.15). After discarding an anomalous result for the first test on a mix with 50% sand replacement the variation of normalised flow table value with percentage sand replacement is as shown in Figure 4.16. Once again, there is clear evidence of a reduction in workability with increasing glass content (upto 50% glass a decrease of 15% of the numerical value for conventional concrete). However, as for the clear (Flint) glass it may be that upto 25% of conventional fine aggregate can be replaced without significant effect on flow value.

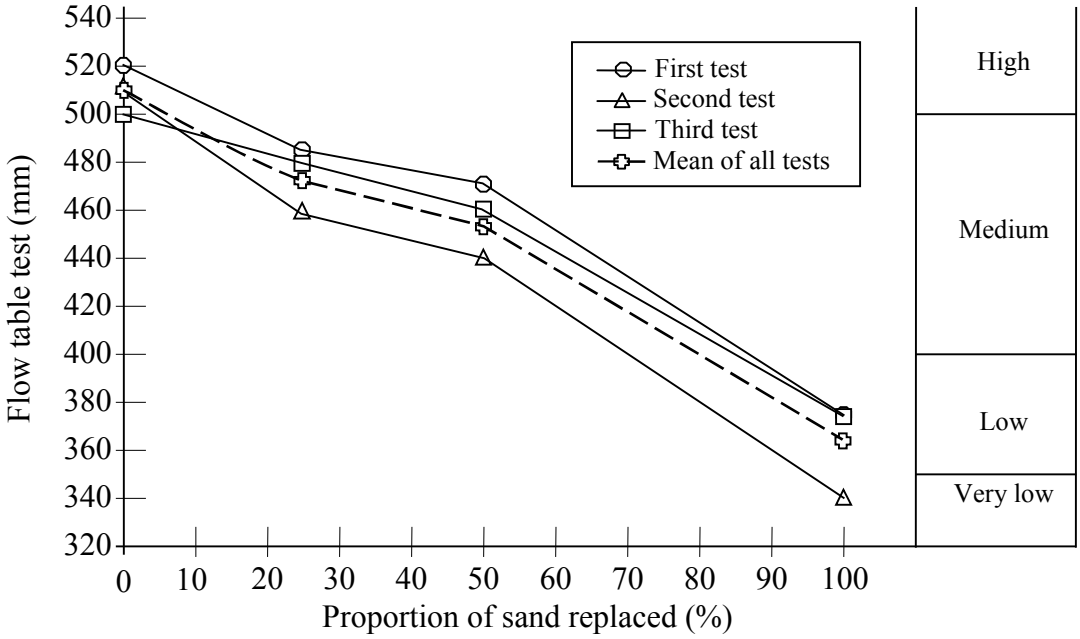

Fig. 4.15 Flow table test of concrete containing amber glass

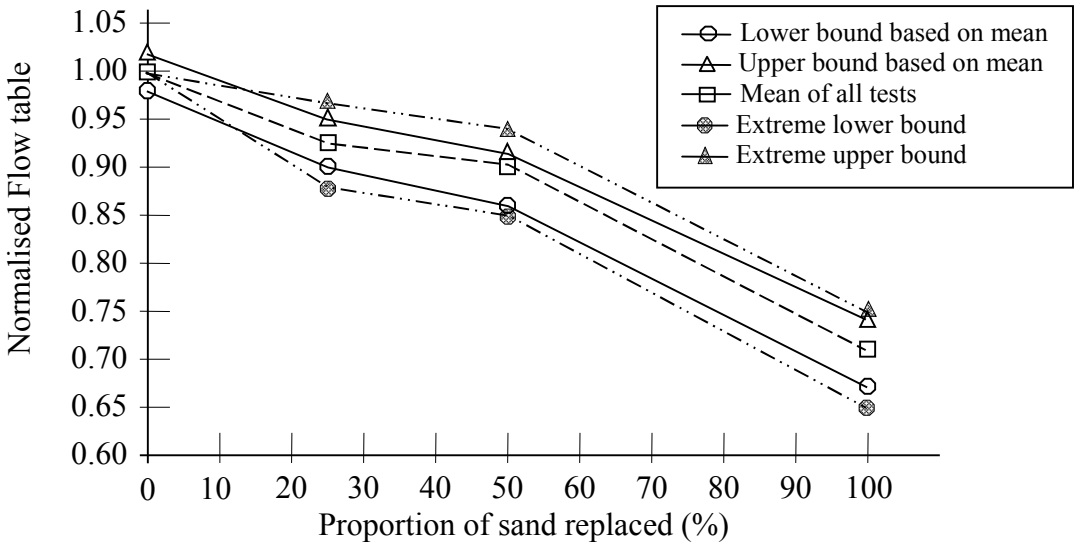

Fig. 4.16 Normalised flow table for concrete containing amber glass

Figures 4.17 and 4.18 show the data obtained for concrete containing green glass. The Figures show trends which are very similar to those seen for clear (Flint) glass and so the same comments are applicable. Interestingly the decrease in the numerical value obtained from the flow table test is of the order of 70% for complete replacement of the sand aggregate and the same percentage decrease was previously reported for the slump test (section 4.1.2).

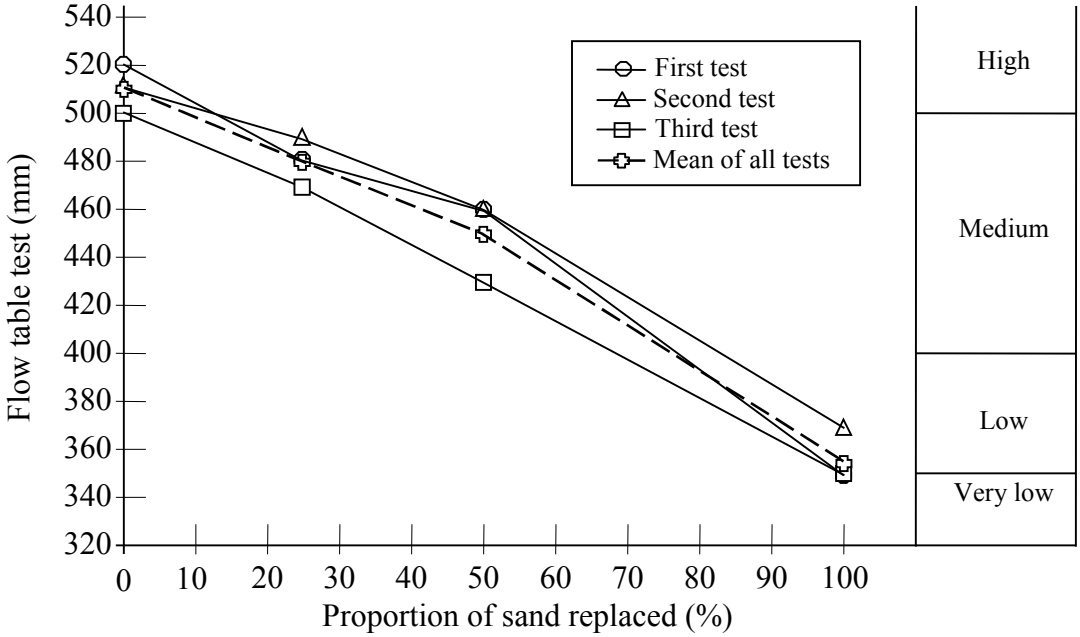

Fig. 4.17 Flow table test of concrete containing green glass

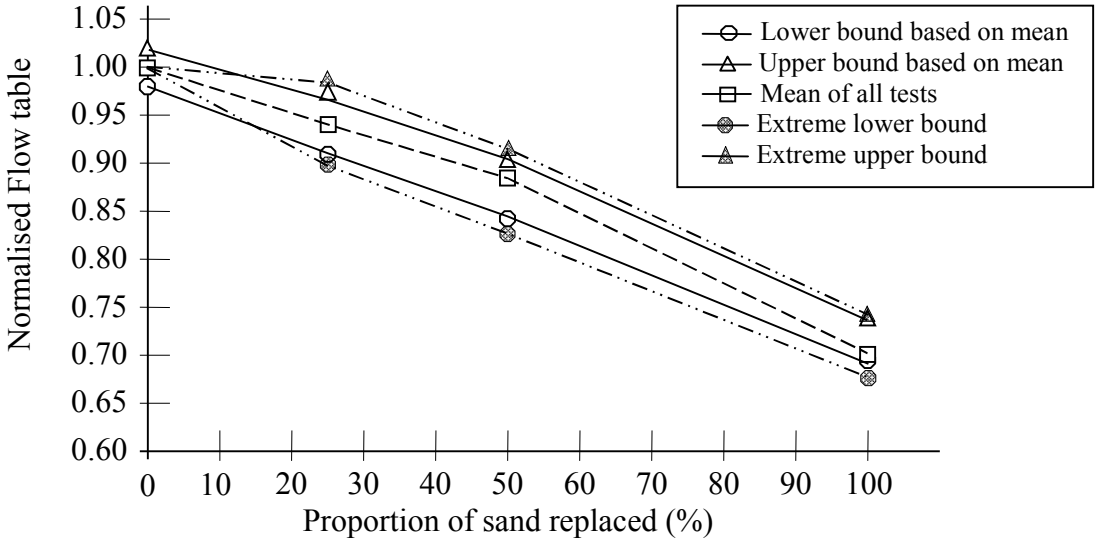

Fig. 4.18 Normalised flow table for concrete containing green glass

Figures 4.19 and 4.20 shows the effect on Flow table value of incorporating mixed washed glass into concrete to the flow table value of the mix. The trend of decreasing workability, which was observed with selected colours of glass, is evident again.

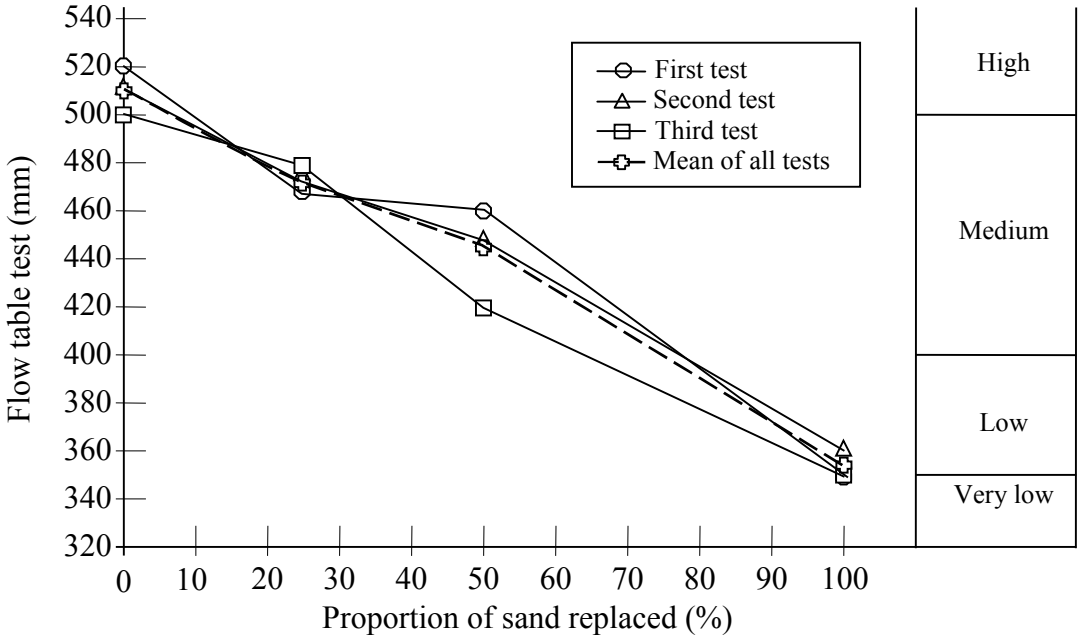

Fig. 4.19 Flow table test of concrete containing mixed washed glass

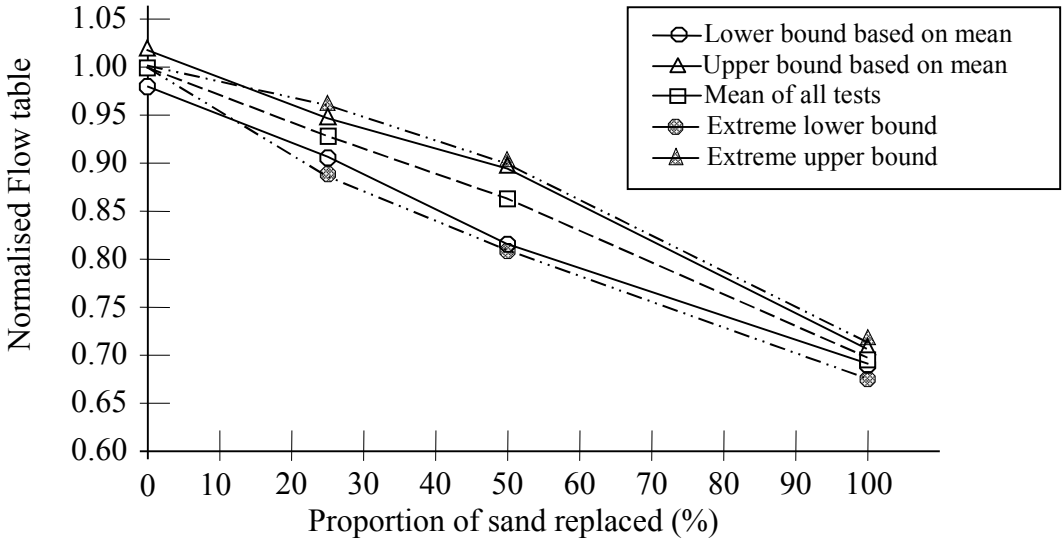

Fig. 4.20 Normalised flow table for concrete containing mixed washed glass

Figures 4.21 and 4.22 show that for unwashed glass aggregate there is an unequivocal tendency for the Flow table value to decrease with increasing proportion of glass in the fine aggregate content. At 25% glass replacement, the flow decreased slightly (by 20-60 mm); with 50% glass replacement the flow decreased by 50-100mm, in the case of 100% glass replacement flow decreased by 150-195mm. The relationship between normalised Flow table value and percentage of fine aggregate which comes from waste glass is essentially linear. Complete replacement of the sand in the concrete used in this investigation resulted in the Flow table value being reduced by about one-third. It is believed that this loss is due to the angularity of the waste glass aggregate which produces high internal friction when the concrete has to flow and this could have implications for pumping concrete containing glass.

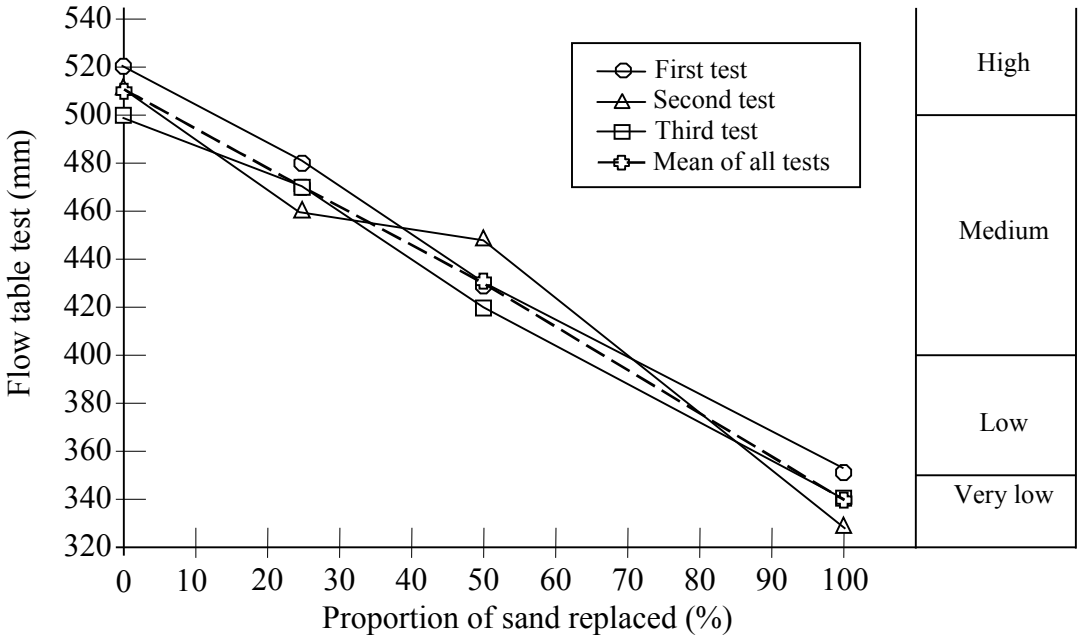

Fig. 4.21 Flow table test of concrete containing mixed unwashed glass

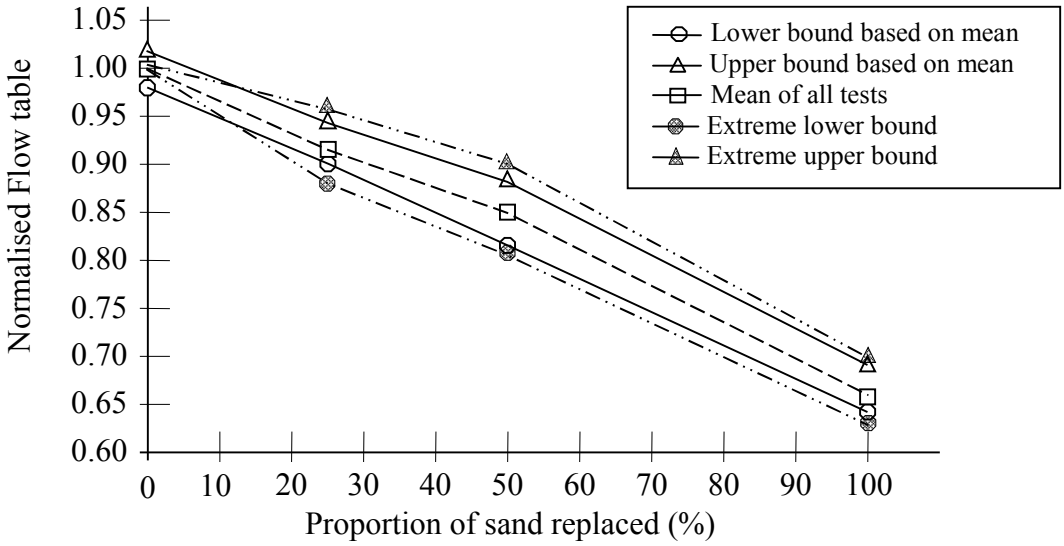

Fig. 4.22 Normalised flow table for concrete containing mixed unwashed glass

The rate of decrease of normalised Flow value with respect to percentage of sand which is replaced is essentially the same for both washed and unwashed glass, i.e. the presence of contaminants from drinks (such as sugars) has no effect on flow of fresh concrete.

4.1.4 Setting times of the washed and unwashed glass

Table 4.4 contains the data relating to initial and final setting times of all mortar mixes made with different amounts of fine aggregate made from waste glass. For each mix the three values measured are sufficiently close for them to be represented by their mean - Figure 4.23.

Both initial and final setting times increase linearly with the amount of washed waste glass which is used as fine aggregate in the concrete mortar essentially - see Figure 4.24. As a consequence of 100% replacement of sand by glass the final setting times were in excess of 8 hours for both washed and unwashed glass aggregate and they were greater than the time for natural sand by 23% and 38%. However, for concrete containing washed glass the rate of increase of setting times, when expressed as a percentage of the respective time for conventional concrete, with respect to proportion of fine aggregate replaced was approximately the same for both initial and final setting.

For concrete containing unwashed glass aggregate the data in Figure 4.24 could be interpreted as showing a non-linear relationship between setting time (both initial and final) and proportion of glass within the fine aggregate. However, an alternative representation of the data is that the use of unwashed glass caused the washed relationship to be displaced upwards. In other words the onset of setting (both initial and final) is delayed by a fixed amount due to the presence of contaminants. For initial setting the delay is approximately 21 minutes and for final setting the delay is approximately 45 minutes. The delay in initial and final setting of the concrete containing waste glass may be due to several reasons, including the presence of impurities, such as sugar, in the glass surface layer, w/c ratio, and low water absorption of the glass relative to the natural aggregates.

Table 4.4 Setting times of waste glass mortar

Waste glass contents mortar	Setting times ranged in order of determination, i.e. 1st, 2nd & 3rd test, and mean values			
	Initial setting time (h:min)		Final setting time (h:min)	
	washed	unwashed	washed	unwashed
Natural sand	2:30, 2:50, 2:45 } 2:41		6:30, 6:50, 6:40 } 6:40	
Waste glass 25%	3:15, 3:10, 2:45 } 3:03	3:30, 3:45, 3:00 } 3:25	6:50, 6:55, 7:10 } 6:58	7:30, 7:50, 7:35 } 7:38
Waste glass 50%	3:20, 3:15, 2:55 } 3:10	3:40, 3:45, 3:15 } 3:33	7:20, 7:10, 7:30 } 7:20	8:25, 8:10, 7:55 } 8:10
Waste glass 100%	3:40, 3:20, 3:30 } 3:30	3:50, 4:05, 3:40 } 3:51	8:10, 8:05, 8:30 } 8:15	9:10, 9:15, 9:30 } 9:18

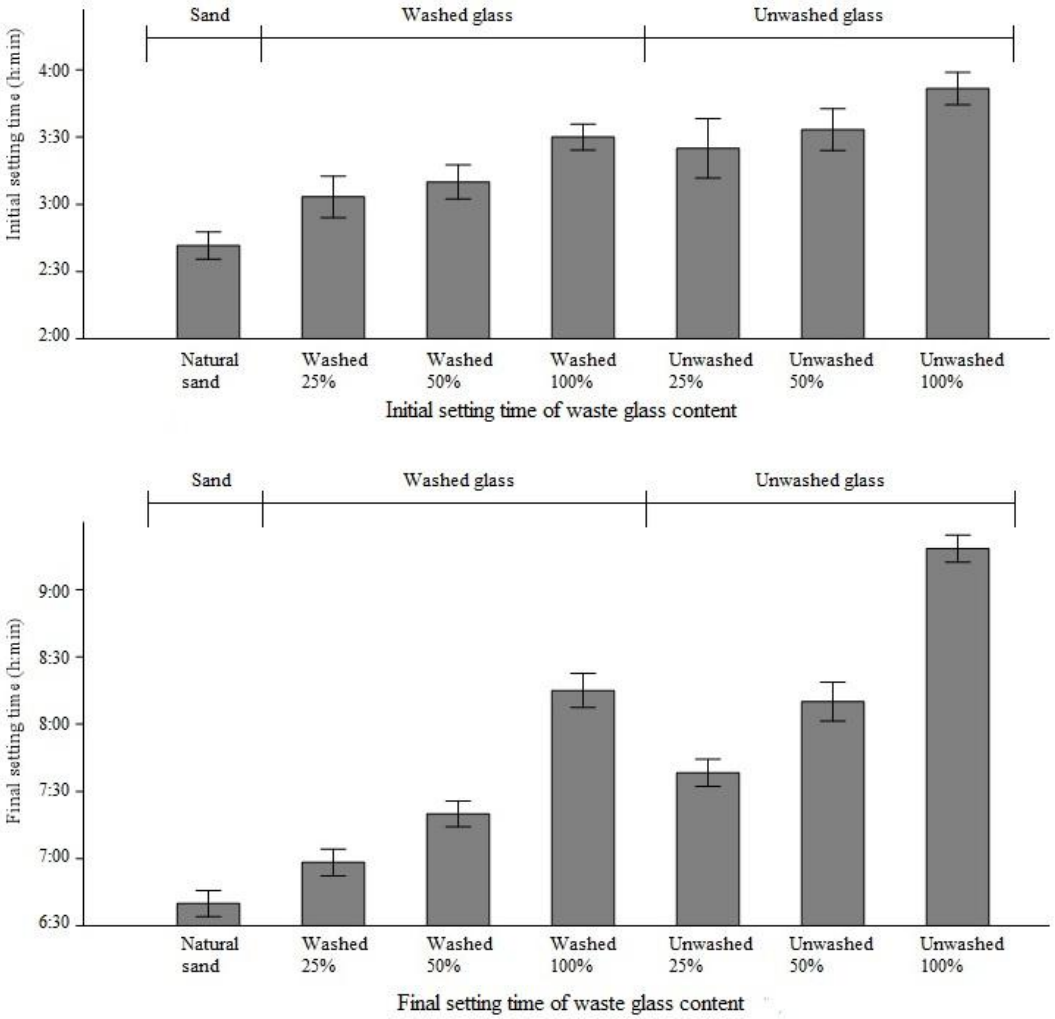

Fig. 4.23 Setting times for mortars containing natural and glass aggregate

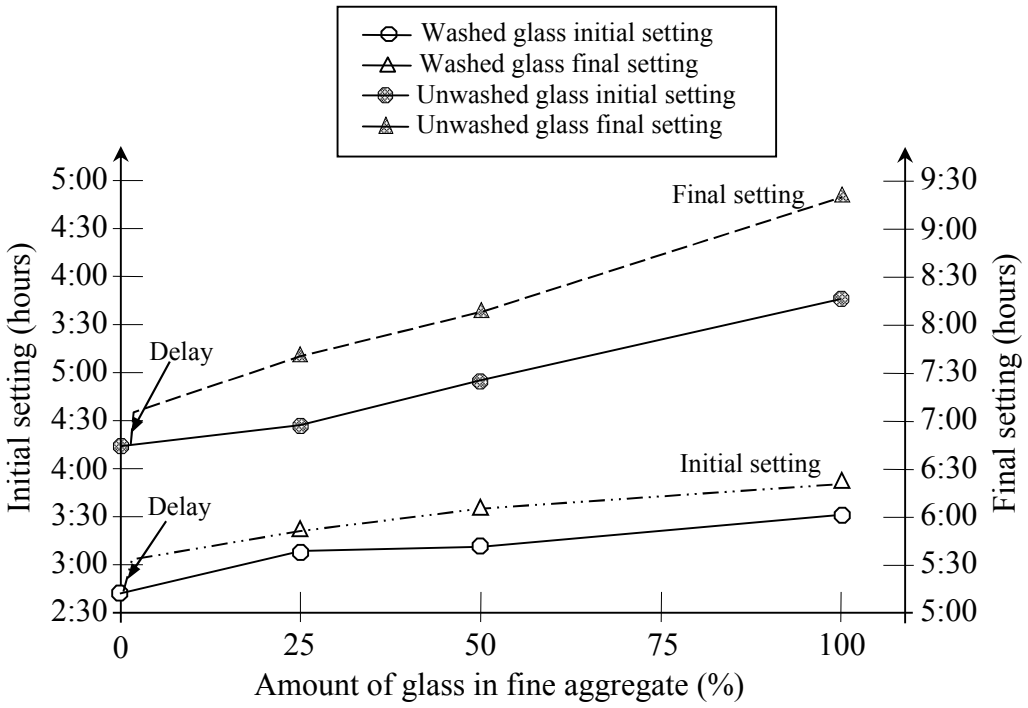

Fig. 4.24 Initial and final setting times

4.2 Hardened concrete

The compressive strength of hardened concrete is usually considered as its most important engineering property. However, ideally the concrete should be designed with the appropriate emphasis on each of its various properties, and not solely with a view to obtaining the maximum possible compressive strength.

4.2.1 Density of hardened concrete

The density of each cube was determined by weighing it in air and water as described in Section 3.4.9. Table 4.5 contains the values of density obtained from cubes the first time that they were measured. For the conventional concrete the values fell in a narrow band, i.e. from 2382kg/m³ to 2405kg/m³ at 28 days which demonstrated that cubes were made and cured in a consistent way. The foregoing values fall within the typical density range quoted for this mix of concrete, i.e. from 2300 to 2425 kg/m³ (Neville, 1995) indicating that there was nothing unusual with the concrete used in the research. The mean specific gravity for the conventional cubes ranged from 2.382 to

2.397, which agrees with normal values quoted by Neville (1995) for the concrete mix used in this research, i.e. 1:2:4.

Density values determined after differing curing times also indicate consistency of value (within a group) thereby confirming suitable experimental techniques. The mean density values suggest a gradual increase in density during the first 28 days of curing.

Table 4.5 Density and specific gravity data for conventional concrete

Age (Days)	Density (kg/m^3)			Specific gravity		
	Values	Range	Mean value	Values	Range	Mean value
1-day old	2358 2339 2345	2358 to 2358	2347	2.391 2.400 2.399	2.391 to 2.400	2.397
7-days old	2369 2379 2386	2369 to 2386	2378	2.380 2.389 2.388	2.380 to 2.389	2.386
28-days old	2382 2397 2405	2382 to 2405	2395	2.377 2.370 2.389	2.370 to 2.389	2.379
112-days old	2350 2366 2427	2350 to 2427	2381	2.362 2.378 2.384	2.362 to 2.384	2.375
365-days old	2395 2402 2383	2383 to 2402	2393	2.383 2.397 2.369	2.369 to 2.397	2.383

Tables 4.6, 4.7 and Figure 4.25 contains density data for the cubes made from concrete where the fine aggregate was replaced by waste glass. As with the conventional concrete the density values for cubes within each age cube demonstrate that a consistent sample preparation methodology was used and there is a trend for the density to increase with curing time.

If one compares mean density values in Tables 4.6 and 4.7 for the same curing period then the values for concrete containing waste glass are consistently lower than those for conventional concrete-by between 0.1% and 1.8%, however, there does not seem to be any trend relating to time.

Table 4.6 Density of concrete verses percentage in the concrete mixes (1-28 days)

Glass (%)	Density of concrete (kg/m³) in order of measurement, i.e. 1st, 2nd & 3rd test, and mean values					
	Natural Sand	**Flint glass**	**Amber glass**	**Green glass**	**Mix washed**	**Mix unwashed**
1-day old						
0	2358 2339 *Mean* 2345 (*2347*)					
25		2329 2338 (*2344*) 2366	2337 2344 (*2336*) 2326	2317 2348 (*2345*) 2370	2326 2356 (*2343*) 2348	2357 2342 (*2344*) 2334
50		2332 2365 (*2345*) 2338	2328 2341 (*2331*) 2325	2340 2326 (*2340*) 2353	2349 2328 (*2343*) 2351	2350 2331 (*2343*) 2347
100		2342 2353 (*2342*) 2330	2355 2327 (*2338*) 2333	2338 2324 (*2329*) 2325	2346 2325 (*2334*) 2332	2348 2331 (*2335*) 2326
7-days old						
0	2369 2379 (*2378*) 2386					
25		2352 2369 (*2366*) 2376	2348 2378 (*2360*) 2355	2326 2381 (*2355*) 2358	2379 2375 (*2367* 2346	2347 2356 (*2354*) 2358
50		2364 2376 (*2363*) 2349	2368 2352 (*2359*) 2358	2354 2337 (*2351*) 2361	2367 2378 (*2362*) 2342	2356 2358 (*2353*) 2344
100		2353 2364 (*2353*) 2343	2366 2337 (*2349*) 2345	2349 2334 (*2340*) 2338	2343 2347 (*2349*) 2358	2367 2325 (*2349*) 2356
28-days old						
0	2382 2397 (*2395*) 2405					
25		2391 2416 (*2397*) 2384	2386 2378 (*2380*) 2376	2368 2358 (*2358*) 2348	2356 2369 (*2364*) 2368	2362 2368 (*2362*) 2355
50		2361 2388 (*2364*) 2342	2380 2376 (*2370*) 2353	2355 2360 (*2358*) 2358	2365 2354 (*2359*) 2359	2365 2352 (*2364*) 2375
100		2353 2339 (*2357*) 2378	2379 2343 (*2352*) 2335	2353 2368 (*2359*) 2356	2362 2333 (*2356*) 2372	2346 2361 (*2354*) 2355

Table 4.7 Density of concrete verses percentage in the concrete mixes (112-365 days)

Glass (%)	Density of concrete (kg/m³) in order of measurement, i.e. 1st, 2nd & 3rd test, and mean values					
	Natural Sand	**Flint glass**	**Amber glass**	**Green glass**	**Mix washed**	**Mix unwashed**
112-days old						
0	2350 2366 (*2381*) 2427					
25		2383 2362 (*2375*) 2379	2366 2386 (*2374*) 2371	2378 2348 *2359*) 2352	2376 2360 (*2365*) 2358	2360 2355 (*2367*) 2387
50		2358 2370 (*2364*) 2364	2363 2379 (*2366*) 2355	2348 2372 *2359*) 2357	2376 2364 (*2366*) 2357	2356 2368 (*2364*) 2369
100		2367 2361 (*2362*) 2358	2369 2354 (*2365*) 2373	2366 2347 *2357*) 2359	2373 2358 (*2362*) 2354	2368 2381 (*2358*) 2324
365-days old						
0	2395 2402 (*2393*) 2383					
25		2395 2384 (*2393*) 2401	2392 2387 (*2386*) 2379	2374 2382 (*2382*) 2390	2376 2398 (*2386*) 2384	2390 2365 (*2381*) 2387
50		2383 2377 (*2383*) 2388	2372 2386 (*2372*) 2357	2401 2382 (*2379*) 2353	2367 2372 (*2375*) 2386	2384 2387 (*2380*) 2370
100		2379 2365 (*2375*) 2380	2378 2381 (*2374*) 2364	2381 2350 (*2368*) 2373	2370 2366 (*2367*) 2365	2376 2371 (*2370*) 2363

Figure 4.25 also shows that replacement of more than 25% fine aggregate by waste glass actually causes the density of the resultant concrete to decrease by 0.1% to 1.6%. This change is probably due to the glass having a lower density than the natural sand which it has replaced.

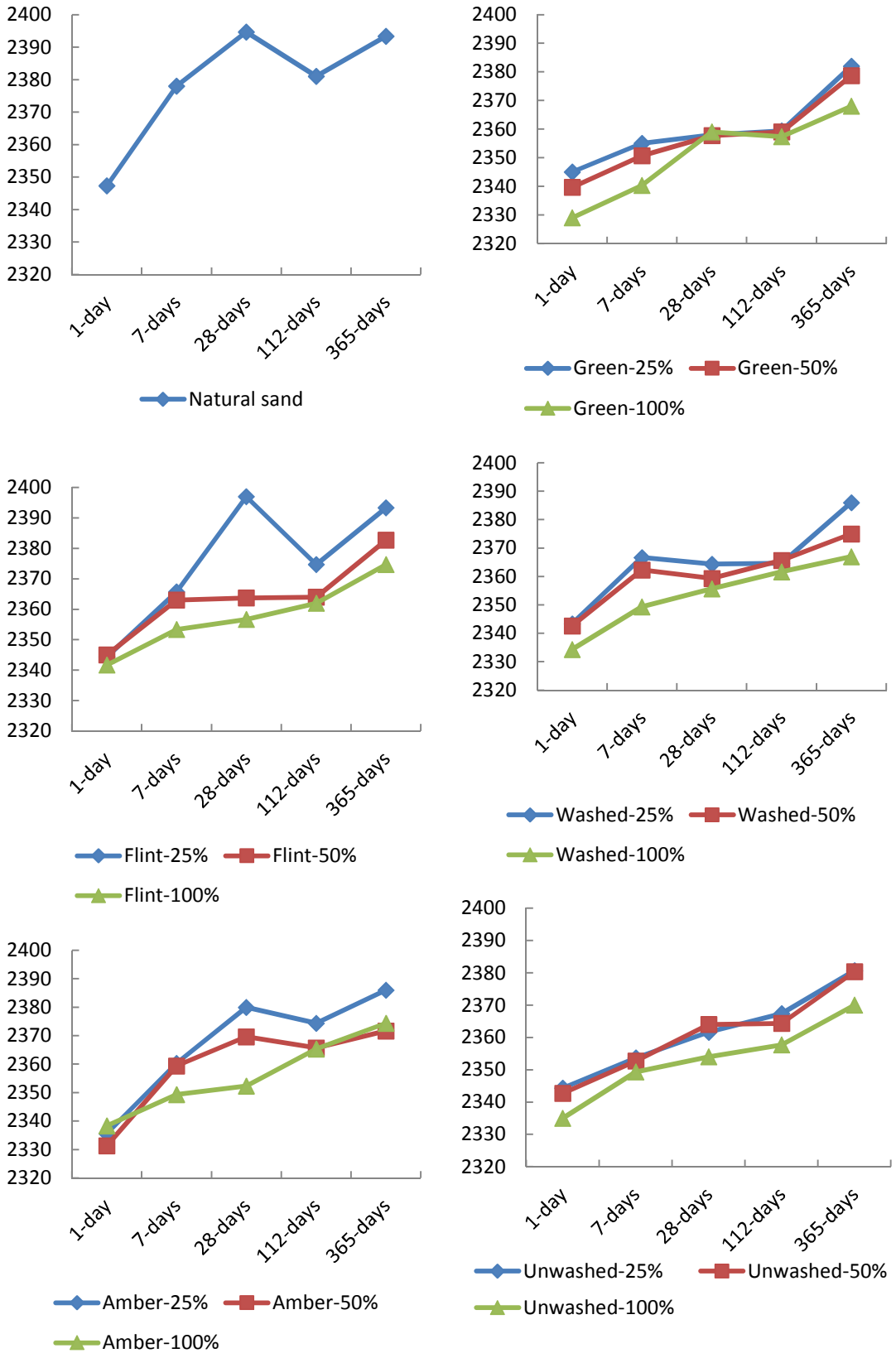

Fig. 4.25 Density of concrete

4.2.2. Ultrasonic Pulse Velocity

The ultrasonic pulse velocity test has the considerable merit of being a non-destructive test which gives information about the interior of a concrete element. The test is, therefore, useful to detect cracking and voids, deterioration due to ASR and air voids content in the concrete. This is possible because ultrasonic pulses do not travel through air. The ultrasound has to travel around an air-filled crack or void so the transit time is longer in cracked or voided concrete than in sound concrete. Small defects often have little or no effect on transit times for the different directions of the concrete cube faces.

There is no unique relationship between ultrasonic pulse velocity and compressive strength but there is a general trend. Figure 4.26 (from Neville, 1995) contains indicative data for compressive strength and ultrasonic pulse velocity (UPV) of hardened concrete. From this Figure UPV values between 4 km/s and 5 km/s typically indicate a compressive strength of between 20 N/mm^2 and 60 N/mm^2, depending on whether a concrete cube is tested in a moist or dry state.

Ultrasonic pulse velocity (UPV) measurements were taken prior to compression testing of the concrete cubes, and the results are given in Table 4.8 and Figures 4.27 to 4.35. The variation of UPV with curing time for the conventional concrete used in this investigation is shown in Figure 4.27. Up to 28 days the difference between upper and lower bound UPV values is small, i.e. 0.11km/s (approximately 2% of the mean values), but for the relationship shown in Figure 4.26 this would correspond to a difference of upper and lower compressive strengths of between 3N/mm^2 and 9N/mm^2. After 28 days the range of UPV values at any time falls to a very small value, i.e. 0.05km/s, but for the relationship in Figure 4.26 this difference would still correspond to approximately 7N/mm^2 between upper and lower bound compressive strengths. Nevertheless the data in Figure 4.27 do show a consistent trend of increasing UPV with curing time and this would suggest an 'improvement' in the internal structure of the concrete with time. Using the mean UPV data and the relationship in Figure 4.26 this 'improvement' would correspond to the following mean compressive strengths; 22N/mm^2 (7days), 34N/mm^2 (28days), 40N/mm^2 (112days), 54N/mm^2 (365days).

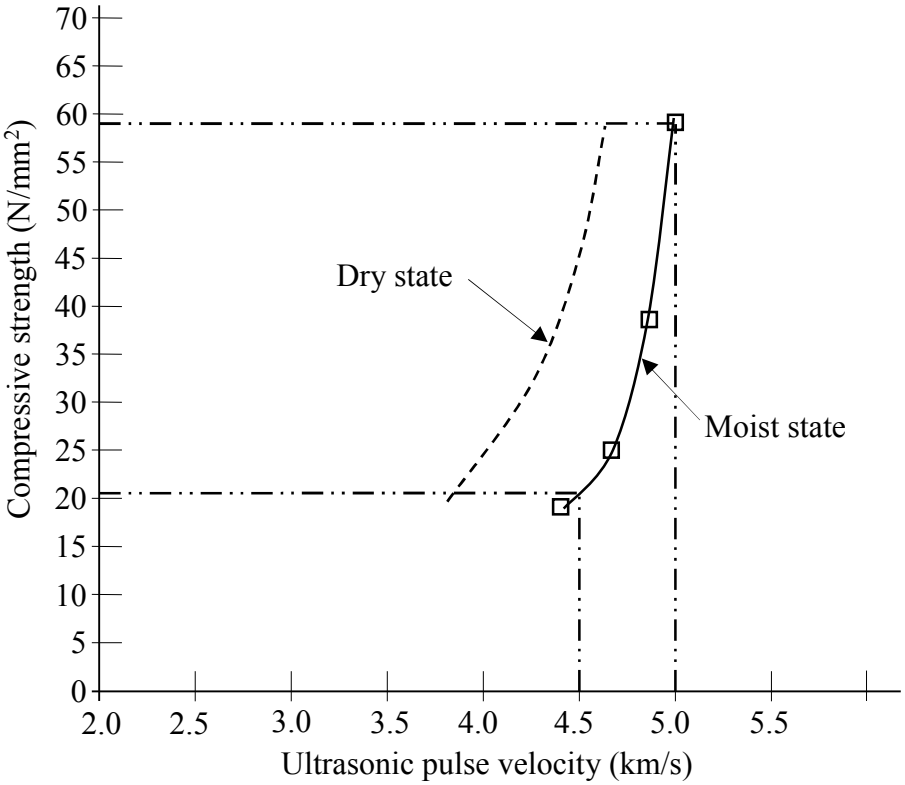

Fig. 4.26 Indicative relation between compressive strength and ultrasonic pulse velocity (Neville, 1995)

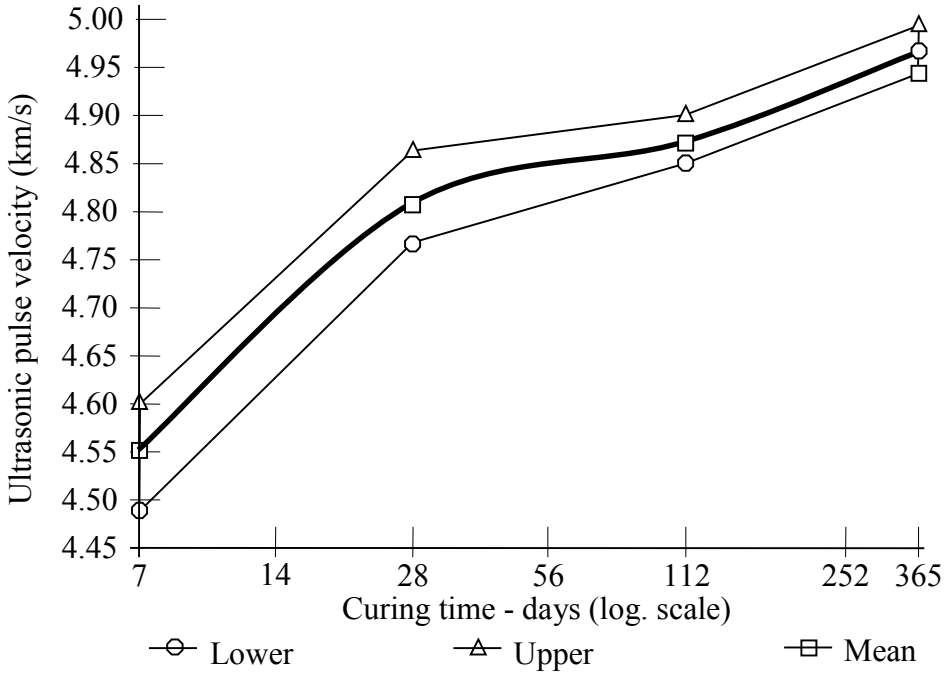

Fig. 4.27 Ultrasonic pulse velocity change with time for conventional concrete

As will be seen later (in Section 4.2.4) the difference between upper and lower bounds for compression strength of cubes with the same composition and age was about half that predicted by the UPV data for conventional concrete. Also, in Figure 4.27, the mean UPV data accurately reflect the trends indicated by the full set of values. Hence mean UPV data will be used in the rest of this section.

Graphs of mean ultrasonic velocity against curing time for concrete containing glass as fine aggregate are presented in Figures 4.28 to 4.35 inclusive. For any given curing time green glass consistently gave the highest UPV value. However, other colours of glass have very similar values and together they form a band with a width of approximately 0.1km/s, i.e. similar to that observed for all conventional concrete results. Furthermore, all concretes made with a single colour of glass exhibited the same shape of UPV versus curing time curve as for the conventional concrete (Figure 4.27). All the different mixes of concrete with glass aggregate showed an increase in UPV value with time –with the exception of the samples containing 50% of mixed washed glass at curing times of 112 and 356 days**,** this may be due to the pozzolanic nature of waste glass in a alkaline environment.

The data in Table 4.8 show that with the exception of two samples containing green glass the incorporation of glass resulted, at all curing times, in UPV values less than those for the equivalent conventional concrete. All samples containing 25% of green glass fine aggregate had for each curing time very similar UPV values to those for conventional concrete. In fact at 7 days and 28 days the concrete contain green glass exhibited UPV values which were 0.4% greater than those for the normal concrete. As there was no significant trend observed with respect to effect of glass aggregate on bulk density (Section 4.2.1), the higher velocities can be attributed either to a higher pulse velocity through glass and/ or to a marginally better bond being developed between the glass and the cement.

In Figures 4.28 to 4.30 the results for unwashed glass consistently fall, by a significant amount, below those for the washed glasses mixes. For 100% replacement of sand aggregate by washed glass the UPV reduced by up to 4% approximately whereas for unwashed glass the decrease is about double that. This difference possibly gives an

indication of the effect (which is likely to be detrimental) of contamination on the surface of the fine aggregate as was noted previously with regard to setting times (Section 4.1.4)

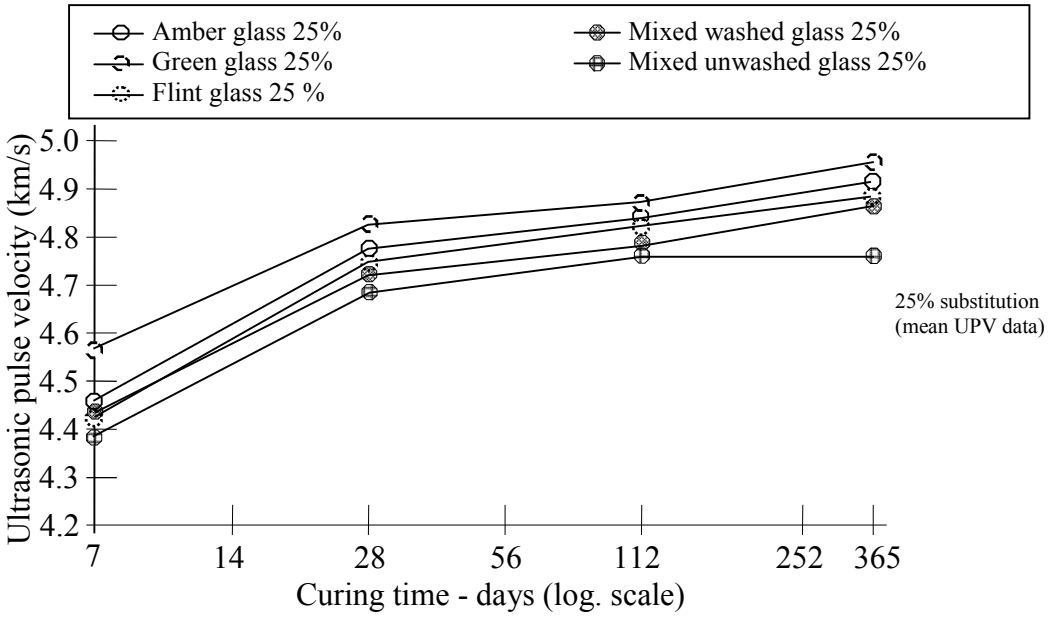

Fig. 4.28 Variation of ultrasonic pulse velocity with curing time for concrete with 25% of fine aggregate replaced by glass

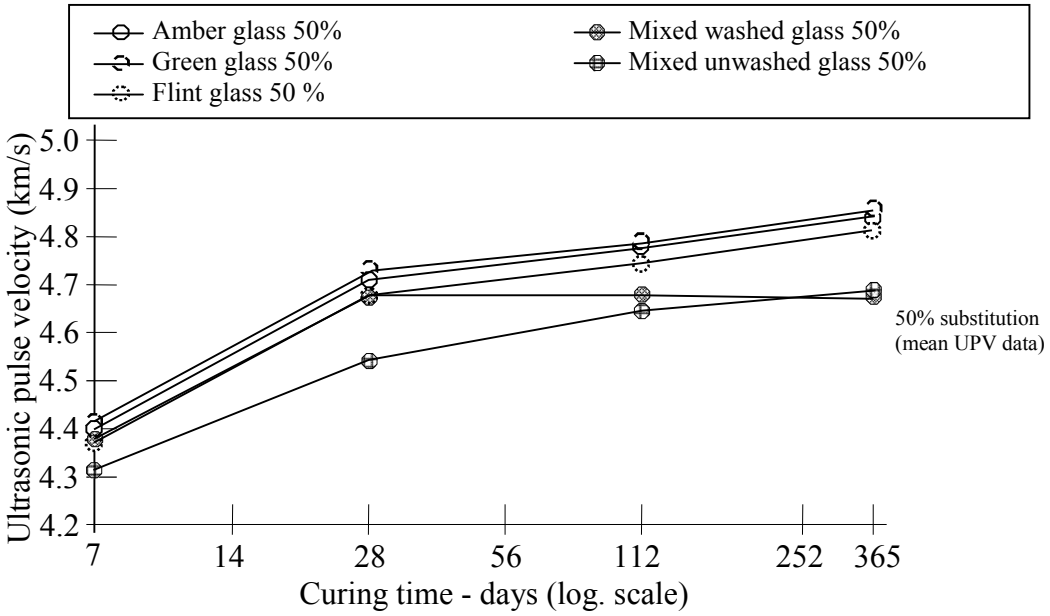

Fig. 4.29 Variation of ultrasonic pulse velocity with curing time for concrete with 50% of fine aggregate replaced by glass

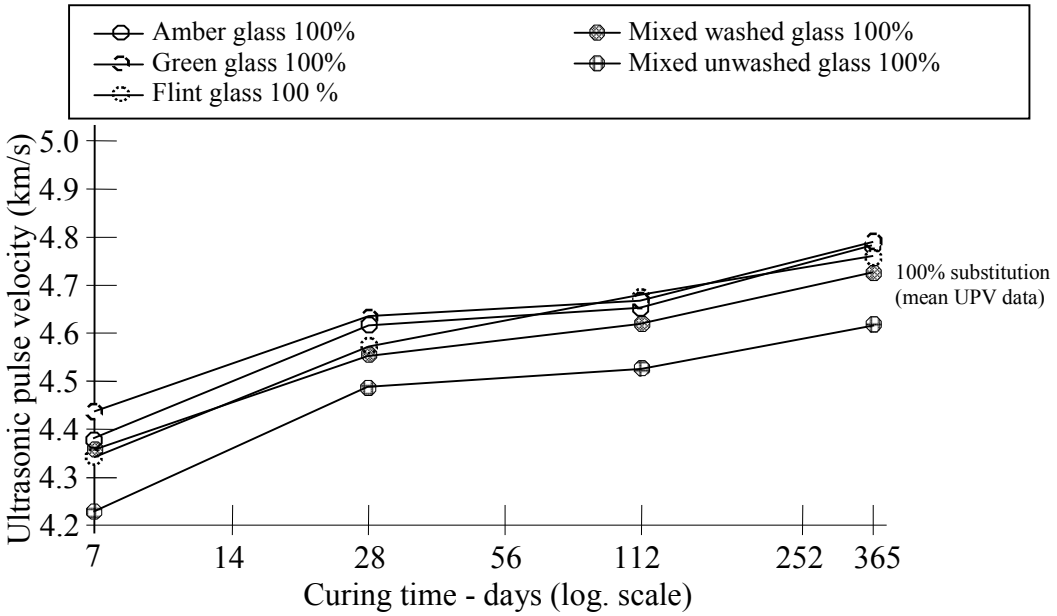

Fig. 4.30 Variation of ultrasonic pulse velocity with curing time for concrete with 100% of fine aggregate replaced by glass

For any colour of waste glass, including mixed washed and mixed unwashed, the UPV values decrease with increasing amount of conventional fine aggregate replaced by glass, for all curing times, as shown in Figure 4.31. Because the UPV for conventional concrete varied with curing time the velocity values for all concrete containing glass have been normalised by dividing them by the mean UPV of conventional concrete after 7 days curing.

Table 4.8 Ultrasonic pulse velocity data

Glass (%)	Ultrasonic pulse velocity (km/s) in order of measurement, i.e. 1st, 2nd & 3rd test, and mean values					
	Natural Sand	**Flint glass**	**Amber glass**	**Green glass**	**Mix washed**	**Mix unwashed**
7-days old						
0	4.57 4.48 *Mean* 4.60 (*4.55*)					
25		4.40 4.50 (*4.42*) 4.36	4.44 4.52 (*4.46*) 4.42	4.63 4.55 (*4.57*) 4.53	4.41 4.39 (*4.43*) 4.49	4.40 4.32 (*4.39*) 4.45
50		4.41 4.31 (*4.38*) 4.41	4.41 4.43 (*4.40*) 4.36	4.41 4.45 (*4.41*) 4.37	4.46 4.31 (*4.39*) 4.40	4.39 4.25 (*4.31*) 4.29
100		4.39 4.29 (*4.35*) 4.37	4.42 4.41 (*4.38*) 4.31	4.42 4.39 (*4.43*) 4.48	4.34 4.29 (*4.36*) 4.45	4.21 4.20 (*4.23*) 4.28
28-days old						
0	4.87 4.76 (*4.81*) 4.80					
25		4.78 4.79 (*4.75*) 4.68	4.76 4.83 (*4.78*) 4.75	4.79 4.79 (*4.83*) 4.91	4.72 4.69 (*4.72*) 4.75	4.71 4.62 (*4.69*) 4.74
50		4.73 4.61 (*4.68*) 4.70	4.70 4.65 (*4.71*) 4.78	4.63 4.78 (*4.73*) 4.78	4.73 4.72 (*4.68*) 4.59	4.48 4.56 (*4.54*) 4.58
100		4.51 4.64 (*4.58*) 4.59	4.60 4.68 (*4.61*) 4.55	4.63 4.55 (*4.62*) 4.68	4.60 4.57 (*4.55*) 4.48	4.45 4.45 (*4.49*) 4.57
112-days old						
0	4.86 4.85 (*4.87*) 4.90					
25		4.82 4.89 (*4.82*) 4.75	4.86 4.79 (*4.84*) 4.87	4.87 4.82 (*4.86*) 4.89	4.78 4.76 (*4.79*) 4.83	4.76 4.80 (*4.76*) 4.72
50		4.75 4.69 (*4.74*) 4.78	4.83 4.76 (*4.78*) 4.75	4.84 4.72 (*4.79*) 4.81	4.68 4.61 (*4.68*) 4.75	4.65 4.59 (*4.64*) 4.68
100		4.68 4.65 (*4.68*) 4.71	4.68 4.58 (*4.65*) 4.69	4.69 4.70 (*4.67*) 4.62	4.62 4.65 (*4.62*) 4.59	4.54 4.56 (*4.53*) 4.49
365-days old						
0	4.98 4.99 (*4.97*) 4.94					
25		4.92 4.90 (*4.89*) 4.85	4.90 4.88 (*4.91*) 4.95	4.96 4.97 (*4.95*) 4.92	4.85 4.91 (*4.87*) 4.85	4.77 4.71 (*4.76*) 4.80
50		4.84 4.78 (*4.81*) 4.81	4.82 4.89 (*4.83*) 4.78	4.86 4.87 (*4.85*) 4.82	4.69 4.72 (*4.68*) 4.63	4.67 4.76 (*4.69*) 4.64
100		4.73 4.80 (*4.75*) 4.72	4.72 4.86 (*4.78*) 4.76	4.79 4.77 (*4.79*) 4.81	4.71 4.69 (*4.72*) 4.76	4.59 4.69 (*4.62*) 4.58

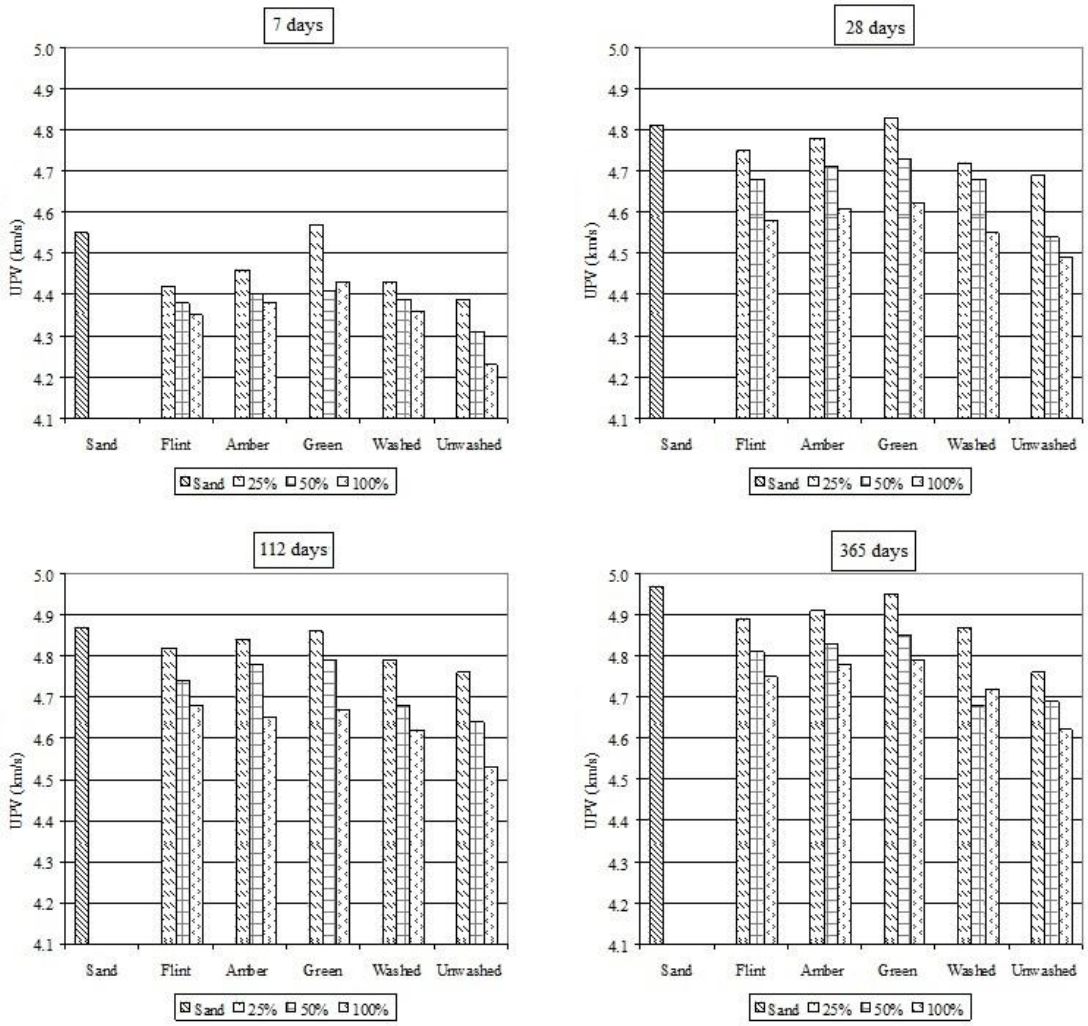

Fig. 4.31 Ultrasonic pulse velocity of all concrete mixes

Figure 4.32 contain normalised UPV values for all concretes containing glass after 7 days of curing. For green glass aggregate there was a very slight increase in UPV (over that for normal concrete) for 25% sand replacement. For higher green glass contents the UPV decreased in line with other colours of glass. The effect of not washing glass before it was used is clearly to depress UPV values. The difference between the UPV for conventional concrete and that of concrete containing 25% of any washed waste glass, at 7 days, was insignificant. The UPV for mixes containing 50% and 100% fine glass was slightly lower (by 3% to 7%), than that for conventional concrete mixes - Figure 4.32.

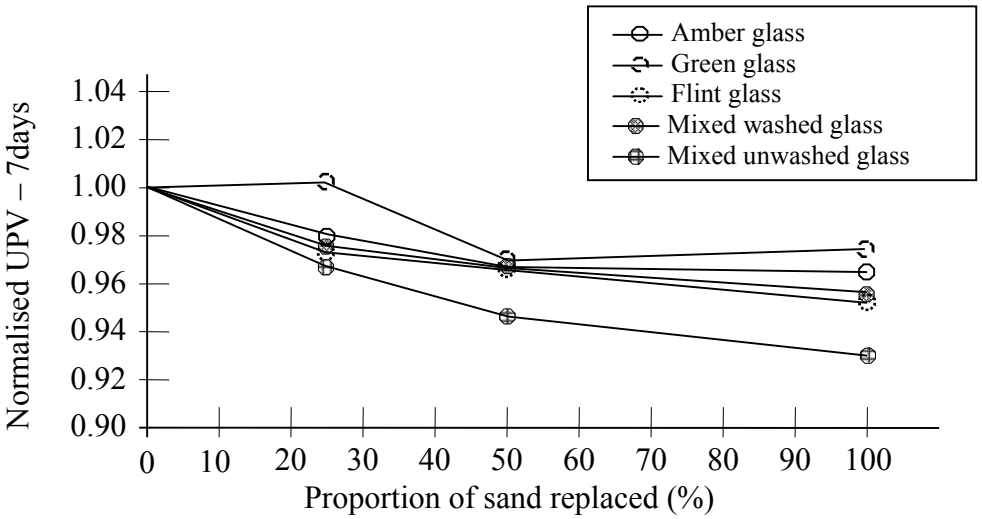

Fig. 4.32 Normalised UPV for concrete at 7 days

Normalised UPV data for concretes cured for 28 days are shown in Figure 4.33. Once again for 25% green glass content the UPV was essentially the same as for the normal concrete. Data for other colours of glass at 28 days (Figure 4.33) revealed a lower UPV value for the concrete containing waste glass in comparison to conventional concrete. The effect of not washing the glass aggregate was significant.

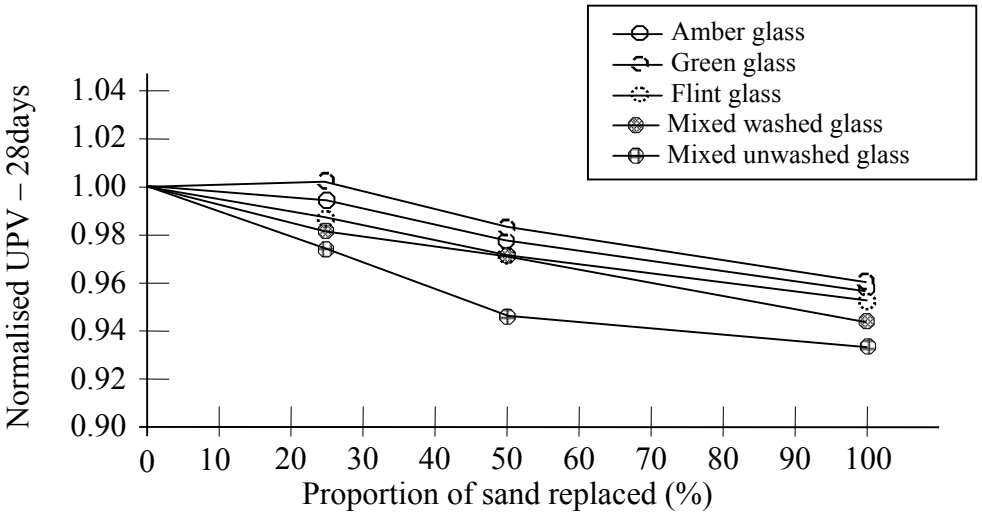

Fig. 4.33 Normalised UPV for concrete at 28 days

The results for concretes cured for 112 days are shown in Figure 4.34. All mixes showed a decrease in UPV compared to the conventional concrete. However, it should be noted that the observed differences between the conventional concrete and 'glass concrete' were small as was the decrease in UPV, i.e. only 1% to 7%. The decrease in

UPV for a 25% green glass content was negligible. The effect of the presence of contaminants in unwashed mixed glass is clearly visible.

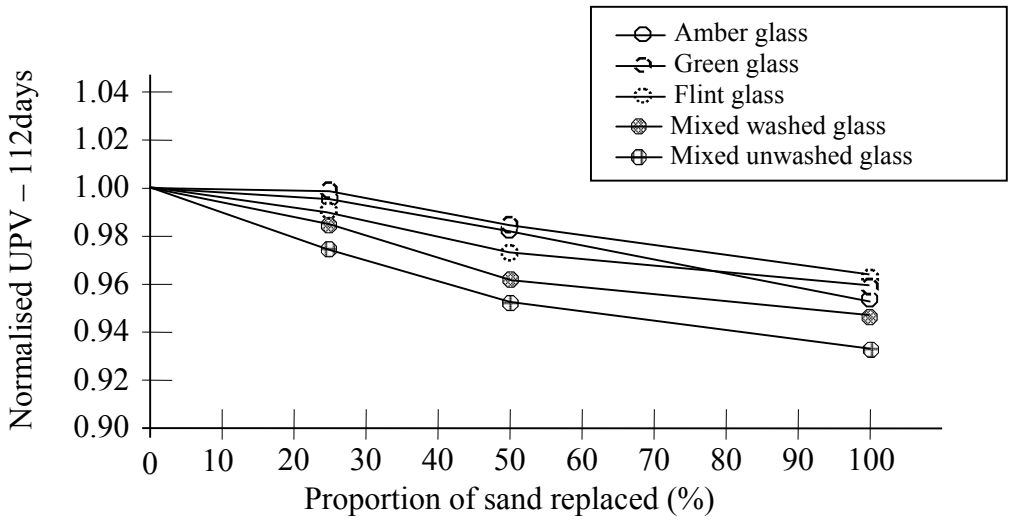

Fig. 4.34 Normalised UPV for concrete at 112 days

The long term tests (365 days of curing) gave the UPV data shown in Figure 4.35. The mean UPV value for 50% sand replacement by mixed washed glass did not follow the trend demonstrated by the other data and, although it is acknowledged to be the result of a pozzolanic reaction and this anomaly, this UPV value should be discounted.

In summary, the UPV values for concrete containing waste glass were generally lower than the mean value for conventional concrete at the corresponding age. Concrete containing green glass showed a better performance than other colours for all curing times and for 25% green glass content the decrease in UPV was negligible. Mixed unwashed glass had poorest performance - the UPV decreased by 4%, 6% and 7% for replacements of 25%, 50% and 100% of the fine aggregate by such glass.

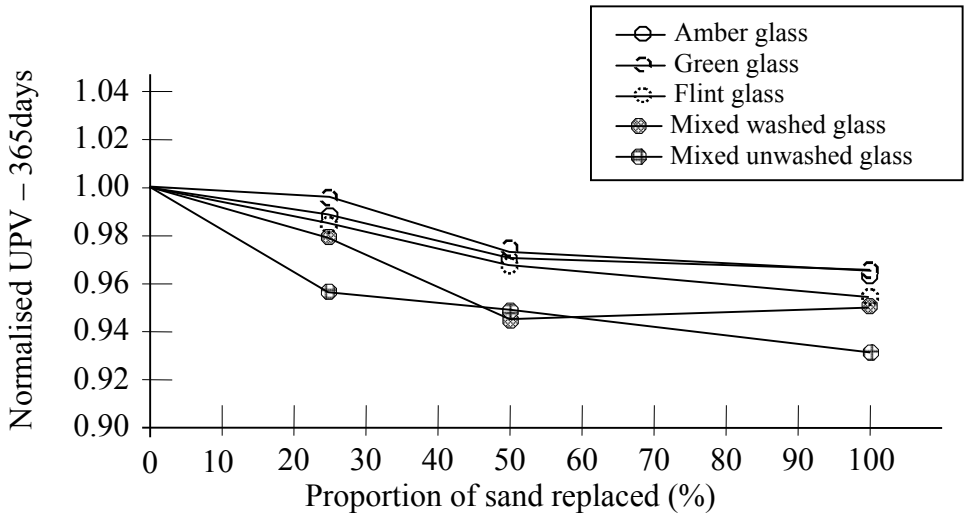

Fig. 4.35 Normalised UPV for concrete at 365 days

4.2.3. Alkali Silica Reactivity (ASR)

Axial Strain Measurements

The results of the ASR of percentage length change tests carried out on prisms of concrete (cast and treated in accordance with the relevant British Standard as described in previous Section (3.4.11) are presented in Figure 4.36 and Tables 4.9 and 4.10. The normal sand showed an expansion of 0.053% after one year and this is acceptable. The data show that expansion increased with increasing glass sand content. The 100% waste glass exhibited high expansion, from 0.107% to 0.174%, after one year. However all expansions of the mortar bars are below the limits for normal reactivity implied by BRE Digest 330, Part 2 (2004), i.e. 0.2% at 365days and 0.1% at 28 days. The results indicate that the unwashed glass has the highest expansion at all ages for 25%, 50% and 100% sand replacement in the mortar. Even so all mixes satisfied the BRE limits for normal reactivity.

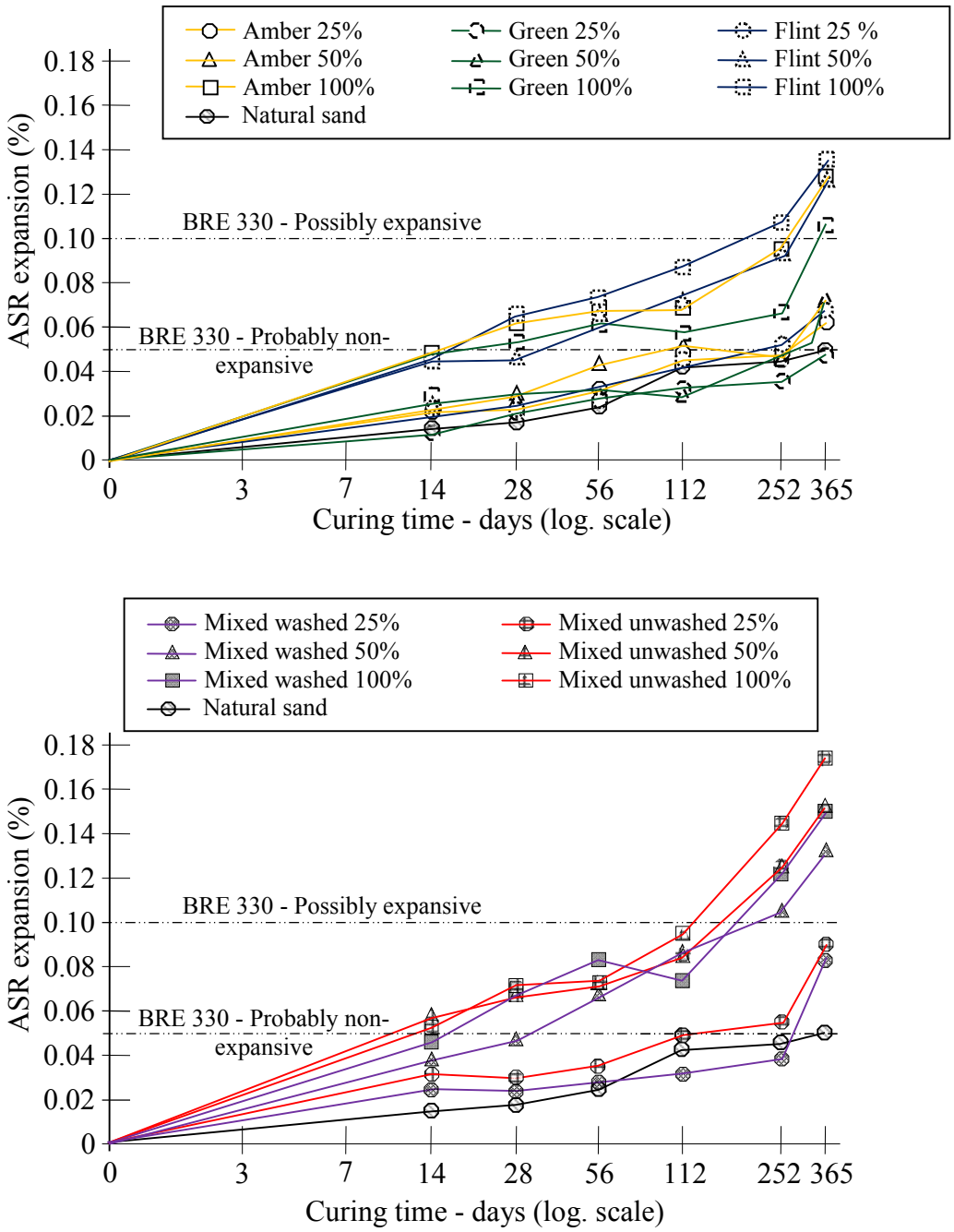

Fig. 4.36 ASR expansion of waste glass mortar via BS 812-123 test

The green glass produced less expansion than other colours, i.e. flint, amber and mixed glass. It appears unlikely that green glass would pose a risk due to ASR expansion. The expansion of concrete containing natural sand was quite small and comparable to concrete with 25% fine glass aggregate. The ASR expansion increased significantly with higher glass sand content, especially beyond 50%. Visual inspection revealed cracks on the sides of mortar bars with a high content of unwashed glass as seen Figure in 4.37.

Table 4.9 Alkali Silica Reactivity (ASR) verses percentage in the concrete mixes via BS 812-123 test (sand, amber and green glass)

Waste glass content in concrete (%)	ASR expansion by length change via BS 812-123 test (%)					
	14 days	28 days	56 days	112 days	252 days	365 days
Natural sand						
Cube 1	0.0171	0.0188	0.0262	0.0413	0.0422	0.0498
Cube 2	0.0140	0.0208	0.0235	0.0443	0.0466	0.0583
Cube 3	0.0151	0.0186	0.0223	0.0434	0.0431	0.0509
	0.0154	0.0194	0.0240	0.0430	0.0440	0.0530
Amber 25%						
Cube 1	0.0190	0.0198	0.0275	0.0390	0.0536	0.0620
Cube 2	0.0278	0.0228	0.0371	0.0559	0.0473	0.0564
Cube 3	0.0227	0.0326	0.0314	0.0461	0.0551	0.0676
	0.0232	0.0251	0.0320	0.0470	0.0520	0.0620
Amber 50%						
Cube 1	0.0257	0.0256	0.0413	0.0566	0.0590	0.0747
Cube 2	0.0320	0.0374	0.0456	0.0464	0.0864	0.0930
Cube 3	0.0329	0.0306	0.0421	0.0500	0.0706	0.0813
	0.0302	0.0312	0.0430	0.0510	0.0720	0.0830
Amber 100%						
Cube 1	0.0433	0.0677	0.0830	0.0755	0.1027	0.1178
Cube 2	0.0539	0.0555	0.0544	0.0619	0.0912	0.1408
Cube 3	0.0471	0.0598	0.0666	0.0666	0.0941	0.1254
	0.0481	0.0610	0.0680	0.0680	0.0960	0.1280
Green 25%						
Cube 1	0.0137	0.0192	0.0322	0.0262	0.0338	0.0539
Cube 2	0.0130	0.0259	0.0264	0.0391	0.0346	0.0451
Cube 3	0.0162	0.0219	0.0284	0.0317	0.0456	0.0480
	0.0143	0.0223	0.0290	0.0323	0.0380	0.0490
Green 50%						
Cube 1	0.0323	0.0414	0.0422	0.0414	0.0533	0.0799
Cube 2	0.0265	0.0339	0.0346	0.0339	0.0437	0.0655
Cube 3	0.0285	0.0366	0.0372	0.0366	0.0470	0.0706
	0.0291	0.0373	0.0380	0.0373	0.0480	0.0720
Green 100%						
Cube 1	0.0309	0.0652	0.0519	0.0652	0.0614	0.0993
Cube 2	0.0302	0.0534	0.0714	0.0534	0.0719	0.0972
Cube 3	0.0385	0.0575	0.0598	0.0575	0.0647	0.1239
	0.0332	0.0587	0.0610	0.0587	0.0660	0.1068

Table 4.10 Alkali Silica Reactivity (ASR) verses percentage in the concrete mixes via BS 812-123 test (flint, mixed washed and unwashed glass)

Waste glass content in concrete (%)	ASR expansion by length change via BS 812-123 (%)					
	14 days	28 days	56 days	112 days	252 days	365 days
Flint 25%						
Cube 1	0.0198	0.0259	0.0209	0.0481	0.0437	0.0657
Cube 2	0.0194	0.0212	0.0218	0.0394	0.0653	0.0592
Cube 3	0.0247	0.0228	0.0293	0.0424	0.0529	0.0702
	0.0213	0.0233	0.0240	0.0433	0.0540	0.0650
Flint 50%						
Cube 1	0.0260	0.0505	0.0722	0.0805	0.1055	0.1432
Cube 2	0.0332	0.0414	0.0592	0.0660	0.0865	0.1174
Cube 3	0.0347	0.0446	0.0637	0.0711	0.0931	0.1264
	0.0313	0.0455	0.0650	0.0725	0.0950	0.1290
Flint 100%						
Cube 1	0.0353	0.0651	0.0889	0.0803	0.1124	0.1363
Cube 2	0.0517	0.0651	0.0692	0.0904	0.0974	0.1566
Cube 3	0.0422	0.0632	0.0699	0.0828	0.1113	0.1421
	0.0431	0.0645	0.0760	0.0845	0.1070	0.1450
Mixed washed 25%						
Cube 1	0.0216	0.0198	0.0249	0.0340	0.0347	0.0771
Cube 2	0.0205	0.0218	0.0336	0.0278	0.0441	0.0886
Cube 3	0.0254	0.0202	0.0284	0.0300	0.0382	0.0804
	0.0225	0.0206	0.0290	0.0306	0.0390	0.0820
Mixed washed 50%						
Cube 1	0.0313	0.0424	0.0733	0.0813	0.1177	0.1292
Cube 2	0.0285	0.0497	0.0601	0.0779	0.0965	0.1455
Cube 3	0.0341	0.0447	0.0647	0.0976	0.1039	0.1333
	0.0313	0.0456	0.0660	0.0856	0.1060	0.1360
Mixed washed 100%						
Cube 1	0.0444	0.0581	0.0899	0.0673	0.1343	0.1408
Cube 2	0.0396	0.0574	0.0737	0.0804	0.1101	0.1392
Cube 3	0.0465	0.0738	0.0794	0.0716	0.1186	0.1790
	0.0435	0.0631	0.0810	0.0731	0.1210	0.1530
Mixed unwashed 25%						
Cube 1	0.0306	0.0256	0.0327	0.0542	0.0557	0.0801
Cube 2	0.0281	0.0262	0.0441	0.0444	0.0528	0.1037
Cube 3	0.0340	0.0346	0.0372	0.0478	0.0655	0.0892
	0.0309	0.0288	0.0380	0.0488	0.0580	0.0910
Mixed unwashed 50%						
Cube 1	0.0562	0.0724	0.0677	0.0946	0.1159	0.1638
Cube 2	0.0620	0.0593	0.0778	0.0775	0.1305	0.1420
Cube 3	0.0573	0.0639	0.0706	0.0835	0.1196	0.1622
	0.0585	0.0652	0.0720	0.0852	0.1220	0.1560
Mixed unwashed 100%						
Cube 1	0.0500	0.0711	0.0733	0.0862	0.1197	0.1792
Cube 2	0.0575	0.0634	0.0601	0.0970	0.1752	0.1757
Cube 3	0.0521	0.0746	0.0647	0.0889	0.1431	0.1670
	0.0532	0.0697	0.0660	0.0907	0.1460	0.1740

Fig. 4.37 Expansion of mortar bars during ASR testing

Volumetric Strain Measurements

Estimates of the volume change of concrete cubes during curing were made directly by monitoring changes in the dimensions of all six cube faces using the demec gauge described in Section 3.3.7. Because the gauge length of the demec gauge was 100mm and cubes were 100mm × 100mm × 100mm the demec studs were located in the corners of each cube face as shown in Figure 4.38. If the axes of a cube and its individual faces are designated as on shown in Figure 4.39 then deformation in the x-direction will be indicated by components of changes in lengths L1 and L2 for cube faces A, B, C and D. For deformation in the y-direction the faces involved are A, B, E and F and for the z-direction the relevant faces are C, D, E and F. The changes in lengths L1 and L2, i.e. ΔL1 and ΔL2, are so small that their components in the x, y and z direction can be taken as ΔL1 cos 45° and ΔL2 cos 45°. The mean change in the size of a cube in the X-direction can then be defined as,

$$\Delta_X = \frac{\cos 45°}{8} \Sigma (\Delta L1 + \Delta L2)_{\text{Faces A, B, C, D}} \qquad \text{Equ. 4.1}$$

Similarly

$$\Delta_Y = \frac{\cos 45°}{8} \Sigma (\Delta L1 + \Delta L2)_{\text{Faces A, B, E, F}} \qquad \text{Equ. 4.2}$$

and

$$\Delta_Z = \frac{\cos 45°}{8} \Sigma (\Delta L1 + \Delta L2)_{\text{Faces C, D, E, F}} \qquad \text{Equ. 4.3}$$

The calculated values of Δ_X, Δ_Y and Δ_Z for cubes composed of conventional concrete cured for different times are shown in Table 4.11. The data in Table 4.11 show that

there was no curing time at which Δ_X, Δ_Y and Δ_Z were all equal. There were some instances where the three increments were quite similar, e.g. Cube 1 after 56 days, but there were other instances where the three increments were quite dissimilar e.g. cube 2 after 365 days. However, it much be remembered that concrete is composed of solid particles ranging in size from clay to gravel and so although a concrete cube may be formed of well-mixed, uniform concrete it will not be an isotropic material. Hence it cannot be expected to deform isotropically, whether under the action of external stress or due to ASR.

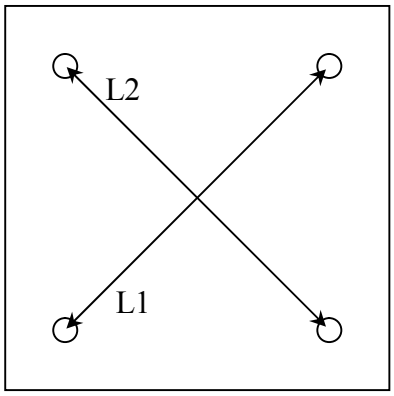

Fig. 4.38 Demec stud locations on a cube face

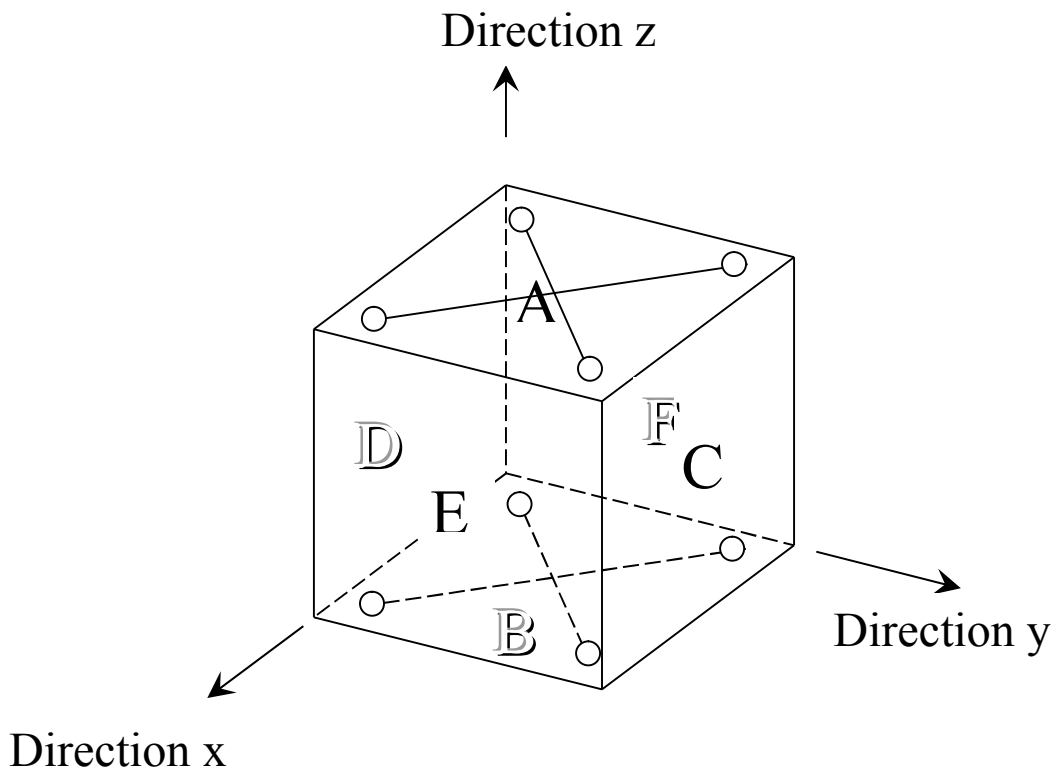

Fig. 4.39 Designation of faces and axes for a cube

Table 4.11 Cube dimensional changes for conventional concrete

Natural sand	Cube expansion				
	Change in dimension			Volumetric strain	Equivalent isotropic axial strain
	Direction x Δ_X (μm)	Direction y Δ_Y (μm)	Direction z Δ_Z (μm)	ε_V (%)	'ε_V /3' (%)
14 days					
Cube 1	10.3	10.3	11.5	0.0321	0.0107
Cube 2	10.5	10.8	9.5	0.0308	0.0103
Cube 3	11.3	10.0	11.5	0.0328	0.0109
Mean				0.0319	0.0106
28 days					
Cube 1	13.4	12.8	15.0	0.0412	0.0137
Cube 2	14.2	15.1	13.1	0.0423	0.0141
Cube 3	12.5	12.0	15.5	0.0400	0.0133
Mean				0.0412	0.0137
56 days					
Cube 1	16.9	16.9	18.1	0.0519	0.0173
Cube 2	19.1	18.8	17.3	0.0553	0.0184
Cube 3	15.1	14.4	18.6	0.0481	0.0160
Mean				0.0518	0.0173
112 days					
Cube 1	20.8	20.8	23.5	0.0652	0.0217
Cube 2	23.9	23.5	20.8	0.0682	0.0227
Cube 3	20.4	17.3	23.3	0.0609	0.0203
Mean				0.0648	0.0216
252 days					
Cube 1	25.0	27.0	30.6	0.0826	0.0275
Cube 2	32.3	30.6	24.9	0.0878	0.0293
Cube 3	26.5	20.7	31.4	0.0787	0.0262
Mean				0.0830	0.0277
365 days					
Cube 1	31.2	35.2	39.7	0.1062	0.0354
Cube 2	43.6	42.8	32.4	0.1188	0.0396
Cube 3	30.4	24.9	37.7	0.0931	0.0310
Mean				0.1060	0.0353

The cube dimensional changes in Table 4.11 have been plotted in Figure 4.40 by arbitrarily choosing one axis, i.e. the x-axis, and plotting changes in the y and z directions relative to the chosen axis. The line representing isotropic behaviour, i.e. $\Delta_X = \Delta_Y = \Delta_Z$, is the bisector of the angle between the upper and lower bounds to the data and neither the Δ_Y nor the Δ_Z valves are consistently above or below the isotropic line.

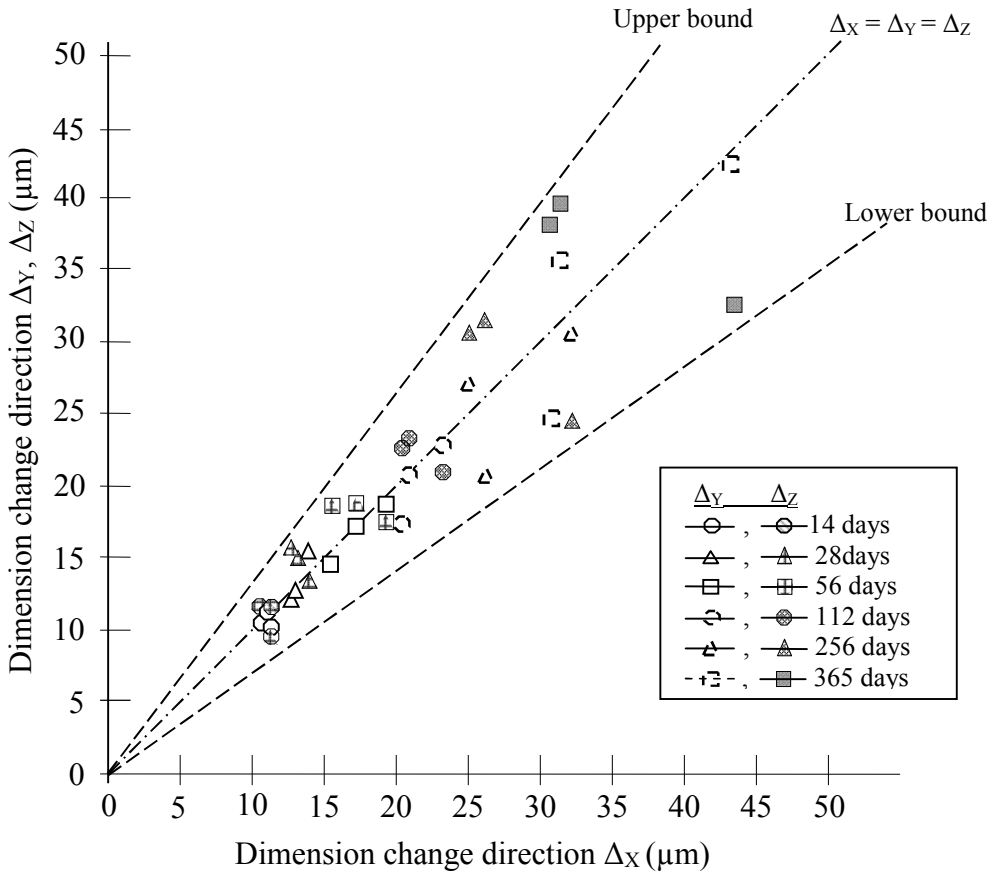

Fig. 4.40 Dimensional change during curing

For a material undergoing small strains the sum of the linear strains in three orthogonal direction is the volumetric strain. Using the values of Δ_X, Δ_Y and Δ_Z the volumetric strains for each cube have been calculated as shown in Table 4.11. At any specific curing time the volumetric strains exhibited by the three relevant cubes are very similar, i.e. mainly within ± 7 % of the mean value. Since ASR is acknowledged to be responsible for volume changes of a concrete the mean volumetric strain for each curing time (as shown in Table 4.11) has been plotted against time (on a logarithmic scale) in Figure 4.41. The axial strain data (from Table 4.9) determined using BS 812-123 test are also shown in Figure 4.41. The volumetric strain data define a smooth curve whereas the axial strain data show considerable scatter about a potential relationship between strain and time. Also shown in Figure 4.41 are values of the equivalent isotropic axial strains for the cubes calculated by assuming isotropic behaviour of the concrete and dividing volumetric strain by 3. These equivalent axial strains are considerably less than these measured directly in the BS 812-123 test, in fact this latter test overpredicts the amount of expansion by approximately 60%. This

difference may be due to the fact that the concrete cubes onto which demec studs were bonded were cured in a tank maintained at 20°C, whereas the BS 812-123 accelerated ASR test uses a curing temperature of 38°C so any time-dependent dimensional changes would occur at a faster rate in this latter test.

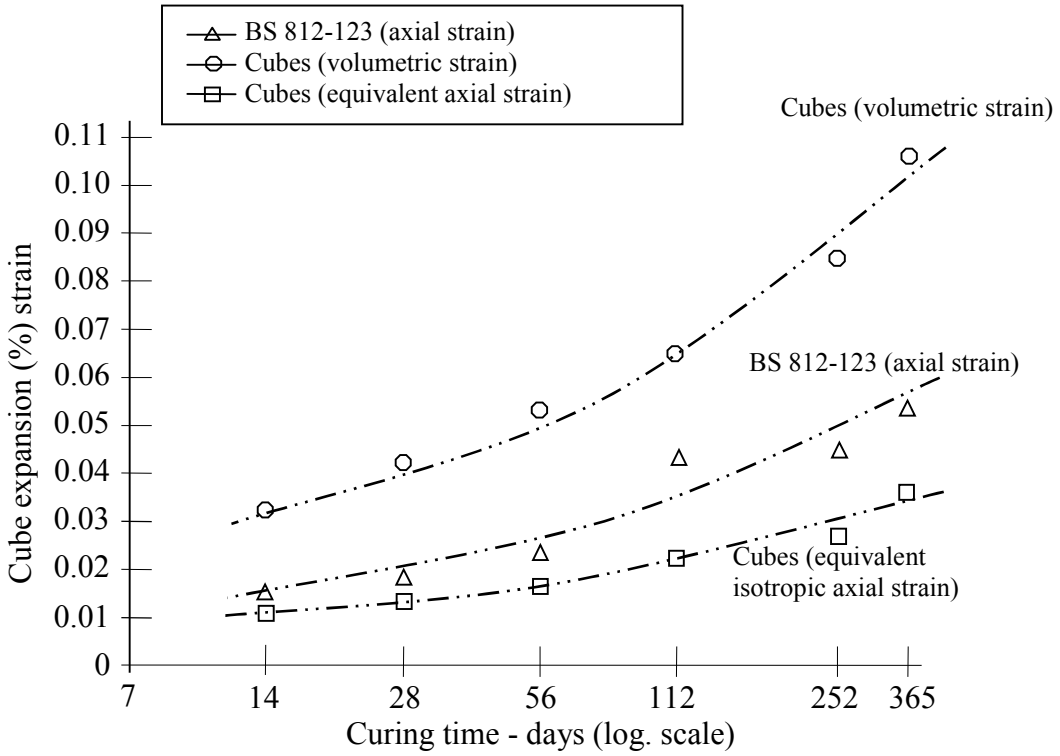

Fig. 4.41 Strain versus logarithm of curing time for conventional concrete

To investigate the conflicting expansion data from the cube measurements and from test BS 812-123 the volumetric strains from the cubes have been plotted against curing time on a log-log plot – Figure 4.42. The cube data from Table 4.11 define a straight line which has an equation of the form

$$\varepsilon_V = A\, t^{\,n} \qquad \text{Equ. 4.4}$$

For ε_V in percentage and t in days the values of A and n are 0.0125 and 0.35, respectively.

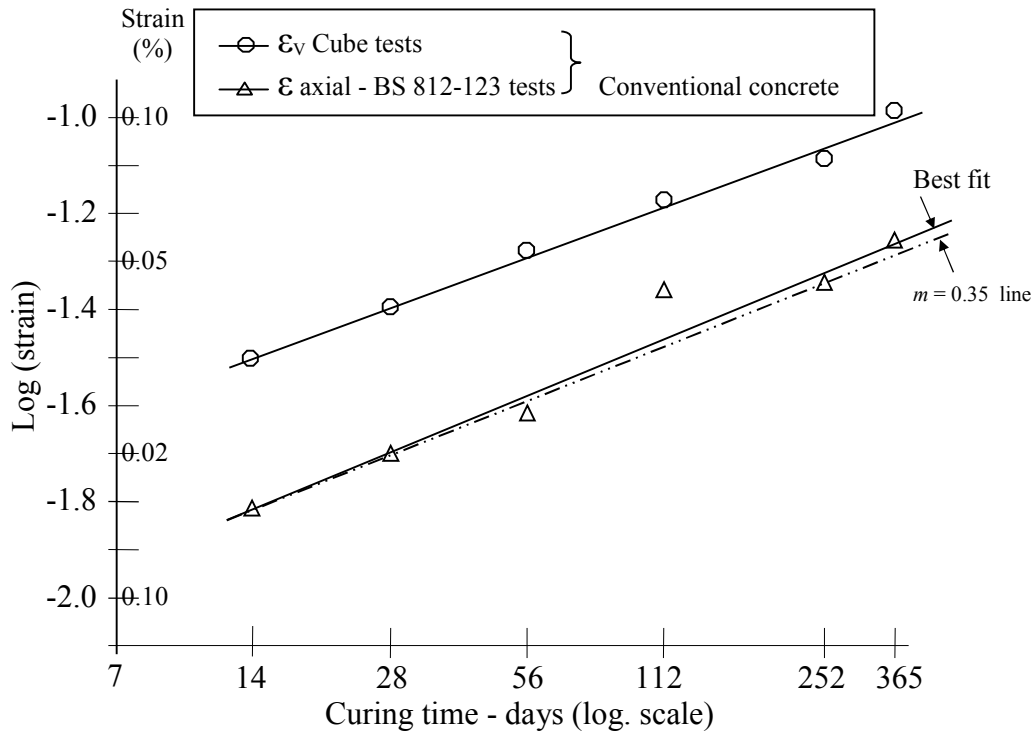

Fig. 4.42 Log (strain) versus Log (curing time) for normal concrete

The results obtained from test BS 812-123 are also plotted on Figure 4.42 in terms of axial strain and the data are a reasonable fit to a straight line with an equation of the form

$$\varepsilon \text{ axial} = B\, t^{m} \qquad \text{Equ. 4.5}$$

For the best fit line m is equal to 0.37 and B is equal to 0.0058 for ε axial in percentage and t in days.

However a line with m equal to 0.35 is also a reasonable fit to the data in Figure 4.42 and for this case B becomes equal to 0.0062

$$\text{Thus} \quad \frac{\varepsilon_V \text{ (cubes)}}{\varepsilon \text{ axial (BS 812-123)}} \approx \frac{A}{B} \equiv \frac{0.0125}{0.0062} \approx 2 \qquad \text{Equ. 4.6}$$

If the tests used to monitor dimension changes of concrete with time were equivalent to one another and if the concrete behaved more-or-less as an isotropic material then the ratio in equation (4.6) should be equal to 3.

The volumetric strain data obtained by mounting demec studs on cubes of concrete containing glass are given in Tables 4.12 and 4.13. and typical data are plotted in Figure 4.43.

Analysis of the measurements from concrete cubes reveals that the cubes containing 50% and 100% glass generally had greater slightly expansion than the conventional concrete, but the concrete containing 25% glass had similar or even less expansion than conventional concrete as shown in Tables 4.11 to Table 4.13.

Table 4.12 Volumetric strains of cubes containing amber and green glass

Waste glass content in concrete (%)	Cube expansion as volumetric strain ε_v (%) mean values					
	14 days	28 days	56 days	112 days	252 days	365 days
Natural sand	0.0319	0.0412	0.0518	0.0648	0.0830	0.1060
Amber 25%	0.0251	0.0314	0.0382	0.0480	0.0618	0.0795
Amber 50%	0.0460	0.0599	0.0764	0.0945	0.1233	0.1489
Amber 100%	0.0888	0.1046	0.1181	0.1366	0.1634	0.1860
Green 25%	0.0217	0.0283	0.0356	0.0449	0.0575	0.0729
Green 50%	0.0397	0.0507	0.0622	0.0783	0.1007	0.1239
Green 100%	0.0759	0.0880	0.0995	0.1163	0.1414	0.1658

Table 4.13 Volumetric strains of cubes containing flint and mixed glass

Waste glass content in concrete (%)	Cube expansion as volumetric strain ε_v (%) mean values					
	14 days	28 days	56 days	112 days	252 days	365 days
Flint 25%	0.0316	0.0413	0.0508	0.0629	0.0796	0.1022
Flint 50%	0.0707	0.0803	0.0938	0.1134	0.1380	0.1616
Flint 100%	0.0899	0.1085	0.1237	0.1438	0.1660	0.1928
Mixed washed 25%	0.0353	0.0454	0.0574	0.0722	0.0933	0.1218
Mixed washed 50%	0.0492	0.0626	0.0801	0.1010	0.1296	0.1615
Mixed washed 100%	0.0709	0.0842	0.1016	0.1233	0.1547	0.1884
Mixed unwashed 25%	0.0503	0.0640	0.0808	0.1009	0.1291	0.1652
Mixed unwashed 50%	0.0675	0.0780	0.0945	0.1148	0.1361	0.1702
Mixed unwashed 100%	0.0891	0.1046	0.1243	0.1485	0.1724	0.1988

Results shown in Figure 4.43 show that the concrete mixes containing 25%, 50%, and 100% mixed unwashed glass exhibited significant expansion, up to 0.165%, 0.172%, and 0.199% respectively, after one year. The volume changes develop more-or-less linearly with logarithmic of curing time.

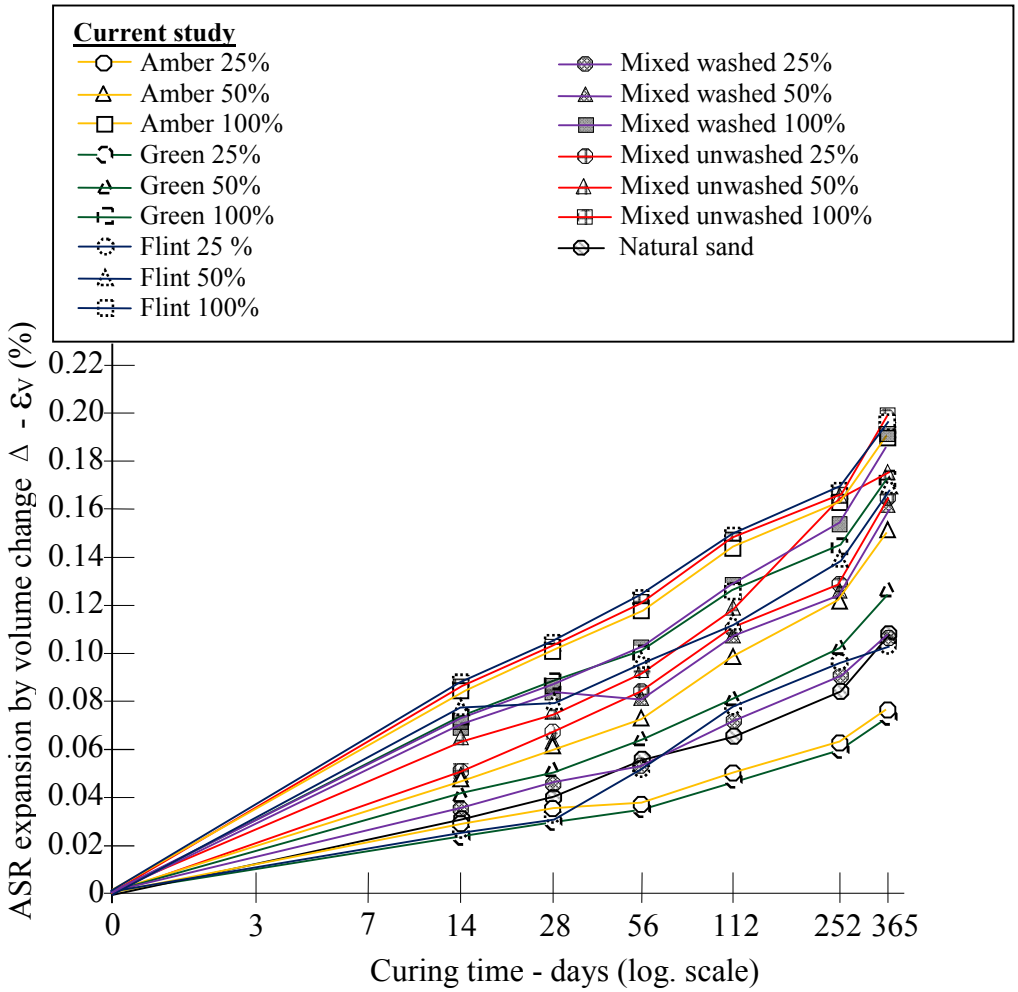

Fig. 4.43 Volumetric expansion for concrete with conventional fine aggregate replaced by glass

However the values in Tables 4.12 and 4.13 are volumetric strains and the BRE 330 reactivity limits are in terms of length change and if the cubes deformed isotropically then the axial strain would be obtained by dividing the volumetric strain by 3. If this procedure is correct then at no time does the concrete containing glass exceed the BRE 330 limits - the calculated maximum axial strains from the cubes would be 0.03%(as opposed to a 0.1% limit) at 28 days and 0.066% (as opposed to a 0.2% limit) at 365 days. On the other hand if the BRE 330 limits relate to specimens cured at 38°C (instead of 20°C) as occurs within test BS812-123 then the cube data cannot

simply be divided by 3. Hence the data in Tables 4.12 and 4.13 have been drawn on log-log plots to determined the dimension change parameters (A, *n*, B and *m* in equations 4.4 and 4.5) so that the strain from the cubes and the prisms (BS 812-123 test) can be compared - sample plots are shown in Figure 4.44 and the resultant parameters are given in Table 4.14.

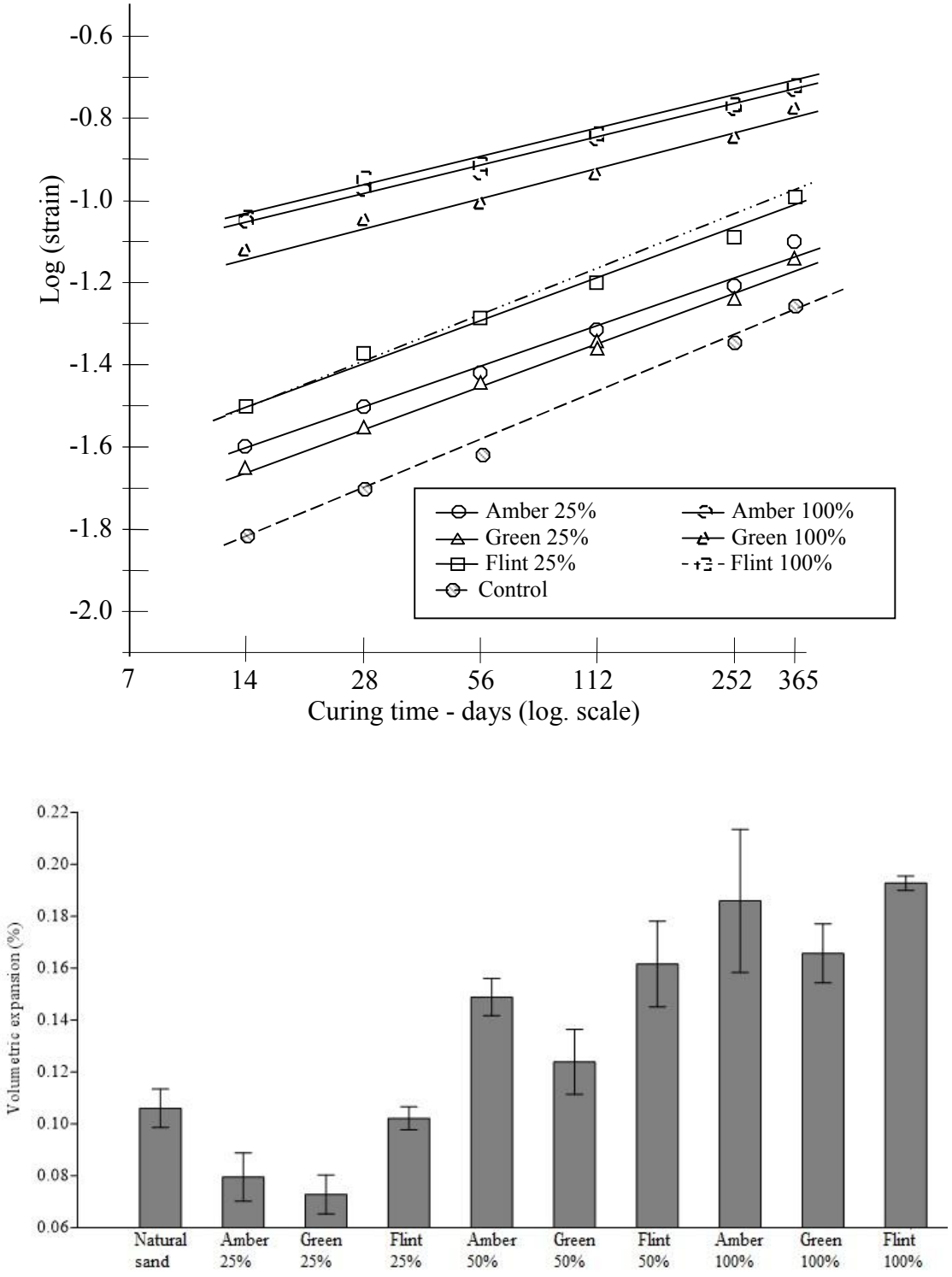

Fig. 4.44 Volumetric expansion for concrete containing glass

Table 4.14 Dimension change parameters (equation 4.4 and 4.5)

Concrete mix	Glass content (%)	Volumetric strains (cubes)		Axial strains (prisms)		A / B	*n* / *m*
		A	*n*	B	*m*		
Normal	0	0.0125	0.35	0.0062	0.35	2.0	1.0
Amber	25	0.0102	0.33	*	0.33	/	1.0
	50	0.0186	0.34	0.0110	0.34	1.7	1.0
	100	0.0452	0.24	0.0240	0.24	1.9	1.0
Green	25	0.0085	0.35	0.0060	0.35	1.4	1.0
	50	0.0166	0.33	*	*	/	/
	100	0.0339	0.24	0.0178	0.24	1.9	1.0
Flint	25	0.0132	0.33	0.0083	0.34	1.6	1.0
	50	0.0300	0.28	0.0151	0.35	2.0	1.0
	100	0.0490	0.23	0.0279	0.24	1.8	1.0
Mixed washed	25	0.0141	0.35	*	*	/	/
	50	0.0202	0.34	*	*	/	/
	100	0.0331	0.27	*	0.25	/	1.1
Mixed unwashed	25	0.0213	0.33	0.0095	0.33	2.2	1.0
	50	0.0351	0.25	0.0263	0.22	1.3	1.1
	100	0.0473	0.24	0.0282	0.25	1.7	1.0

***** Data too scattered to estimate B and / or *m* accurately

As illustrated in Figure 4.44 the volumetric strain data from cubes showed good fit to a relationship of the form described by equation (4.4). The results in Tables 4.12 to 4.14 show that:

a) For all mixes with glass replacing 25% of the fine aggregate the value of the power function *n* was the same as for conventional concrete.

b) For all mixes containing 25% of glass fine aggregate (except for the unwashed glass, the value of A was either marginally greater than, or significantly less than, that for conventional concrete. The result for unwashed mixed glass would suggest that contaminants on the surface of waste glass may have a significant effect on concrete behaviour but that this effect can be drastically reduced by simple washing of the waste glass.

c) The foregoing remarks demonstrate that the concrete mixes containing 25% of glass fine aggregate did not exhibit volume changes significantly greater than that of conventional concrete.

d) Concrete mixes containing 50% of glass fine aggregate exhibited significantly greater volume change than that of conventional concrete, ranging from approximately +30% for green glass (the best performer) to +50% for flint glass.

e) All mixes containing 100% of glass fine aggregate exhibited a volumetric strain-time relationship characterised by a value of the power function *n* (equation 4.4) of 0.23 to 0.24. These mixes underwent considerable greater volume change than conventional concrete - from +50% (green glass the best performer) to +90% (mixes unwashed glass).

f) Using the correlation between *n* and *m* and between A and B shown in Table 4.14 volumetric strains have been converted to equivalent BS 812-123 axial strains. The following are the maximum axial strains obtained for any of the washed glasses - 0.05% (at 14 days) 0.06% (at 28days) and 0.11% (at 365 days).

4.2.4. Compressive strength

The compression strength of all concrete cubes tested is shown in Table 4.15 and the values for conventional concrete have been plotted against time (on a logarithmic scale) in Figure 4.45.

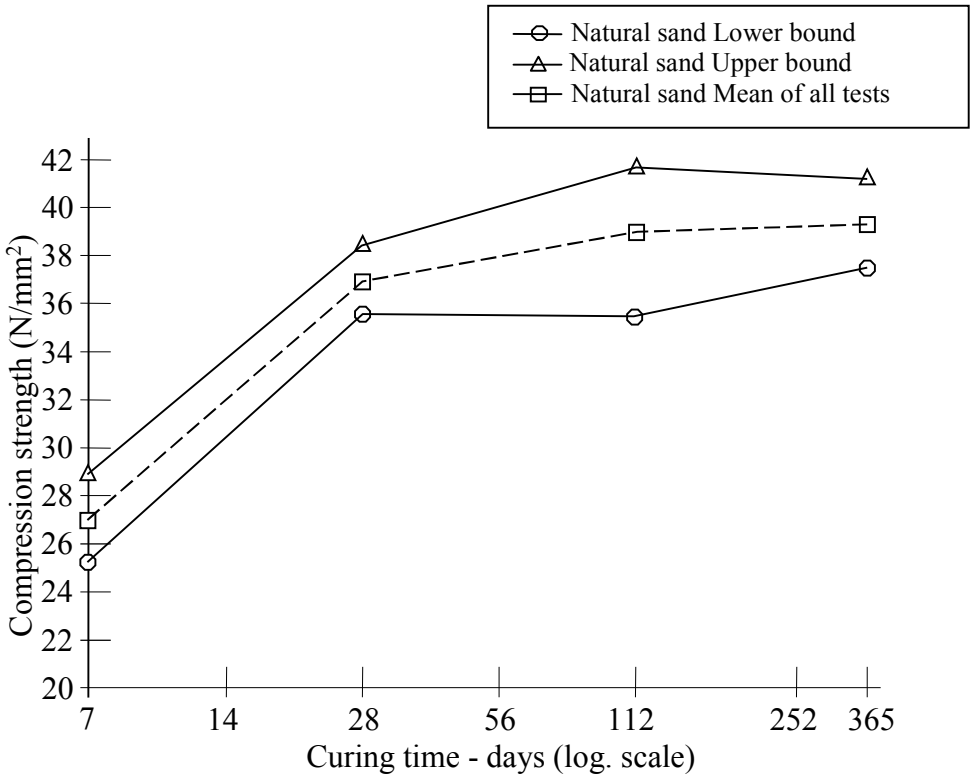

Fig. 4.45 Strength of cubes made of normal concrete

The results in Figure 4.45 show a significant increase in compressive strength from 7 to 28 days - the upper bound, lower bound and mean values all conform to the 'rule-of-thumb' guide (CP110, 1972) that 7-day strength is approximately 75% of the 28-day strength. For curing times beyond 28 days there is a significant difference between measured upper and lower bound values. However, the mean values indicate the trend that would be expected, i.e. continuing time-dependent strength grain after 28 days but at a rapidly diminishing rate after this curing period.

Table 4.15 Compressive strength verses percentage in the concrete mixes

Glass (%)	Compressive strength (MPa) in ranged 1st, 2nd & 3rd test and mean values					
	Natural sand	Flint glass	Amber glass	Green glass	Mix washed	Mix unwashed
7-days						
0	25.12					
	28.91 *26.92*					
	26.73					
25		25.22	26.19	26.65	26.18	23.23
		26.13 *25.96*	25.16 *25.52*	25.19 *26.18*	24.26 *25.26*	24.45 *24.66*
		26.54	25.21	26.69	25.33	26.29
50		23.55	26.91	25.33	26.76	23.99
		25.66 *24.55*	25.03 *25.48*	26.18 *25.74*	25.49 *25.44*	22.87 *23.94*
		24.45	24.51	25.71	24.07	24.95
100		26.13	22.66	22.98	23.66	23.31
		23.11 *23.77*	22.87 *23.21*	24.67 *24.22*	22.99 *23.62*	22.97 *22.02*
		22.06	24.11	25.01	24.21	19.78
28-days						
0	35.81					
	38.22 *36.81*					
	36.41					
25		36.22	32.24	36.57	36.73	36.69
		33.53 *35.11*	34.77 *35.12*	36.28 *36.92*	37.34 *35.95*	35.41 *34.43*
		35.58	38.34	37.91	33.79	31.18
50		36.53	32.77	34.42	32.78	32.76
		31.45 *33.61*	35.68 *33.75*	35.96 *35.50*	34.64 *33.79*	29.55 *31.27*
		32.86	32.79	36.12	33.96	31.49
100		32.34	33.77	32.52	31.36	30.53
		31.79 *31.71*	29.34 *31.97*	31.42 *33.03*	29.95 *31.39*	29.67 *30.07*
		30.99	32.79	35.14	32.85	30.01
112-days						
0	39.21					
	41.90 *38.91*					
	35.62					
25		38.91	34.79	37.14	38.79	37.88
		35.88 *37.33*	38.56 *36.71*	38.11 *37.31*	37.67 *37.15*	33.55 *35.63*
		37.21	36.78	36.67	34.98	35.47
50		36.55	33.97	35.44	37.29	35.77
		37.54 *35.92*	36.88 *35.25*	35.97 *35.88*	35.12 *35.44*	32.54 *33.43*
		33.68	34.91	36.23	33.91	31.99
100		32.14	32.78	34.98	32.43	30.95
		33.92 *32.61*	32.73 *33.41*	35.33 *34.86*	31.57 *32.51*	32.84 *31.79*
		31.77	34.71	34.28	33.54	31.57
365-days						
0	38.81					
	41.23 *39.20*					
	37.55					
25		37.62	35.23	38.54	36.87	37.69
		36.55 *37.37*	37.87 *37.04*	36.21 *37.55*	37.43 *37.42*	35.08 *36.55*
		37.95	38.01	37.90	37.97	36.87
50		36.88	35.77	37.41	36.78	35.79
		35.12 *36.36*	34.48 *36.07*	35.96 *36.55*	34.67 *35.80*	34.54 *35.08*
		37.09	37.96	36.27	35.94	34.92
100		34.43	35.77	36.05	35.79	33.78
		32.48 *33.87*	34.73 *34.50*	35.94 *35.57*	34.91 *34.49*	32.76 *32.74*
		34.71	32.99	34.71	32.76	31.67

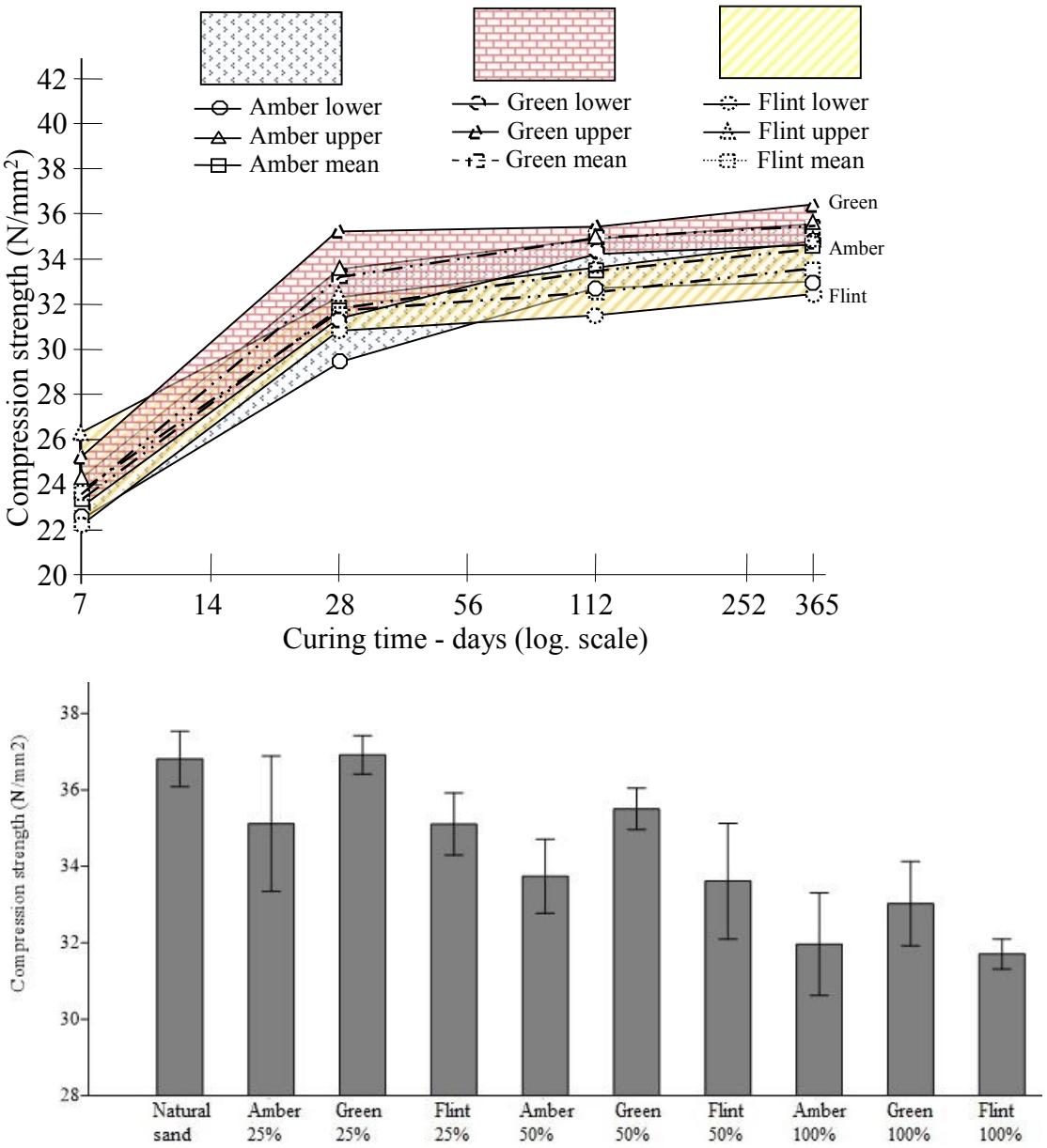

Fig. 4.46 Strength of cubes containing glass as fine aggregate

Figure 4.46 shows the gain in compressive strength with time for concrete containing only different colours of waste glass i.e. amber, green and flint, as fine aggregate. The strength envelopes for the three colours of glass have the same shape as that for the conventional concrete (Figure 4.45). In addition, for each colour, the variation of mean strength with time is the same shape as, that for the normal concrete. Figure 4.47 contains the mean compressive strength curves, as a function of curing time, of all concrete mixes tested. It is evident that all curves have the same general shape even though there is a significant range of strength values between the upper and lower bound curves.

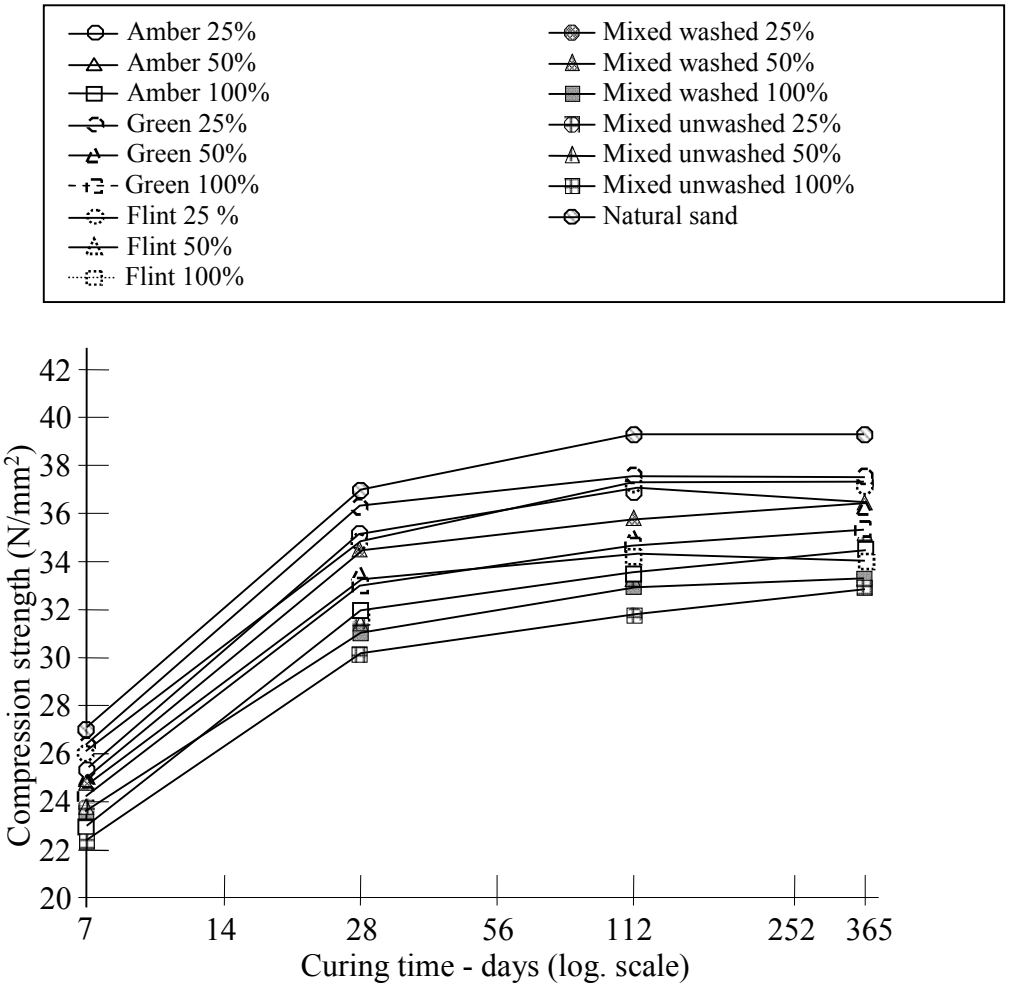

Fig. 4.47 Compression strength of concrete containing glass fine aggregate

Because of the aforementioned similarity of compressive strength-time curves 'Age factors' have been calculated from the mean strengths of the various concrete mixes at differing curing times, where:

$$\text{Age factor} = \frac{\text{Mean compressive strength at time } t \text{ (days)}}{\text{Mean strength of the same mix at 7 days}} \qquad \text{Equ. 4.7}$$

Age factor values are tabulated in Table 4.16 and are plotted against curing time in Figure 4.48. The results show that:

- The Age factor values lie in a narrow band, which is widest at 28 days (difference between upper and lower bounds is 0.10) and which is narrowest at 365 days (difference of 0.07).
- The data for conventional concrete lie in the middle to upper part of the band formed by the Age factor values, but are never the upper bound.

- There is no one material or waste glass content that consistently defines the upper or lower bounds. For instance; a green glass content of 25% has the maximum Age factor at 28 days but at 365 days the factor lies in the lower part of the band, a mixed unwashed glass content 50% has the minimum Age factor at 28 days but at 365 days the factor lies in the upper part of the band and above conventional concrete.

Thus it is contended that neither the colour of glass used as fine aggregate, nor the proportion of fine aggregate which it replaces, has a consistent effect on the rate of gain of compressive strength with time relative to the strength of a particular mix of concrete at 7 days, i.e. curing and 'setting' process is unaffected by the presence of glass.

Table 4.16 Age factor values for all mixes

Amount of glass as aggregate	**Colour of glass**	**Age factor - Curing time (days)**			
		7	**28**	**112**	**365**
0%	N/A	1.00	1.37	1.45	1.46
25%	Amber	1.00	1.38	1.44	1.45
	Green	1.00	1.41	1.43	1.43
	Flint	1.00	1.35	1.44	1.44
	Mixed washed	1.00	1.42	1.47	1.48
	Mixed unwashed	1.00	1.40	1.44	1.48
50%	Amber	1.00	1.32	1.38	1.42
	Green	1.00	1.38	1.39	1.42
	Flint	1.00	1.37	1.46	1.48
	Mixed washed	1.00	1.33	1.39	1.42
	Mixed unwashed	1.00	1.31	1.40	1.47
100%	Amber	1.00	1.38	1.44	1.49
	Green	1.00	1.36	1.44	1.47
	Flint	1.00	1.33	1.37	1.42
	Mixed washed	1.00	1.33	1.38	1.46
	Mixed unwashed	1.00	1.37	1.44	1.49

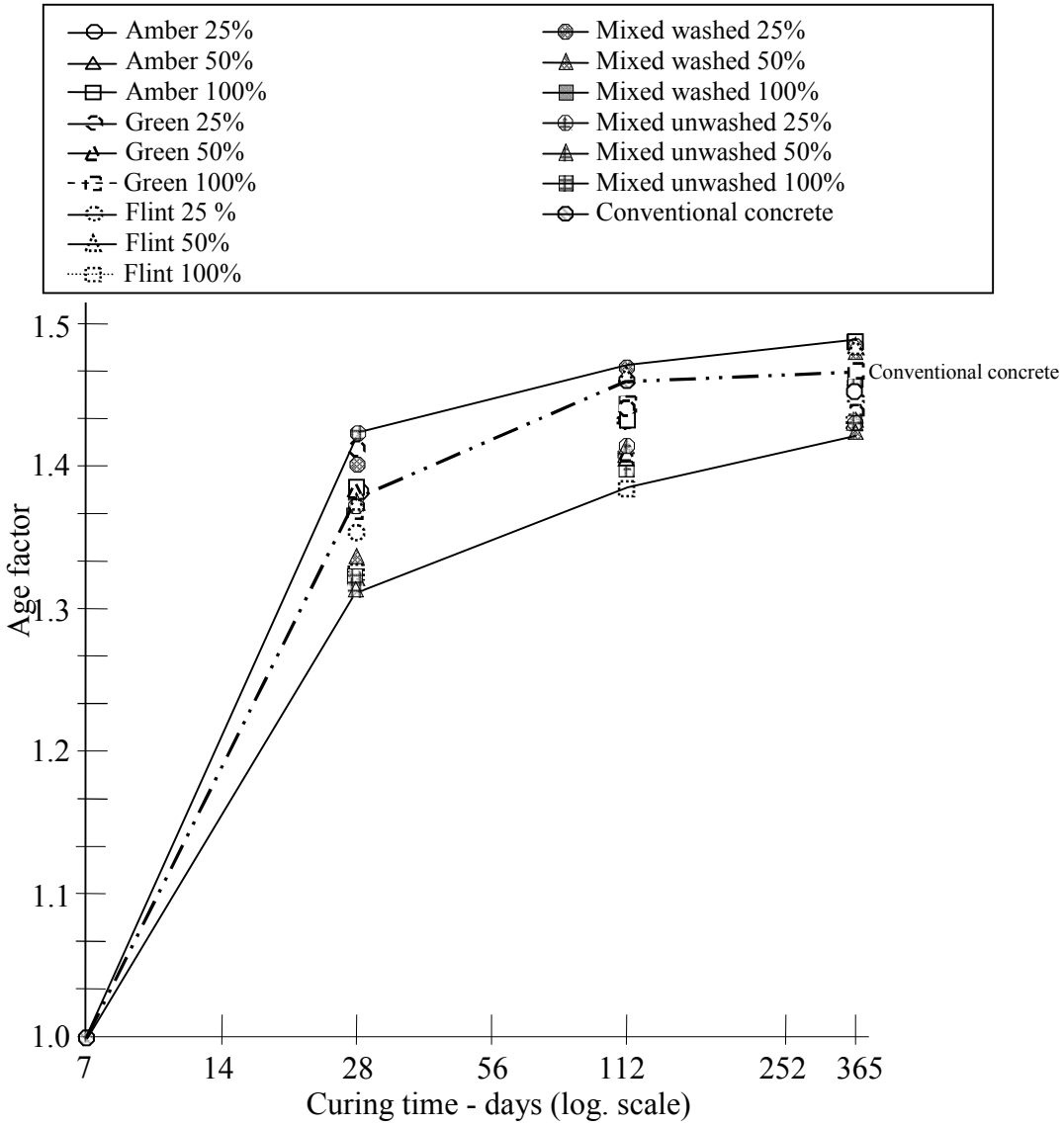

Fig. 4.48 Age factors for all mixes

However, the boxplots in Figure 4.49 to Figure 4.52 of the concrete cubes do show that as the amount of waste crushed glass used as fine aggregate increases then the compressive strength achieved at 7 days (and afterwards) is reduced. All ages of the concrete containing waste glass aggregate had compressive strengths that were lower than conventional concrete- the sole exception was concrete with 25% green glass aggregate after 28 days curing with a strength slightly higher (0.11 N/mm^2) than normal concrete as shown in Figure 4.47. However use of up to 25% waste crush glass as fine aggregate replacement gives only minor reduction in compressive strength when compared with natural sand at all ages. Concrete containing fine aggregate made from unwashed mixed glass manifested the largest reduction in compressive strength i.e. 18% at 28 days.

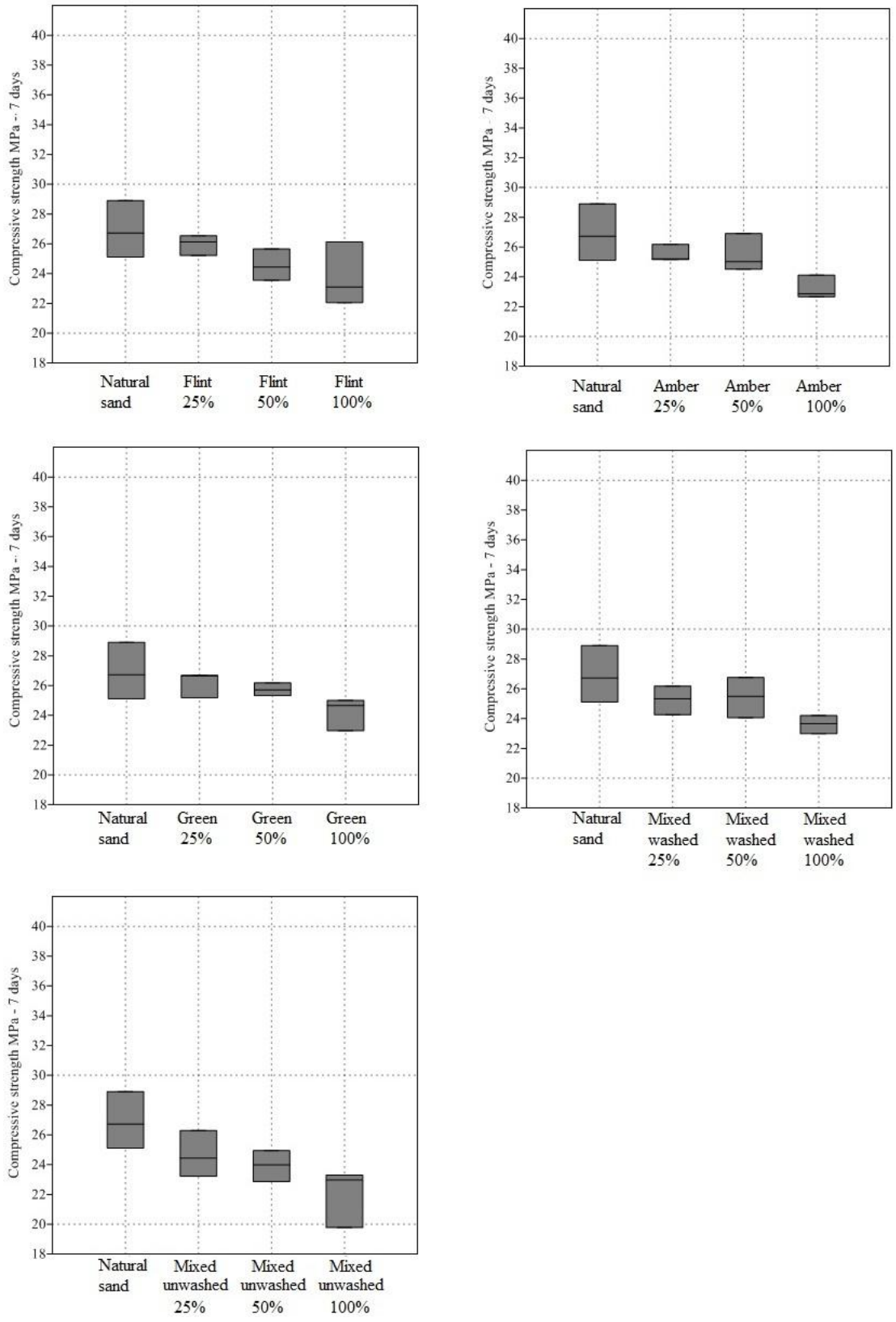

Fig. 4.49 7-day compressive strength of concrete containing glass fine aggregate

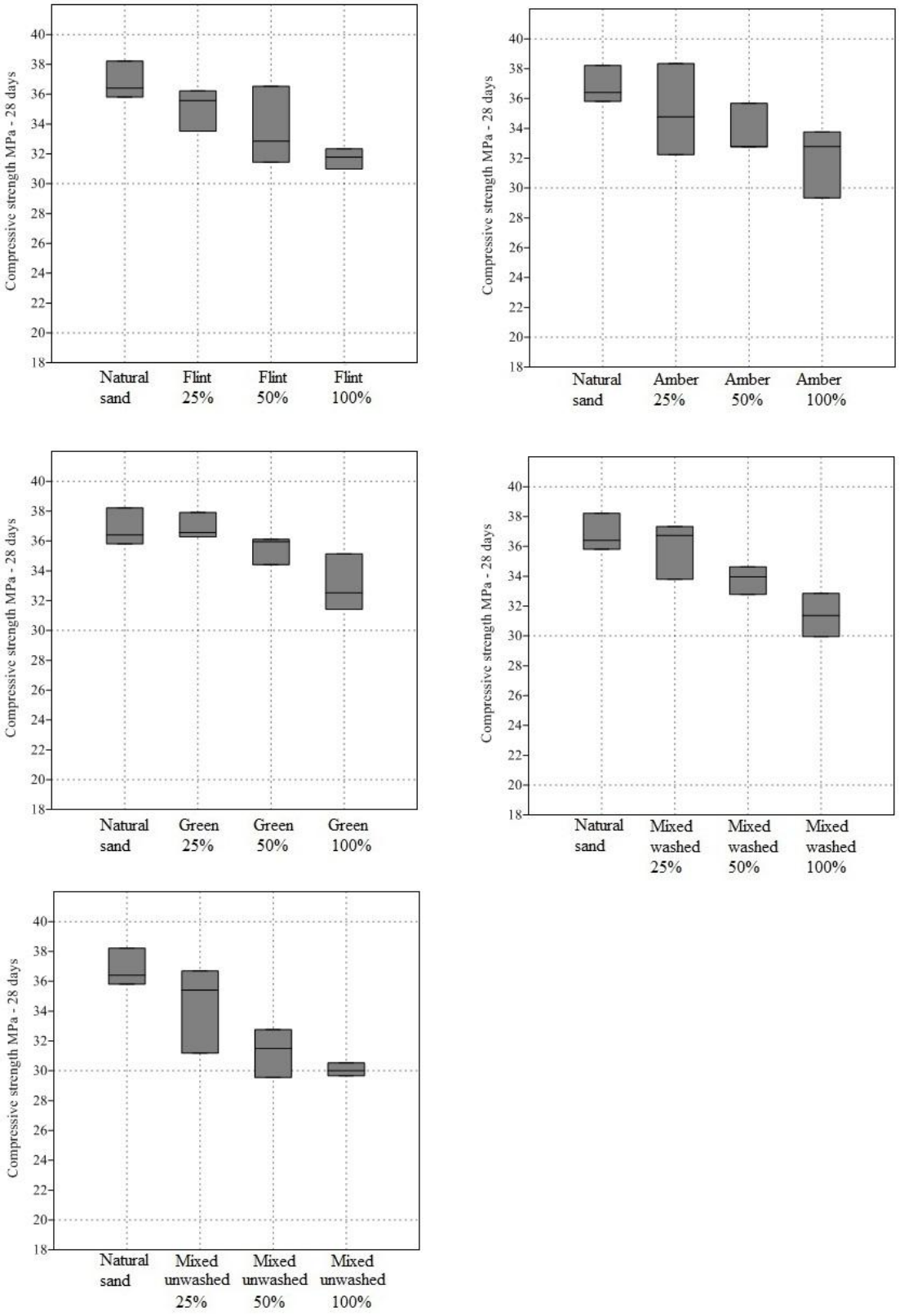

Fig. 4.50 28-day compressive strength of 'glass concrete'

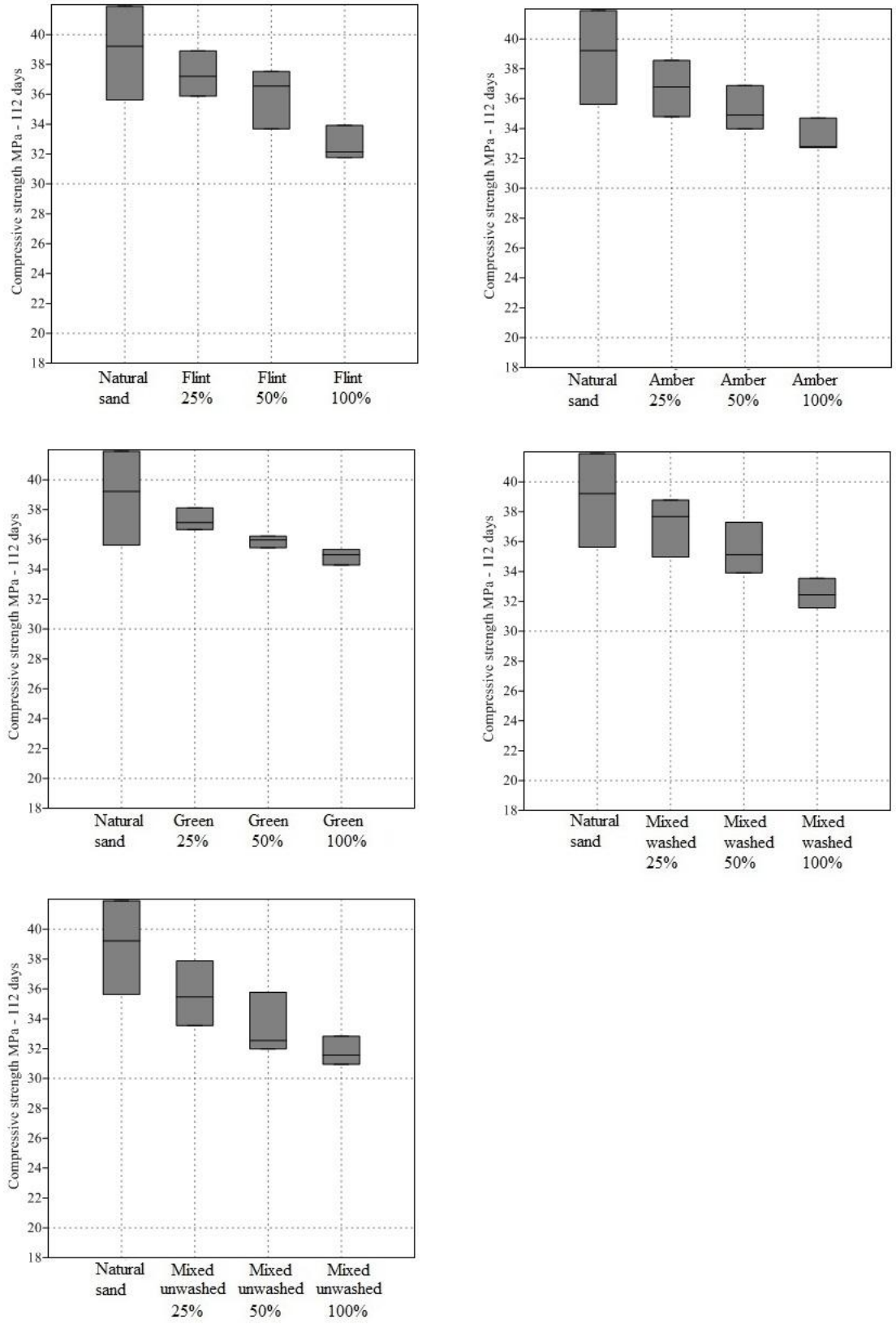

Fig. 4.51 112-day compressive strength of 'glass concrete'

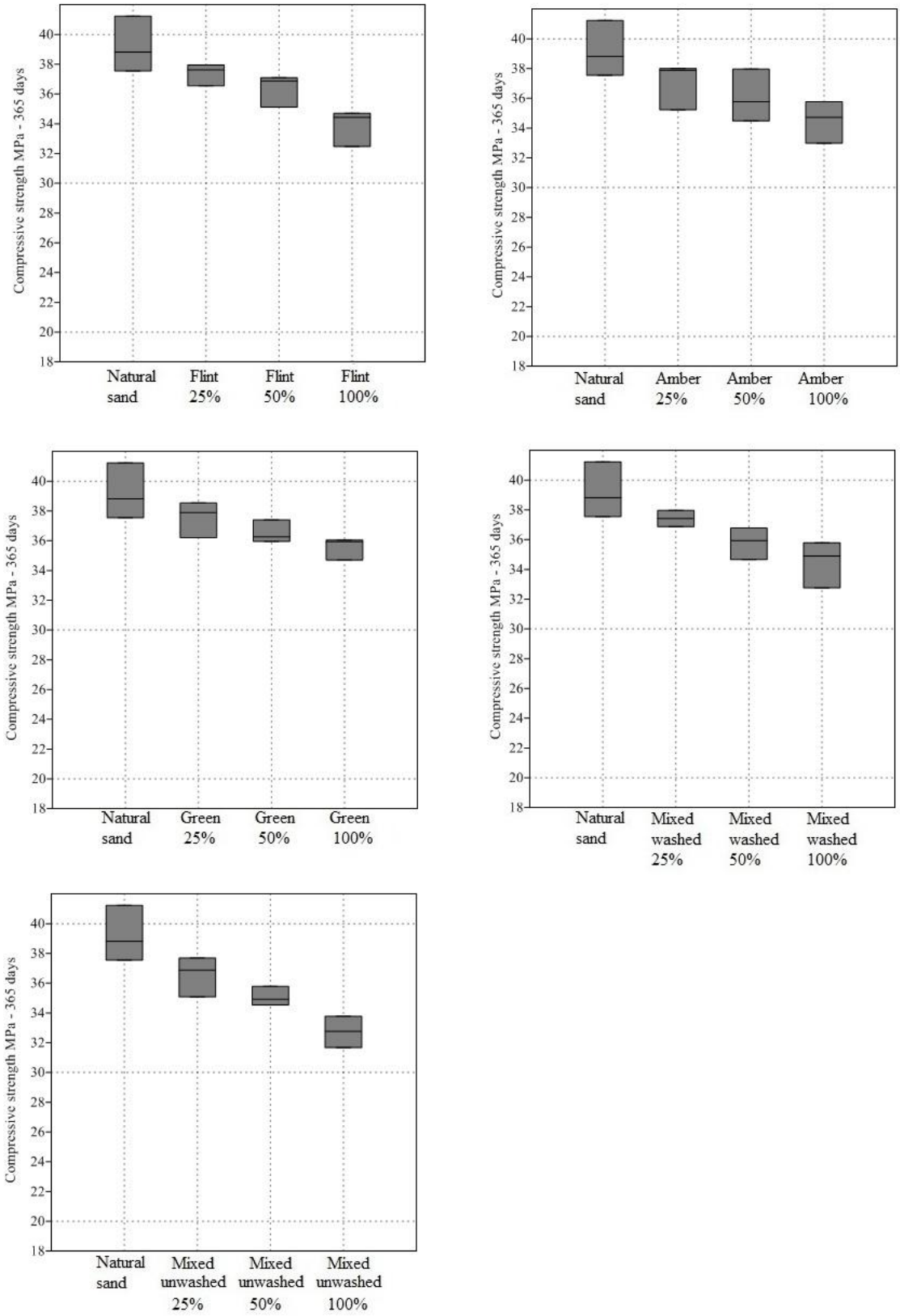

Fig. 4.52 365-day compressive strength of 'glass concrete'

In order to quantify the trends illustrated in Figures 4.49 to 4.52 the compressive strengths have been normalised, whereby

$$\text{Normalised compressive strength} = \frac{\text{Strength of a concrete mix at T days}}{\text{Strength of conventional concrete at T days}} \quad \text{Equ. 4.8}$$

The normalised strength values have been plotted against waste glass content in Figures 4.53 to 4.60.

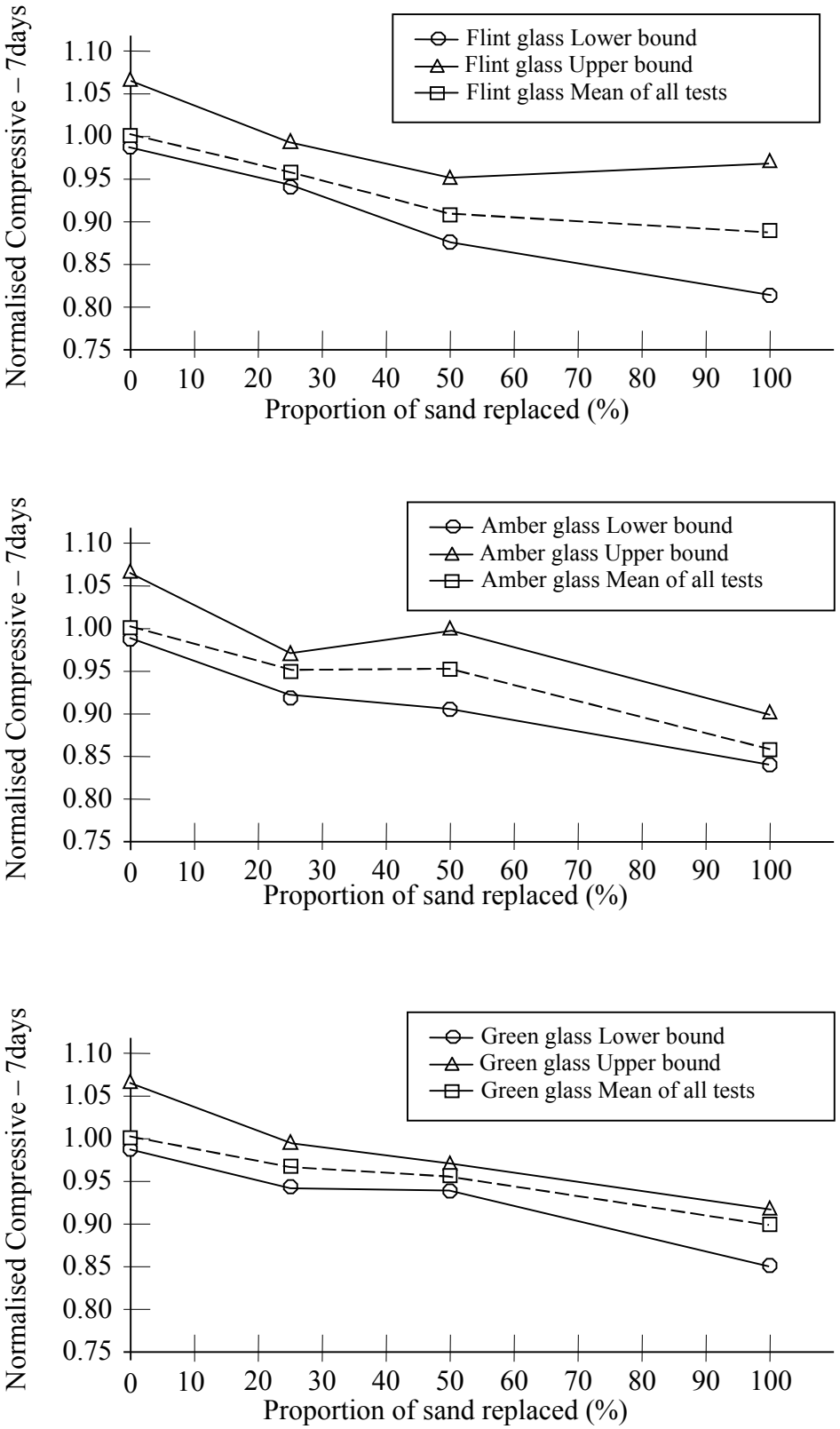

Fig. 4.53 Normalised compressive strength for 'glass concrete' at 7 days (flint, amber and green glass)

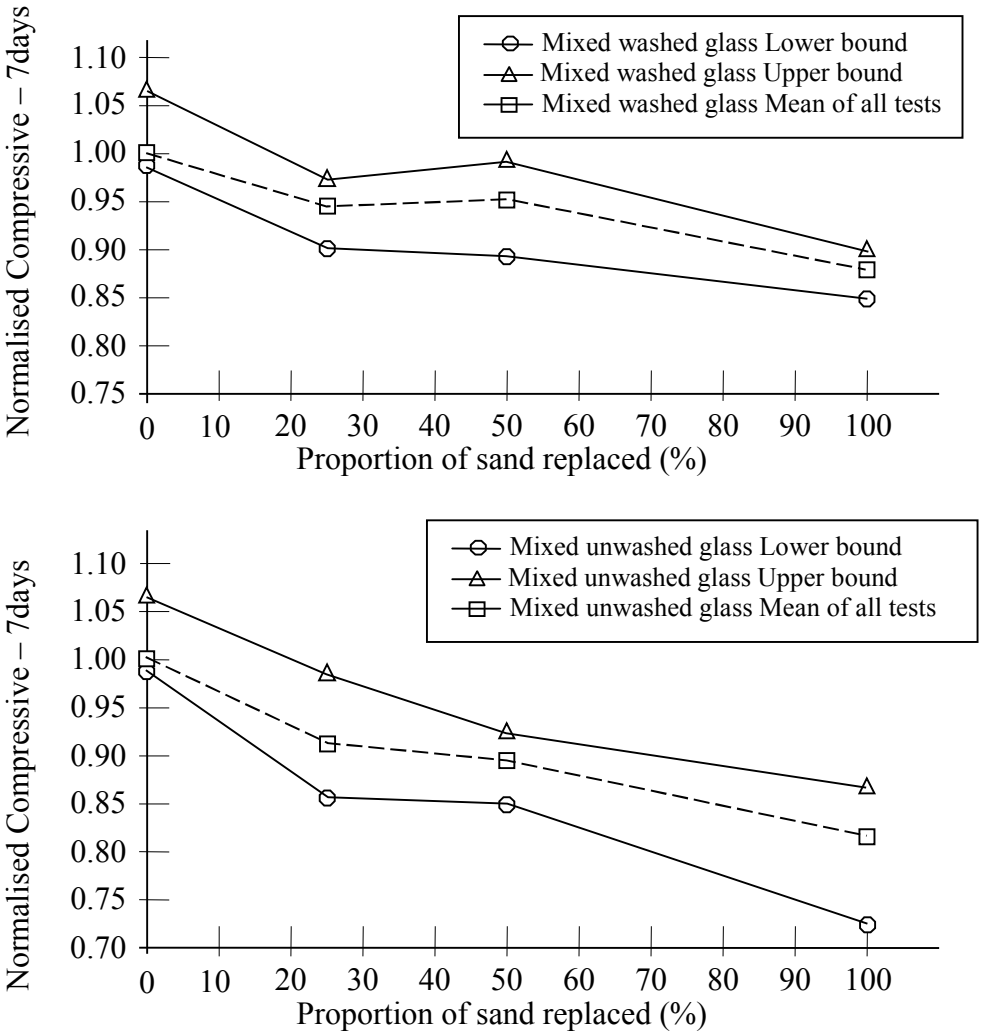

Fig. 4.54 Normalised compressive strength for 'glass concrete' at 7 days (mixed washed and unwashed glass)

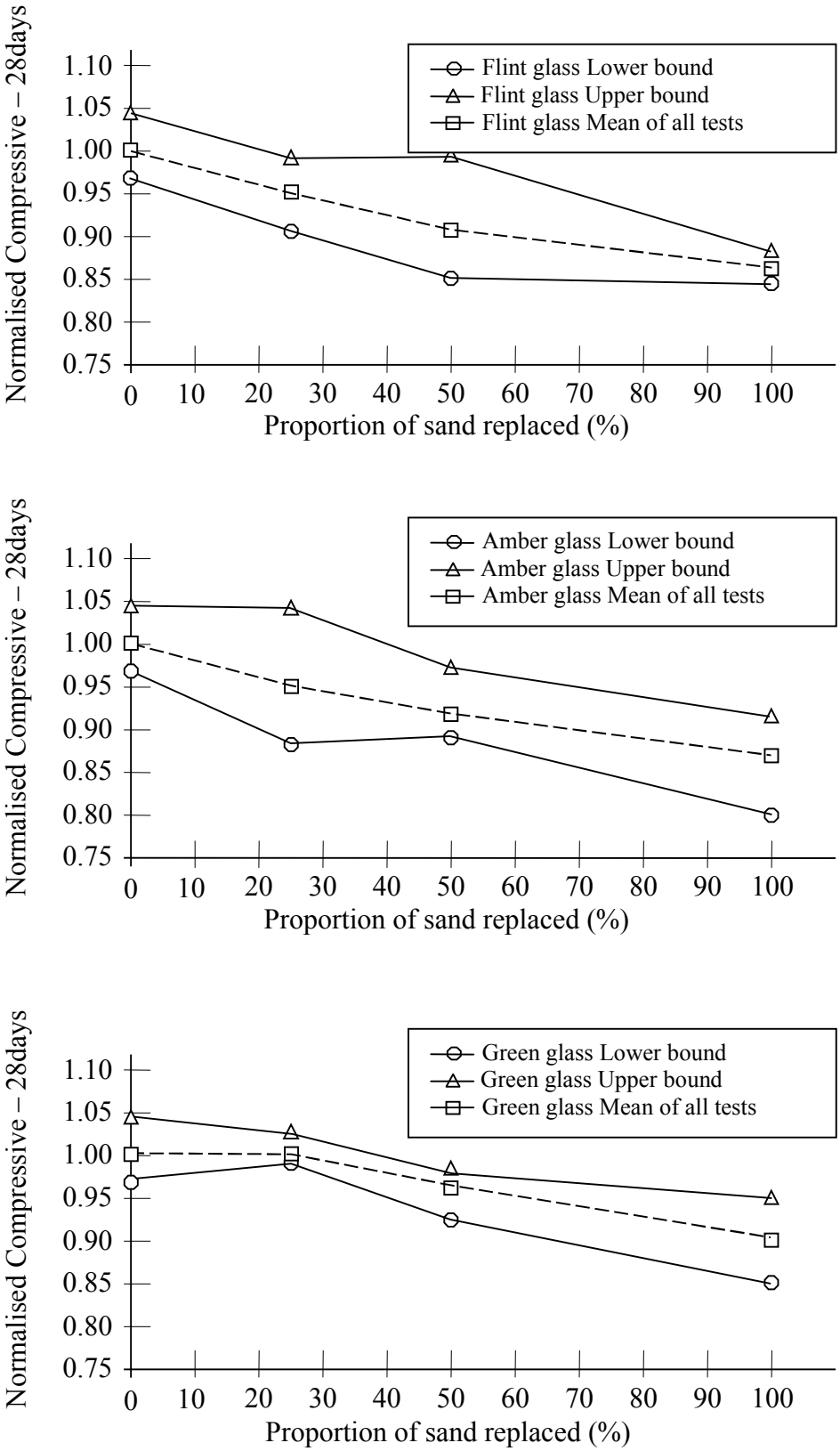

Fig. 4.55 Normalised compressive strength for 'glass concrete' at 28 days (flint, amber and green glass)

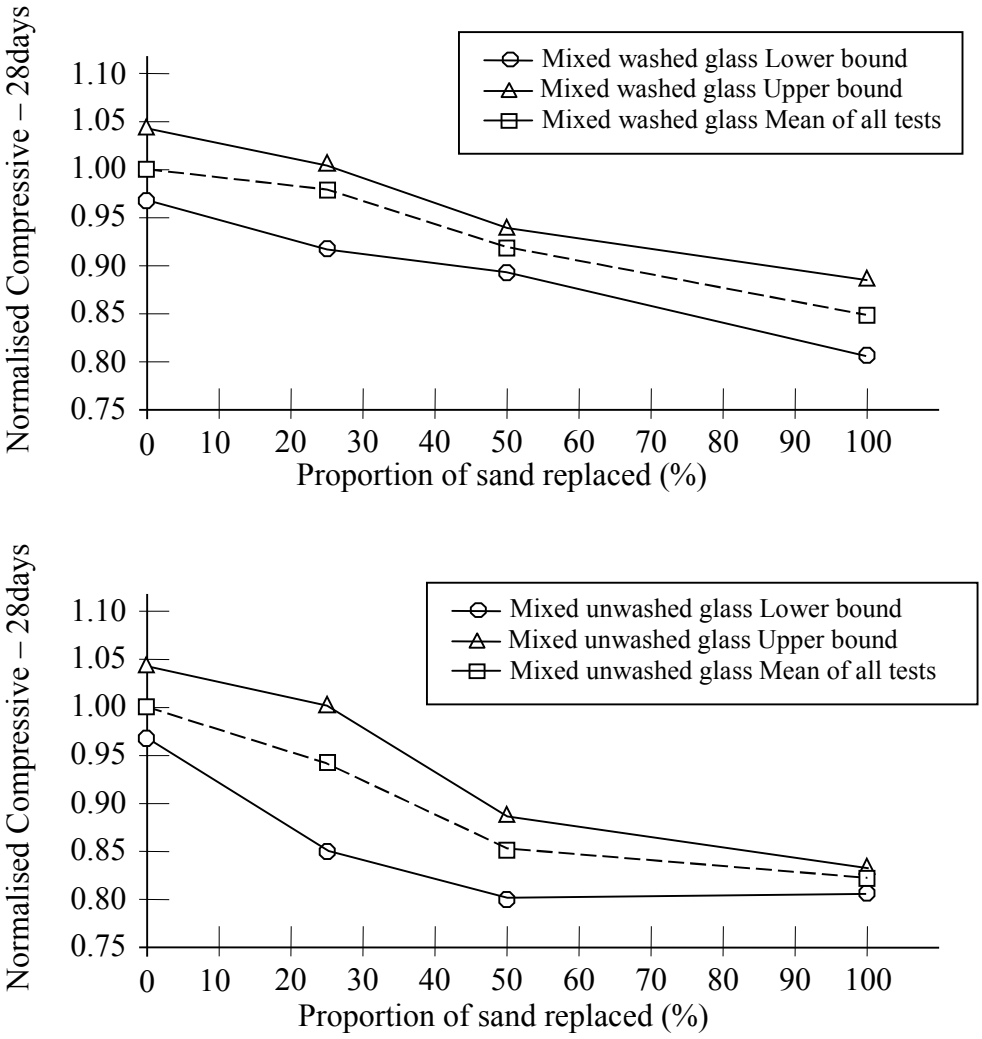

Fig. 4.56 Normalised compressive strength for 'glass concrete' at 28 days (mixed washed and unwashed glass)

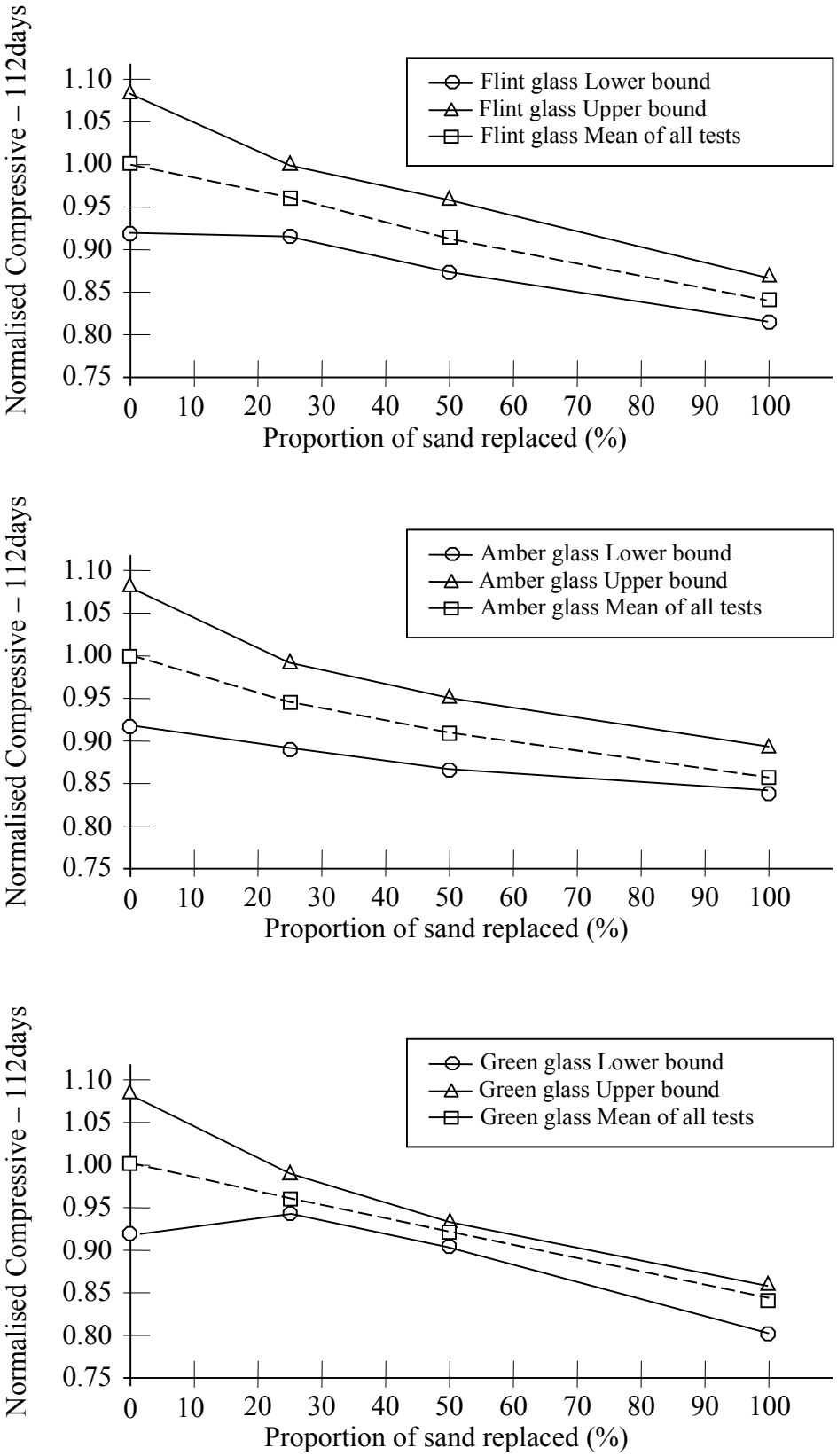

Fig. 4.57 Normalised compressive strength for 'glass concrete' at 112 days (flint, amber and green glass)

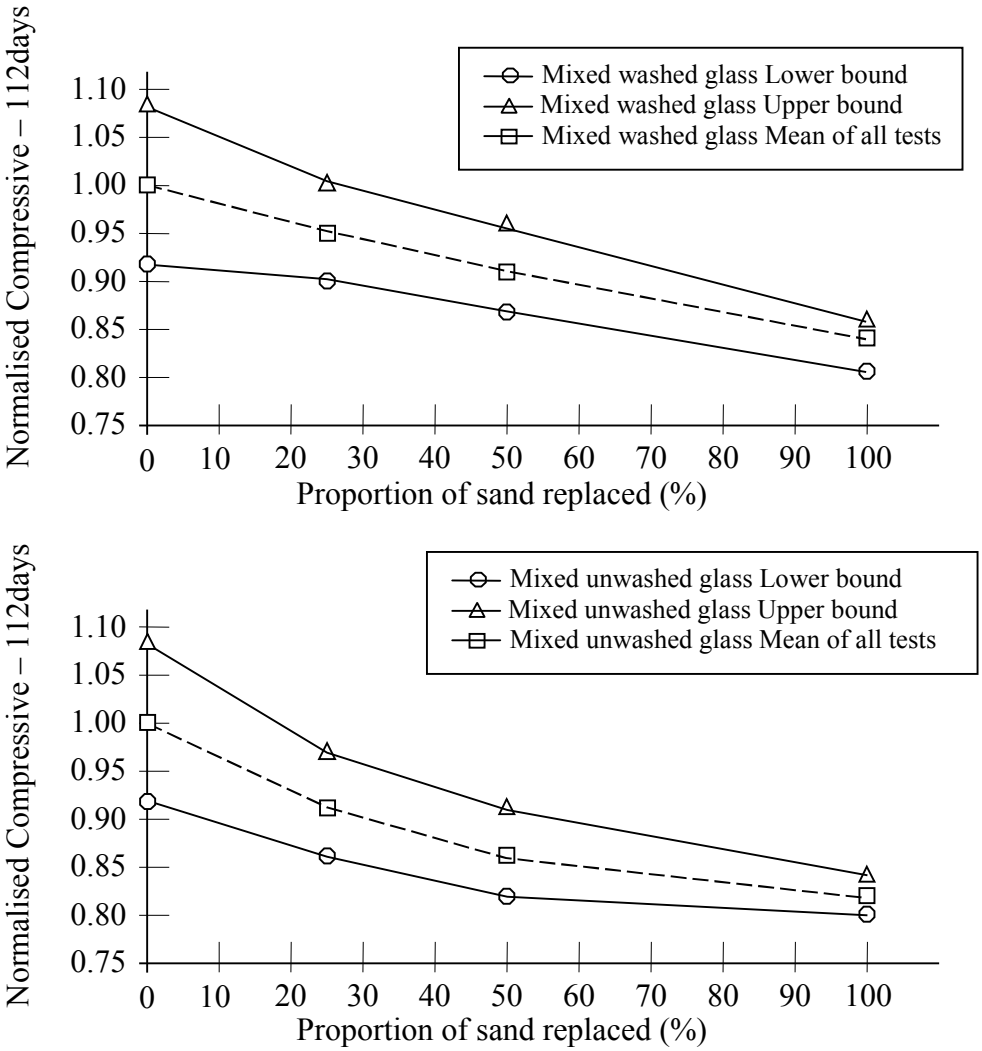

Fig. 4.58 Normalised compressive strength for 'glass concrete' at 112 days (mixed washed and unwashed glass)

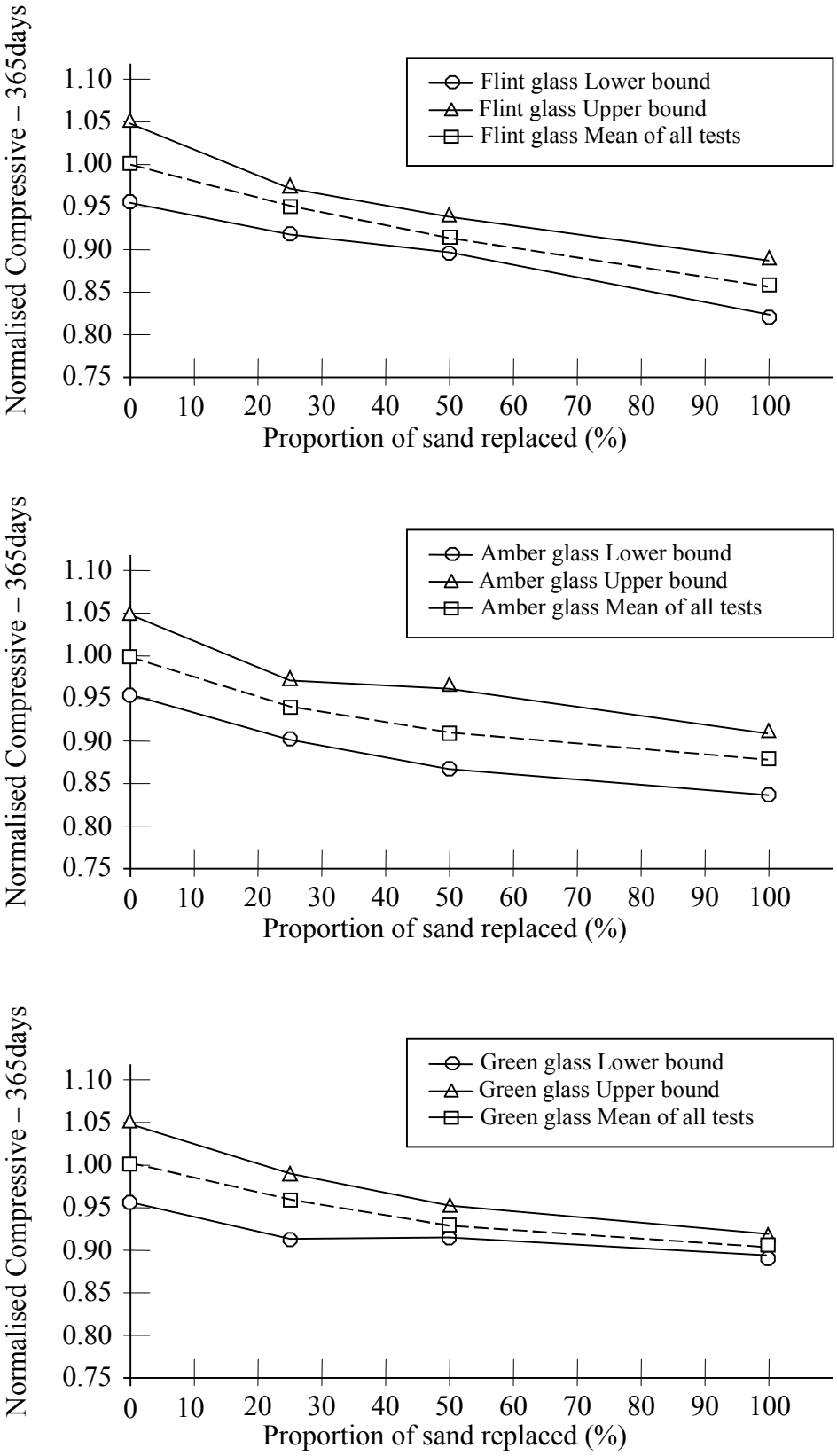

Fig. 4.59 Normalised compressive strength for 'glass concrete' at 365 days (flint, amber and green glass)

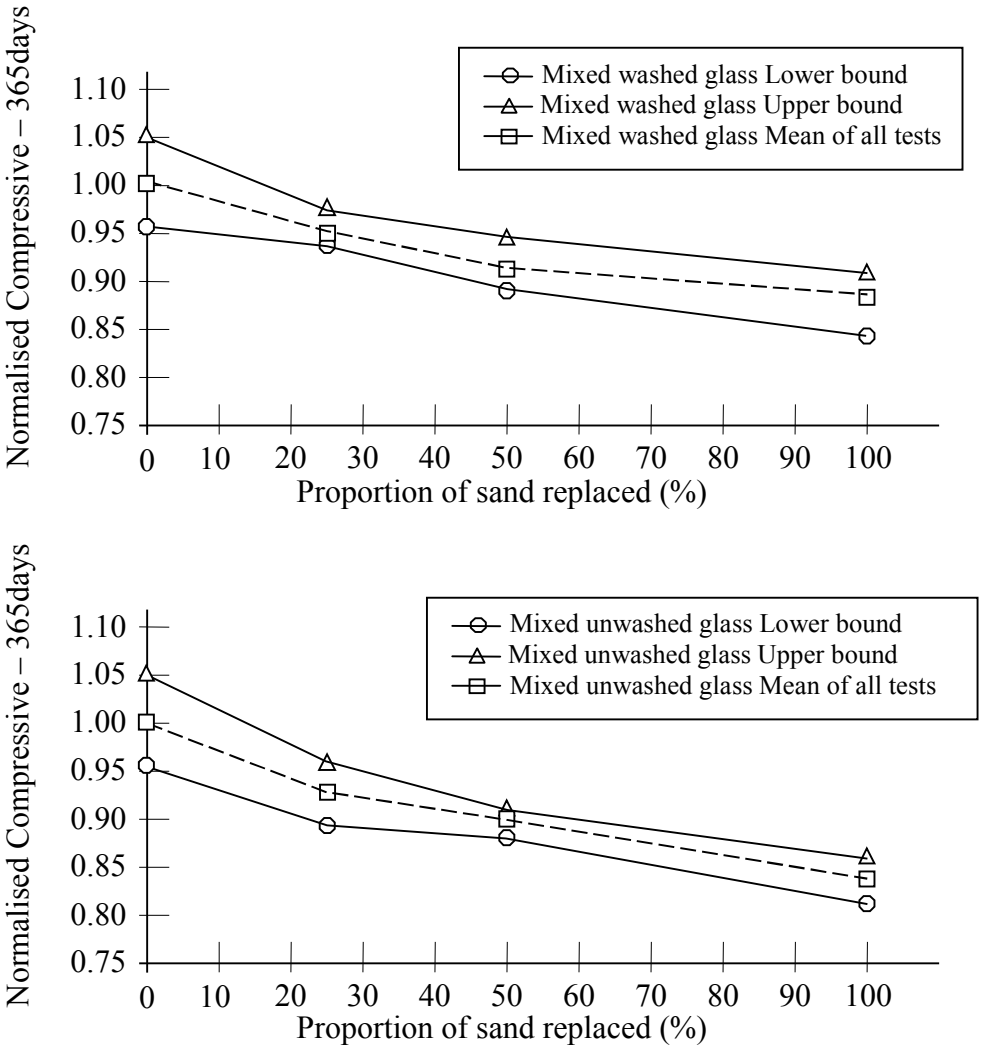

Fig. 4.60 Normalised compressive strength for 'glass concrete' at 365 days (mixed washed and unwashed glass)

The normalised strength plots show that:-

- On average replacement of 25% of conventional fine aggregate by glass led to a 2% to 8% reduction in compressive strength. Replacement of half of the fine aggregate by glass caused a 4% to 15% reduction in strength but total replacement of the normal fine aggregate by glass only caused a 10% to 18% reduction in strength.
- Concrete with green glass fine aggregate replacement exhibited better performance than concretes with other colours of glass, i.e. the 365 day strength was only 4%, 7% and 9% lower than normal concrete for 25%, 50% and 100% glass contents.

- Mixed unwashed glass gave the worst performance of any fine aggregate with 7%, 10% and 16% reduction of strength compared with the control as shown Figure 4.60.
- The performance of concrete containing mixed waste glass was very similar to that of concrete containing flint glass. This would be expected as flint glass was the major component in the mixed waste - as would occur in bottle banks where bottles are not segregated by colour.
- Since the colour and amount of glass replacing fine aggregate cause a reduction in the compressive strength of a mix but do not appear to effect the curing or hardening process (Table 4.16) then the reduction is due to volume changes (as a result of ASR) during curing and/or the 'quality' of the bond between cement paste and glass aggregate (as affected by surface properties of the glass particles).

4.2.5 Water absorption by immersion

Tables 4.17 and 4.18 and Figure 4.61 contain data on the amount of water absorbed over a period of 7 days for all concrete mixes. At the start of the immersion period there is little difference between the values for normal concrete and the mixes containing glass and all mixes showed the same of trend as increasing moisture absorption at a more-or-less uniform rate with the logarithm of time over a period of 8 hours as illustrated in Figure 4.62.

However, after 8 hours of soaking the rate of water absorption for conventional concrete decreased significantly. On the other hand, concretes containing glass aggregate continued to absorb water at a rate that was approximately proportional to logarithm of time right up to the end of testing. For these concretes the rate of water absorption increased with the amount of sand replaced by glass so the results for mixes containing only 25% of glass fine aggregate were similar to the conventional concrete. Even after 7 days of soaking the concretes containing 100% mixed glass still seemed to be absorbing water at about the same rates (with respect to log-time) that they showed after 1 hour.

Since the concrete containing waste glass particles had higher water absorption values than conventional concrete this would suggest that there was a difference between the form (or the location) of the voids in the concretes containing glass and that of the voids within the conventional concrete.

Table 4.17 Water absorption by immersion for concretes containing sand and flint, amber and green glasses

Waste glass content in concrete	Weight increase (%)								
	10min	30min	60min	2hrs	4hrs	8hrs	24hrs	3days	7days
Natural sand	1.88	2.46	3.01	3.80	4.13	4.63	5.10	5.30	5.46
	1.99	2.59	3.13	3.92	4.05	4.65	5.16	5.28	5.43
	1.89	2.42	2.92	3.70	4.12	4.58	5.07	5.32	5.40
	1.92	2.49	3.02	3.80	4.10	4.62	5.11	5.30	5.43
Flint glass 25%	2.21	2.97	3.30	4.16	4.52	4.80	5.61	5.83	5.98
	2.12	3.01	3.38	4.35	4.49	4.78	5.65	5.84	5.86
	2.30	2.95	3.29	4.40	4.58	4.85	5.54	5.76	5.78
	2.21	2.98	3.32	4.30	4.53	4.81	5.60	5.81	5.87
Flint glass 50%	2.07	2.77	3.52	4.19	4.40	4.81	6.24	6.52	6.52
	2.06	2.65	3.50	4.30	4.42	4.70	6.20	6.50	6.55
	2.16	2.59	3.60	4.21	4.50	4.68	6.31	6.42	6.62
	2.10	2.67	3.54	4.23	4.44	4.73	6.25	6.48	6.56
Flint glass 100%	2.10	2.61	3.03	4.00	4.60	4.86	6.30	6.31	6.64
	2.10	2.51	3.10	3.91	4.62	4.85	6.26	6.53	6.69
	2.20	2.60	2.95	3.89	4.73	4.96	6.40	6.51	6.57
	2.13	2.57	3.03	3.93	4.65	4.89	6.32	6.45	6.63
Amber glass 25%	1.57	2.08	2.76	3.33	3.89	4.58	5.57	5.68	5.68
	1.68	2.21	2.81	3.51	3.79	4.45	5.54	5.56	5.72
	1.72	2.10	2.68	3.38	3.81	4.56	5.51	5.65	5.66
	1.66	2.13	2.75	3.41	3.83	4.53	5.54	5.63	5.69
Amber glass 50%	1.64	1.99	2.64	3.30	3.90	4.33	5.46	5.85	5.86
	1.77	2.12	2.59	3.45	3.89	4.45	5.60	5.83	5.86
	1.65	1.94	2.68	3.39	3.76	4.36	5.62	5.78	6.01
	1.69	2.01	2.64	3.38	3.85	4.38	5.56	5.82	5.91
Amber glass 100%	1.18	1.48	1.89	2.90	3.45	4.00	5.52	5.58	5.65
	1.06	1.46	1.86	2.79	3.46	4.03	5.59	5.68	5.78
	1.19	1.56	1.79	2.88	3.59	3.91	5.48	5.60	5.65
	1.14	1.50	1.85	2.86	3.50	3.98	5.53	5.62	5.69
Green glass 25%	1.27	2.03	1.85	2.64	4.09	4.47	5.86	6.04	6.05
	2.33	3.17	3.56	4.79	4.03	4.46	5.79	5.93	6.13
	2.26	2.99	3.28	3.90	3.97	4.57	5.87	5.97	5.99
	1.95	2.73	2.90	3.78	4.03	4.50	5.84	5.98	6.06
Green glass 50%	1.40	2.02	2.36	3.19	3.87	4.42	6.03	6.13	6.32
	1.52	2.06	2.39	3.09	4.00	4.56	5.89	6.06	6.22
	1.56	2.15	2.46	3.08	4.01	4.58	6.05	6.20	6.25
	1.49	2.08	2.40	3.12	3.96	4.52	5.99	6.13	6.26
Green glass 100%	1.48	1.81	2.36	2.32	3.90	4.33	6.29	6.33	6.46
	1.45	1.85	2.30	2.75	3.79	4.43	6.19	6.35	6.38
	1.56	1.75	2.19	3.33	3.92	4.29	6.15	6.19	6.29
	1.50	1.80	2.28	2.80	3.87	4.35	6.21	6.29	6.38

Table 4.18 Water absorption by immersion for concretes containing mixed washed and mixed unwashed glasses

Waste glass content in concrete	Weight increase (%)								
	10min	30min	60min	2hrs	4hrs	8hrs	24hrs	3days	7days
Mixed washed glass 25%	1.96	3.00	3.51	4.09	4.52	4.81	6.00	6.09	6.19
	1.92	3.05	3.51	4.26	4.58	4.90	5.97	6.06	6.25
	2.03	2.89	3.34	4.21	4.49	4.81	5.88	6.12	6.13
	1.97	2.98	3.45	4.19	4.53	4.84	5.95	6.09	6.19
Mixed washed glass 50%	1.57	2.26	3.08	3.28	3.99	4.50	6.21	6.38	6.41
	1.63	2.29	3.06	3.33	4.09	4.38	6.30	6.32	6.37
	1.91	2.67	3.53	3.85	3.95	4.50	6.18	6.29	6.46
	1.70	2.41	3.23	3.49	4.01	4.46	6.23	6.33	6.41
Mixed washed glass 100%	1.69	2.12	2.69	3.06	3.95	4.69	6.54	6.57	6.63
	1.70	2.14	2.70	3.17	3.93	4.86	6.50	6.59	6.66
	1.60	1.99	2.81	3.08	4.06	4.82	6.40	6.46	7.01
	1.66	2.08	2.73	3.10	3.98	4.79	6.48	6.54	6.77
Mixed unwashed glass 25%	2.15	2.50	3.04	4.07	4.56	4.91	5.96	6.24	6.43
	2.21	2.60	3.07	3.64	4.60	4.81	5.93	6.10	6.26
	2.30	2.67	3.10	4.15	4.49	4.92	5.87	6.26	6.33
	2.22	2.59	3.07	3.96	4.55	4.88	5.92	6.20	6.34
Mixed unwashed glass 50%	1.77	2.35	3.03	3.53	4.02	4.62	6.00	6.12	6.20
	1.89	2.37	3.03	3.46	4.09	4.60	5.90	6.11	6.20
	1.77	2.45	3.16	3.60	3.98	4.46	5.98	6.01	6.10
	1.81	2.39	3.07	3.53	4.03	4.56	5.96	6.08	6.17
Mixed unwashed glass 100%	1.89	2.50	2.97	3.33	3.98	4.74	6.51	6.71	6.76
	1.95	2.57	2.87	3.48	4.01	4.69	6.44	6.80	6.93
	1.84	2.49	2.89	3.42	3.89	4.58	6.55	6.68	6.80
	1.89	2.52	2.91	3.41	3.96	4.67	6.50	6.73	6.83

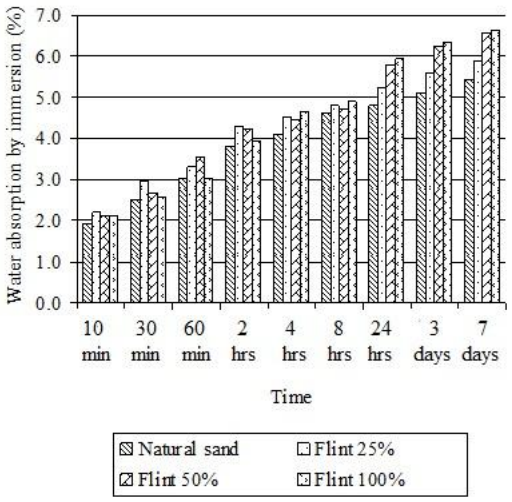

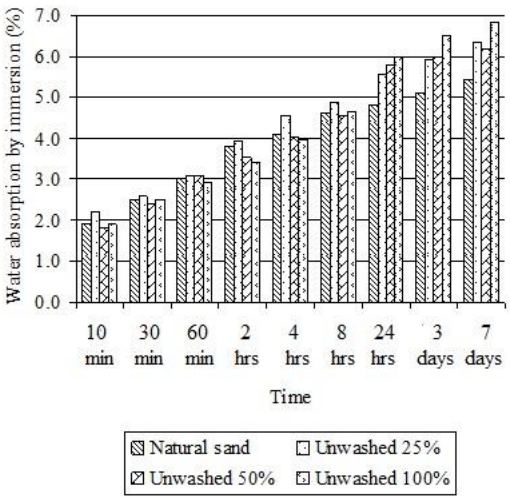

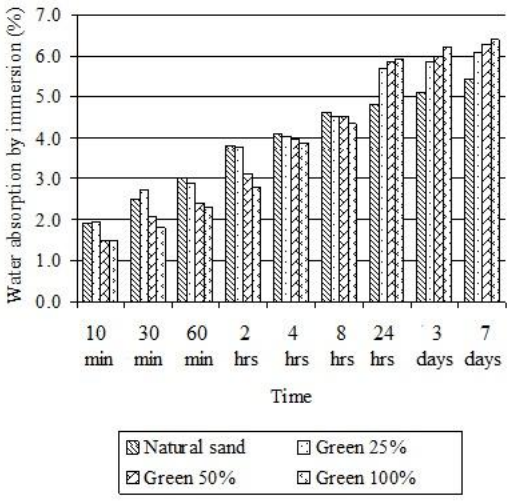

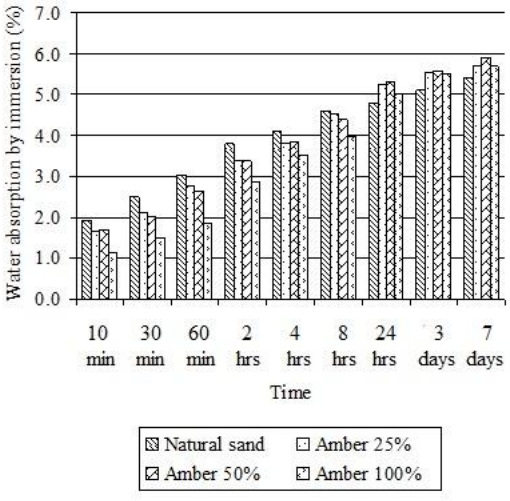

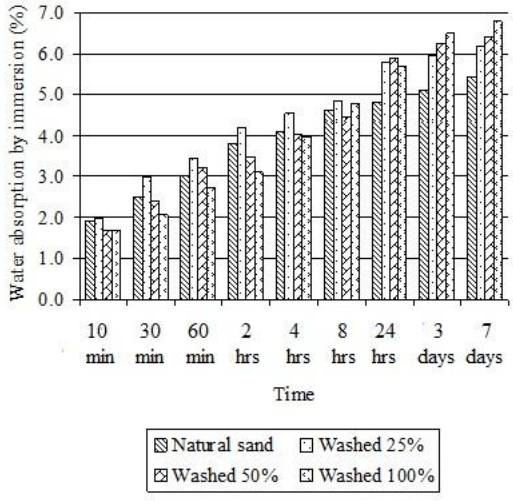

Fig. 4.61 Water absorption by immersion

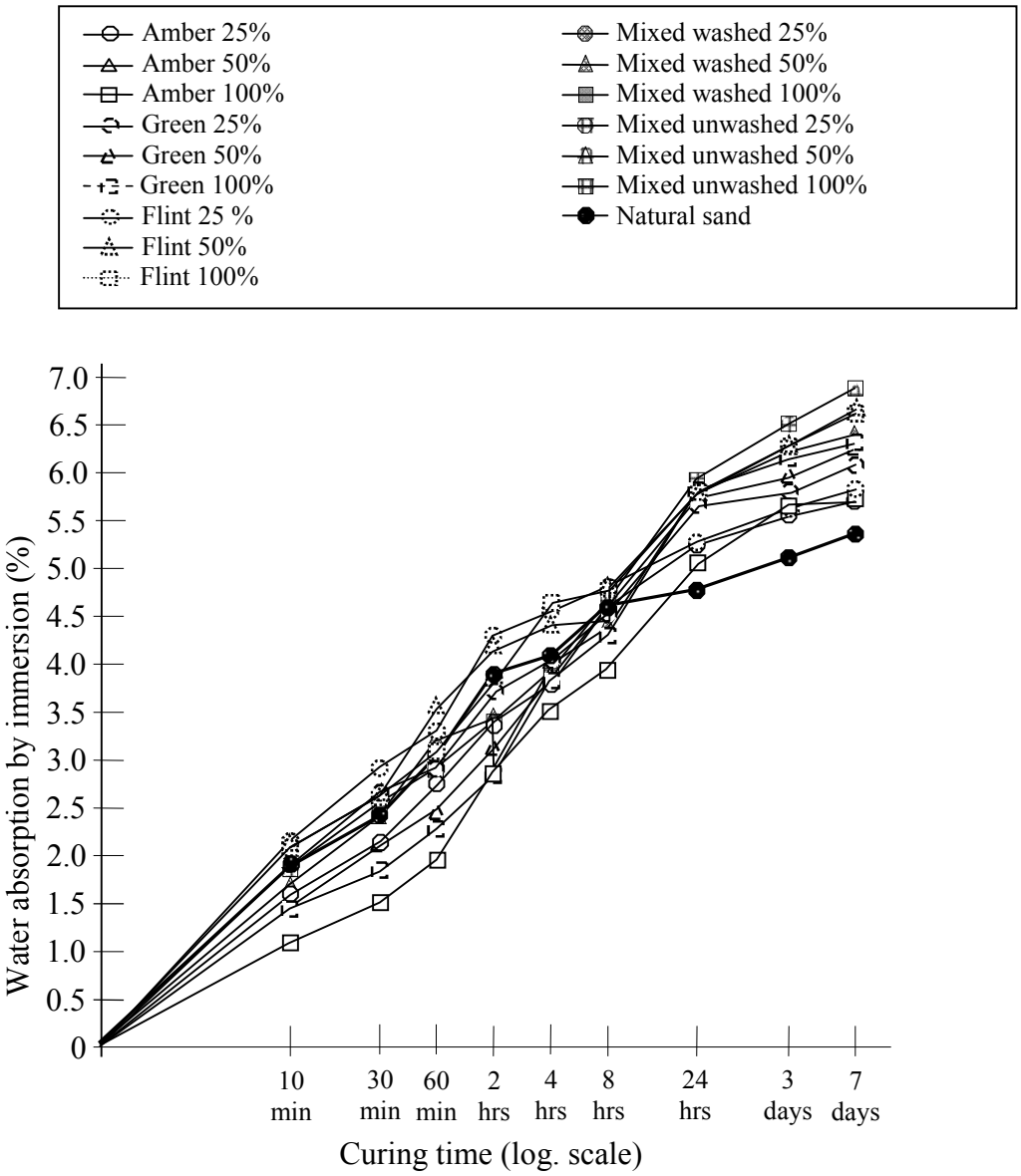

Fig. 4.62 Water absorption by immersion as a function of time

4.2.6 Water absorption by capillary rise (sorptivity)

For each concrete mix three bars were cured and dried as described in Section 3.4.14 and were sat in water for up to a week. The change in mass of each bar was determined at various times after the start of immersion as indicated in Table 4.19. Because the results for each of the bars made from a given mix were very similar the data in Table 4.19 are the mean weight gain (in grams) for each value of elapsed time.

Table 4.19 Mean weight gain (in grams) with time for concrete bars subjected to capillary rise test

Mix		Elapsed Time								
		10min	30min	1hr	2hr	4hr	8hr	1day	3day	7day
Control		2.9	4.7	6.4	9.8	12.2	13.8	15.3	15.8	16.2
Flint glass	100%	2.4	4.1	5.0	7.0	8.4	8.9	11.5	11.7	12.1
	50%	2.6	4.2	5.6	7.9	9.6	10.1	13.5	13.9	14.1
	25%	3.5	4.5	5.9	8.6	10.6	11.3	13.1	13.6	13.8
Amber glass	100%	2.4	3.8	4.9	6.8	8.8	9.9	13.8	14.0	14.2
	50%	3.1	4.4	5.4	7.4	9.2	10.5	13.3	14.0	14.2
	25%	3.2	4.4	5.3	7.3	9.3	11.0	13.4	13.7	13.8
Green glass	100%	2.8	3.9	4.6	6.2	8.0	8.9	12.8	12.9	13.1
	50%	2.7	4.1	5.3	7.6	10.2	11.6	15.1	15.6	15.8
	25%	3.2	4.4	5.6	7.7	9.7	11.0	14.1	14.4	14.7
Mixed glass (washed)	100%	3.0	4.1	5.2	7.2	8.2	9.9	13.4	13.5	14.0
	50%	3.7	4.6	5.5	7.3	9.1	10.0	14.1	14.2	14.5
	25%	3.1	4.3	5.8	8.1	10.2	10.9	13.3	13.6	13.9
Mixed glass (unwashed)	100%	3.7	4.7	5.6	7.5	8.5	10.0	14.0	14.4	14.6
	50%	3.4	4.4	5.4	7.1	8.2	9.3	12.1	12.4	12.6
	25%	3.5	4.6	5.4	6.9	7.9	8.2	9.9	10.4	10.6

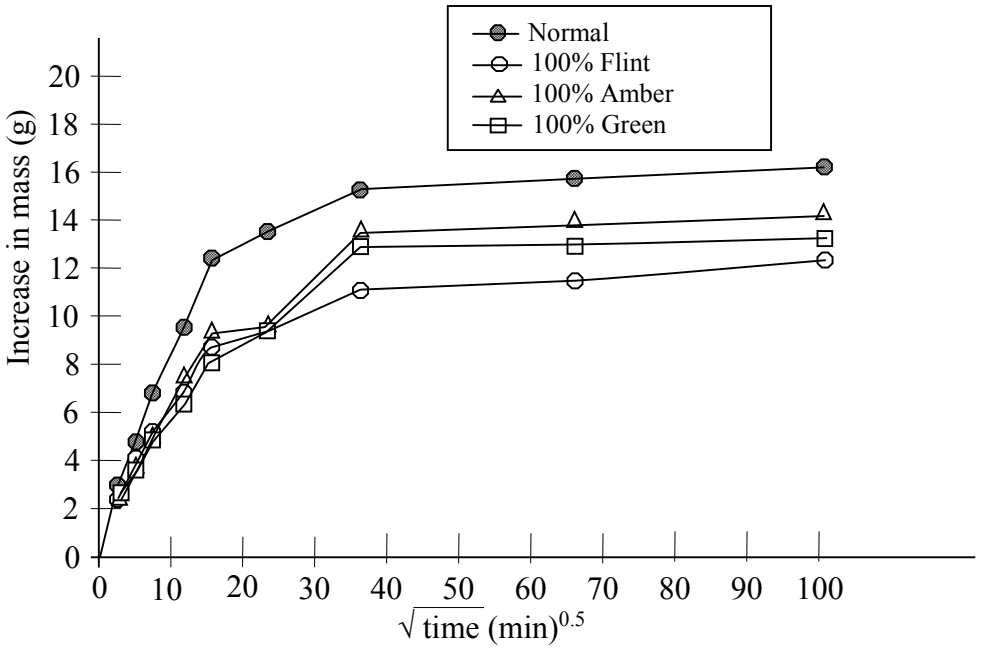

Fig. 4.63 Mean increase in mass of bars with time

From equation 3.3, if the sorptivity (S) is a constant then the gain in mass of a concrete bar during a capillary rise test will be proportional to the square root of time which has elapsed from the start of the test. Figure 4.63 shows plots of mean increase in bar mass for selected concrete mixes. Shortly after the start of a test a linear relationship is established between gain in mass and square root of time. After several hours the rate of capillary rise progressively decreases with time and by the time that one week has elapsed the concrete bars have effectively ceased to gain any further mass, i.e. there is no further increase in the height to which water rises in the concrete due to capillary action. Neville (1995) recommended that sorptivity should be determined using data obtained during the first 4 hours of testing and that the point of origin (of the data in Figure 4.63) should be ignored because of initial extraneous soaking effects. The resultant sorptivity values are given in Table 4.20. This Table also contains the final notional water rise due to capillary action, which is equal to the increase in mass (per unit are of contact between concrete and water) after 7 days divided by the density of water.

Table 4.20 Sorptivity and final notional water rise for concrete mixes

Replacement fine aggregate	Sorptivity, *S*, (mm/min$^{0.5}$)				Final notional water rise, (Final), mm			
	Glass content (%)				Glass content (%)			
	0	25	50	100	0	25	50	100
Flint glass	0.149	0.115	0.110	0.099	3.24	2.76	2.82	2.42
Amber glass	0.149	0.112	0.101	0.099	3.24	2.76	2.84	2.84
Green glass	0.149	0.107	0.107	0.092	3.24	2.94	3.16	2.62
Mixed washed	0.149	0.111	0.091	0.091	3.24	2.78	2.90	2.80
Mixed unwashed	0.149	0.083	0.081	0.079	3.24	2.12	2.52	2.92

The data in Table 4.20 show that the replacement of conventional fine aggregate by any crushed glass causes a substantial fall in Sorptivity of the hardened concrete. The sorptivity also falls as the amount of glass used as fine aggregate increases but to a much smaller degree as it can be seen from Figure 4.64. This figure also shows that sorptivity value is essentially independent of the colour of the glass aggregate.

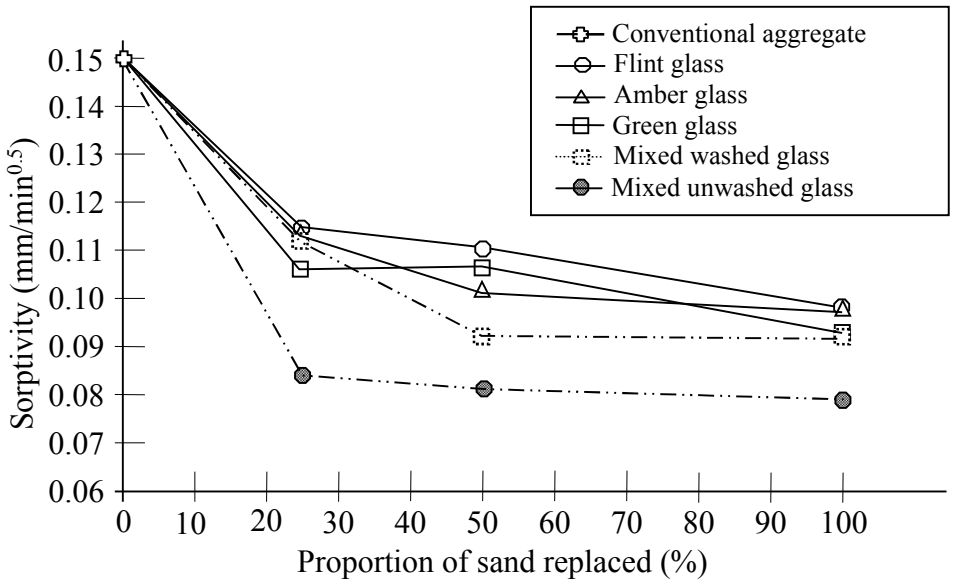

Fig. 4.64 Effect of glass content on Sorptivity

Figure 4.65 shows the effect of glass content on the final notional height of capillary rise. All glass mixtures are below that for conventional concrete but there are no obvious trends relating to glass colour or amount of natural aggregate replaced by glass.

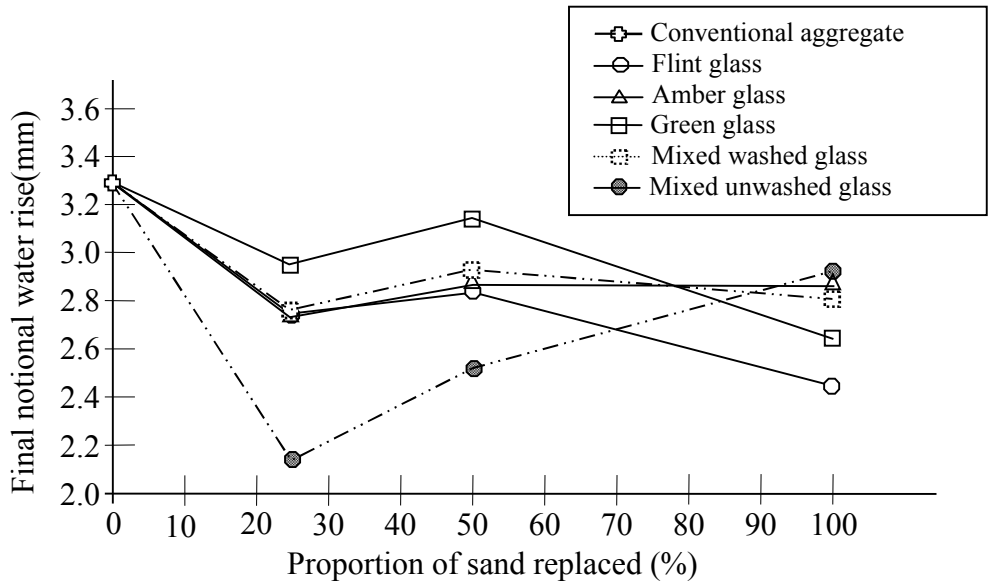

Fig. 4.65 Effect of glass content on capillary rise

4.3 Fine aggregate characterisation

The aggregate used in the research was not a collection of grains which were manufactured to make them more-or-less identical in shape. Hence four descriptors have been chosen to define and quantify the form, i.e. shape and surface texture, of the fine aggregate particles in order to assess their influence on the immediate and long-term properties of concrete containing glass aggregate, which the shape and texture have a significant impact on the strength of concrete. This is because the degree of packing of the aggregates, and hence the voids content in the concrete.

4.3.1 Particle shape

According to BS 812 (1975) angularity, or absence of rounding, of particles of an aggregate is a property which is important because it affects the ease of handling a mixture of aggregate and binder, e.g. the workability of the concrete or the stability of mixtures that rely on the interlocking of the particles (as indicated by slump and flow table tests). To classify the shapes of natural particles in terms of their angularity, Zingg (1935) introduced the concept of using a particle's overall dimensions, in three mutually-perpendicular directions, to define Elongation and Flatness Ratios (Section 2.3.1). For particles whose shape is classified by their appearance in two-dimensions, as is undertaken in particle shape measurement by image processing, then an equivalent to Zingg's parameters is a simple Aspect Ratio, i.e.

$$\text{Aspect Ratio} = \frac{\text{Maximum Feret length}}{\text{Breadth}} \qquad \text{Equ. 4.9}$$

wherein "Feret length" is the distance between two parallel lines which are tangential to the particle being measured. Figure 3.39 shows the circumscribing rectangular prism that is used to define feret values. The larger dimension, which would traditionally be measured using a caliper is also known as the Max.Feret diameter or Max.Feret length. The breadth measurement is the dimension of the circumscribed rectangle that is orthogonal to the Max.Feret length. Aspect Ratio can be considered as indicating elongation as well as being a measure of Shape Index as defined in BS EN 933-4:2000.

The data in Table 4.21 shown the results of determination of the Aspect Ratio for the four different types of fine aggregate used in the research.

The natural sand contains particles with cross-section ranging from approximately circular or square, i.e. with an Aspect Ratio essentially to unity, to approximately rectangular or elliptical (with an Aspect ratio of about 2.6). Whilst all of the glass aggregates had some particles that were approximately circular or square in cross-section they also contained particles that were more elongated than the sand particles, with Aspect Ratios up to 3.9 approximately (for the flint glass). Consequently the natural sand has a mean value of Aspect Ratio which is lower than all those for crushed glass particles. There are differences between the shape factors for coloured manually-crushed glass and commercial glass supplies of the glass aggregate.

Figures 4.66 and 4.67 shows the distribution and range of Aspect Ratios for all aggregates used in concrete mixes. The distributions are asymmetrical because the lower limit of Aspect Ratio is unity (for short particles with square or circular cross-section) and the upper limit is infinity. However for each type of fine aggregate, i.e. the natural sand and the individual colours of glass, the frequency distribution of Aspect Ratio is a reasonable fit to a non-normal distribution about a peak value as can be seen by overlaying a suitably-sized 'Bell shape' over the frequency plots in Figure 4.66. The foregoing peak value is not the mean value given in Table 4.21 because Aspect Ratios cannot be less than unity so the non-normal distribution curve is automatically truncated by this boundary. The respective peak values for the normal distribution fits occur at Aspect Ratios of 1.25 (sand), 1.40 (flint glass), 1.15 (amber glass) and 1.25 (green glass), approximately. The Kruskal-Wallis test may also be used to compare distributions that are not necessarily normal if two, or more, distributions are similar or from the same source. Kruskal-Wallis was does not test the null hypothesis that the distributions have identical means, which is the null hypothesis of a one-way anova.

The Kruskal-Wallis test supports the consideration that the fine aggregate particles can be considered in three groups in terms of the Aspect Ratio. The manual crushed glass sample and the commercial glass suppliers sample indicates similar population distributions. Natural sand and most of glass aggregate for the H:test values being below p=0.05 (same) most strongly indicated dissimilar population, except the amber glass at 0.1217 and 0.1144, at the above p=0.05 significance level.

Table 4.21 Univariate statistics for Aspect Ratio of fine aggregate particles

Univariate Statistics	Natural sand	Manual crushed glass			Commercial glass suppliers		
		Flint	Amber	Green	Flint	Amber	Green
N	50	50	50	50	50	50	50
Min	1.068	1.019	1.064	1.062	1.106	1.023	1.078
Max	2.562	3.878	2.871	2.830	3.146	3.190	3.189
Sum	69.215	84.590	76.417	76.893	80.599	76.012	85.463
Mean	1.384	1.692	1.528	1.538	1.612	1.520	1.709
Std. error	0.039	0.079	0.059	0.055	0.063	0.060	0.059
Variance	0.078	0.312	0.175	0.150	0.196	0.177	0.173
Stand. Dev	0.279	0.558	0.419	0.387	0.443	0.421	0.416
Median	1.335	1.590	1.411	1.399	1.554	1.414	1.580
25 prcntil	1.190	1.261	1.219	1.263	1.249	1.233	1.408
75 prcntil	1.533	1.930	1.737	1.764	1.755	1.769	1.929
Skewness	2.025	1.643	1.366	1.230	1.805	1.731	1.111
Kurtosis	5.980	3.797	1.531	1.277	4.105	4.166	2.001
Georm. Mean	1.361	1.617	1.480	1.496	1.563	1.473	1.664

Mann-Whitney pairwise comparisons
Bonferroni corrected/ uncorrected:

Kruskal-Wallis test	Natural sand	Manual crushed glass			Commercial glass suppliers		
		Flint	Amber	Green	Flint*	Amber*	Green*
Natural sand	0	0.0013	0.1217	0.0448	0.0015	0.1144	0.00001
Flint glass		0	0.0861	0.1938	0.5625	0.0953	0.4566
Amber glass			0	0.7329	0.1744	0.9533	0.0073
Green glass				0	0.3610	0.6294	0.0154
Flint glass*					0	0.2096	0.1546
Amber glass*						0	0.0054
Green glass*							0
H (chi^2):		24.64					
Hc (tie corrected):		24.64					
p(same):		0.000398					

* Commercial glass suppliers

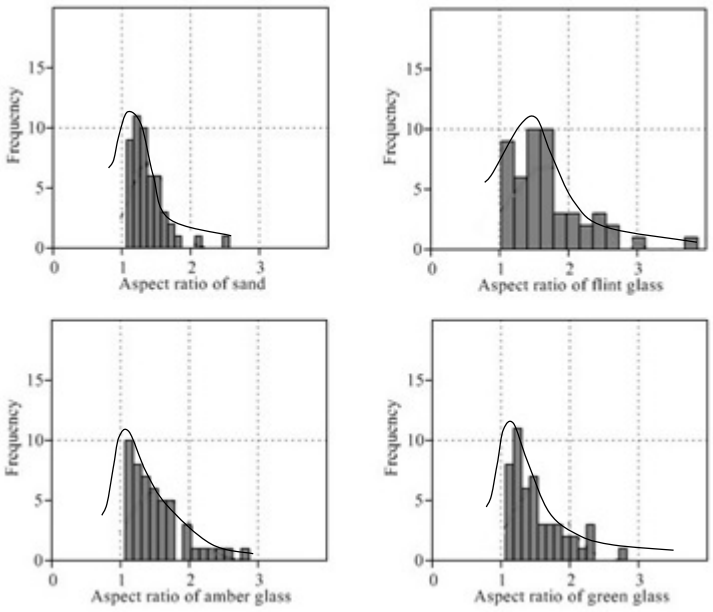

Fig. 4.67 Frequency distribution for Aspect Ratio data

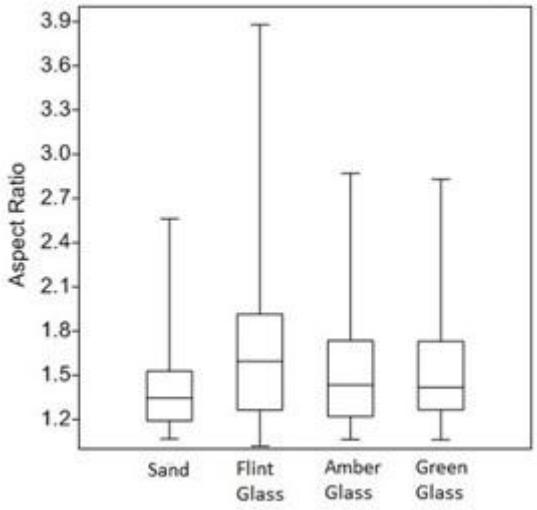

Fig. 4.67 Box plot for Aspect Ratio data

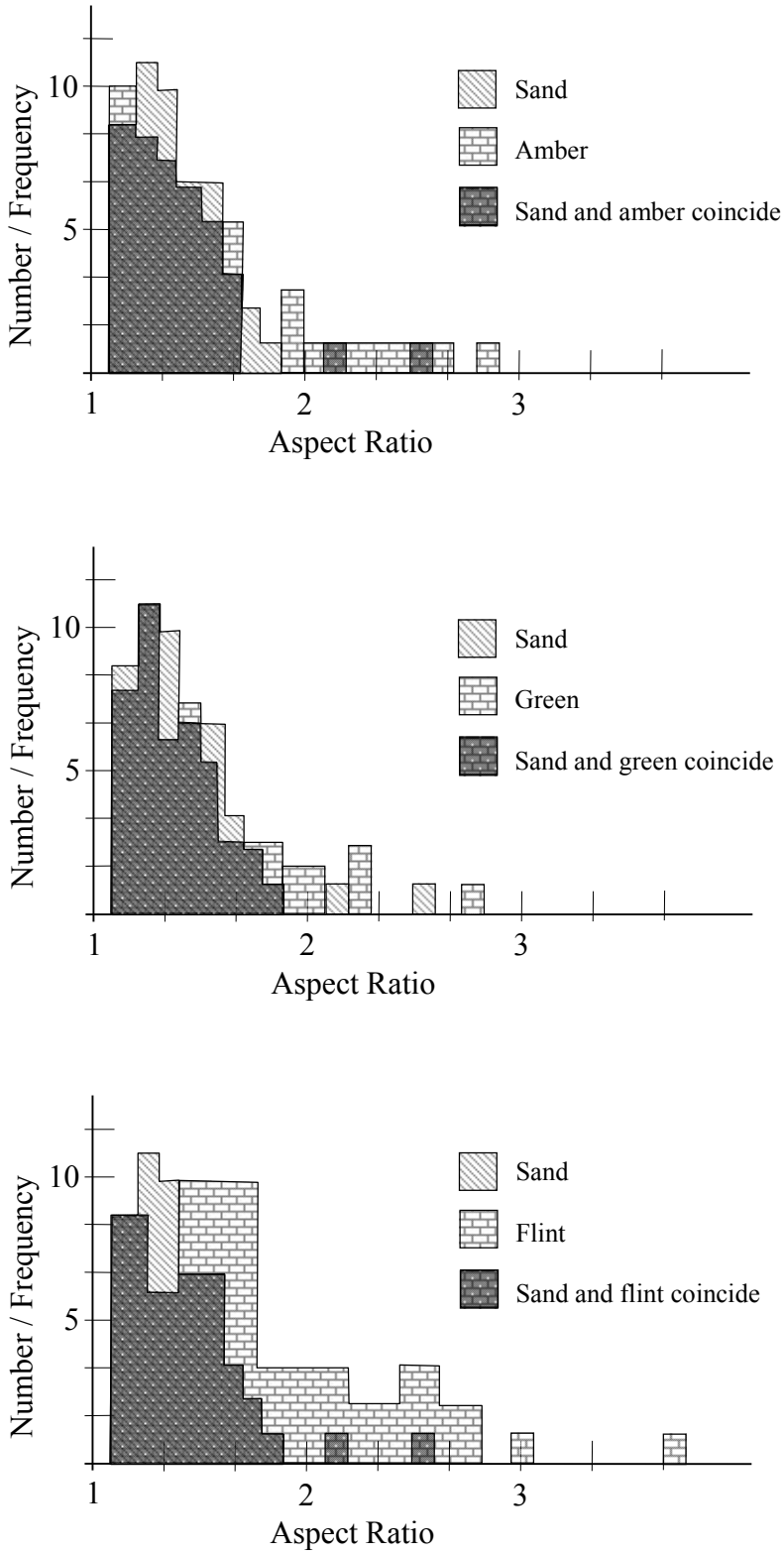

Fig. 4.68 Comparison of frequency distributions for Aspect Ratio

Figure 4.68 shows that there is close correspondence between the Aspect Ratio frequency distributions for green and amber glasses and sand with each aggregate

having a distribution with a well-defined peak. On the other hand the Aspect Ratio distribution for flint glass was noticeably flatter than that for sand and with a less well-defined peak. The box plot in Figure 4.67 and the distributions in Figure 4.68 show that all glass aggregates had more outlying Aspect Ratio values than the natural sand.

Aspect Ratio has been plotted against its cumulative frequency in Figure 4.69. The aggregate dimensions were measured by image analysis of particles which had been arranged in stable positions on a flat screen (Section 3.3.1). Hence the recorded breadth dimension will be similar to the minimum dimension in the classification system of Zingg (1935) for cuboidal or rod-like particles or it will be significantly greater than the minimum dimension for disk-shaped particles. In Zingg's classification system (Figure 2.2 in Section 2.3.1) particle shape would have a significant effect on rolling motion and traction when Aspect Ratio exceeds a value of approximately 1.5. From Figure 4.69 it is seen that 20% of the particles of natural sand had an Aspect Ratio of greater than 1.5. For amber and green glass aggregates approximately 35% of the particles had Aspect Ratios greater than 1.5 and for flint glass the value was only 50%.

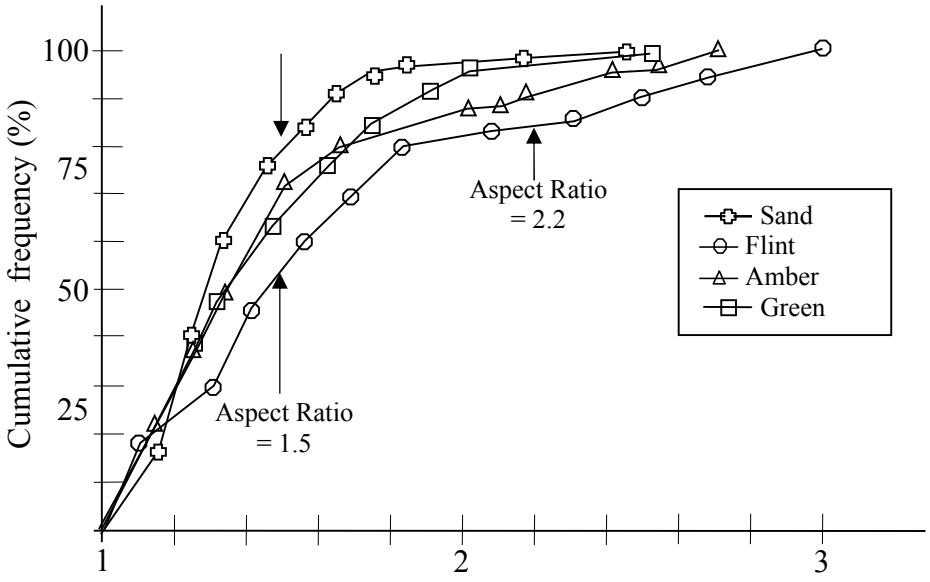

Fig. 4.69 Cumulative Aspect Ratio frequency

BS 812 (1990) defines particles as being elongated when they have a length (greatest dimension) of more than 1.8 times their mean sieve size. The test procedure for assessing whether particles are elongated involves passing the particles through slots which have widths intermediate between the aperture sizes of 'adjacent' pairs of grading sieves. The sieve aperture dimension are such that for 'adjacent' sieve sizes the ratio of the areas of the holes are between 2 and 4 approximately. Hence the BS 812 (1990) definition of elongation would correspond to particles having an Aspect Ratio of 2.2, i.e. $1.8 \times [(1 + \sqrt{2}) \div 2]$, or more. From Figure 4.69 it is seen that the natural sand had only 2% of particles with an Aspect Ratio of greater than 2.2 whilst green, amber and flint glass aggregates contained only 5%, 9% and 15%, respectively, of such particles. Even if all of the elongated flint particles were at the coarse end of the particle size distribution curve (Figure 3.11) these particles would only account for approximately 15% of the total volume of the concrete when used to fully replace the natural sand aggregate.

Riley Inscribed Circle Sphericity ($Ø_{Riley}$) is a measure of sphericity closely related to the shape factor proposed by Wadell (1935) for assessing how easy it is for a particle to more by rolling/ flowing. For two-dimensional image profiles $Ø_{Riley}$ is a measure of circularity and, for the particle shown in Figure 4.70, it is given by

$$Ø_{Riley} = \sqrt{\frac{\text{Minimum Radius}}{\text{Maximum Radius}}} \qquad \text{Equ. 2.5}$$

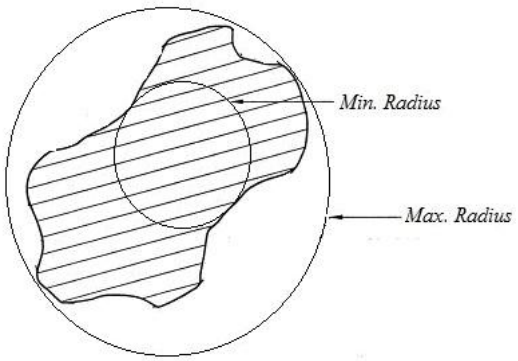

Fig. 4.70 Dimensions used to calculate Riley Sphericity

Table 4.22 contains data relating to Riley Sphericity values obtained by image analysis and in Figure 4.71 the frequency distribution of $Ø_{Riley}$ values is given for each type of fine aggregate. For an approximately circular particle the Riley sphericity would be essentially unity whilst for a square-shaped image the value would be about 0.84. The data in Table 4.22 and Figure 4.71 show that the natural sand contained particles that ranged in shape from almost round to noticeably rectangular. For the glass aggregate the Riley Sphericity values indicated particles ranging in shape from approximately square to rectangular with greater angularity than sand.

Table 4.22 Univariate statistics for Riley Sphericity values of fine aggregate particles

Univariate	Natural	Manual crushed glass			Commercial glass suppliers		
Statistics	sand	Flint	Amber	Green	Flint	Amber	Green
N	50	50	50	50	50	50	50
Min	0.539	0.399	0.295	0.485	0.424	0.410	0.328
Max	0.930	0.815	0.853	0.852	0.824	0.860	0.769
Sum	37.697	32.501	33.807	33.839	32.798	33.747	31.918
Mean	0.754	0.650	0.676	0.677	0.656	0.675	0.638
Std. error	0.011	0.014	0.015	0.011	0.012	0.014	0.012
Variance	0.006	0.010	0.011	0.006	0.008	0.010	0.007
Stand. Dev	0.079	0.101	0.107	0.078	0.087	0.100	0.085
Median	0.760	0.651	0.694	0.682	0.662	0.696	0.661
25 prcntil	0.696	0.574	0.615	0.640	0.598	0.603	0.586
75 prcntil	0.803	0.736	0.746	0.730	0.713	0.747	0.695
Skewness	-0.355	-0.434	-1.172	-0.498	-0.294	-0.576	-1.199
Kurtosis	0.246	-0.525	2.351	0.397	0.074	0.132	2.404
Georm. Mean	0.750	0.642	0.666	0.672	0.650	0.667	0.632

Mann-Whitney pairwise comparisons
Bonferroni corrected/ uncorrected:

Kruskal-	Natural	Manual crushed glass			Commercial glass suppliers		
Wallis test	sand	Flint	Amber	Green	Flint*	Amber*	Green*
Natural sand	0	7.83E-07	0.000154	4.78E-06	2.09E-07	7.15E-05	1.36E-09
Flint glass		0	0.1961	0.2626	0.8822	0.2237	0.5037
Amber glass			0	0.6665	0.1311	0.8308	0.0132
Green glass				0	0.1637	0.8442	0.02395
Flint glass*					0	0.2172	0.41
Amber glass*						0	0.03927
Green glass*							0
H (chi^2):		47.73					
Hc (tie corrected):		47.73					
p(same):		1.337E-08					

*Commercial glass suppliers

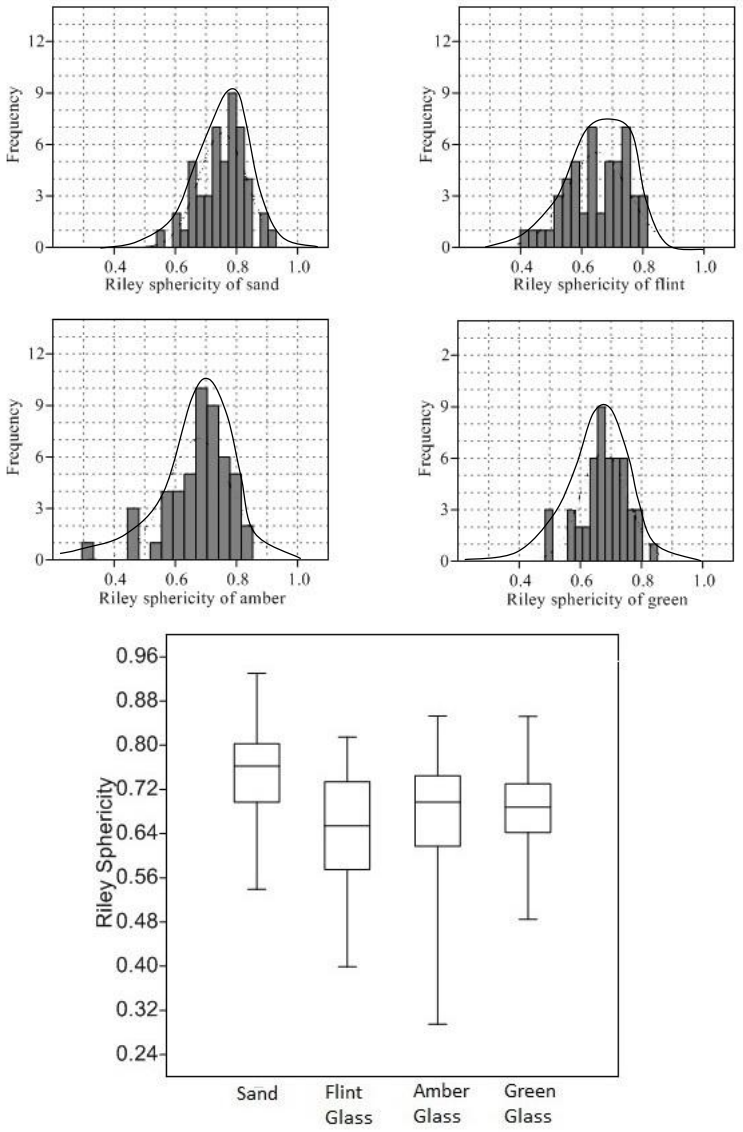

Fig. 4.71 Frequency distribution and box plot of Riley Sphericity values

Figure 4.72. illustrates the differences and similarities in the distribution of Ø $_{\text{Riley}}$ values within the different aggregate types. The Riley Sphericity distributions for sand and amber glass have quite similar shapes. The sand has a higher mean value, i.e. in general it is more rounded, but there is a significant overlap of the distributions. The situation is similar for sand and green glass particles but the latter aggregate contains a small proportion of the more-rounded particles. The flint glass aggregate has a noticeable flatter distribution of Riley Sphericity values with a significant tail of angular particles.

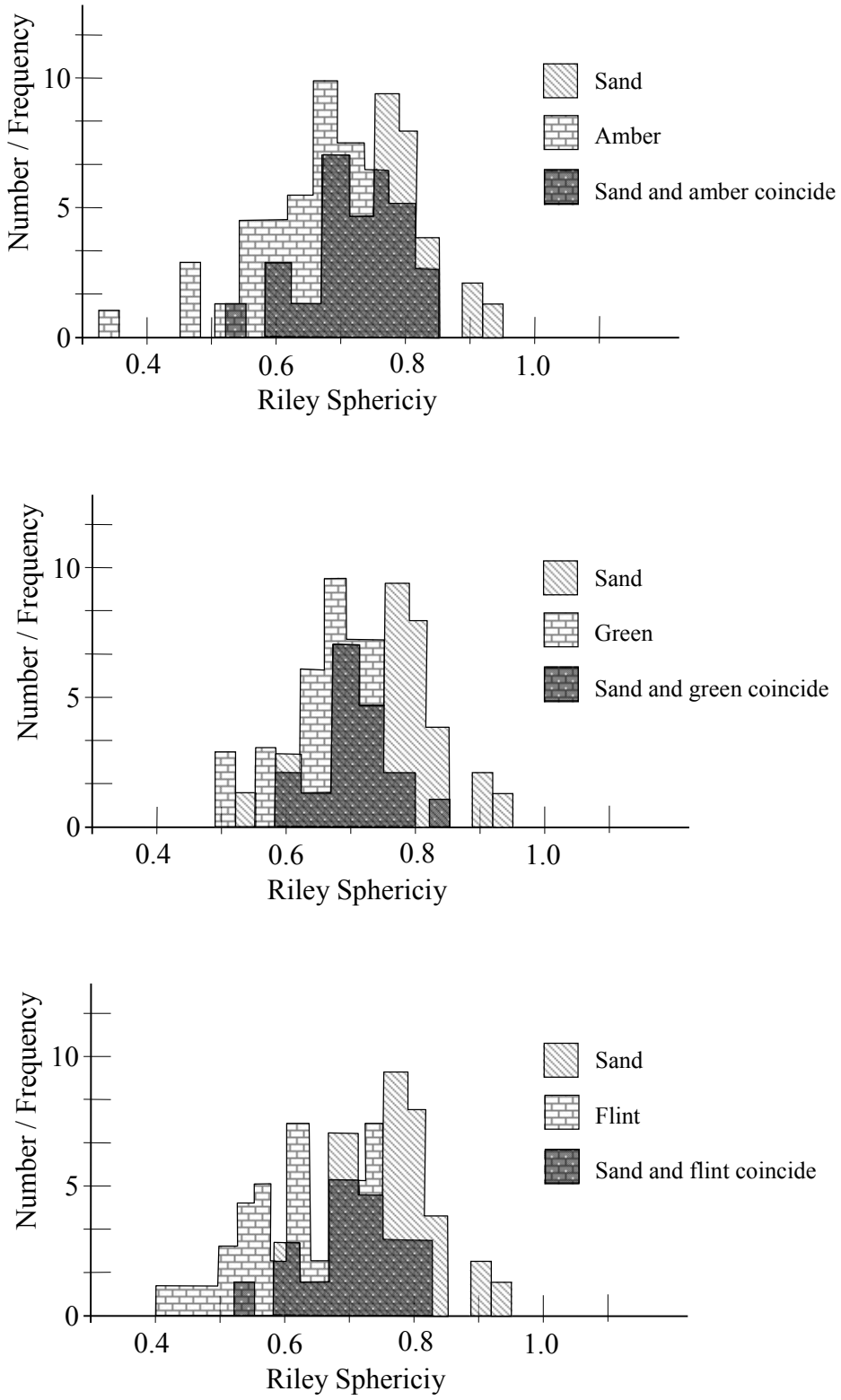

Fig. 4.72 Comparison of frequency distributions for Riley Sphericity

Figure 4.73 is the notional shape of an idealised rectangular particle viewed in two dimensions.

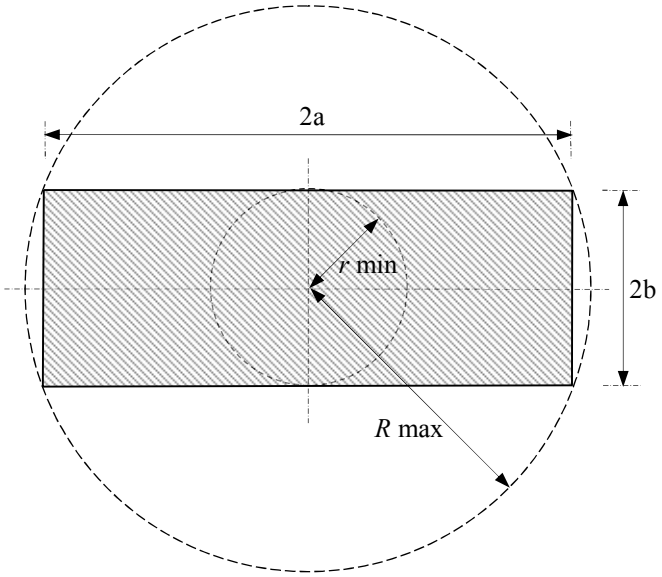

Fig. 4.73 Notional particle showing inscribed and circumscribed circles

For the particle shown in Figure 4.73,

$$\text{Aspect Ratio (AR)} = \frac{2a}{2b} = \frac{a}{b}$$

$$\text{Riley Sphericity } (\text{Ø}_R) = \sqrt{\frac{2\,r\,\text{min}}{2\,R\,\text{max}}}$$

But, r min = b and R max $= \sqrt{b^2 + a^2}$ Equ. 4.10

$$\text{Thus } \text{Ø}_R = \left(\frac{b}{\sqrt{b^2 + a^2}}\right)^{1/2} = \left(\frac{1}{1 + (AR)^2}\right)^{1/4}$$ Equ. 4.11

It is not possible to identify the Aspect ratios and Riley Sphericity values for specific particles (from the data sets given in Tables 4.21 and 4.22) and thereby test equation 4.10. However, it is logical to assume that the extreme values of each parameter will relate to the same or very similar particles. Also it could be assumed that the mean Aspect Ratio and Riley Sphericity values correspond to some notional particle shape because they are based on a large number of values which have similar frequency distributions. Using the foregoing assumptions values of Riley Sphericity have been

predicted using equation 4.10 and the values are compared against the measured values in Table 4.23.

Table 4.23 Predicted and actual Riley Sphericity values using Equation 4.11

Aggregate	**AR**			**$Ø_R$**					
				Predicted			**Actual**		
	Max	Min	Mean	Min	Max	Mean	Min	Max	Mean
Sand	2.564	1.068	1.384	0.603	0.827	0.765	0.539	0.930	0.754
Flint glass	3.878	1.019	1.692	0.500	0.837	0.713	0.399	0.815	0.650
Amber glass	2.871	1.064	1.528	0.574	0.828	0.740	0.295	0.853	0.676
Green glass	2.830	1.062	1.538	0.577	0.828	0.738	0.485	0.852	0.677

Whilst there is some similar between minimum and maximum Riley Sphericity values the results for sand highlight the problems of assuming two different parametral values relate to the same particle; the predicted maximum $Ø_R$ value for sand (0.827) corresponds to a particle having an approximately square cross-section whilst the measured maximum $Ø_R$ value of 0.930 indicates a particle which is almost circular in profile. However, there is better correspondence between predicted and actual mean values of $Ø_R$.

Looking at Figure 4.73 it can be seen that there is another way that an elongated particle can simultaneously satisfy the definitions of Aspect Ratio and Riley Sphericity, as shown in Figure 4.74.

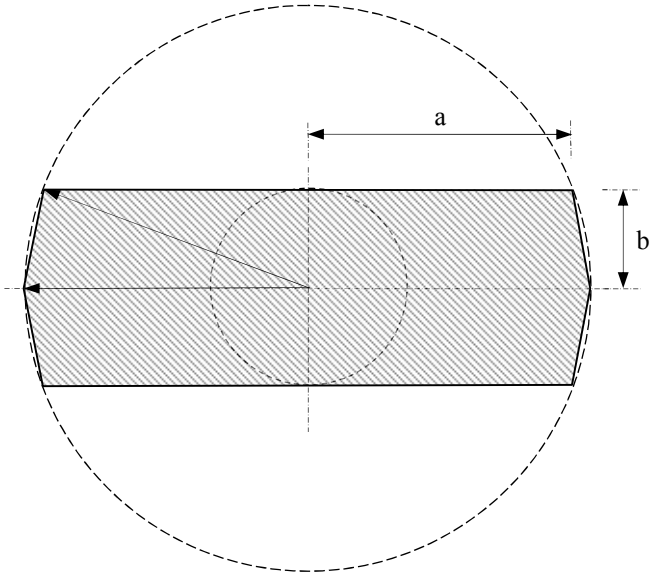

Fig. 4.74 Alternative Notional particle

For the alternative notional particle the terms in the expression for Riley Sphericity are unchanged from those given in equation 4.10. However the value of Aspect Ratio is changed to

$$AR = \frac{2\sqrt{a^2 + b^2}}{2b} = \frac{\sqrt{a^2 + b^2}}{b} \qquad \text{Equ. 4.12}$$

Thus the expression correlation between Aspect Ratio and Riley Sphericity changes to

$$Ø_R = \left(\frac{b}{\sqrt{b^2 + a^2}}\right)^{1/2} = \sqrt{\left(\frac{1}{AR}\right)} \qquad \text{Equ. 4.13}$$

Revised predicted Riley Sphericity values are given in Table 4.24.

Table 4.24 Riley Sphericity values using Equation 4.11 and 4.13

Aggregate	$Ø_R$								
	Predicted (Eq. 4.11)			**Actual**			**Predicted (Eq. 4.13)**		
	Min	Max	Mean	Min	Max	Mean	Min	Max	Mean
Sand	0.603	0.827	0.765	0.539	0.930	0.754	0.652	0.969	0.850
Flint glass	0.580	0.837	0.713	0.399	0.815	0.650	0.508	0.991	0.769
Amber glass	0.574	0.828	0.740	0.295	0.853	0.676	0.590	0.969	0.809
Green glass	0.577	0.828	0.780	0.485	0.852	0.677	0.594	0.970	0.806

Only one prediction of Riley Sphericity (the highlighted value in Table 4.24) is improved (but then it gives an overestimation) by the modification to the shape of the notional particle. This improvement is for the particle closest in shape to a rounded pebble. On the other hand eight other predictions (approximately 67% of the total), shown shaded in Table 4.24, are made significantly worse by the shape modification. In addition the particle shapes in Figures 4.73 and 4.74 and the associated AR and $Ø_R$ values relate to the resistance due to rolling of such particles but do not reflect the fact that undulations in a particle's surface will produce frictional resistance and therefore affect resistance to sliding motion. Hence the original notional particle shape has been modified to that shown in Figure 4.75.

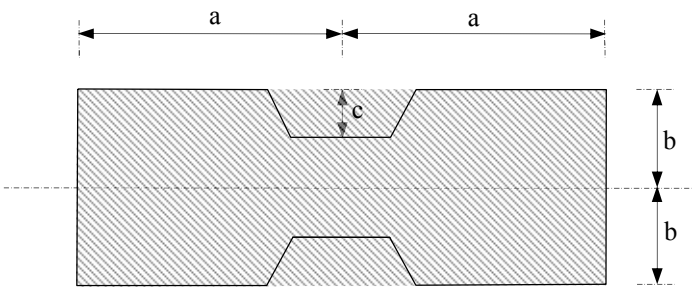

Fig. 4.75 Notional (analogous) particle exhibitory elongation and surface texture

$$\text{Aspect Ratio (AR)} = \frac{2a}{2b} = \frac{a}{b}$$

Riley Sphericity ($Ø_R$) = $\sqrt{\frac{(b - c)}{\sqrt{b^2 + a^2}}}$ if c is small. Equ. 4.14

If the mean values of Aspect Ratio and Riley Sphericity can be considered to apply to the same average notional particle, even though the distributions are not necessarily the same, (as was found by Riley (1941)) and, if c = s × b (where s in an indentation parameter), then

$$(Ø_R)_{mean} = \sqrt{\frac{(1 - s)}{\sqrt{1 + (AR_{mean})^2}}} \equiv \left(\frac{(1 - s)^2}{1+(AR_{mean})^2}\right)^{1/4} \quad \text{Equ. 4.15}$$

For natural sand $(Ø_R)_{mean} = 0.754$ and $(AR)_{mean} = 1.384$
which given s = **0.029**

For glass aggregates, using mean values of $Ø_R$ and AR gives values of s of; 0.170, 0.165 and 0.159 for flint, amber and green, respectively. If the value of s is an indicator of surface profile and particle 'roughness' then the glass aggregates will generate significant increased friction by comparison to sand aggregate, in a flow situation. The flint aggregate is likely to general marginally greater frictional resistance than the other two glass colours.

Table 4.25 contains all values of s calculated using Equation 4.15 together with mean values of $Ø_R$ and AR and combinations of the maximum and minimum values of these shape factors. There is no consistency between values of s determined using $(AR)_{max}$ combined with $(Ø_R)_{min}$ and $(AR)_{min}$ combined with $(Ø_R)_{max}$ with some values indicating concavity on the surface of particles and some values indicating convexity. The value of s of 0.735 is particularly dubious because a particle with such a large indent would be likely to be broken during manufacture.

If the notional, analogous particle shown in Figure 4.75 is modified in the same way as the original stylised particle was, i.e. with the addition of convex ends, then the expression relating Riley Sphericity and Aspect Ratio becomes

$$Ø_R = \sqrt{\frac{(1 - s)}{AR}} \qquad \text{Equ. 4.16}$$

Calculated values of s are shown in Table 4.25. In the final column of this table the s values are cited at an appropriate level of precision and the unrealistic value of 0.750 is discounted, because a particle with such a large indent would be likely to be broken during manufacture. The ranges of s shown in Table 4.25 support the proposition that the sand particles would exhibit least resistance to rolling (and possibly to sliding also) whilst the flint glass grains would exhibit greatest resistance with amber and green glass aggregates being in between.

Table 4.25 Calculated value of indentation parameter (s)

Aggregate	Values of s						
	From Eq. 4.15			From Eq. 4.16			
	$RA_{max} + Ø_{R\,min}$	$RA_{min} + Ø_{R\,max}$	Mean	$RA_{max} + Ø_{R\,min}$	$RA_{min} + Ø_{R\,max}$	Mean	Range
Sand	0.201	-0.265	0.029	0.256	0.076	0.213	0.1-0.3
Flint glass	0.362	0.052	0.170	0.383	0.323	0.285	0.3-0.4
Amber glass	0.735*	-0.062	0.165	0.750*	0.226	0.302	0.2-0.3
Green glass	0.294	-0.059	0.159	0.334	0.230	0.295	0.2-0.3

* Value discounted because it is not compatible with the manufacturing process

4.3.2 Particle surface texture

Aspect Ratio and Riley Sphericity characterise the shape of a particle and thus indicate rolling resistances but there is a need to characterise particle surface texture, as well because this affects friction and interlock and thus stability in slump and flow test and adhesion for the concrete in a hardened state.

If the surface of a particle has depression and bumps then the overall perimeter will be greater than that of a smooth pebble having the same overall shape. These irregularities effect interparticle friction and interlock and their effect on the magnitude of the particle perimeter is the basis of the Surface Texture Index, where

$$\text{Surface Texture Index (STI)} = \left(\frac{\text{Outline perimeter - Convex outline perimeter}}{\text{Convex outline perimeter}} \right) \quad \text{Equ. 4.17}$$

The perimeters are defined in Figure 4.76 and data relating to a randomly collection of 50 grains of each type of aggregate are given in Table 4.26. The sample size is considered to be adequate for the statistical analysis used in this study.

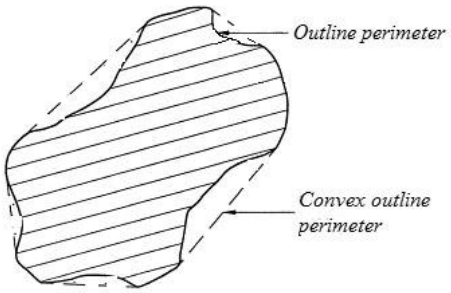

Fig. 4.76 Perimeters used in the determination of Surface Texture Index

Table 4.26 Univariate statistics for Surface Texture Index values of fine aggregate particles

Univariate Statistics	Natural sand	Manual crushed glass			Commercial glass suppliers		
		Flint	Amber	Green	Flint	Amber	Green
N	50	50	50	50	50	50	50
Min	0.053	0.054	0.064	0.058	0.064	0.052	0.045
Max	0.096	0.161	0.147	0.143	0.134	0.113	0.141
Sum	3.577	4.305	4.671	4.091	4.443	4.121	3.855
Mean	0.072	0.086	0.093	0.082	0.089	0.082	0.077
Std. error	0.002	0.003	0.003	0.002	0.002	0.002	0.002
Variance	0.000	0.000	0.000	0.000	0.000	0.000	0.000
Stand. Dev	0.011	0.019	0.020	0.015	0.016	0.015	0.017
Median	0.072	0.087	0.092	0.080	0.087	0.082	0.077
25 prcntil	0.062	0.072	0.077	0.072	0.077	0.075	0.065
75 prcntil	0.079	0.098	0.103	0.088	0.101	0.094	0.084
Skewness	0.459	1.249	0.853	1.670	0.501	0.026	1.397
Kurtosis	-0.412	3.763	0.430	4.648	-0.090	-0.379	3.640
Georm. Mean	0.071	0.084	0.091	0.081	0.087	0.081	0.075

All aggregates exhibited approximately the same minimum value but the glass aggregate had maximum values which were significantly higher than those for sand, as indicated in the box plot in Figure 4.77. The Surface Texture Index frequency histograms (in Figure 4.77) are all similar in form and do not have unique, well-defined peaks.

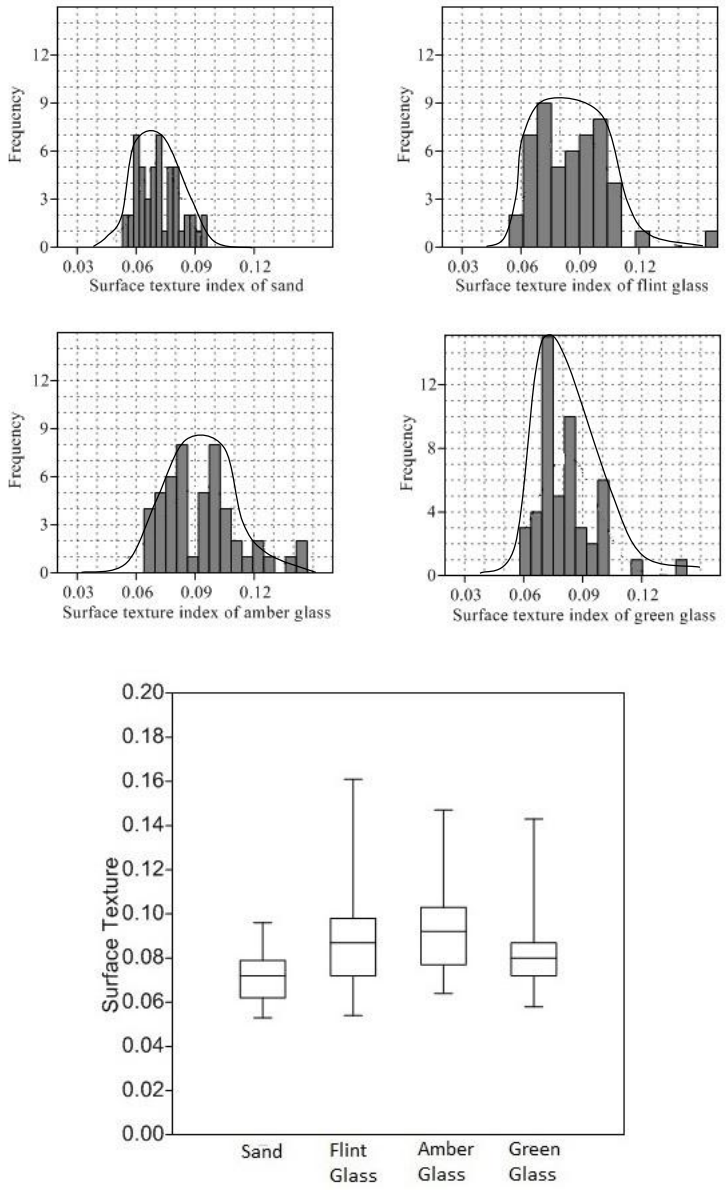

Fig. 4.77 Histograms and box plot of Surface Texture Index

An alternative measure of particle surface texture, termed Percentage Concavity, has been proposed by True (2011). This parameter is related to the proportion of the plan area of a particle which comprises hollows and troughs (Figure 4.78). It is claimed that this parameter is measure of roundness/angularity as well as macro-texture. In Figure 4.78, the fine dotted line circumscribing the convex parts of the particle then traversing across particle projections, i.e. akin to a elastic band stretched around the particle, is known as the Convex Hull and contains an area known as the Convex Polygon. Percentage Concavity is a measure of the convexity and is evaluated from the two-dimensional projection of the particle, as illustrated in Figure 4.78.

$$\text{Percentage Concavity} = \frac{100 \times (\text{convex polygon - particle area})}{\text{particle area}} \qquad \text{Equ. 4.18}$$

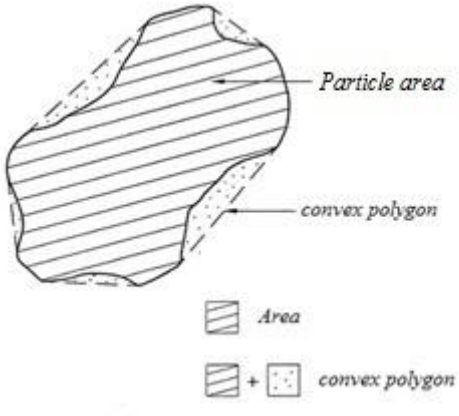

Fig. 4.78 Terms in the definition of Percentage concavity

Data relating to Percentage Concavity, obtained by image analysis of a collection of particles, are presented in Table 4.27 and frequency histograms are given in Figure 4.79. There are significant differences between the numerical values given for each aggregate and the form of the frequency histograms. The sample size was 50 for all statistical tests.

Table 4.27 Univariate statistics for Percentage Concavity to fine aggregate shape

Univariate	Natural	Manual crushed glass			Commercial glass suppliers		
Statistics	sand	Flint	Amber	Green	Flint	Amber	Green
N	50	50	50	50	50	50	50
Min	1.206	1.844	2.401	2.826	2.774	3.317	3.974
Max	7.191	22.413	30.525	17.815	24.933	27.929	32.058
Sum	195.04	400.13	436.52	348.27	484.80	452.44	421.31
Mean	3.901	8.003	8.730	6.965	9.696	9.049	8.426
Std. error	0.222	0.582	0.803	0.442	0.660	0.756	0.673
Variance	2.454	16.949	32.280	9.775	21.801	28.552	22.675
Stand. Dev	1.567	4.117	5.682	3.126	4.669	5.343	4.762
Median	3.667	6.736	7.556	6.704	9.017	7.482	7.661
25 prcntil	2.679	5.162	5.013	5.162	5.818	5.477	5.777
75 prcntil	5.416	11.126	10.527	8.346	12.441	10.454	8.845
Skewness	0.193	1.333	2.266	1.561	1.322	1.914	3.187
Kurtosis	-0.982	2.543	6.219	3.561	2.430	3.816	12.815
Georm. Mean	3.566	7.074	7.459	6.383	8.733	7.938	7.640

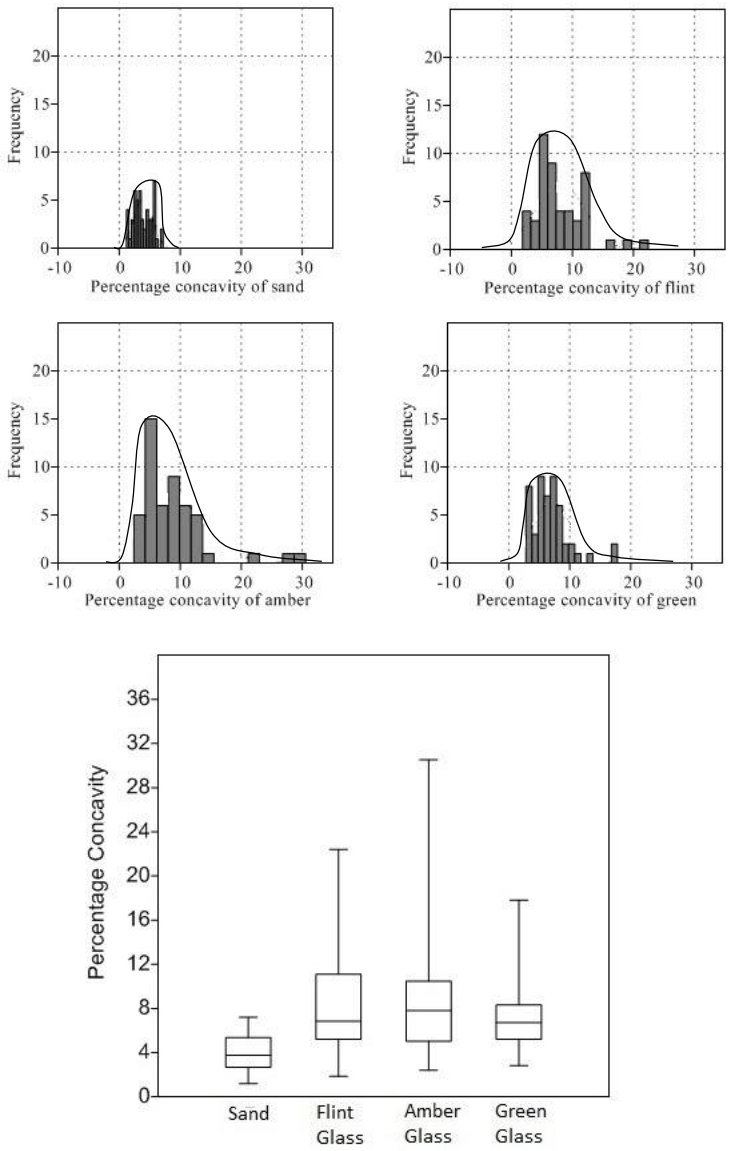

Fig. 4.79 Frequency distributions and box plot of Percentage concavity values

The mean Percentage Concavity for the natural sand is 3.90 and this is much lower than the mean values for crushed glass with different colours. However it should be remembered that this parameter is expressed as a percentage so one is actually comparing small values. The natural sand has a much smaller standard deviation than the values for crushed glass and this spread of values is apparent in the histograms in Figure 4.78.

Figure 4.80 shows the final schematic aggregate particle containing rectangular indentations. If each upper and lower surface contains *n* such indentations, each of width *w*, so that they occupy a proportion *k* on each surface then

$$n\,w = k\,(2a) \qquad \text{Equ. 4.19}$$

and total area of surface indentations = $2 \times k\,(2a)\,c$ Equ. 4.20

Also, total particle area = $4\,a\,b + 2\,[\,½ \times \{\sqrt{a^2 + b^2} - a\}\,] - 4\,k\,a\,c$ Equ. 4.21

From the definition of Percentage Concavity (PC),

$$k = \frac{PC}{2s\,(1+PC)} \left\{ 1 + \frac{AR}{\sqrt{AR^2 - 1}} \right\} \qquad \text{Equ. 4.22}$$

For PC expressed as a pure number and using the mean values of relevant parameters the values of *k* are obtained as shown in Table 4.28

Table 4.28 Parameter for schematic particle with rectangular indentations

Aggregate	**Mean values**						
	AR	s	PC	*k*	PTI	*n*	*w*
Sand	1.384	0.213	0.03901	0.216	0.072	1.27	0.170
Flint glass	1.692	0.285	0.08003	0.291	0.086	1.40	0.208
Amber glass	1.528	0.302	0.08730	0.309	0.093	1.29	0.240
Green	1.538	0.295	0.06965	0.256	0.082	1.17	0.218

For the module in Figure 4.80 using the definition of Surface Texture Index (STI)

$$n = \frac{PTI}{s} \left\{ 1 + \sqrt{AR^2 - 1} + \sqrt{AR^2 + AR\,\sqrt{AR^2 - 1}} \right\} \qquad \text{Equ. 4.23}$$

Using this expression the values for *n* are obtained and then *w* is calculated - Table 4.28.

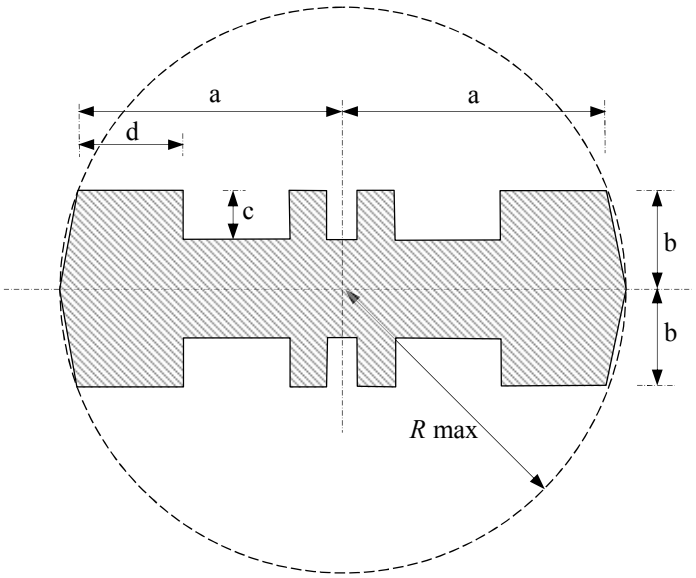

Fig. 4.80 Final schematic particle

Figure 4.81 shows the final schematic particles which satisfy all of the mean values of Aspect Ratio, Riley Sphericity, Percentage Concavity and Surface Texture Index for all of the fine aggregates used. These diagram are not intended to replicate the shape and surface undulations of the actual aggregate particles. Furthermore it should be remembered that the size of the schematic particles are intended to be applicable to the whole of the particle size distribution curves (Figure 3.11) with sizes ranging between 0.15 mm and 10 mm.

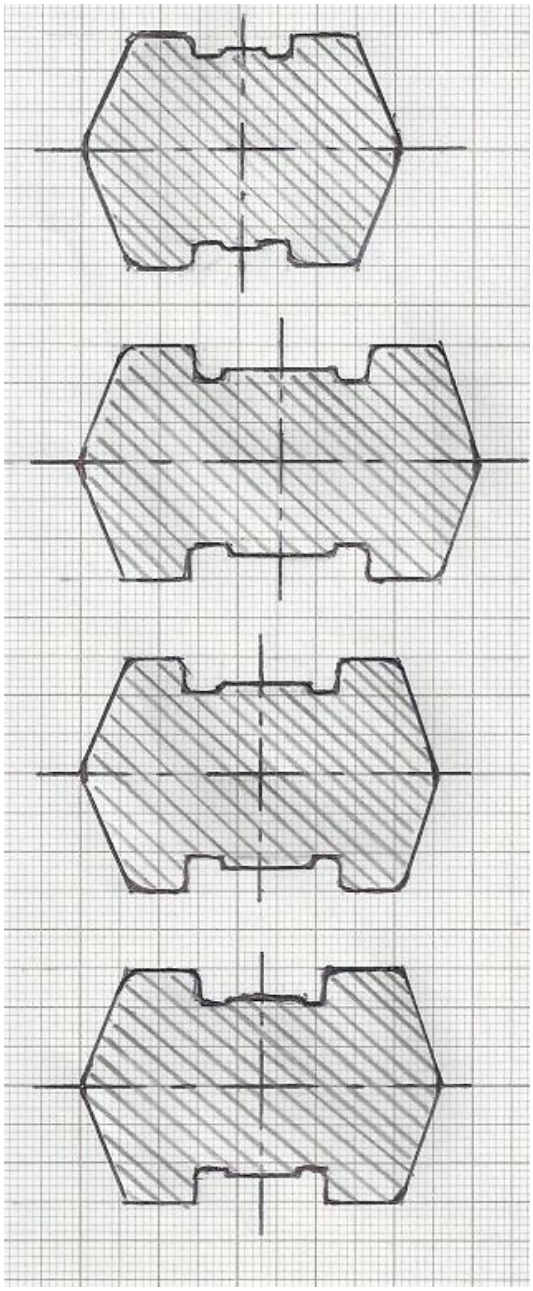

Fig. 4.81 Final schematic particles

Scatter diagrams are shown in (Figure 4.83) to compare the univariate statistics for the various shape and form parameters. As expected natural sand is different from the crushed glasses (flint, amber and green) although there is a good deal of variation of all parameters.

Figure 4.84 shows normal probability plots for the shape and texture factors of the natural sand and waste glass fine aggregates. These plots demonstrate that the data for the natural sand and waste glass aggregates generally obey the normal distribution in

respect of the factors of aspect ratio, percentage concavity, riley sphericity and surface texture index. More waste glass aggregate samples deviate from the normal distribution than sand samples and this is believed to be due to the crushing process used to create the glass aggregates. The images in Figures 3.12 to 3.17 show that crushed glass particles have a range of sharp corners and edges. However, these images also show that the glass particles have smoother surfaces than the sand particles (Figures 3.9 and 3.10). The schematic particles in Figure 4.81 are intended to incorporate both shape and texture characteristics.

The shape of the aggregate particles is important, because the shape of aggregates are affects both the flow workability and compressive strength of the concrete. Smooth rounded aggregates produce advantageous flow workability and ease of placing of concrete. Angular materials tend to produce higher voids content (Figure 4.82), while flaky and elongated materials promote segregation and reduce workability. Therefore these latter materials require more water and cement paste to achieve comparable performance to conventional concrete.

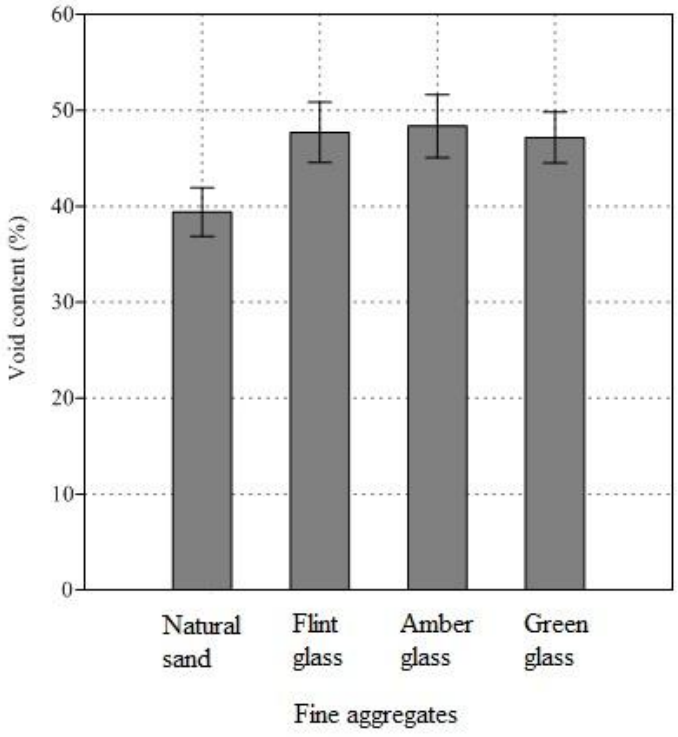

Fig. 4.82 Uncompacted voids content in fine aggregate

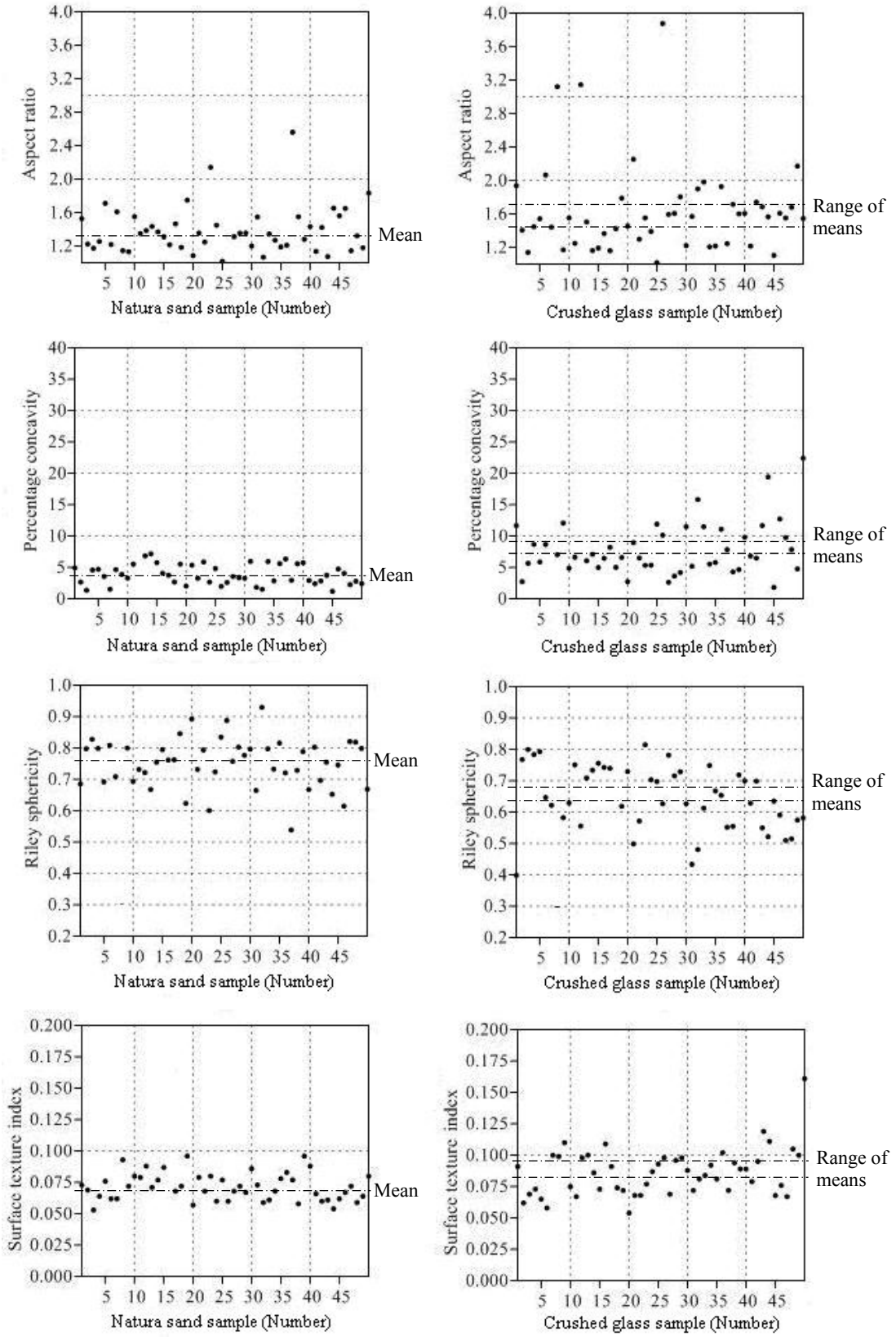

Fig. 4.83 Scatter diagrams of fine aggregates shape factors

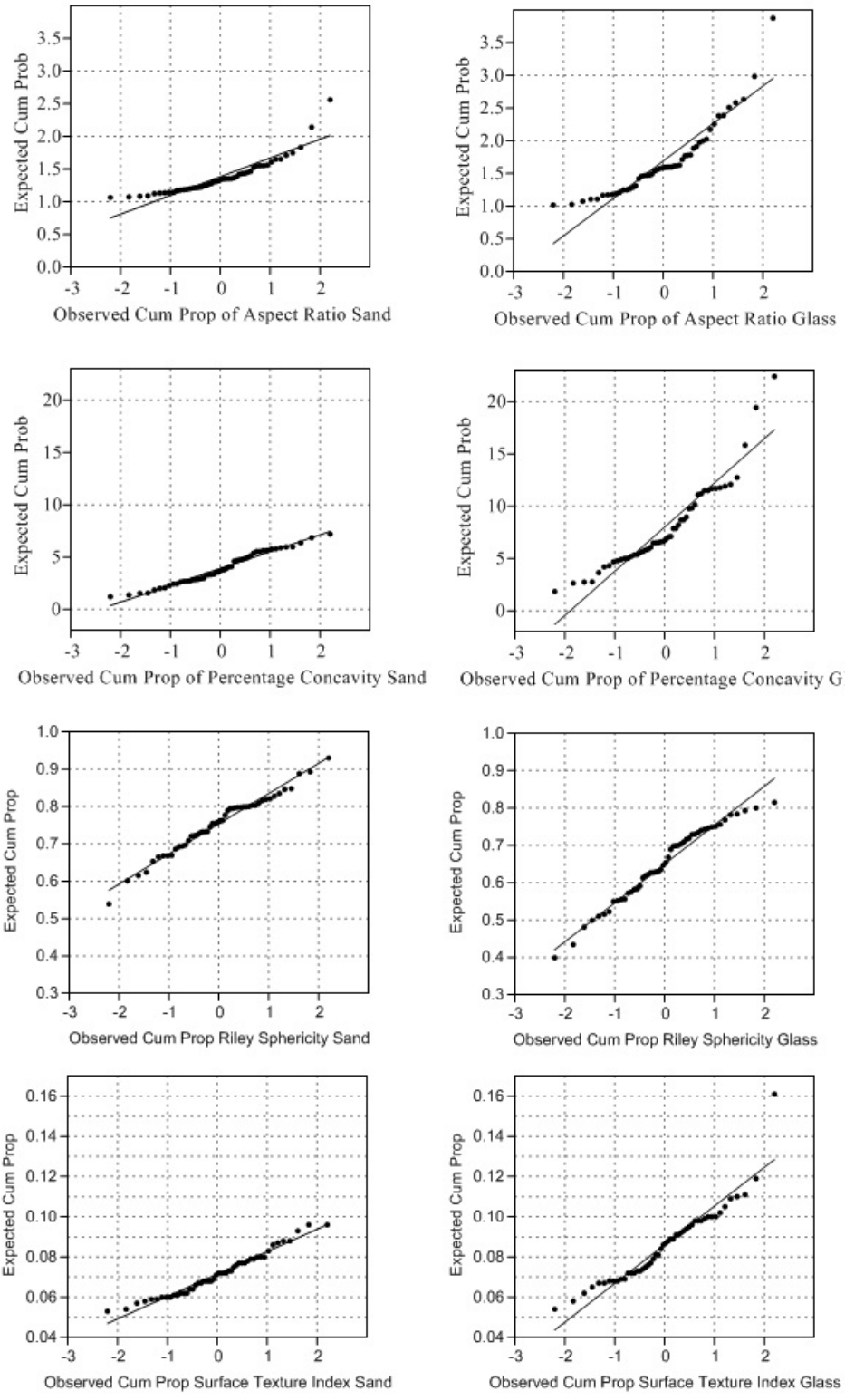

Fig. 4.84 Normal probability plot of fine aggregates shape factors

Results from tests to measure voids content in uncompacted masses fine aggregate are shown in Figure 4.82 and individual values are given in Table 4.29.

The lower bulk density of the crushed glass aggregate was indicative of a higher voids content. The green and amber glass particles in Figure 4.81 are very similar in form and would be expected to form very similar loose packings. These glass particles are not very dissimilar in degree of roundness from the sand particles but they contain larger surface indentations. Hence if the sand and green and amber particles formed similar structures when loosely packed the sand would have the lowest voids content. The schematic flint glass particles (Figure 4.81) had surface indentations which were wider, but approximately the same depth, as the other glass colours. However the elongated nature of the flint glass particles could lead to more dense packing in a loose state.

Table 4.29 Bulk density and voids content of loose fine aggregate

Fine aggregate	**Loose bulk density (*Pd*) kg/m³**	**Pre-dried particle density (*Pb*) kg/m³**	**Un-compacted voids %**
Natural sand	1582	2611	39.4%
Flint glass	1318	2520	47.7%
Amber glass	1307	2531	48.4%
Green glass	1334	2525	47.2%

Table 4.30 Previous findings relating to glass shape factors was affected use in concrete

Finding	Researchers
1. Waste glass was more angular and sharp edges that natural sand - as found in this study.	Park *et al*. (2004), Limbachiya *et al*. (2012), Cassar and Camilleri (2012), Topcu and Canbaz (2004), Castro and Brito (2013), Lee *et al.* (2013), Ismail and AL-Hashemi, (2009), Liu (2011), Borhan (2012), CCANZ (2011), Persson (1998), Pereira-de-Oliveira *et al.* (2012), Ai *et al*. (2013), Shao *et al*. (2000), Tan and Du (2013)
2. Waste glass shape was affected the concrete workability and decreased (i.e. slump, flow table, and flow slump) - as found in this study.	Park *et al*. (2004), Limbachiya *et al*. (2012), Ismail and AL-Hashemi (2009). Liu (2011), Borhan (2012), Shao *et al*. (2000), Tan and Du (2013),
3. Waste glass shape was unaffected the concrete performance	Persson (1998)
4. Waste glass sizes was affected the performance of concrete - as found in this study.	Park *et al*. (2004), Castro and Brito (2013), Borhan (2012), Persson (1998), Shao *et al*. (2000)
5. Waste glass shape and surface texture/ smooth surface was affected bonding to cement paste are weak and decreased concrete strength - as found in this study.	Cassar and Camilleri (2012), Topcu and Canbaz (2004), Lee *et al*. (2013), CCANZ (2011), Ai *et al*. (2013), Tan and Du (2013)
6. Waste glass shape was affected the performance of concrete which contributed to increased air content.	Park *et al*. (2004), Topcu and Canbaz (2004), Tan and Du (2013)
7. Waste glass shape was affected the performance of concrete which contributed to reduced air content.	Wang and Huang (2010)

There is no major difference between manually crushed waste glass and waste glass from commercial glass suppliers in terms of shape or surface texture so the preparation method was not a factor in the results attained.

Table 4.31 is a summary of calibration of aggregate shape factors. The table shows the difference between schemes and the difficulty of coming to a consensus on the most important definition of a shape factor for a particle.

Table 4.31 Calibration of aggregate shape factor, based on True (2011)

Grade term	Property	Roads research technical paper 5	Shepard & young	Hughes & Ali-Ani	P. Owens prime mix method	Com-bines values	True 2011	Current study	
								Sand	Waste Glass
Well-rounded	% concavity		2.556	1.664	1.237	2.5	0-2.5		
	Aspect ratio		1.514	1.518	1.420	1.5	1-3		
	Riley sphericity		0.894	0.884	0.941	0.9	1-0.895		
Rounded	% concavity	2.901	3.873	3.001		3.25	2.5-3.25		
	Aspect ratio	1.655	1.364	1.440		1.5	1-3	**1.34**	
	Riley sphericity	0.862	0.866	0.863		0.86	0.895-0.775		
Sub-rounded	% concavity		6.162		8.908	6.0	3.25-6	**3.67**	
	Aspect ratio		1.445		2.091	1.6	1-3		
	Riley sphericity		0.800		0.743	0.80	0.775-0.635	**0.76**	
Sub-angular	% concavity	8.781	7.695	7.602; 7.514	9.159	7.5	6-7.5		
	Aspect ratio	1.734	1.638	1.829; 1.548	1.797	1.7	1-3		**1.40-1.59**
	Riley sphericity	0.809	0.786	0.799; 0.846	0.681	0.78	0.635-0.445		**0.65-0.70**
Angular	% concavity		15.341			15	7.5-15		**6.7-9.0**
	Aspect ratio		1.611				1-3		
	Riley sphericity		0.739				0.445-0.23		
Very angular	% concavity		17.266			17	15-20		
	Aspect ratio		1.624				1-3		
	Riley sphericity		0.657				0.23-0		

CHAPTER 5: DISCUSSION

5.1 Fresh concrete

The results of laboratory tests used to determine the characteristics of fresh concretes containing various amounts of glass fine aggregate, e.g. slump, flow value, have been presented previously in Section 4.1. These results are discussed herein, in the context of the findings reported by other researchers, with the aim of drawing sound conclusion about the effect on workability and consistency of replacing a conventional fine aggregate by waste glass aggregate crushed to achieve the same particle size distribution.

5.1.1 Slump

Figure 5.1 contains a pictorial summary of all of the numerical data (relating to slump) from the research reported herein (Sections 4.1.1 and 4.1.2), together with relevant data from other researchers. It is evident that the majority of previous researchers have reported that using glass as a replacement fine aggregate in concrete has caused some change in slump. The change has usually been a decrease but modest increases in slump have also been reported - the overall conclusion from previous work are summarised in Table 5.1

Table 5.1 Previous findings relating to slump of concrete containing fine waste glass aggregate

Finding	Water cement ratio	Researchers
Replacing sand by waste glass in concrete has decreased the slump values	1.0 0.5 0.5 0.7 0.65 0.6	Chen *et al.* (2006) E-glass Kou and Poon (2009) Mixed glass Park *et al.* (2004) Bottles reduced to 0-5mm Shayan&Xu (2006) Powdered glass 10-15μm in size Tang *et al.* (2005) Clean green bottle glass Current study (all colours of glass)
Increasing the waste glass in concrete has caused a slight increase the slump values	0.48 0.4 Not specified	Terro (2006) From bottles mixed Wang & Huang (2010a) LCD glass Zammit *et al.* (2004) Clean mineral bottles; Particles reduced to 0-5mm

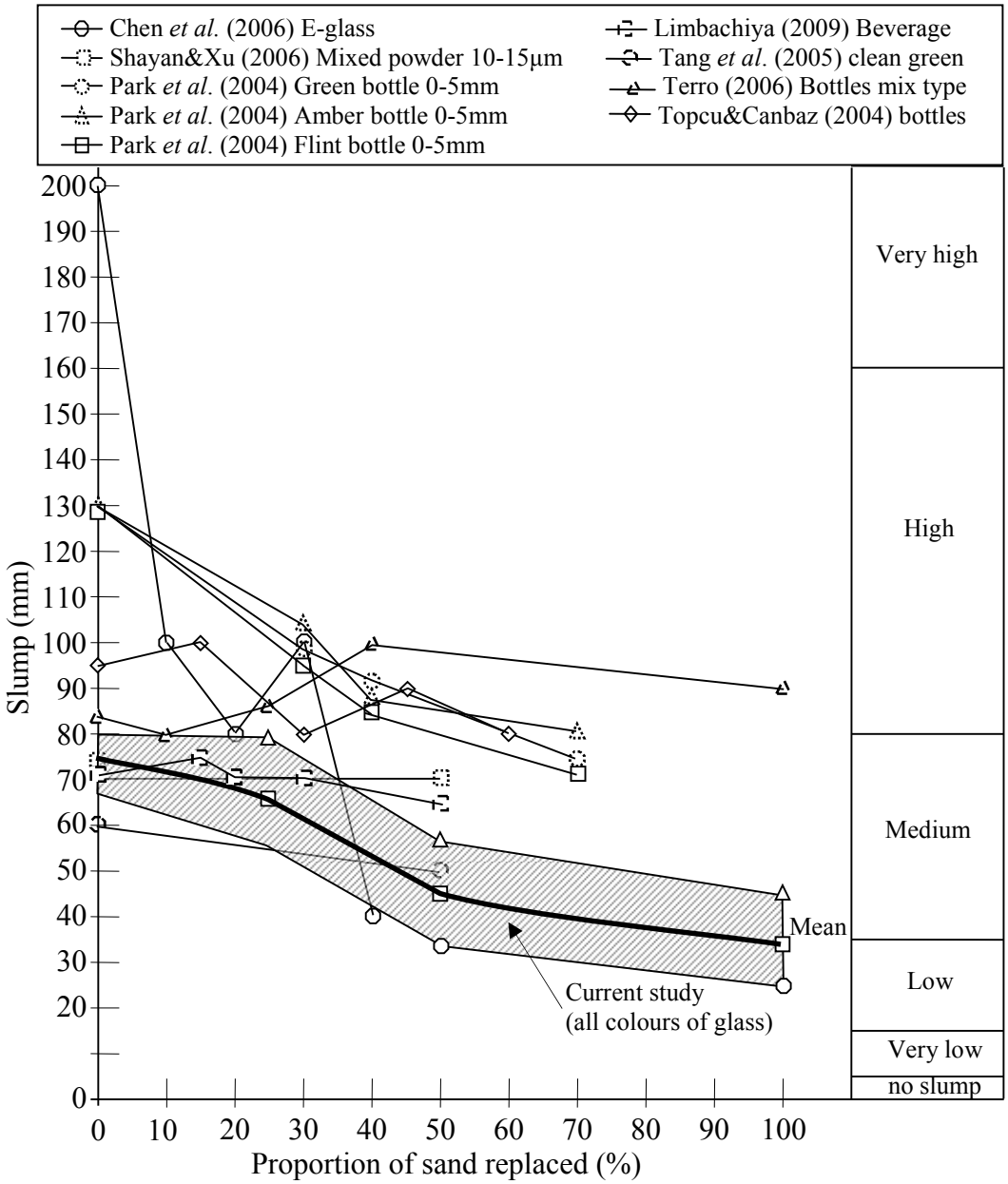

Fig. 5.1 Slump data for concrete containing glass as replacement for conventional fine aggregate (sand)

Because previous research work has related to a variety of concrete mixes containing fine glass aggregate the 'starting' slump values, i.e. those for concrete containing only conventional fine aggregate (sand), for most of this earlier work have not been the same as the author's. Hence all data presented in Section 4.1.1 have been normalised, by dividing slump values by the mean slump value for the relevant conventional concrete, and the resultant values are presented in Figure 5.2.

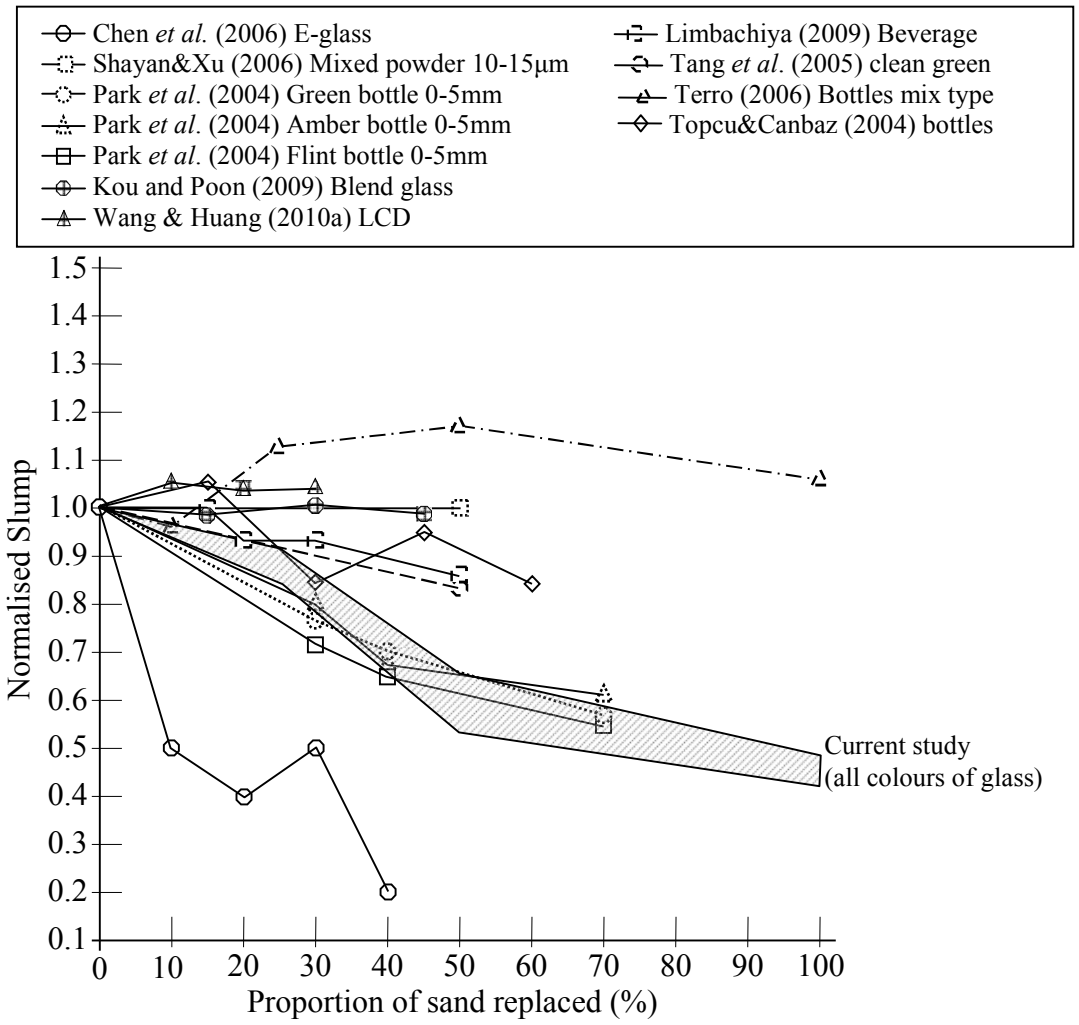

Fig. 5.2 Normalised mean slump values for concrete containing fine glass aggregate

The results from this investigation into the effect on slump of using fine glass aggregate, as presented in Section 4.1.1, can be summarised as:

a) *Slump values were decreased by the use of fine glass aggregate and the greater the glass content the greater was the reduction.*

In early work on the use of coarse glass particles in concrete (Polley *et al*., 1998) it was reported that the use of glass aggregates required a higher water content in a mix to achieve the same workability as a conventional mix. A similar finding was reported by Castro and Brito (2013) who found that the size of waste glass aggregate had a significant effect on concrete workability. They specifically stated that if waste glass was used as fine aggregate the water-cement ratio needed to be increased to

compensate for the loss of workability. No such compensation was applied during the author's work and all concrete mixes had the same water-cement value.

Park *et al.* (2004) reported that the tendency for slump to reduce may be related to the mixing ratio of waste glass to aggregate because cement paste tended to become attached to the surface of the waste glass, resulting in less cement paste being available for the fluidity of the concrete. Furthermore, Park *et al*. noted that their waste glass aggregates had sharper edges and more angular grain shapes than sands and this resulted in more friction within the concrete and hence less fluidity. In addition the glass aggregate contained a significant proportion of grains larger than 0.6mm which affected workability. Figure 5.3 illustrates the effect of particle shape and surface texture on the author's results for slump.

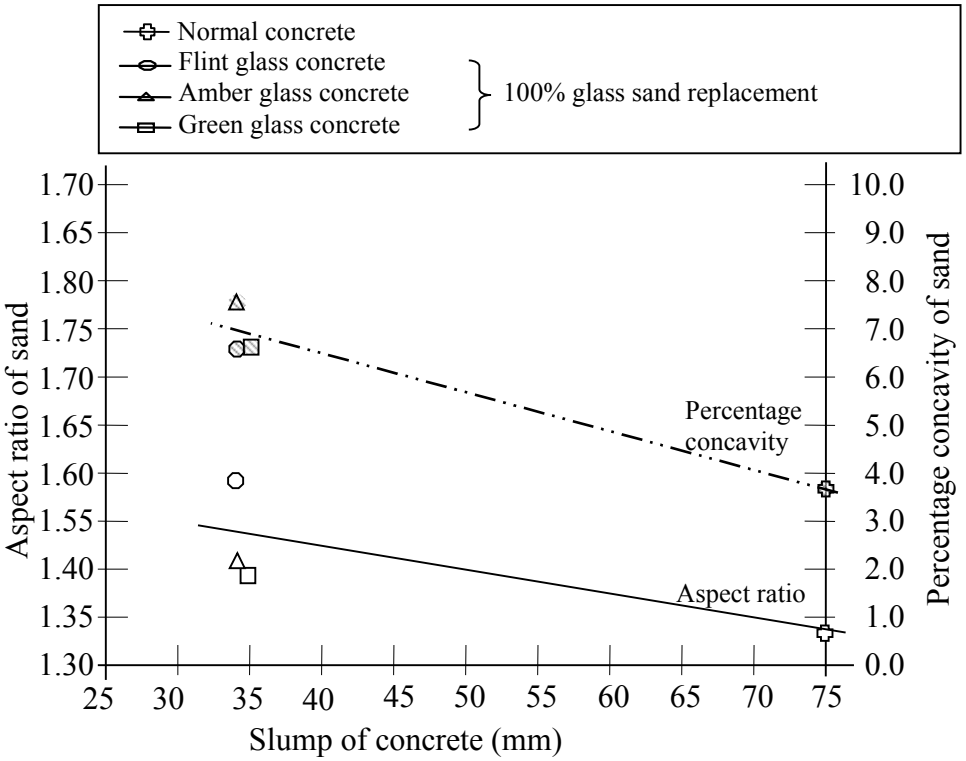

Fig. 5.3 Relationship between slump and Aspect Ratio and Percentage Concavity of fine aggregate

The normalised results of Park *et al.* (2004) show very good agreement with the author's data. Topcu and Canbaz (2004) also reported a decrease of slump with concrete containing waste glass and they believed that this was due to the geometry/ shape of the glass particles. However, it should be noted that the observed differences

between the shape of the sand and glass particles used by Topcu and Canbaz reported were small as the decrease in slump was itself quite small, i.e. only 5 mm. It should be noted that this decrease is of the same order as the likely variation of the slump value of a normal structural concrete, i.e. ± 5 mm (Neville, 1995).

There would appear to be an overall trend that the higher the workability the greater will be the decrease in slump when the sand component is replaced by crushed bottle glass as it can be seen in the results of Park *et al.* (2004) and Chen *et al.* (2006).
The data from Chen *et al.* (2006) show a decrease in slump which is much greater than that of the general trend and this is probably due to their use of "E-glass" with glass particles which were cylindrical in shape. Such a shape would promote slump due to particle rolling whereas the author's particles had greater angularity. The waste E-glass particles were obtained from electronic grade glass yarn scrap by grinding to give a particle sizes from 38 μm to 300 μm with about 40% the particles being less than 150 μm. Hence the particles of glass were much finer than conventional fine aggregate whereas in the author's work the conventional and glass fine aggregates had identical particle size distributions.
Shayan and Xu (2006) reported that mixes of 40% and 75% glass powder as fine aggregate replacement with a 0.7 water cement ratio decreased slump values by 29%. In the research reported herein replacement of conventional fine aggregate by the foregoing amounts of glass would have caused slump values to decrease by 30 to 50%. According to Limbachiya (2009) an increase in glass content beyond 20/30% (of the fine aggregate) produced a measureable reduction in workability of the concrete but the fall did not exceed the allowable slump variation, i.e. ±25mm.
Kou and Poon (2009) reported that rate of slump loss decreased with the increase in recycled glass aggregate content, as has been found in this investigation - see Figure 5.2.
Unlike the author, Zammit *et at.* (2004) found that glass slightly increased slump and reported 50% waste glass replacement produced the highest slump values. Camilleri *et al*. (2004) also found that incorporation of glass fines in concrete reduced the amount of water required by the mix to achieve a specific slump. This is directly the opposite of the findings of Castro and Brito (2013). However the white bottle glass added by Camilleri was crushed to such an extent that it was described as completely amorphous. The addition of this very fine glass would have changed the particle size

distribution within the concrete (a change which the author was very careful to avoid) and would have affected the internal mechanism and stability of fresh concrete.

Terro (2006) stated that replacement of up to 10% of fine aggregate by glass had no effect on fresh concrete but slump values generally increased with higher percentages of waste glass. This was attributed to the poorer cohesion between the glasses aggregates with smooth impermeable surfaces in contact with the cement paste which leads to reduced inter-particle friction.

Wang and Huang (2010a) used Liquid Crystal Display (LDC) glass in self-compacting concrete and reported that for increasing glass replacement of aggregate in concrete the slump flow showed a distinct tendency to increase. For a glass replacement of 10% to 30% the slump flow went from 20 to 100 mm due to the higher compactness of the concrete granular skeleton. However, according to Wang and Huang their "glass sand" was finer than conventional sand so the results do not relate to equivalent mixes - unlike the author's data. Ali and Al-Tersawy (2012) also reported that the use of glass fine aggregate increased slump flow for self-compacting concrete. Scanning electron microscope micrographs showed that the surface of the glass used was very smooth so there was poor adhesion between glass and cement paste as suggested by Terro (2006). Measurements of particle shape and texture reported in Section 4.3, indicate that the surface of the glass aggregate used by the author was anything but "smooth" (as illustrated schematic in Figure 4.81). Furthermore, percentage concavity values (Section 4.3.2) indicate that the glass particles used had considerably 'rougher' surfaces than the sand that they replaced so that using glass aggregate would be expected to inhibit slump.

However Liu (2011) used ground glass as a partial replacement for fine aggregate in self-compacting concrete and reported that in order to keep the "filling ability" of the concrete constant an increase in water/ powder ratio was required, as stated by Castro and Brito (2013). Chen *et al*. (2011) noted that when LCD glass was used in conventional concrete the slump was not detrimentally affected.

b) *The observed decrease in slump occurred for all colours of glass and regardless of whether the glass aggregate was in a washed or unwashed state (Figures 4.12 and 5.1)*

For amber glass, Park *et al*. (2004) reported that a concrete with 30% sand replacement had ‘high workability’ whilst for 70% replacement the concrete had only

'medium workability'. However, this only equated to a change in slump value range from 95-110mm down to 72-80mm, i.e. an approximate reduction in slump value of around 25%. The corresponding reduction obtained from the research reported herein would be around 20 to 30%.

Park *et al*. (2004) showed that the actual colour of waste glass aggregates did not markedly affect the slump, as found in the research reported herein. Therefore, a small amount of admixture or water could be used to ensure the necessary fluidity to prevent a decrease in slump value.

c) *Upto 25% of fine aggregate (sand) could be replaced by crushed glass before there was a significant change in slump (Figures 4.12 and 5.1).*

As indicated earlier in this section the form of the waste glass used as fine aggregate, e.g. particle size distribution, particle shape, grain surface texture, affects which way the slump changes. Shao *et al*. (2000) reported that the use of glass powders within concrete reduced the workability (by about 18%) compared to that of conventional concrete. Shao *et al*. (2000) stated that the angular shape of the glass particles was the likely cause of this decrease in workability and showed pictures of their aggregates to demonstrate the difference in shapes. Similar comments about waste glass grain shape and slump of fresh concrete were made by Ismail and Al-Hashmi (2009) and Borhan (2012). Lee *et al*. (2013) stated that in contrast to the rounded, smooth shape of natural sand fine glass aggregate was generally elongated, flat and angular and they presented pictures to illustrate the difference. This difference was quantified by Castro and Brito (2013) using a shape index. However, according to CCANZ (2011) the flat and elongated nature of glasses particles could improve the rheological properties of fresh concrete containing glass, i.e. the workability would not be decreased.

Figures 5.4 to 5.7 show that the waste glass particles used in this research have sharper edges, higher aspect ratio and more angular shape than the conventional aggregate (Figures 3.9-3.10 and 3.12-3.17) and this is confirmed by the surface texture index of the crushed glass being 0.082 to 0.093 as compared to 0.072 for the sand (Section 4.3.2), i.e. the conventional aggregate has greater sphericity and roundness. The greater 'roughness' of the glass particles hinders the movement of

cement paste and particles and thus reduces the workability of the concrete. Therefore concrete with the glass aggregate used in this research requires greater water content to give a more liquid paste which can coat and lubricate. It is believed that concrete with low workability would exhibit increasing air content adjacent to aggregate particles and this would be especially true for the higher percentage of waste glass aggregate replacement.

There is no consensus from previous research as to whether the use of glass as fine aggregate increases or decreases the slump of a mixture. However, it would appear that there is negligible change in slump with substitution of glass up to about 25% of the fine aggregate - Park *et al.*, Topcu & Canbaz, Terro, Limbachiya, etc. Further increase in glass content does produce a change in slump, but generally not sufficient to change the workability category.

Fig. 5.4 Shape and texture of natural aggregate

Fig. 5.5 Flint glass aggregate shape and texture

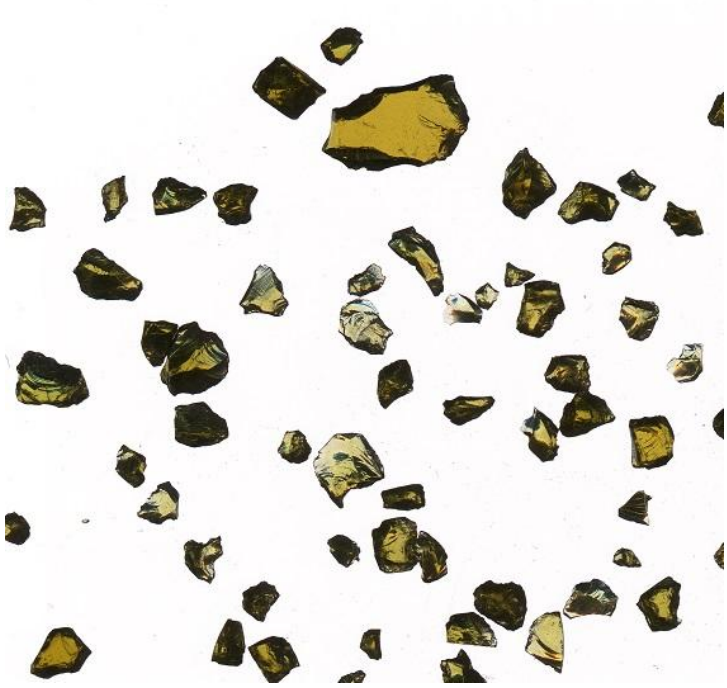

Fig. 5.6 Amber glass aggregate shape and texture

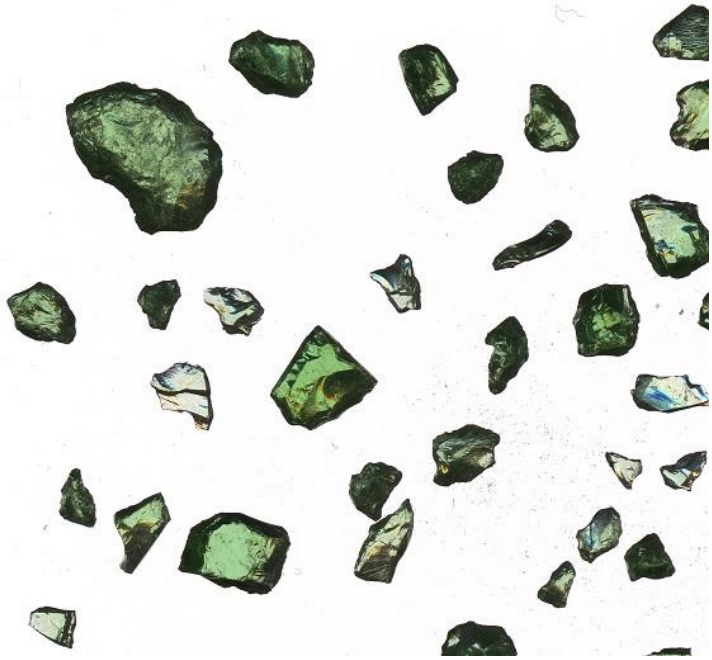

Fig. 5.7 Green glass aggregate shape and texture

5.1.2 Flow table value

Figure 5.8 contains a pictorial summary of all of the numerical data (relating to the flow table test) from the research reported herein (Section 4.1.3) together with relevant data from other researchers. The foregoing data have been normalised by dividing flow table values by the mean flow table value for the relevant conventional concrete, and the resultant values are presented in Figure 5.9. Previous findings are summarised in Table 5.2.

In Figures 5.8 and 5.9 the flow table value is shown to reduce with increasing waste glass content of the fine aggregate. The value dropped from 510 to 475 to 443 to 355mm as the glass content increased from 0% to 25% to 50% to 100%. Similar results were reported by Saccani and Bignozzi (2010) and Tan and Du (2013), who used a similar source of beverage bottle glass to the author's and a mortar flow test as indicated at Table 5.2. The colour of the glass has no significant affect on the workability of the concrete, as shown by the work reported herein and the research of Tan and Du (2013).

On the other hand Wang (2009), Wang & Chen (2010) and Chen *et al*. (2011) reported that slump flow increased with increasing percentage of sand replaced by thin film transition liquid crystal display optical (LCD) waste glass powder. The flow table value peaked when the waste glass amounted to 30% of the total volume of fine aggregate. It must be noted that the three foregoing publications relate to the same test results which used self-compacting concrete. Because low water-cement ratios were used (around 0.3 to 0.4) in the concrete the mixes also contained fly ash, blast furnace slag and super- plasticiser. Ali and Al-Tersawy (2012) also reported that when self-compacting concrete was made using fine glass aggregate the flow value increased as the glass content increased. This effect was attributed to the smoothness of the surface of the glass used in their mixes with SEM micrographs showing reduced contact between the cement matrix and the glass surface. According to Matos and Coutinho (2012) SEM investigations showed that fine glass particles could be completely encapsulated by gel produced during hydration of cement so that in effect they behaved like balls. Ali and Al-Tersawy (2012) also used mixes with a low water-cement ratio (0.4) and super plasticizer. Paradoxically, Wang and Chen (2010) reported that concrete made with a high water-binder ratio (1.1) and 10% glass-sand substitution exhibited a slump flow which was less than other concrete mixes. So with fine glass aggregate there may be same effect on internal resistance to flow resulting from surface tension, surface wetting, etc. and the composition of the 'liquid phase' within the concrete.

As indicated in the previous section (5.1.1) the shape and surface texture of the conventional fine aggregate and its glass replacement affects the slump/ workability of a concrete mix. The influence of aggregate grain characteristic (tendency to roll and resistance to sliding) on flow table values is indicated in Figure 5.10. However, with the flow table test the effects may be masked to some extent by differences in the composition of the 'fluid' occupying the pores in the concrete skeleton, e.g. its viscosity, air content, because the flow table test invokes a liquefaction failure rather than testing internal shearing resistance as the slump test does. It is contended that a good way to assess the integrity of the concretes containing glass made by the author is to compare their flow values against slump (Figure 5.10).

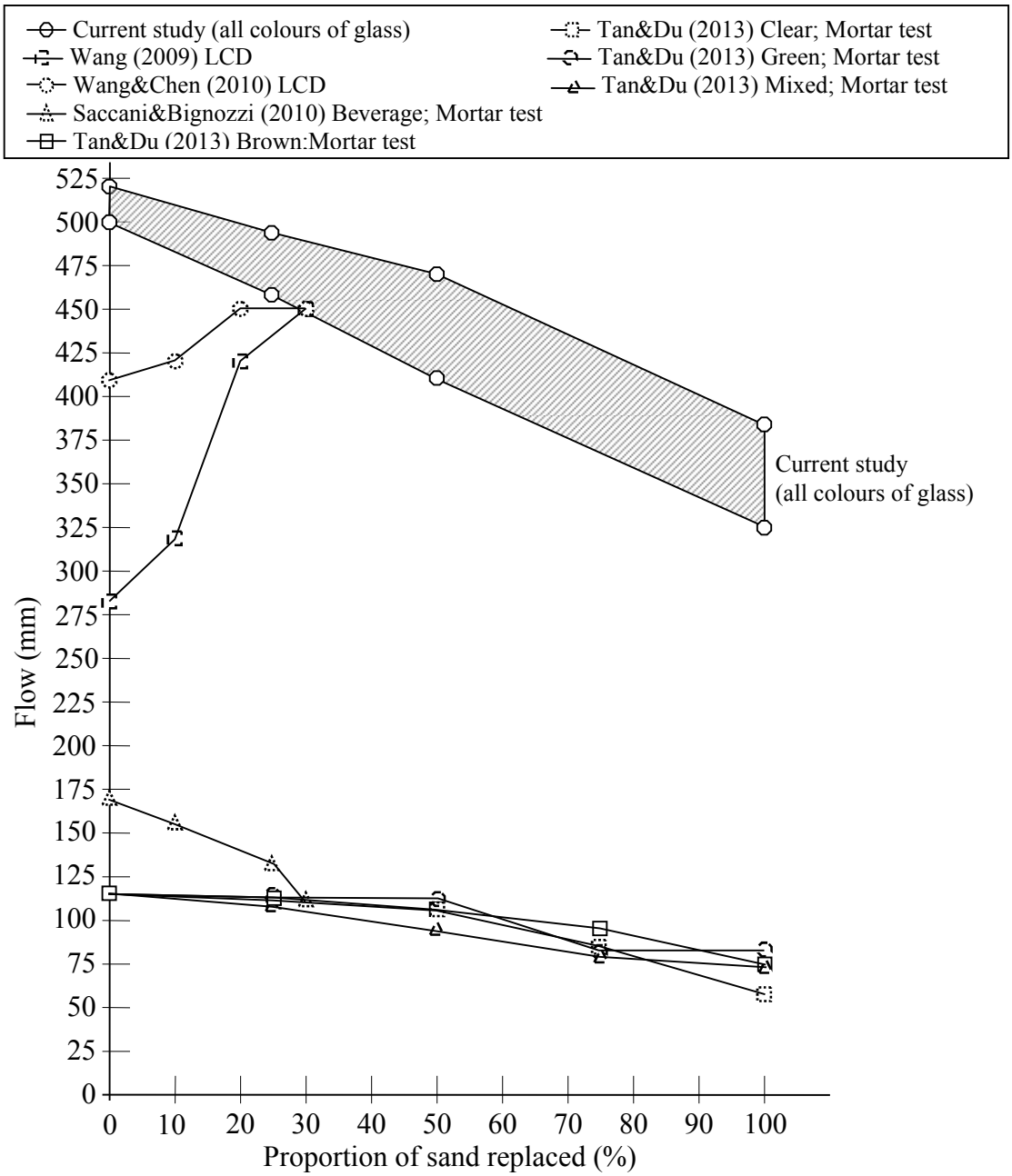

Fig. 5.8 Flow table data for work on replacement of fine aggregate by glass

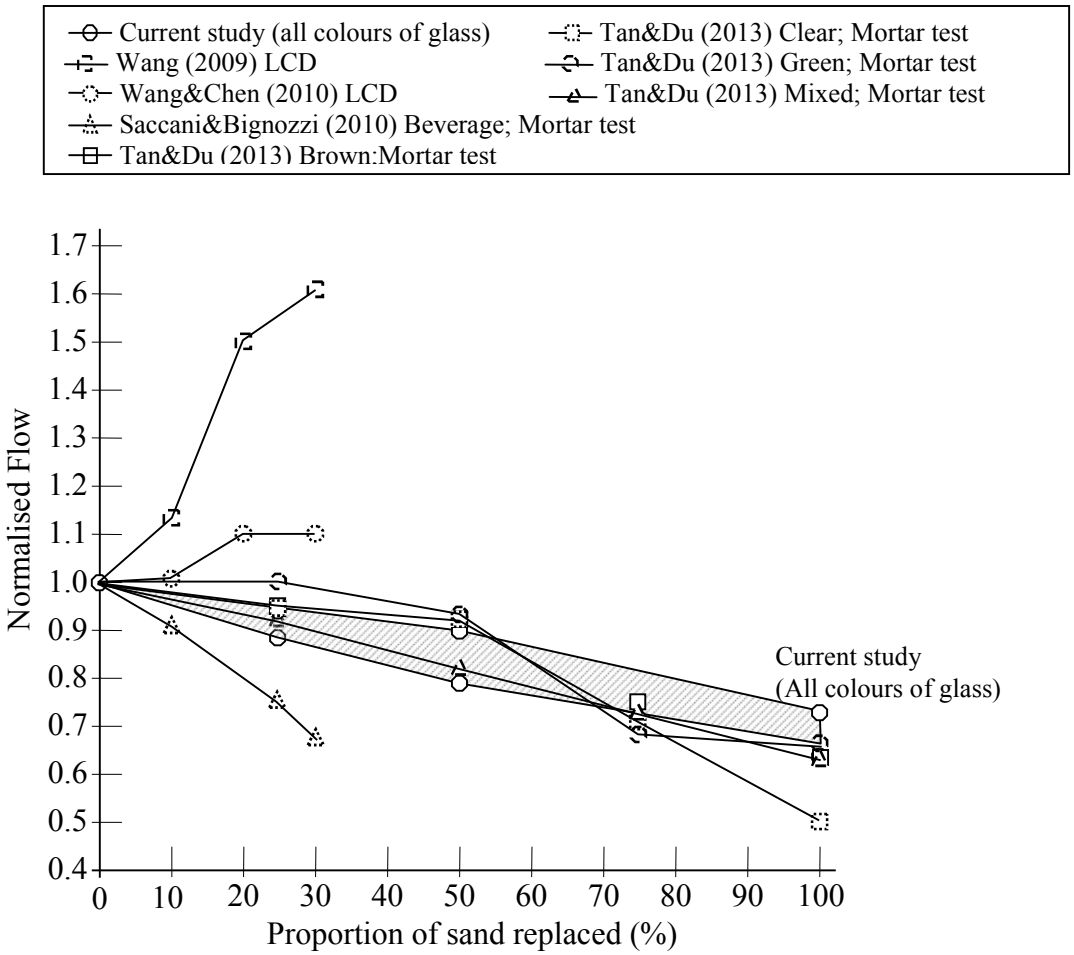

Fig. 5.9 Normalised flow values for concrete containing fine glass aggregate

Table 5.2 Previous findings relating to flow table values and use of waste glass as fine aggregate in concrete

Finding	Researchers
1. Using waste glass as replacement in the concrete has increased flow table value compared to using sand as aggregate.	Wang (2009), Wang and Chen (2010)
2. Using waste glass as replacement in the concrete has decreased the flow table value compared to natural sand - as found in this study.	Saccani and Bignozzi (2010), Tan and Du (2013)

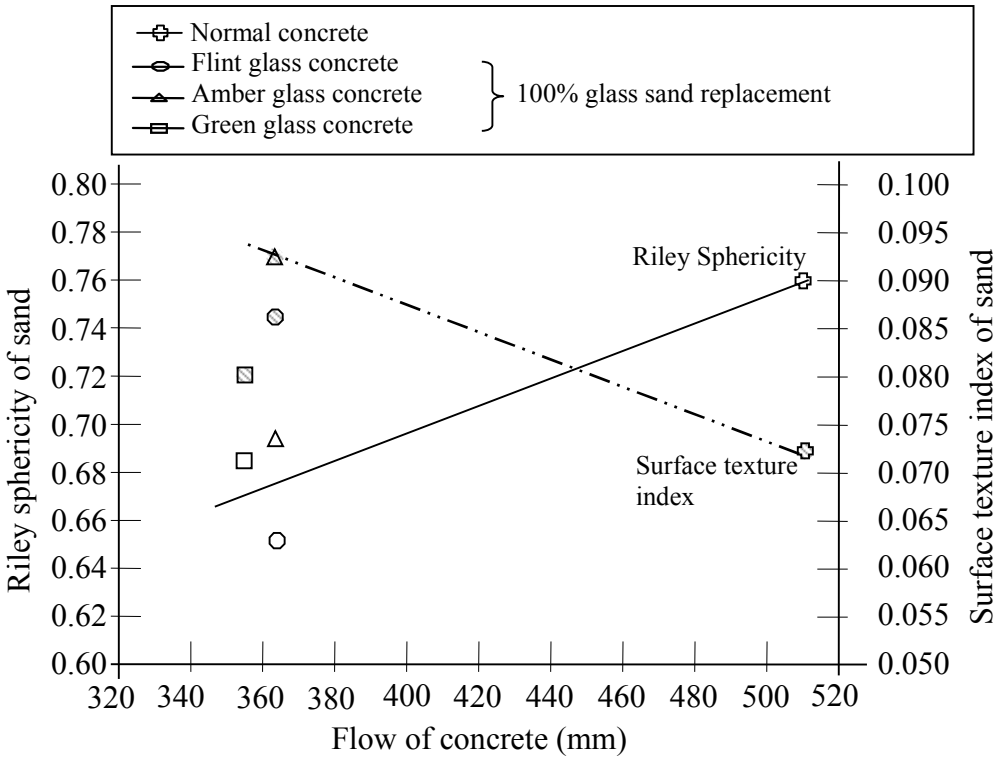

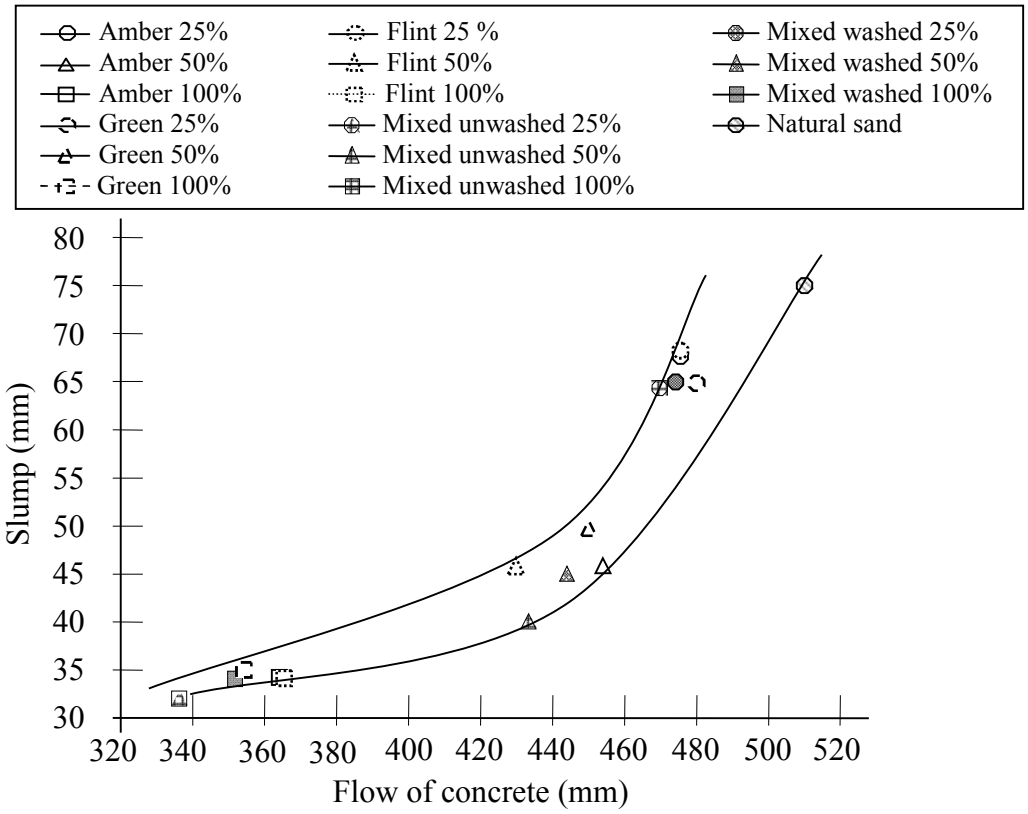

Fig. 5.10 Relationship between flow, slump and particle surface texture of fine aggregate

5.1.3 Setting times

A summary of the numerical data obtained relating to initial setting time (Section 4.1.4) and relevant results from other researchers are presented in Figure 5.11. To account for differences in mixes between the various source of information included in this figure (as shown by the range of setting times for zero-glass mortar) setting times have been normalised by dividing by the respective setting times for zero glass content and these values are shown in Figure 5.12.

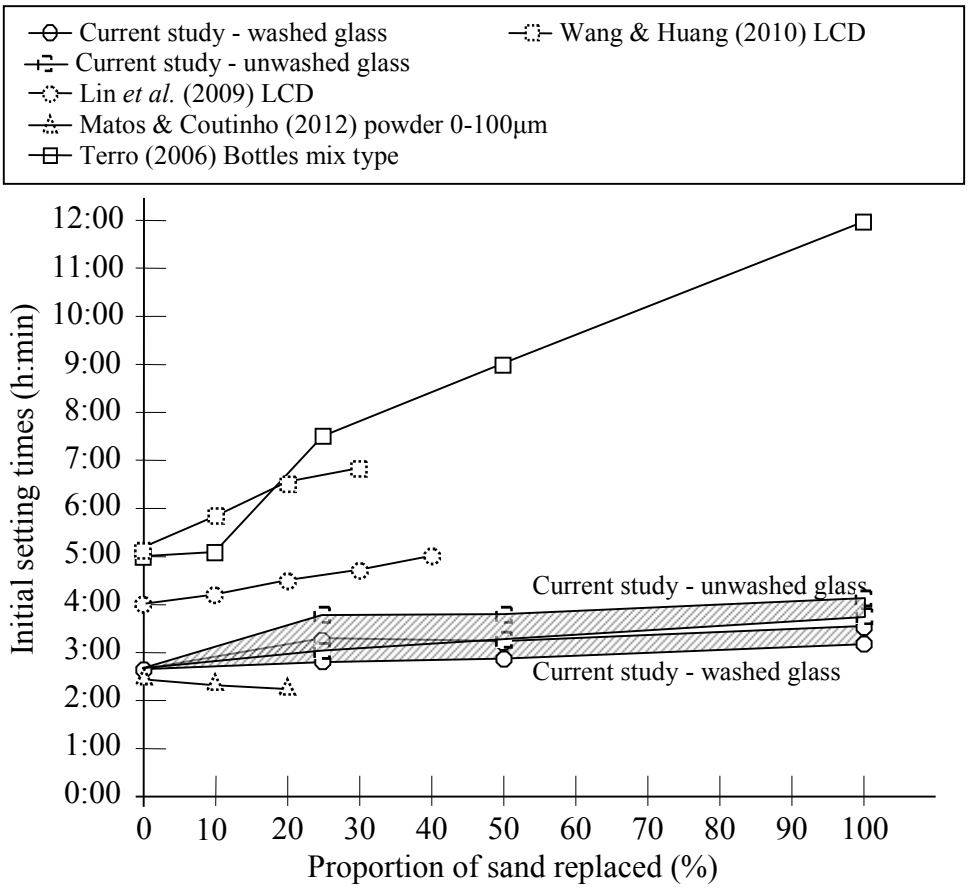

Fig. 5.11 Initial setting times for work on replacement of fine aggregate by glass

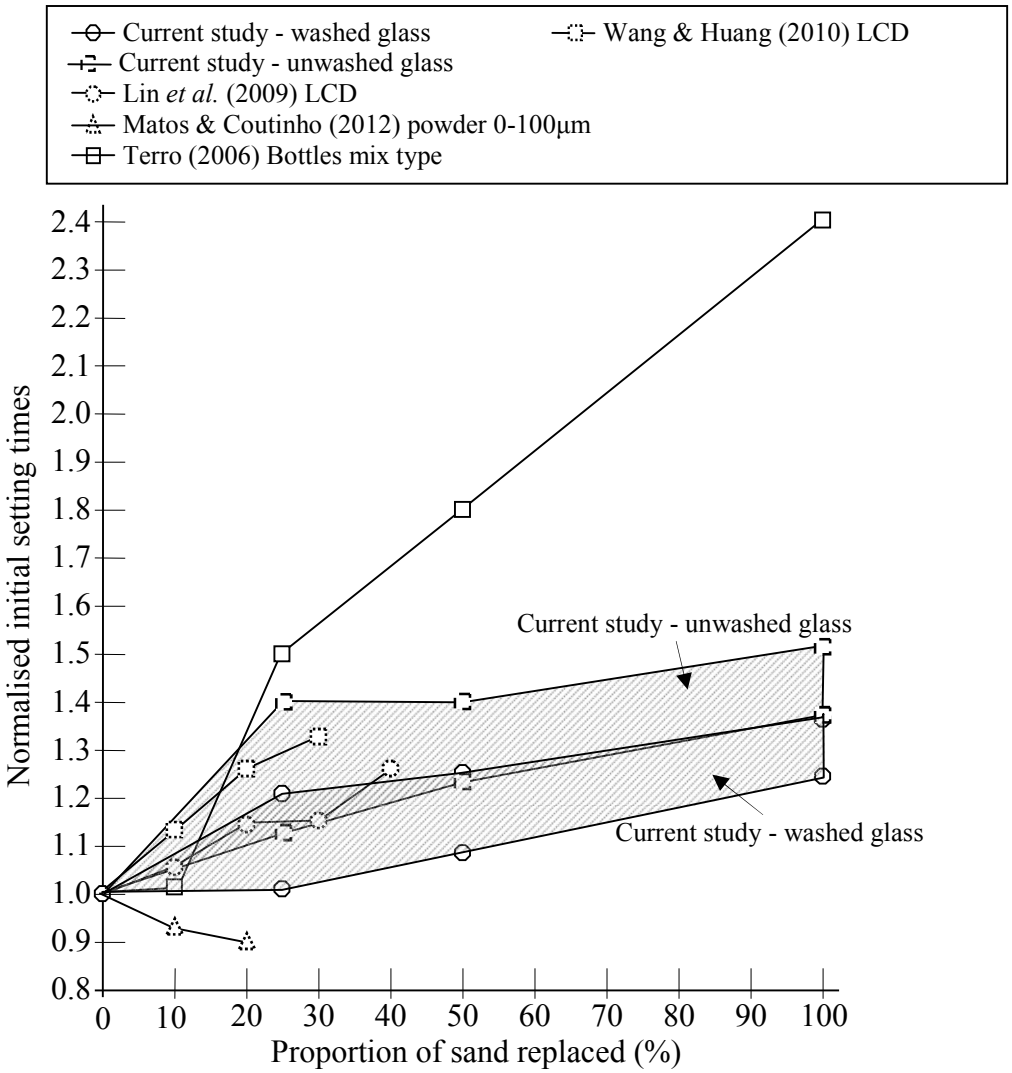

Fig. 5.12 Normalised initial setting times values for concrete containing fine glass aggregate

The relevant findings reported by the other researchers are summarised in Table 5.3.

Table 5.3 Findings relating to setting times when waste glass is used in concrete

Finding	Researchers
1. Increasing the waste glass content extends the initial setting time - as found in this study.	Terro (2006), Wang & Huang (2010), Wang (2009) and Lin *et al.* (2009)
2. Increasing the waste glass content extends the final setting time - as found in this study.	Terro (2006), Wang & Huang (2010), Wang (2009) and Lin *et al.* (2009)
3. Increasing the glass content has shortens the initial setting time.	Matos and Coutinho (2012)
4. Increasing the glass content has shortens the final setting time.	Matos and Coutinho (2012)

In section 4.1.4 it was reported that the setting time increased linearly with amount of conventional fine aggregate replaced by glass and that the effect of not washing the glass aggregate was to cause all setting times to be delayed by 21 minutes (13% of the initial setting time for normal concrete). Figure 5.12 demonstrates that Terro (2006), Lin *et al*. (2009) and Wang and Huang (2010) reported similar findings. However each of the foregoing pieces of research had a different rate of increase of initial setting time with amount of glass present and different 'delay times'. The Vicat penetration test measures primarily the fluidity of the cement paste and its ability to flow as it is 'pushed aside' and into the surrounding aggregate skeleton by the penetrating needle. Hence setting time could be delayed by the surface chemistry of the glass particles (presence of contaminants such as sugars as found by Terro (2006) exposure of particular elements during glass crushing, for instance) or by there being less adhesion (at any particular time) between the cement paste and glass. Both Terro (2006) and Wang & Huang (2010) reported increases in slump when they replaced sand by their fine glass. Also Lin *et al*. (2009) used LCD glass as their source of fine

aggregate and Wang and Huang (2010) pointed out that this type of glass was hydrophobic and hence it could affect the internal chemistry of concrete by altering the amount of water available for hydration.

In Figure 5.12 it is seen that Matos and Coutinho (2012) reported a reduction in initial setting time as the amount of fine glass replacing sand increased. However this glass was in the form of fine powder (0-100μm) and it has been widely reported that glass powder is pozzolanic - Dyer and Dhir (2001), Shao *et al.* (2000), Byars *et al*. (2004b), etc. Schwarz *et al.* (2008) demonstrated specifically that glass powder facilitated an enhancement in cement hydration at early stages and so its use as a replacement for sand aggregate would reduce initial setting time.

Figure 5.13 contains the results obtained for the effect of glass fine aggregate on final setting time together with the results presented by previous researchers who investigated the same topic. Figure 5.14 contains data which have been normalised of with respect to the final setting time of the relevant normal concrete.

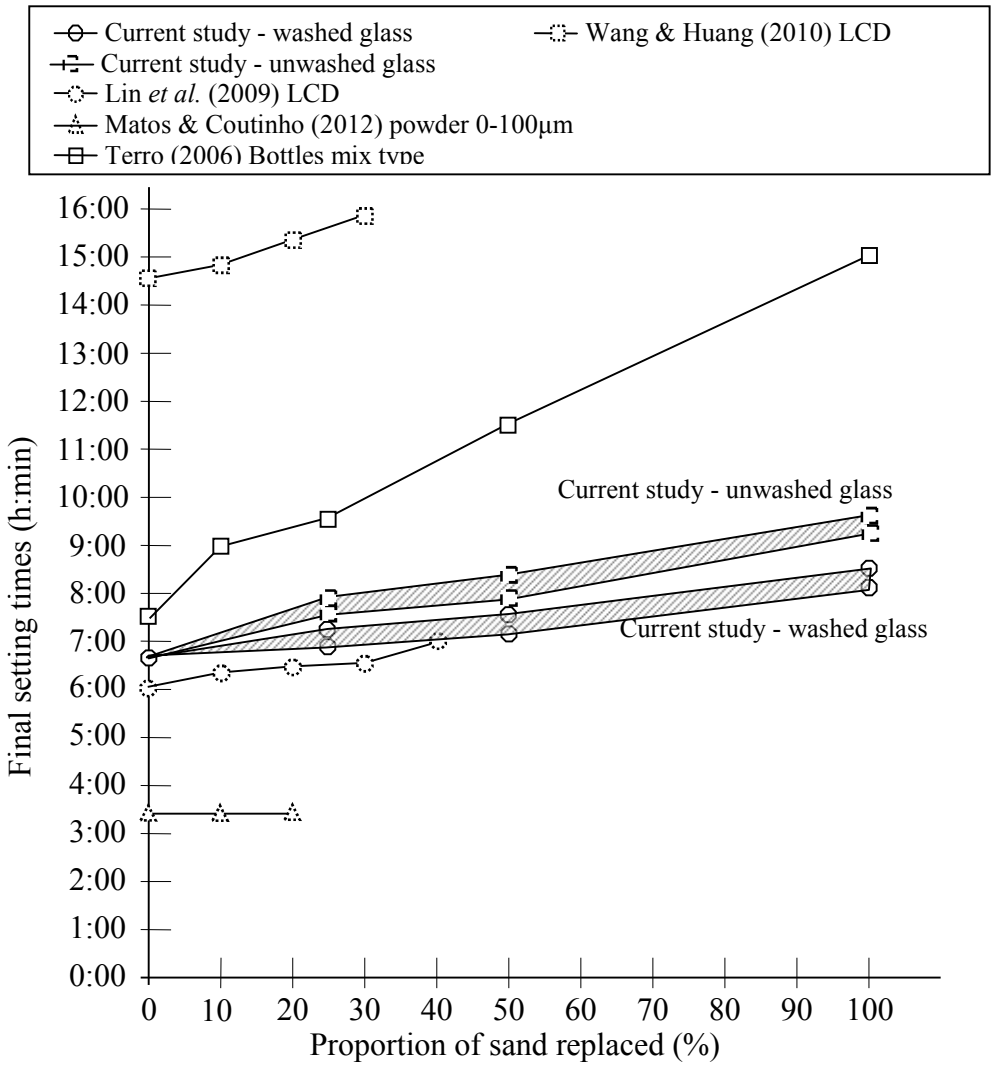

Fig. 5.13 Final setting times for work on replacement of fine aggregate by glass

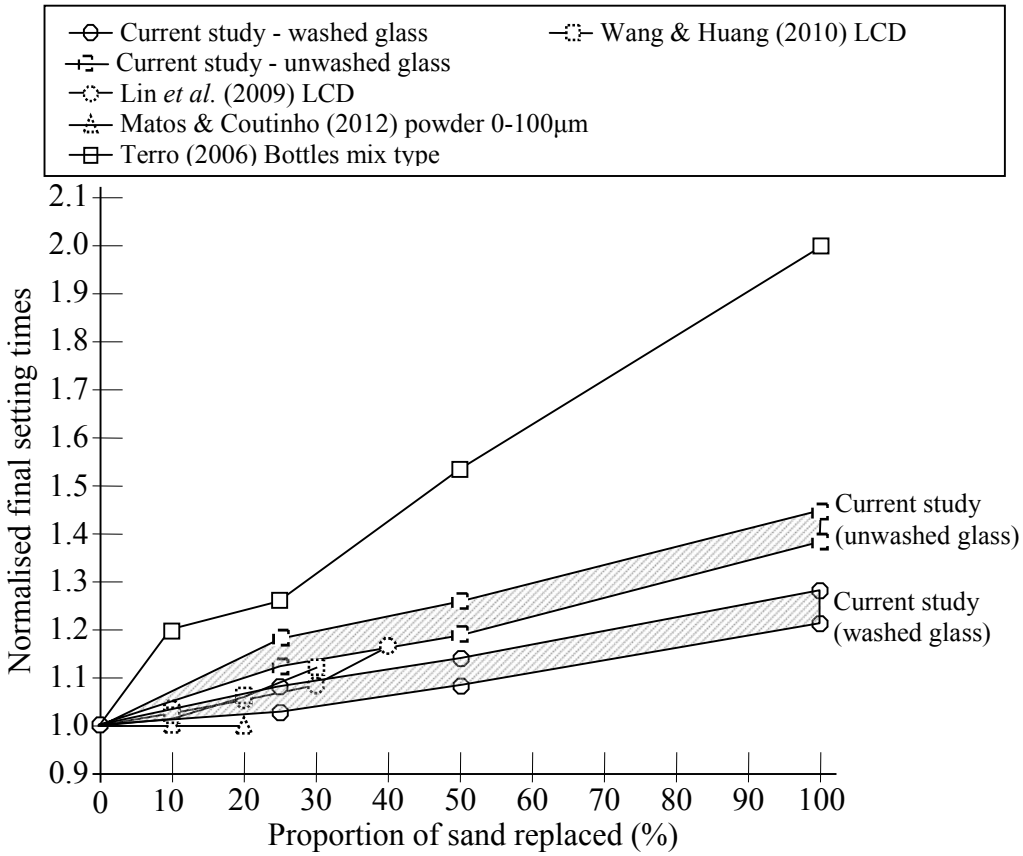

Fig. 5.14 Normalised final setting times values for concrete containing fine glass aggregate

The data in Figures 5.13 and 5.14 demonstrate very similar trends to the findings for initial setting time, i.e. the final setting time increased linearly with the proportion of fine aggregate which was crushed glass and not washing the glass aggregate caused all setting times to be delayed (by 45 minutes, approximately 11% of the final setting time for normal concrete). The data published by Lin *et al*. (2009) and Wang & Huang (2010) exhibited very similar trends and values (when normalised) to those observed in the course of the author's research. The results from Terro (2006) show a much larger increase in setting time with proportion of sand replaced. It was stated that the delay was a result of a relative increase in water-cement ratio due to the glass aggregate having a low water absorption property. However, Terro (2006) replaced both fine and coarse aggregate by waste glass and found that this reduced the compressive strength of the resultant concrete by a significant amount. Since the test for final setting time relates to stiffness/ surface hardness of the concrete with respect to a given load then the weaker concrete containing glass would require significantly greater curing time. On the other hand, Matos and Coutinho (2012) replaced normal

sand with fine glass powder (which is acknowledged to be pozzolanic), so one would expect their final setting time to be reduced or unchanged. Taha and Nounu (2008) claimed that contamination and organic content in waste glass fine aggregate, can be considered as the main issue in decreasing setting time and creating voids in the microstructure of concrete.

5.2. Hardened concrete

5.2.1 Density

In Section 4.2.1 it was shown that the density of the cast concrete was reduced (by between 0.1 and 1.8%) when glass was used as fine aggregate in the mix. There was no evidence that the magnitude of the density reduction was affected by either curing time or the colour of the glass aggregate. The density data for 28 days curing are summarised in Figure 5.15 which also includes information from other researchers' work.

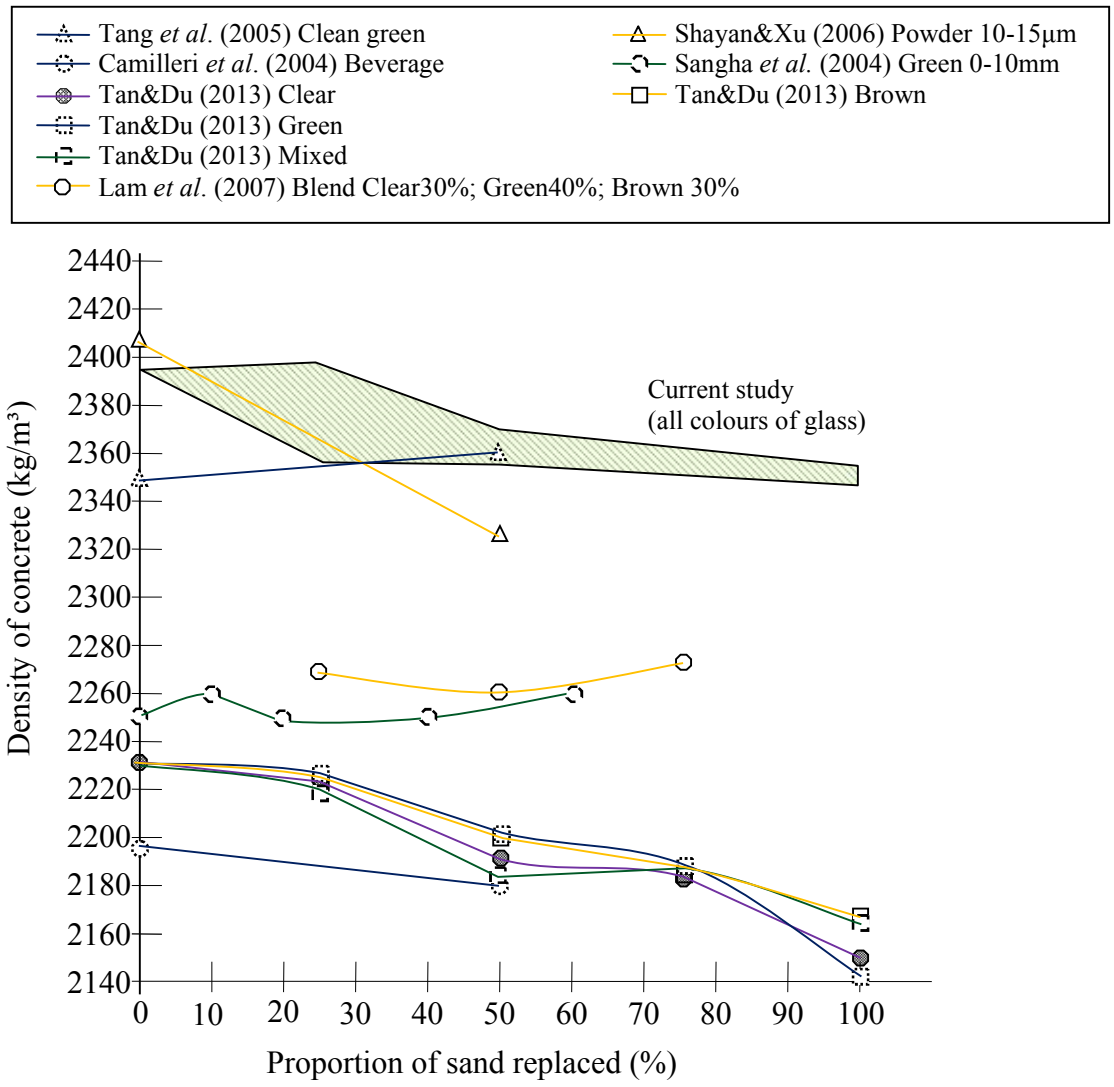

Fig. 5.15 Density of concrete for other researchers' glass replacement aggregate

In Section 4.2.1 it was mentioned that the concrete containing fine aggregate made from crushed glass could have a lower overall density than conventional concrete due to the glass having lower density than sand. The specific gravity of the waste glass was 2.5 while the Specific Gravity of the replaced sand was 2.61. Similar differences in the Specific Gravity of sand (as fine aggregate) and crushed glass have been reported by other researchers as shown in Table 5.4.

Table 5.4 Fine aggregate Specific Gravities

Aggregate	**Specific Gravity**				
	Park *et al*. (2004)	Polley *et al*. (1996)	Kou and Poon (2009)	Shayan and Xu (2006)	Current study
Natural gravel	2.70	2.68	2.62	No specify	2.65
Natural sand	2.65	2.63	2.62	2.63	2.61
Waste crushed glass	2.5-2.52 (0 – 5mm)	2.15 (75µm – 2mm)	2.49 (0 – 5mm)	2.5 (Powder 10-15µm)	2.5 (0 – 5mm)

Table 5.5 contains values relating to estimation of the effect of the Specific Gravity/ density of a fine aggregate on the bulk density of a typical concrete. The estimation is based on BS1881: Part 107:1983 for a design mix of 1:2:4 of cement: fine aggregate: coarse aggregate with water-to-cement ratio 0.6.

Table 5.5 Calculations of quantities per cubic metre for concrete mixes

Materials	**Weight (kg)**	**Specific gravity**	**Volume (m^3) × 10^{-3}**
Conventional concrete			
Cement	313.16	3.15	99.4
Fine aggregate (100% sand)	626.32	2.61	240.0
Coarse aggregate	1252.63	2.65	472.7
Water	187.89	1.0	187.9
Total	2380.00		1000.0
Concrete containing 100% glass fine aggregate			
Cement	313.16	3.15	99.4
Fine aggregate (100% glass)	626.32	2.5	250.5
Coarse aggregate	1252.63	2.65	472.7
Water	187.89	1.0	187.9
Total	2380.00		1010.5

The estimated density of the conventional concrete is 2380 kg/m³. The estimated density of the concrete containing 100% fine glass aggregate

$= 2380 \times 1000 \div 1010.5$ kg/m³

$= 2355$ kg/m³

The difference between the estimated densities of a conventional concrete and an equivalent glass concrete containing all glass fine aggregate is thus $(2380 - 2355) \div 2355 \times 100\%$ which equals 1.1%, as compared to the reduction of between 0.1 and 1.8% found in this research. Furthermore the estimated density for a conventional concrete, i.e. 2380kg/m³, is very similar to the mean value for 7-day old concrete which was measured in this research, i.e. 2378 kg/m³ (in Table 4.6). The corresponding measured mean densities for concretes wherein all of the fine aggregate had been replaced by glass were (Table 4.6): 2353 (flint glass), 2349 (amber glass), 2340 (green glass), 2349 (mixed glass) and 2349 (mixed unwashed glass). These latter values are in good agreement with the estimated value calculated as shown in Table 5.5. Consequently the mean density values measured for conventional concrete at all ages have been used to estimate the equivalent concrete density values which could be expected of there was some replacement of the fine aggregate by crushed glass and the resultant data are presented in Table 5.6. There is generally close agreement between the estimated/ predicted density values and those actually measured. The very good correspondence between estimated and measured density values after 365 days curing tends to suggest that in the long-term there is negligible difference, in terms of internal porosity and volume change during curing, of the conventional concrete and the mixes containing waste glass.

Table 5.6 Estimation of effect on concrete density of using glass as fine aggregate

Age (days)	Normal concrete		Concrete containing waste glass fine aggregate Proportion of glass (%)		
			25	50	100
1	2347	Measured	2336-2345	2331-2345	2329-2342
		Calculated	2340	2334	2321
7	2378	Measured	2354-2367	2351-2363	2340-2353
		Calculated	2371	2365	2352
28	2395	Measured	2358-2397	2358-2370	2352-2359
		Calculated	2388	2382	2366
112	2381	Measured	2359-2375	2359-2366	2357-2365
		Calculated	2374	2368	2355
365	2393	Measured	2381-2393	2372-2383	2367-2375
		Calculated	2386	2378	2366

Other researchers (Figure 5.15) have found that the use of waste glass as replacement fine aggregate in concrete has affected the bulk density of cubes by up to 4%. Some previous research has shown that the incorporation of glass aggregate leads to either a reduction, or essentially no change in density.

A density decrease of up to 2% was reported by Camilleri *et al*. (2004), Shayan & Xu (2006), Taha & Nounu (2008a), Wang & Huang (2010)). This reduction falls within the range observed in the research project reported herein. Tan and Du (2013) reported a density decrease of 3% to 4%. This was probably due to the combination of a low water cement ratio, i.e. 0.485, as opposed to the author's 0.6, and the additional internal friction due to the 'rough' glass aggregate which prevented good compaction of the concrete. In fact Tan and Du (2013) reported that the air content (5.9%) of the 'glass concrete' was almost double that of the concrete incorporating sand. Camillari *et al.* (2004) reported a reduction in density of normal concrete cubes during initial curing with a decrease from 2250 kg/m³ to 2180 kg/m³ from fresh to 7 days of age. However, after 28 days the density of concrete had risen to 2200 kg/m³. It was also observed that with long term curing the concrete containing waste glass replacement

for fine aggregate had a density increase from 2170 kg/m³ to 2180 kg/m³ i.e. about 0.5%.

The schematic particles (Figure 4.81) satisfy two specific shape factors and two specific surface texture factors. The schematic mean glass particles contain surface in indentation which are considerably wider than those for the schematic mean sand particle and the depression are significantly deeper for the glass grains. Hence the glass grains after greater opportunity for entrapment of bubbles or treads of air in surface recesses unless a high water-cement ratio is used. The recessed grooves which are evident in the schematic particles in Figure 4.81 would also facilitate water entry into finished concrete if they contained air voids, as was observed in immersion and capillary tests (Section 4.2.6)

Some researchers have reported that use of glass aggregate results in an increase in density. Sangha *et al*. (2004) Tang *et al*. (2005) and Lam *et al*. (2007) reported that concrete density increased when there was significant replacement of conventional fine aggregate by glass. For Sangha *et al*. (2004) and Lam *et al*. (2007) the maximum increase was 0.4% but there was no clear relation between increase in density and proportion of fine aggregate which was glass. The increase reported by Tang *et al*. (2005) was 1% but this was only based on 50% replacement of fine aggregate and there was no indication of a specific trend. The Figure

5.2.2. Ultrasonic pulse velocity

In Section 4.2.2 it was shown that, at all curing times, the UPV values for concrete containing glass in the form of fine aggregate were lower than those for conventional concrete. However for replacement of 25% of fine aggregate by green glass the effect on UPV was negligible at all curing times. The use of mixed unwashed glass gave the greatest reduction in UPV. After 28 days curing the reductions in mean UPV value ranged from 0 to 2%, 2 to 6% and 4 to 7% for glass contents of 25%, 50% and 100% respectively. Concrete cured for 365 days exhibited virtually identical reductions in UPV value due to use of glass as fine aggregate. The data for 28 days curing are illustrated in Figure 5.16 which also contains finding from other researchers. To account for the various UPV values measured by previous researchers the data in Figure 5.16 have been normalised by dividing them by the respective UPV value for conventional concrete. The normalised data are presented in Figure 5.16.

It is believed that the reduction of UPV, as a result of inclusion of fine glass aggregate, is due to loss of contact between particles and surrounding binder due to presence of small air pockets. These voids would be located in small recesses adjacent to the surface of an aggregate particle. The diagrams illustrating the form of the notional particles, in Figure 4.81, show that glass particles potentially have a greater volume of deeper voids within the grains themselves than sand particles. Because the diagram in Figure 4.81 represent all particle sizes within an aggregate the recesses in the glass particles could be only 20μm wide. So unless a concrete was made with a high water content or with some agent to eliminate surface tension effects the crevices within glass particles would promote the presence of trapped air voids. The plot of UPV value again density, in Figure 5.17 support this contention.

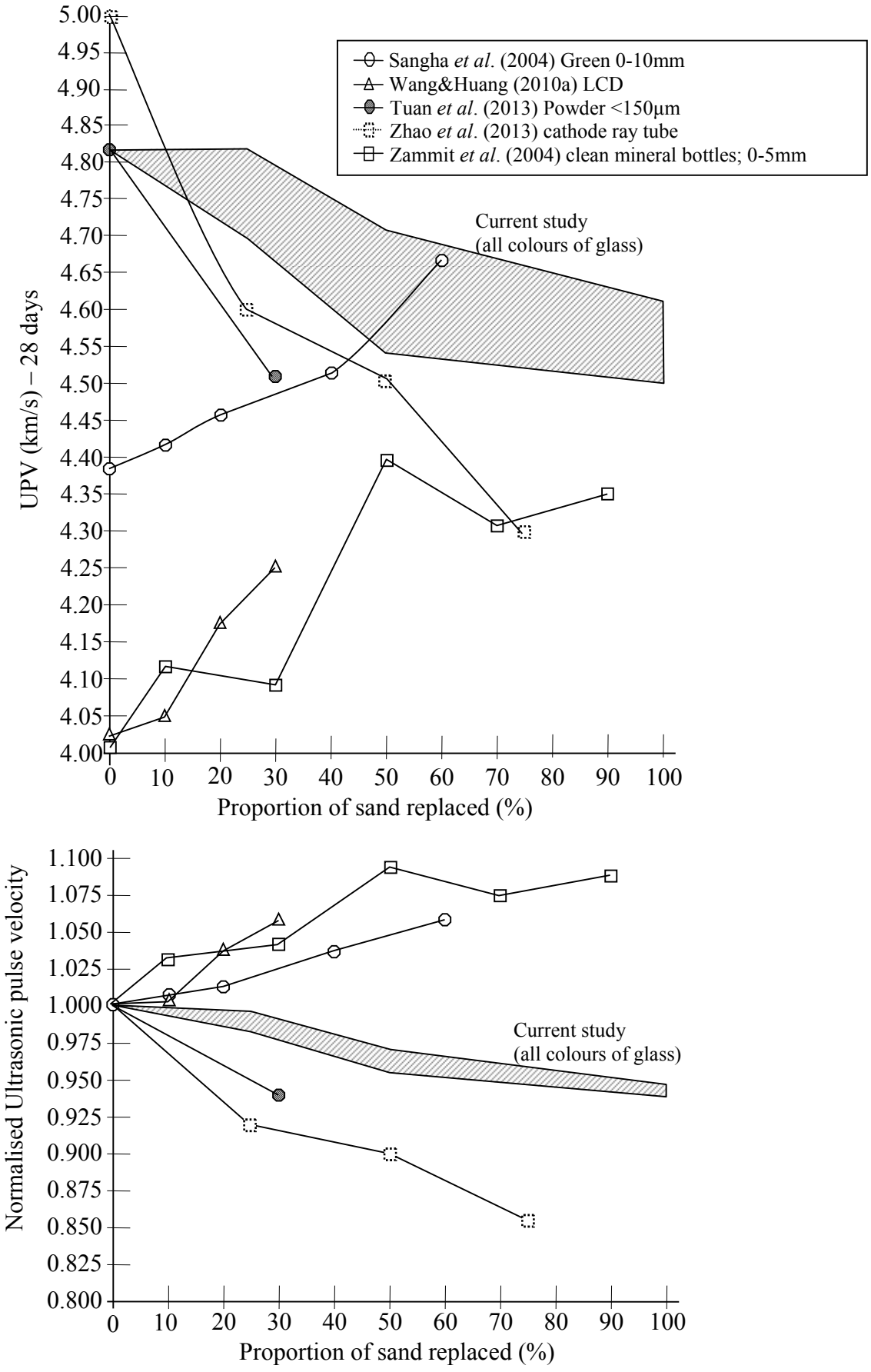

Fig. 5.16 Ultrasonic Pulse Velocity data after 28days of curing

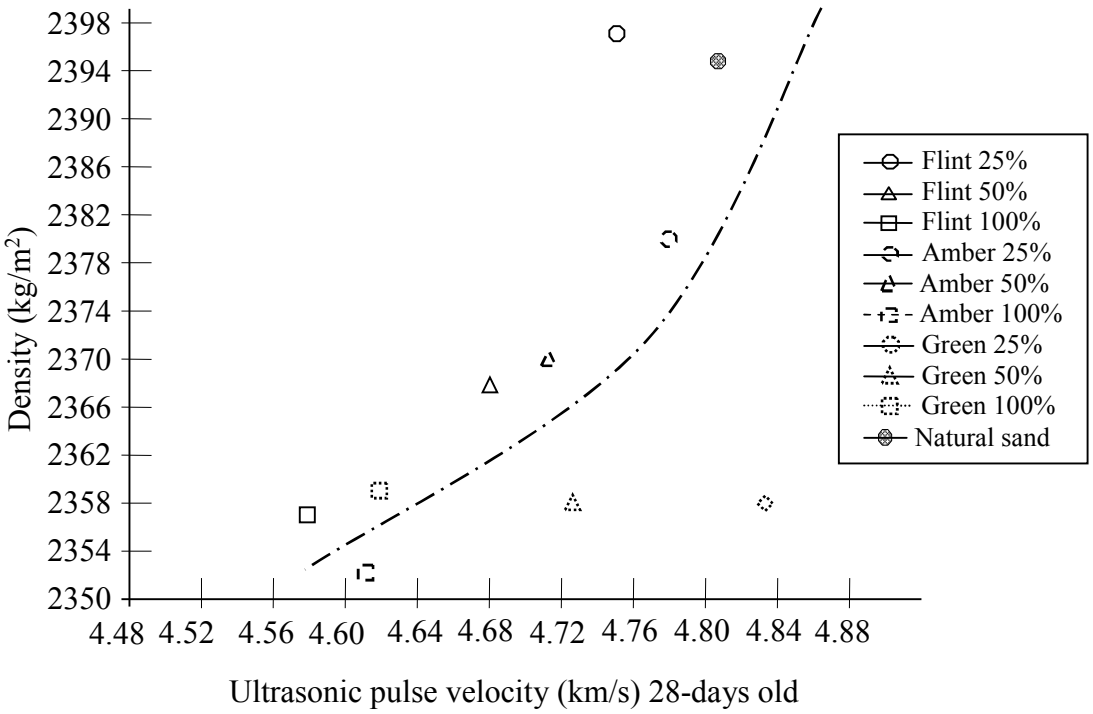

Fig. 5.17 Relationship of density and UPV glass replacement aggregate

Tuan *et al*. (2013) and Zhao *et al*. (2013) have previously reported that concrete with waste glass exhibited decreased ultrasonic pulse velocity. However, both researchers found that the rate at which UPV drops with amount of glass present was much greater than that observed herein. This may be due to the form/ type of glass used by Tuan *et al*. (2013) and Zhao *et al*. (2013). Tuan *et al*. (2013) used glass crushed to a powder with particles finer than 0.15mm which did not conform to size requirements for conventional fine aggregate. Zhao *et al*. (2013) used glass originating from cathode ray tubes and they believed that the lead content of the glass both retarded the cement hydration process and the formation of hydration products. These effects then resulted in a concrete which contained more pores and had a more open structure.

Sangha *et al*. (2004), Zammit *et al*. (2004) and Wang and Huang (2010a) have previously reported increases in UPV due to the incorporation of glass into concrete. Sangha *et al*. (2004) found that the increase was directly proportional to the amount of sand replaced by glass - the UPV increased by 6% for a 60% replacement using glass cullet. The waste glass used was green and in the investigation reported herein it was

found that green glass had the least detrimental effect on UPV - for 25% replacement it gave a marginal increase of 0.4% and for 50% replacement it gave a decrease of only 1.7%. Sangha *et al*. (2004) stated that in order to achieve better strength, there must be better bonding at the aggregate-matrix interface. A higher pulse velocity may thus indicate that there is less cracking at these interfaces. This hypothesis was assessed by slicing concrete samples in the direction of casting and studying them under a microscope. There was clear visual evidence that better bonding is achieved with glass in comparison to the flint aggregate that was used as control. Exceptionally low levels of cracking and air voids were observed at the interface of the cement matrix and glass aggregate. It was believed that these effects may have resulted from the smoothness of the surface, inability to absorb water and possible chemical characteristics.

Zammit *et al*. (2004) found that UPV increased approximately in proportion with glass content up to replacement of half of the conventional fine aggregate. The increase (9%) remained approximately constant as more glass was used. Zammit *et al*. (2004) also found that the maximum slump was achieved with 50% glass content so the concrete that they tested would have been denser than the conventional concrete.

Wang and Huang (2010a) reported that UPV increased from 4.02km/s to 4.25km/s with 30% content of LCD glass in concrete. This was attributed to the smaller glass grains being able to fill pores in a constant-weight sand content and reduce concrete voids. Therefore both ultrasonic pulse velocity and resistance rose with increasing glass sand content.

It is noticeable that the UPV values for conventional concrete measured by the author of this thesis were significantly greater than the corresponding UPV values reported by Sangha *et al*. (2004), Wang and Huang (2010a) and Zammit *et al*. (2004). In fact their values were typical of those for cubes being tested in a dry condition or for poorly-compacted concrete. Hence the increases in UPV values which were quoted may have resulted from differences in manufacture and testing of their concretes, e.g. use of additives, superplasticisers.

5.2.3 Alkali Silica Reactivity (ASR)

The results for all colours of glass aggregate and the various combinations of sand and glass (in the fine aggregate) were presented in Section 4.2.3. After 365 days, i.e. 12 months, the linear expansion of prisms containing normal aggregate was between 0.05 and 0.06%. According to BRE 330 (2004) the aggregate combination for this conventional concrete would be classified as being on the border between "Non-expansive" and "Probably non-expansive" for which it was noted that the aggregate combinations either "have no record of curing damage in concrete" or "have rarely been associated with actual causes of damage to concrete structures", respectively.

The linear expansion of concrete prisms containing various amounts of glass fine aggregate is illustrated in Figures 5.18 and 5.19 together with the findings of other researchers (which are summarised in Table 5.7). The results show that:

a) For all glass colours and combinations of glass the expansion increased as the of amount of glass used as fine aggregate increased.

   Numerous researchers have reported the same finding as indicated in Table 5.7. On the other hand Shao *et al*. (2000) reported that the use of ground glass helped to reduce concrete expansion. However the glass was from fluorescent lamps and was ground so that the size of the particles was a maximum of 38 μm and many researchers (Nishikawa *et al*. (1995), Byars *et al.* (2004), Shi and Wu (2005), etc.) have reported that ground glass exhibits pozzolanic behaviour which reduces the amount of alkali available for reaction with aggregate. Shao *et al*. (2000) themselves suggested that the pozzolanic nature of ground glass was responsible for suppression of alkali-aggregate interaction. Similarly, Shayan and Xu (2004) noted that no deleterious expansion was noted in their concrete prism tests because the glass powder which was added to the concrete had particles 10 to 15 μm and therefore added as a pozzolana thereby binding excess alkali. Schwarz *et al*. (2008) reported that the incorporation of fine glass into concrete reduced expansion. However, their 'conventional concrete' which contained no glass had a reactive siliceous and as fine aggregate. Hence the replacement of this sand by glass powder with a particle size range of 0 to 100 μm, which was itself a pozzolanic material, would be expected to reduce concrete expansion due to alkali-aggregate reaction.

b) Green glass produced less expansion than other colours of glass, mixed glass or unwashed glass.

Figg (1981) reported that the expansion of mortars containing glass was dependent on the colour of the glass. It was stated that clear glass was most reactive and green glass caused less expansion. Park and Lee (2004) and Topcu *et al*. (2008) observed similar behaviour Meyer and Baxter (1997), and Jin *et al*. (2000) suggested that the chromium within green glass could be responsible for inhibition of expansion of the concrete. Zhu and Byars *et al.* (2004) found that there was essentially no difference in the expansion behaviour of concretes containing green, amber or clear glass. Dhir *et al*. (2003) reported a similar finding for concretes wherein upto 50% of conventional fine aggregate was replaced by fine glass. However, for complete replacement of this aggregate by glass Dhir *et al.* (2003) reported that green glass produced much more expansion than other colour. Dhir *et al.* (2003) commented that elements other than chromium could be playing a role in controlling ASR expansion and that the waste glasses used contained different trace impurities due to variations in the composition of the raw materials used to make the glasses. Since no chemical testing of the glass aggregates was undertaken during the course of this research it not is possible to say whether the presence of chemicals in the glass (and their exposure as a result of the crushing process) was significant or not.

For the concrete mixes containing upto 25% replacement of sand by washed glass the mean linear expansion (after 365 days) ranged between 0.05% (green) and 0.08% (mixed). According to BRE 330 (2004) the foregoing aggregate combinations would be classified as being in the lower half of the expansion range (after 12 months curing) defined as "Probably non-expansive". This classification is very similar to that for the conventional concrete used and it corresponds to a combination of aggregates that "have rarely been associated with actual cases of damages". Hence it is proposed that upto 25% of conventional fine aggregate may be replaced by washed waste glass which originates from bottles which were used to hold drinks without causing detrimental expansion of the concrete. A similar conclusion was reacted by Chi (2006) and Topcu *et al.* (2008) and is supported by the results from Dhir *et al.* (2013).

If more than 50% of the conventional aggregate is replaced by glass then the aggregate combination becomes "possibly reactive".

Table 5.7 Previous findings relating to expansion due to use of waste glass as fine aggregate in concrete

Finding	Researchers
1. Concrete containing glass as fine aggregate has greater expansion than concrete containing only natural sand as fine aggregate - as found in this study.	Taha and Nounu (2008), Park and Lee (2004), Topcu *et al*. (2008), Lam *et al*. (2007), Pike *et al*. (1960), Kou and Poon (2009), Bignozzi and Sandrolini (2004), Park *et al*. (2004), Limbachiya (2009) and Dhir *et al.* (2003)
2. Use of glass as fine aggregate reduces concrete expansion.	Schwarz *et al*. (2008), Shao *et al*. (2000)
3. 50% waste glass sand replacement in concrete has less that 0.1% expansion at 28 days - as found in this study.	Taha and Nounu (2008), Lam *et al*. (2007), Shayan and Xu (2004).
4. 100% waste glass sand replacement in concrete has less that 0.1% expansion at 28 days - as found in this study.	Taha and Nounu (2008), Lam *et al*. (2007), Shayan and Xu (2004)
5. 50% waste glass sand replacement in concrete has less that 0.2% expansion at 365 days - as found in this study.	Taha and Nounu (2008) and Lam *et al*. (2007)
6. 100% waste glass sand replacement in concrete has less that 0.2% expansion at 365 days - as found in this study.	Park and Lee (2004), Topcu *et al*. (2008), Topcu and Canbaz (2004), Shayan and Xu (2004)

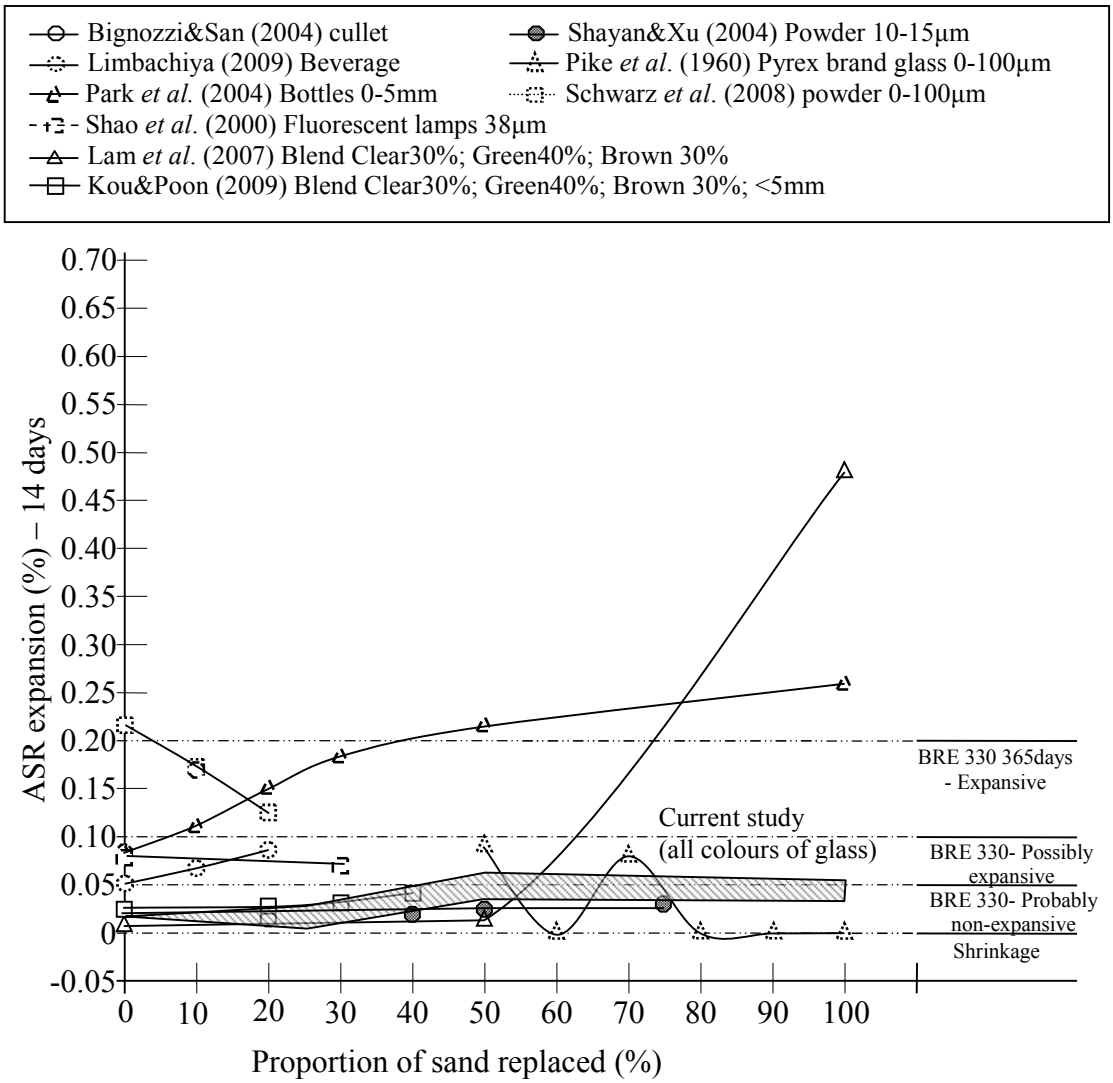

Fig. 5.18 ASR expansion after 14 days curing

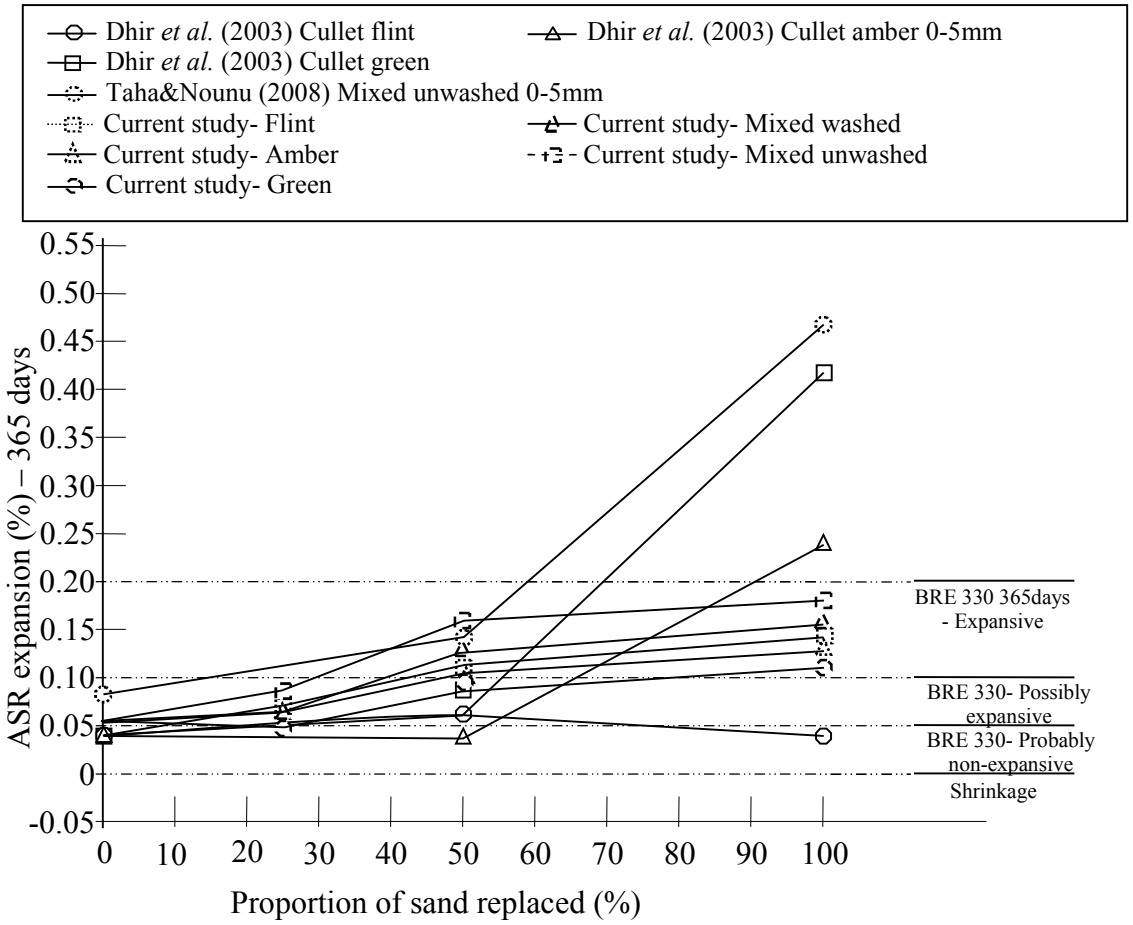

Fig. 5.19 ASR expansion of 365 days other researchers' glass replacement aggregate

Stanton (1941) demonstrated that the effect of alkali-aggregate reaction was to create an internal volumetric expansion within concrete. If this expansion can be accommodated within the pore spaces between aggregates then the reaction will not have a detrimental effect on the concrete (Meyer and Baxter (1998), Suwito (1998)). If the volumetric expansion cannot be accommodated internally then stresses will be induced due to the expansion of the concrete and its strength will be affected detrimentally (Bazant *et al*., 2000). Hence in this research project reported herein the volume change of concrete cubes as they cured was monitored directly as reported in Section 4.2.3. This monitoring showed that concrete specimens did not expand isotropically either after any particular curing time or consistently with curing duration. - Figure 4.41. These observations explained the erratic behaviour (in terms of linear expansion as time as shown in Figure 4.37) of specimens tested in accordance with BS 812-123. Furthermore the volumetric expansion data (shown in

Figure 5.20) confirmed the trends relating to linear expansion which were reported earlier, i.e.

- expansion increased as the amount of glass used as time aggregate increased,
- green glass generally produced the least expansion (although the difference between all glasses was small).

However, the data in Figure 5.20 demonstrated clearly that for washed waste glass, up to 25% of fine aggregate within the conventional concrete could be replaced by any single colour of glass without any significant change in the volumetric expansion of the concrete. Furthermore the replacement of 25% of sand by clean crushed green glass actually reduced the expansion of the concrete. The limited amount of directly comparable data which are available, i.e. from Liu (2011), also show that a small amount of glass may be used as fine aggregate without any influence on the expansion of a concrete during curing.

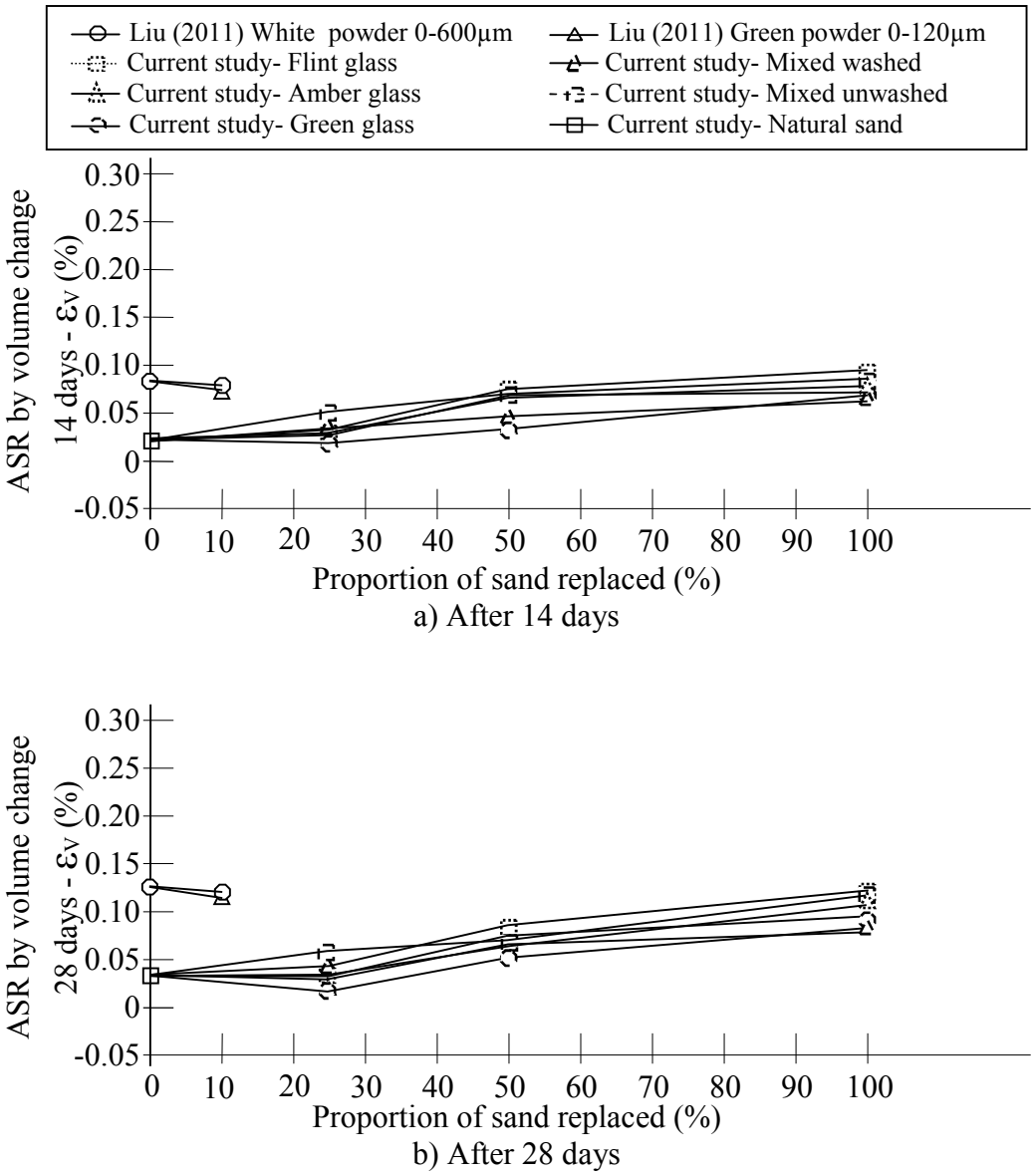

Fig. 5.20 Measured volumetric strain of concretes

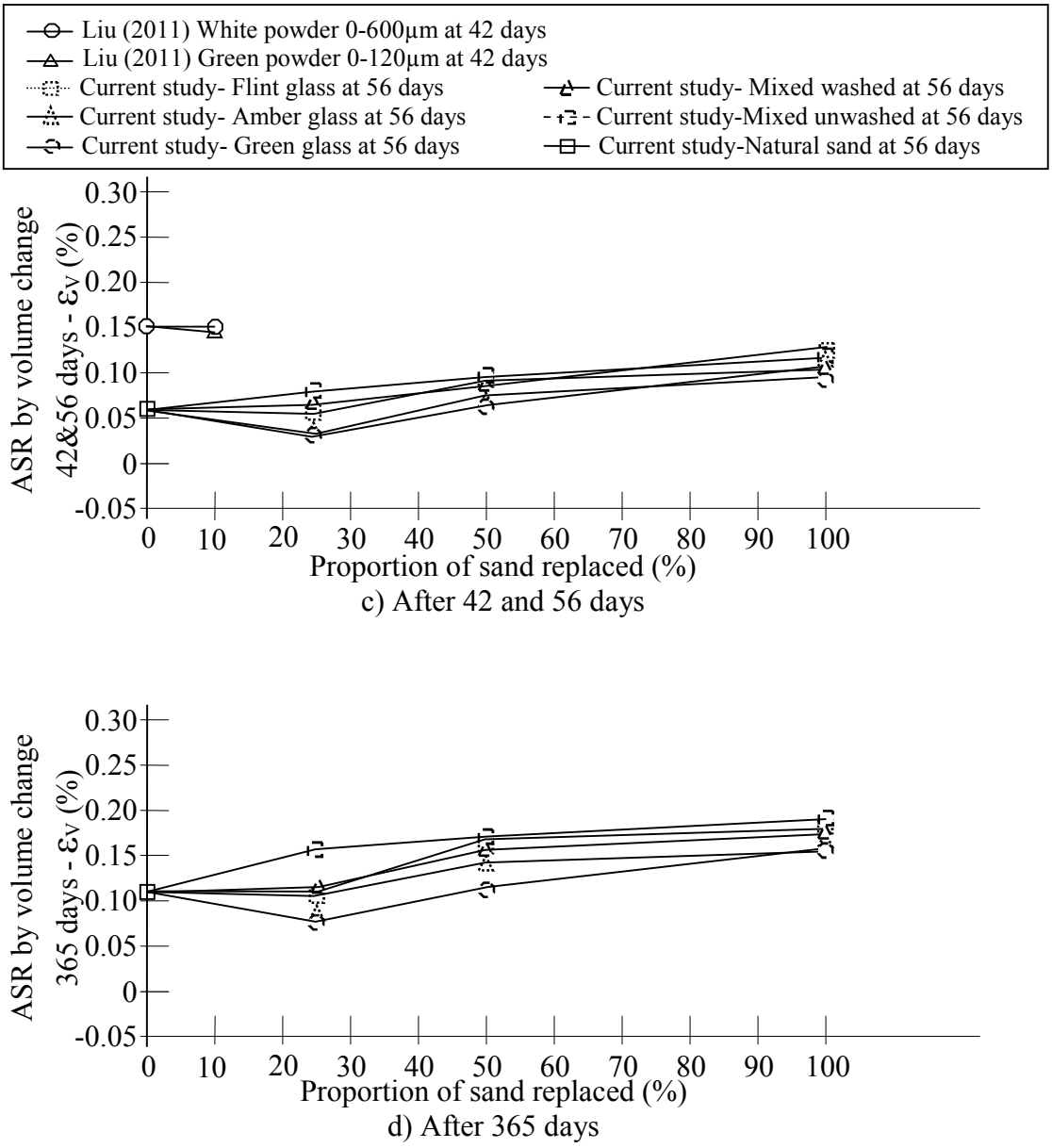

Fig. 5.20 (Cont'd) Measured volumetric strain of concretes

Using the correlation between volumetric strain of cubes (presented herein) and linear strain of prisms (determined according to BS 812 - 123) which was established in Section 4.2.3, i.e. equation 4.6, the data summarised in Figure 5.21 have been compared to the guidance given in BRE 330 (2004) regarding expansiveness of aggregate combination. The outcome of the foregoing comparison is presented in Figure 5.21. This figure demonstrates clearly the feasibility of replacing 25% of the fine aggregate within the concrete mix which was used as a standard in this research project with single colour glass crushed to give the appropriate grading. Figure 5.21

also shown that replacement of more than 25% of the conventional fine aggregate with glass gave concrete mixes which lay in the 'grey area' between being "non-expansive" and being "possibly expansive".

% of fine aggregate which is glass	Glass colour	Expansion category for the aggregate combination		
		Non-expansive (<0.05%)	Probably non-expansive (0.05-0.1%)	Possibly expansive (0.1-0.2%)
0	N/A			
25	Green			
	Amber			
	Flint			
	Mixed			
50	Green			
	Amber			
	Flint			
	Mixed			
100	Green			
	Amber			
	Flint			
	Mixed			

Fig. 5.21 Categorisation of expansion potential of aggregate combinations

5.2.4. Compressive strength

The data relating to compressive strength of the various concrete mixes were presented in Section 4.2.4. The strength data (for 28 days curing) are summarised in Figure 5.22 which also contains the findings of previous investigation into the effect on compressive strength of replacing fine aggregate by crushed glass. To account for the different concretes represented in Figure 5.22 each data set has been normalised (with respect to the strength of the corresponding conventional concrete) and the results are presented in Figure 5.23.

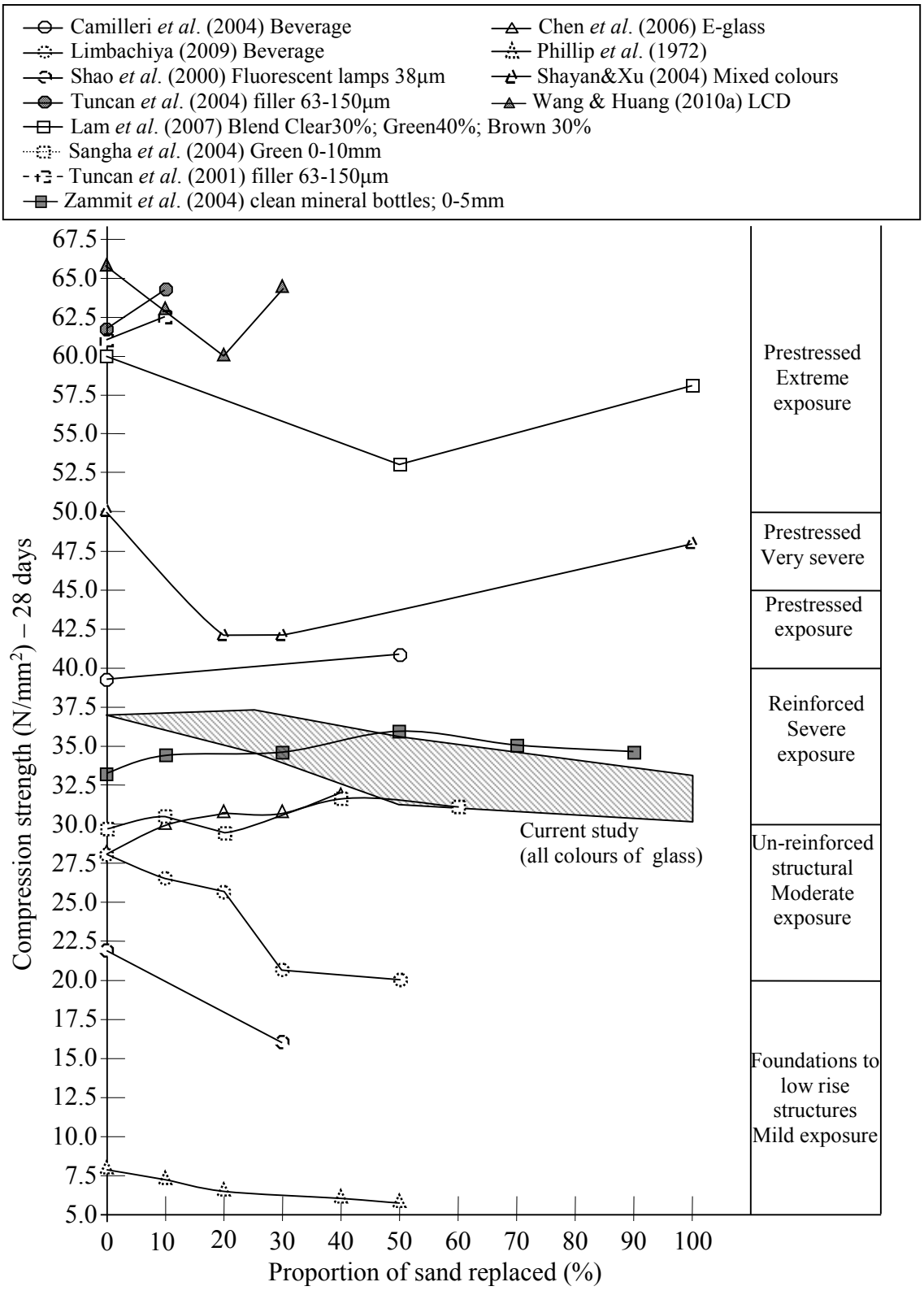

Fig. 5.22 Compression strength of 28days other researchers' glass replacement aggregate

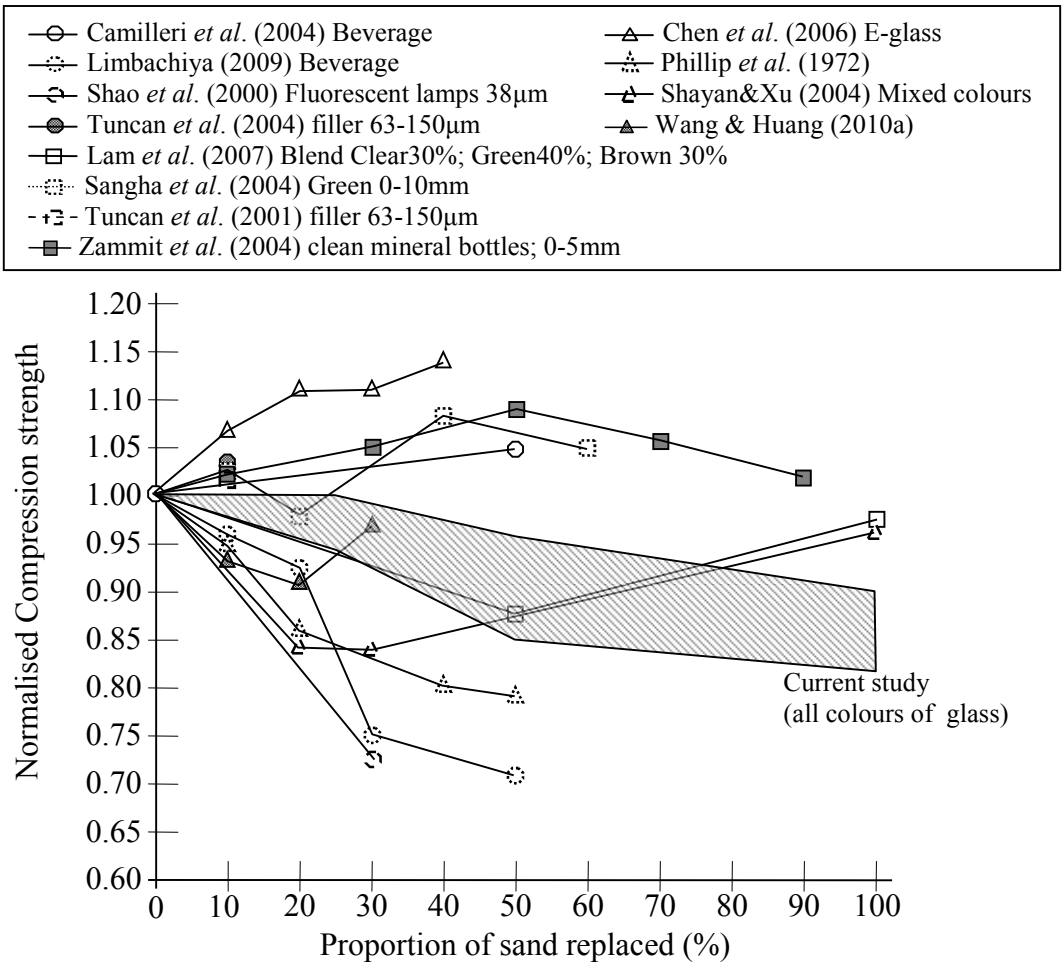

Fig. 5.23 Normalised Compression strength values for concrete containing fine glass aggregate

Examination of the results presented in Section 4.2.4 led to the following observations:-

a) The replacement of conventional fine aggregate (sand) by crushed glass causes some reduction in compressive strength of the concrete mix. The greater the amount of fine aggregate which originates from waste glass the greater is the reduction in strength.

b) For practical purposes up to 25% of the fine aggregate may be crushed glass before the reduction in compressive strength is significant, i.e. it is less than 10%. Overall, green glass gave the best performance and unwashed mixed glass gave the worst, e.g. after 1 year of curing complete replacement of sand by green glass resulted in a compressive strength of 91% of conventional concrete whilst complete replacement by unwashed glass gave a strength of 84% of the control mix.

c) The aforementioned reduction in strength was unlikely to be due to the small volume changes which occurred as the concrete cured and probably resulted from a reduction of the 'effectiveness' of the bond between cement paste and glass aggregate, due to air pockets trapped in sharp-sided 'crevices' in the surface of glass particles. This views is supported by the data in Figure 5.24 which shows effect of Percentage Concavity of the fine aggregate. The higher Percentage Concavity of crushed glass is associated with a decrease in strength of 3.78 to 5.1 N/mm^2. The presence of voids content in concrete reduces the compressive strength significantly; 5% of voids content can lower compressive strength by as much as 30%, and even 2% voids content can result in a drop of compressive strength of more than 10% (Neville, 1995). Concrete voids content increases as aggregate angularity increases.

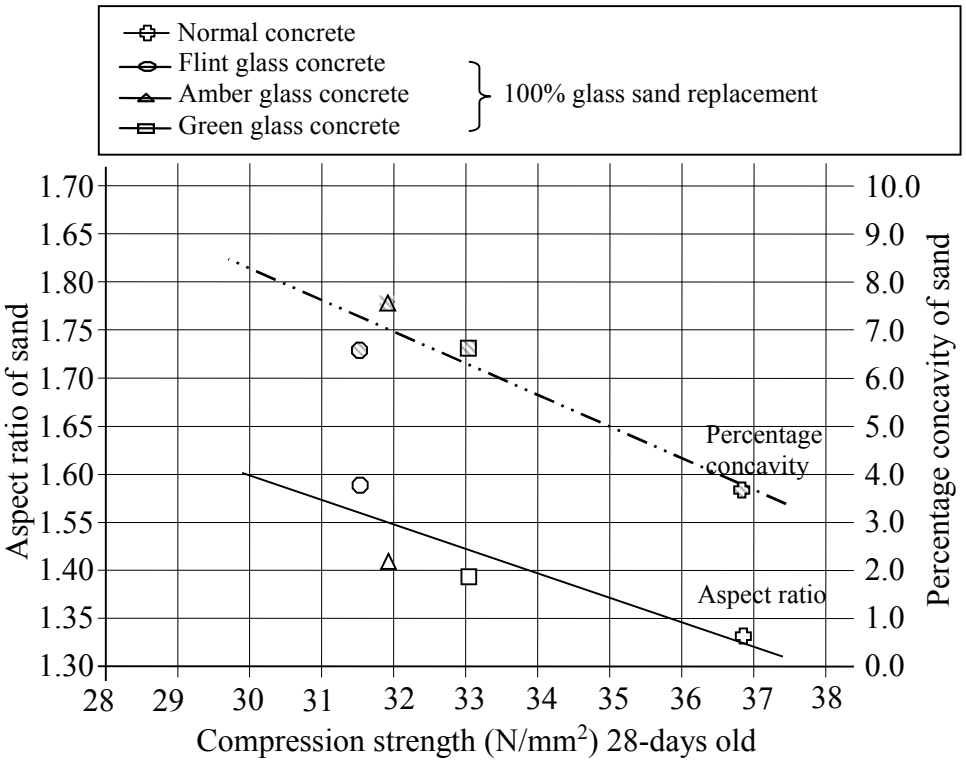

Fig. 5.24 Effect of Aspect Ratio and Percentage Concavity of fine aggregate on 28-days strength

In Figure 5.25 the mean compressive strength of each concrete mix has been plotted against the mix's mean Ultrasonic Pulse Velocity.

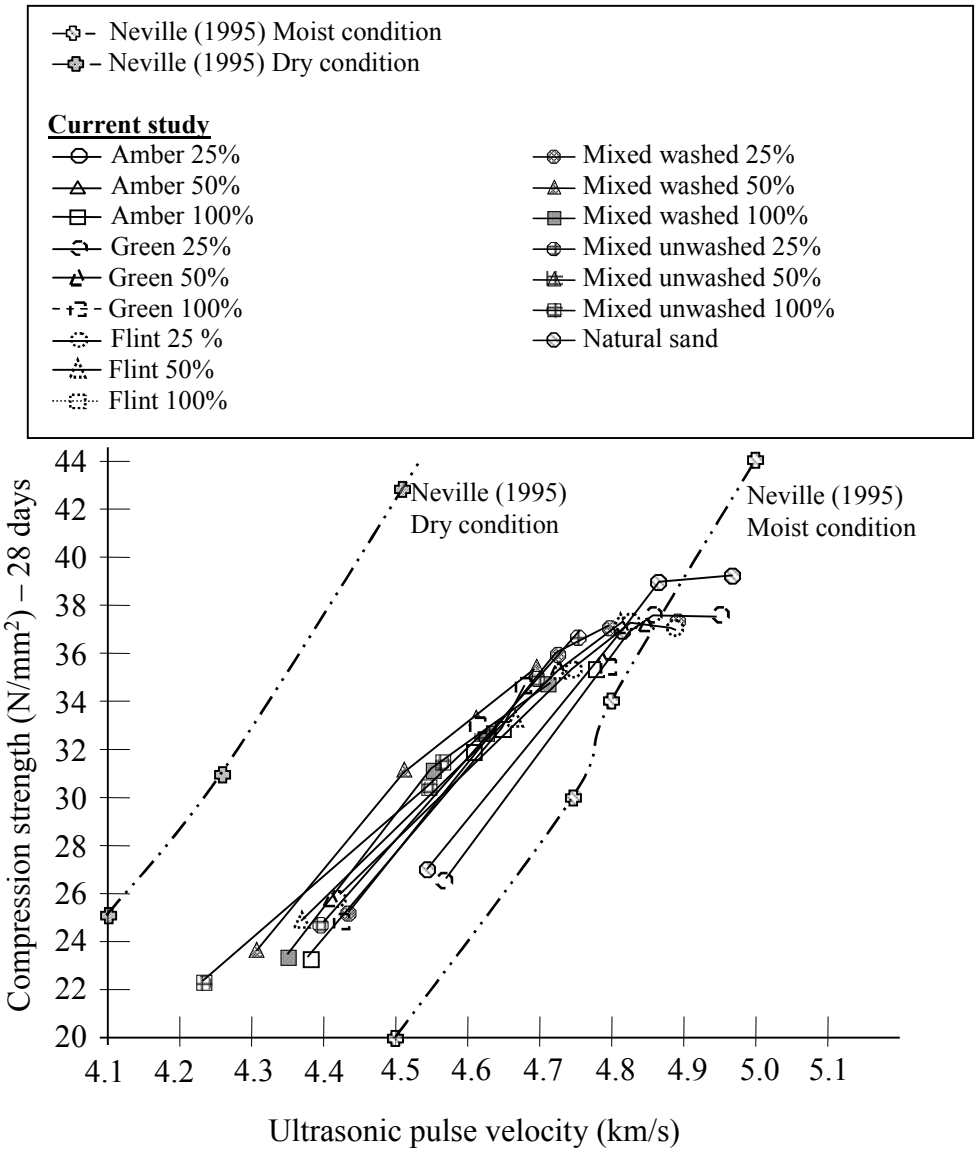

Fig. 5.25 Relationship of compression strength and UPV glass replacement aggregate

The relevant findings from previous investigations are summarised in Table 5.8.

Table 5.8 Findings relating to compressive strength and waste glass fine aggregate from previous investigations

Finding	Researchers
The compressive strength of a concrete decreased as the amount of fine aggregate which was glass increased - as found in this study.	Lam *et al*. (2007), Limbachiya (2009), Park & Lee (2004), Park *et al*. (2004), Phillips *et al*. (1972), Shao *et al*. (2000), Shayan & Xu (2004), Shayan & Xu (2006), Tan & Du (2013), Topcu&Canbaz (2004), Ali & Al-Tersawy (2012), Cassar and Camilleri (2012)
Replacement of normal fine aggregate by glass increased the compressive strength of a concrete.	Camilleri *et al*. (2004), Chen *et al*. (2006), Sangha *et al*. (2004), Tuncan *et al*. (2001), Tuncan *et al*. (2004), Wang & Huang (2010) and Zammit *et al*. (2004)
Replacement of 25% of the normal fine aggregate by glass only changed the strength by ± 10% - as found in this study.	Lam *et al*. (2007), Limbachiya (2009), Park & Lee (2004), Park *et al*. (2004), Chen *et al*. (2006), Sangha *et al*. (2004), Tuncan *et al*. (2001), Tuncan *et al*. (2004), Wang & Huang (2010), Camilleri *et al*. (2004), Sangha *et al*. (2004), Zammit *et al*. (2004), Tan and Du (2013)

With regard to the reduction in compressive strength of concrete containing glass fine aggregate it can be seen that numerous other researchers have observed the same trend. On the other hand some researchers have reported that the use of glass as fine aggregate has caused an increase in compressive strength. However, with regard to these latter investigations: Tuncan *et al*. (2001, 2004) used a glass which only had about 60% of the usual silica content of common waste glass and the sand which was replaced, some of the glass used by Chen *et al*. (2006) and Camilleri *et al*. (2004) was so fine as to be pozzolanic (and it replaced unreactive sand), Sangha *et al*. (2004) just used green glass which previous research has shown to be able to reduce volumetric expansion, Wang and Huang (2010) incorporated fly ash and super-plasticizer in their mixes containing glass and the glass particles were finer than the sand they replaced.

Figure 5.26 shows the effect of using glass as fine aggregate on the long- term strength of concrete. The shape of the relationship between strength and percentage of aggregate replaced by glass is the same as that for the 28-day strength as indicated by

the 'Age factors' given in Table 4.16 of Section 4.2.4. This confirms the proposal made earlier that the presence of washed glass particles which lie within the grading for fine aggregate does not affect the rate of hardening of the cement paste. The results of Limbachiya (2009) for long-term strength also mirror the trend for 28-day strength as shown in Figure 5.23. The data of Chen *et al.* (2006) show that after 365 days curing the increase in strength generated by the incorporation of glass aggregate was much greater than that observed after 28 days curing (Figures 5.22, 5.23 and 5.26). This was due to the nature and fineness of the fine aggregate used by Chen *et al*. (2006) which appears to have had a pozzolanic nature.

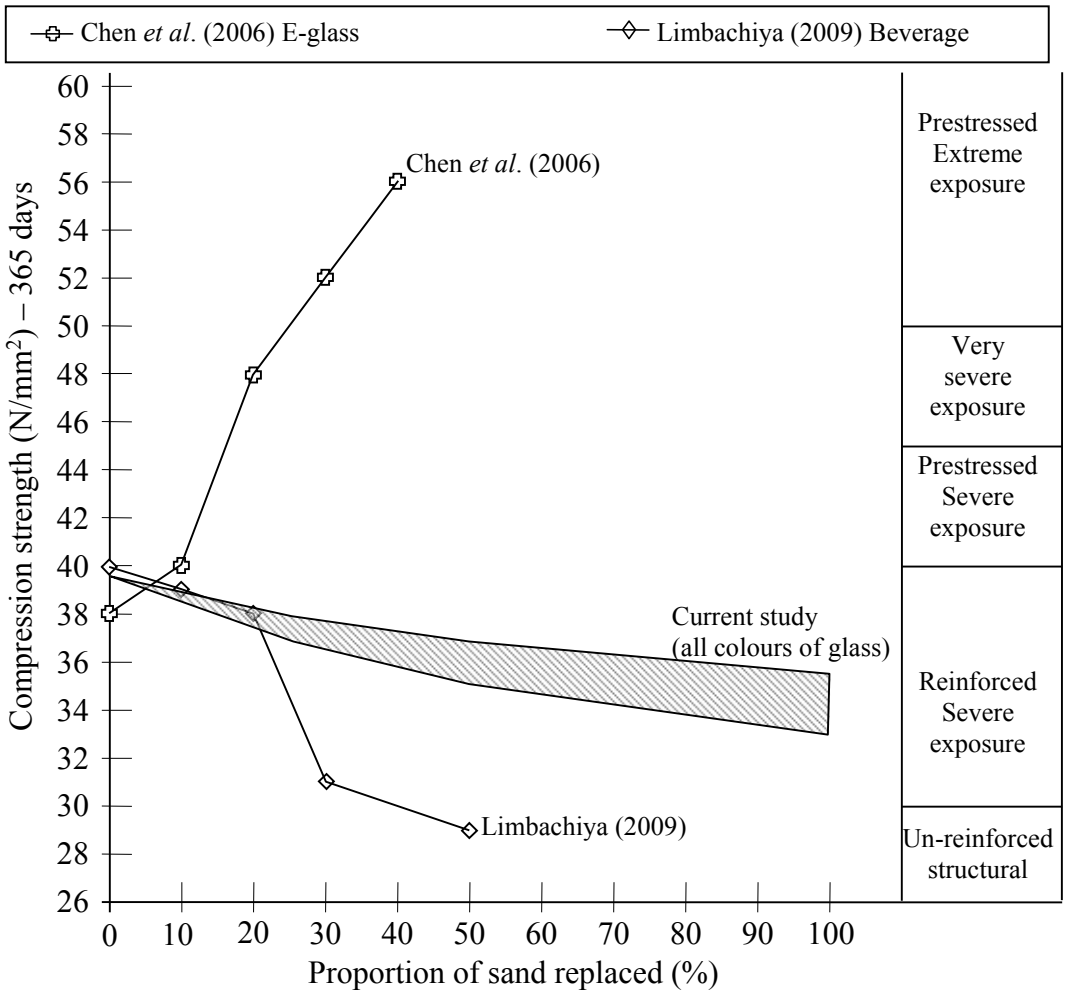

Fig. 5.26 Compression strength of 365 days other researchers' glass replacement aggregate

As the different concrete mixes hardened both their compressive strength and UPV values increased and the data are in general agreement with the trend given by Neville (1995). However it is noticeable that most of the author's data lie to the left of the relationship for conditions given by Neville (1995). In other words, for the author's mixes combining measured-UPV with Neville's relationship would have consistently underestimated the compressive strength of the cured concrete. For a particular aggregate and a given richness of the mix, the Ultrasonic Pulse Velocity of the concrete is affected by difference in the hardened cement paste, such as difference in water cement ratio, which affects the modulus of elasticity of the hardened cement paste. Consequently the strength and UPV data for the individual cubes made from conventional concrete during this research have been plotted in Figure 5.27.

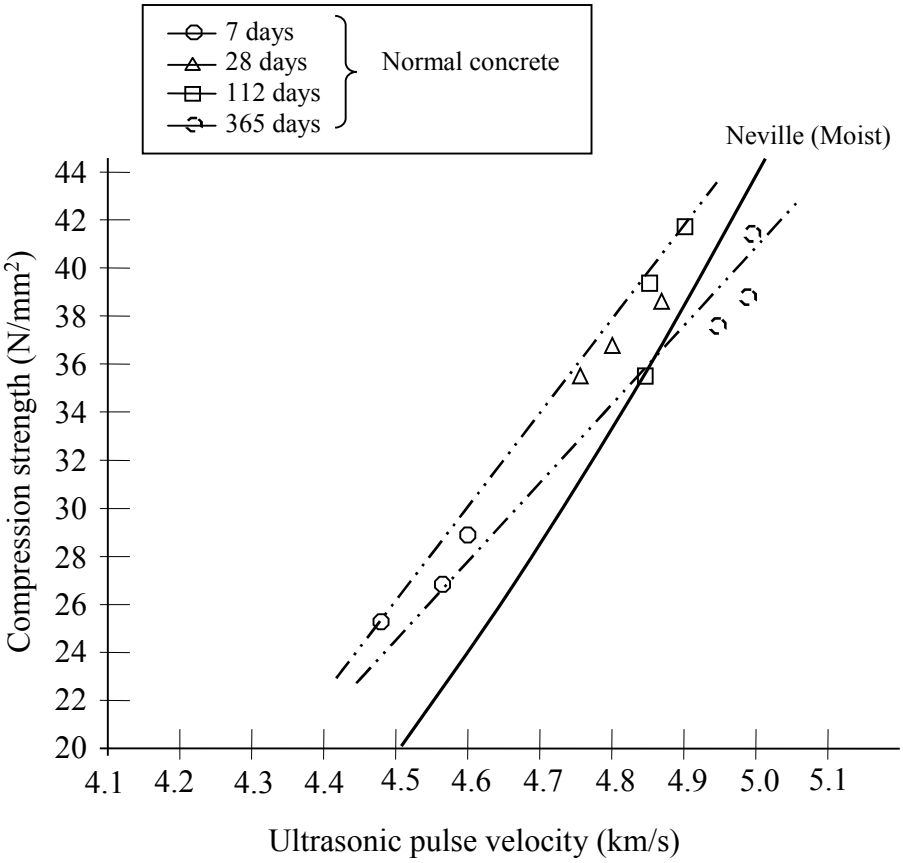

Fig. 5.27 Relationship between strength and UPV for conventional concrete

Up to 28 days all of the strength data in Figure 5.26 lie to the left of the relationship given by Neville (1995) and so this relationship would be an overconservative way of testing the integrity of the concrete by measuring UPV. It is contended that a good way to assess the integrity of the concretes containing glass made by the author is to

compare their UPV values against those measured for conventional concrete - as shown in Figure 5.28 for concrete mixes where all the sand used as fine aggregate has been replaced by crushed glass.

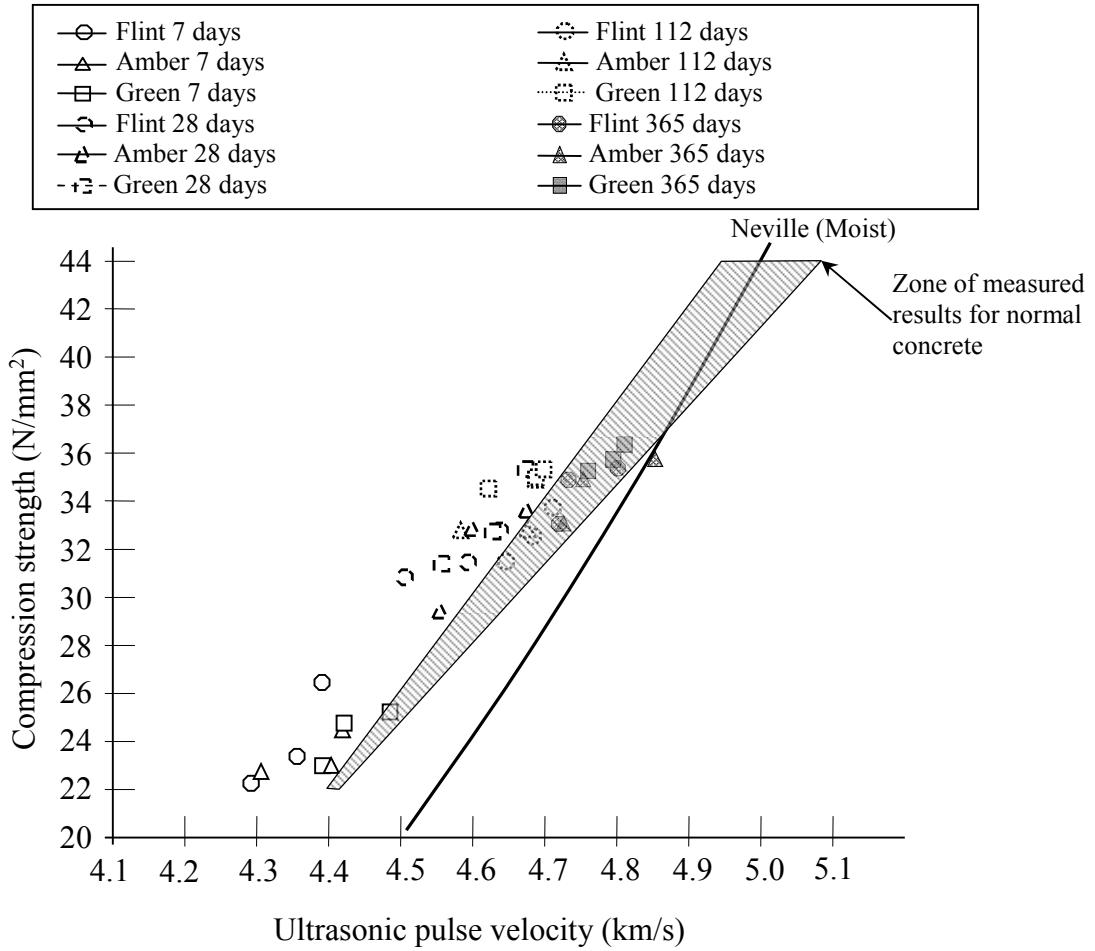

Fig. 5.28 Compressive strength and UPV data for concretes wherein all fine aggregate has been replaced by crushed glass

Once again all of the data lies to the left of the Neville (1995) relationship. The data also generally lie to the left of the proposed relationship for the author's conventional concrete - particularly for curing times up to 112 days. Thus, for a given compressive strength a concrete containing 100% glass fine aggregate will exhibit a lower UPV than the conventional concrete containing 100% sand fine aggregate. This would normally suggest that the internal structure of the 'glass concrete' will contain more pores or voids than the conventional concrete. However the measured density values (Table 5.6) do not support this view. Hence the reduced UPV values must indicate some differences in the interface between cement past and fine aggregate and it is believed that this is due to air being trapped within the angular grooves contained by

glass particles. The schematic particles shapes in Figure 4.81 and the plot of UPV value again Surface Texture Index, in Figure 5.29 support this contention.

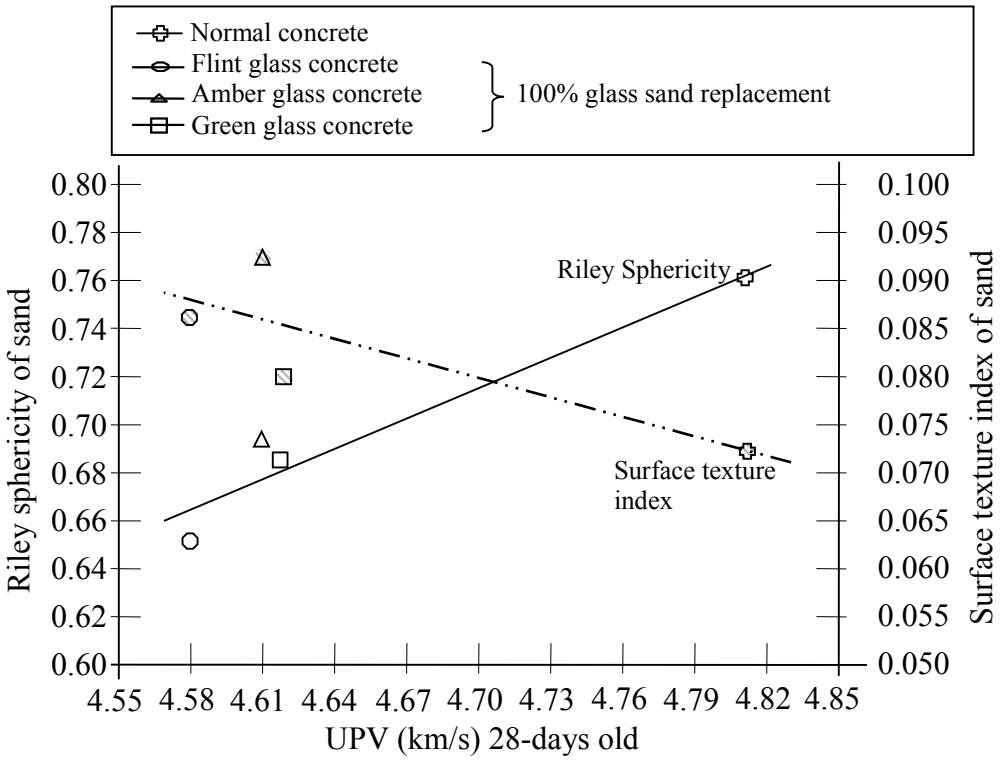

Fig. 5.29 UPV, Riley Sphericity and Surface Texture Index values for fine aggregate

After 365 days curing the 'glass concrete' data lie within the zone of results for normal concrete. So it would seem likely that the pulse transmission properties of the fine glass aggregate (which accounts for approximately 30% of the hardened concrete) are similar to those of the sand fine aggregate. Furthermore the volumetric expansion produced by the glass particles has caused compression and reduction of the volume of the trapped air 'bubbles' and hence the rise in UPV.

5.2.5 Concrete internal structure

At the start of the 'Water absorption by immersion test' a concrete specimen is subjected to a water head difference between its centre because it has been oven-dried. This head difference creates a hydraulic gradient (i), which causes water to flow into the concrete, where

$$i = \frac{\text{head difference}}{\text{water path length through the concrete}} \qquad \text{Equ. 5.1}$$

The flow velocity (v) is given by Darcy's law (because flow rates are small) i.e.

$$v = \mathrm{k}\, i \qquad \text{Equ. 5.2}$$

where k is the water permeability of the concrete. If the area through which the concrete flows is A then in time t the quality of water (Q) entering the concrete is given by

$$Q = \mathrm{A}\, v\, t = \mathrm{A}\, \mathrm{k}\, i\, t \qquad \text{Equ. 5.3}$$

To make an estimate of the quantity of water that could enter a concrete prism during an immersion test the following assumptions will be made:

1) For flow purposes, the concrete prism (which is almost cuboidal) can be represented by an equivalent sphere with a volume equal to that of the prism. This approximation is necessary because during the immersion test there will be converging flow within the prism and thus the area through which water flows cannot be simply taken as the surface area of a prismoidal block.
2) The average water head difference is the vertical distance between the free water surface and the mid-height of the sphere, i.e. 25mm + sphere radius. This assumption is made because the hydraulic gradient acting on the equivalent sphere will vary from the top to the bottom. However the variation will be linear with depth and the sphere has identical surface areas above and below its mid-height.
3) The water path length is equal to the radius of the equivalent sphere, by virtue of symmetry of flow paths within the equivalent sphere.
4) The water permeability of the concrete is 10^{-11} m/s - published literature indicates that this value is typical of the upper limit for a well-made concrete block.
5) The area through which water flows is equal to the total surface area of the equivalent sphere since the water pressure acts normally to the surface of the sphere.
6) The permeation period (t) is 7 days because this is the duration of the immersion test.

If r_e is the radius of the equivalent sphere, then

$$\frac{4}{3}\pi (r_e)^3 \equiv 100\times100\times50 \text{ mm}^3$$

$$r_e = 49.2 \text{ mm}$$

Thus; average water head = 25+49.2mm = 74.2 mm

water path length = 49.2 mm

area through which water flows = $4\pi (r_e)^2 = 30.4 \times 10^3$ mm²

and Q $= 30.4 \times 10^3 \times \left(\frac{10^3}{10^{11}}\right) \times \left(\frac{74.2}{49.2}\right) \times (7\times24\times60\times60)$ mm³

$= 277$ mm³

$\equiv$ 0.277 grams of water

But the data from actual immersion tests (Section 4.2.5, specifically Table 4.17) shows that the 7-days gain in weight of prisms made of conventional concrete was between 57 and 63 grams. Hence the amount of water that enters the concrete due to the externally-applied head is negligible and the permeation of the concrete can be considered to be entirely due to an internal hydraulic head, i.e. internal suction. This head results from surface tension effects within very fine passages within the concrete which cause capillary rise and lead to the weight gains described in Section 4.2.6 and illustrated in Figure 4.63.

For conventional concrete the average weight gain of prisms after a certain period of immersion has been plotted, in Figure 5.30, against the average weight gain in sorptivity tests over same period of time. There is clearly a linear relationship between the two weight gains over a period of 7 days which confirms the belief that the permeation in both the sorptivity and immersion tests is due to capillary rise. If the weight gains in the first 10 minutes of testing are discounted, as suggested by Neville (1995), then the data define a straight line which passes through the origin of the graph (Figure 5.30). The slope of this straight line is 0.355 and this corresponded to a ratio of 2.8 between the weight gain values for immersion and those from the sorptivity test. The ratio of the two weight gain values will depend on the relative

magnitudes of the wetted surface areas in the two tests. However, it will not simply be the direct ratio because the actual flow paths will be different, i.e. essentially parallel in the sorptivity test and convergent in the immersion test. Furthermore the concrete specimens are unlikely to be isotropic in terms of permeability.

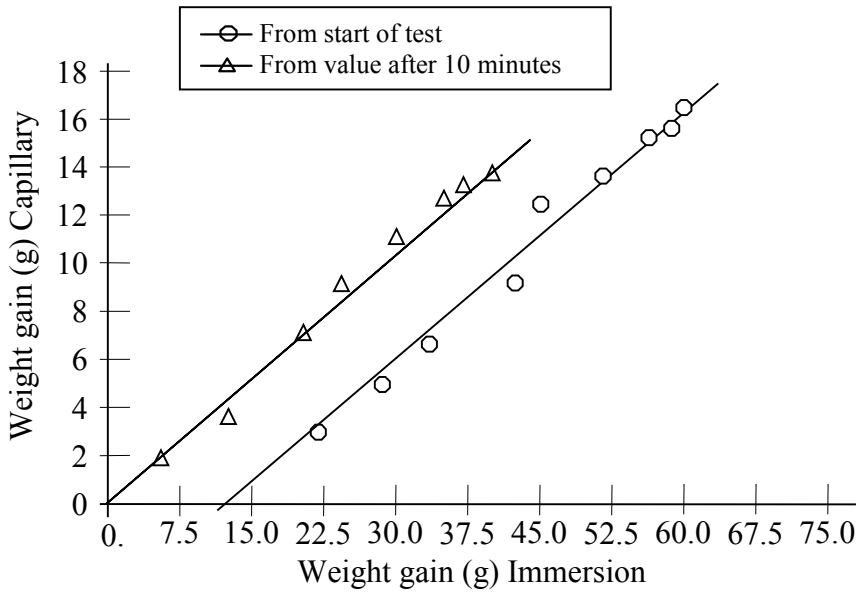

Fig. 5.30 Comparison of immersion and sorptivity test weight-gain data for conventional concrete

If the weight gains of concrete prisms containing glass are plotted (Figure 5.31) as for conventional concrete then the same trends are observed. If the data obtained during the first 10 minutes are once again discounted then the weight gain values lie on straight lines passing through the origin. For these linear the ratio of immersion and sorptivity weight gains are given in Table 5.9. The values of the ratio for concretes containing mixed glass aggregates are also included in this Table.

Table 5.9 Ratio of weight gain rates for immersion and sorptivity tests

Fine aggregate combination	Amount of replacement	$\left(\frac{\text{Weight gain - immersion}}{\text{Weight gain - capillary}}\right)$
Normal sand	0	2.8
Flint glass + sand	25%	4.0
	50%	4.1
	100%	5.2
Amber glass + sand	25%	3.9
	50%	4.1
	100%	4.2
Green glass + sand	25%	3.8
	50%	3.8
	100%	4.7
Mixed washed glass + sand	25%	3.8
	50%	4.2
	100%	4.7
Mixed unwashed glass + sand	25%	3.9
	50%	5.3
	100%	4.7

For the immersion test if flow is assumed to be primarily in the direction of maximum hydraulic gradient then the flow regime would be more-or-less parallel flow lines between the two largest faces. For this situation the ratio of weights gains between immersion and capillarity tests would be approximately four. If flow in the immersion test is taken as radially inwards through the equivalent sphere then the ratio of weight gains would be approximately six. The ratios calculated for concrete containing glass aggregate (in Table 5.9) generally fall within the foregoing range. The normal content has a ratio (2.8) which falls well outside of the normal range observed. This may reflect a reduction in water capillary absorption due to the very low absorption characteristic of the waste glass itself and the voidage due to a reduce bond strength.

The water permeation test data (particularly Figures 4.63, 5.30 and 5.31) show that after 7 days the water intake into all concrete via capillary action was essentially complete. This does not mean that after 7 days of immersion the concrete prisms were completely saturated because some air could still be tapped in voids. However,

because of the fineness of passages within the concrete (typically around 0.15×10^{-3} mm in diameter according to Ahmad *et al.* (2005)) the surface tension within the pore fluid would have meant that any air in the voids would be occluded and under high pressure. This would drastically reduce the volume of the trapped air and also cause some air to be dissolved in the pore fluid. Hence the volume of water which has entered a prism after 7 days of immersion will be used to provide an estimate of the mean porosity (volume of voids/ total volume) of each type of concrete.

The porosity values (percentage) in Table 5.10 have been derived from the weight gains contained in Tables 4.17 and 4.18. There is no significant difference between the mean porosity value for conventional concrete and the mean values for mixes containing washed glass aggregate. The values of porosity in Table 5.10 are in good agreement with data published by other researchers e.g. Shayan and Xu (2006) - 13% (normal) and 14% (with glass), Nassar and Soroushian (2012) - 14% for normal and concrete with glass aggregate.

Table 5.10 Porosities from weight gains during immersion

Mix	Percentage of glass in aggregate			
	0	25	50	100
Normal concrete	12	/	/	/
Concrete with flint glass	/	13	14	14
Concrete with amber glass	/	12	13	12
Concrete with green glass	/	13	13	13
Concrete with mixed washed glass	/	13	13	14
Concrete with mixed unwashed glass	/	13	14	15

The mean value of the Sorptivity of the conventional concrete was established as $0.149 mm/min^{0.5}$ (Table 4.20) . This value decreased, by up to 40%, as the amount of sand which was replaced by crushed glass increased. Similar values of Sorptivity have been reported by other researchers: $0.125\ mm/min^{0.5}$ and $0.094\ mm/min^{0.5}$ for normal concrete and a mix with 15% fine glass (Nassar and Soroushian, 2012), $0.135 mm/min^{0.5}$ and $0.123\ mm/min^{0.5}$ for normal concrete and a mix containing 10%

fine glass (Schwarz *et al*., 2008). All colours of washed glass exhibited similar values of Sorptivity but there was a significant reduction when unwashed glass was used. In fact for 100% sand replacement by mixed unwashed glass the Sorptivity was virtually halved. This change in Sorptivity results from the changes in the magnitude of the surface tension of the water in the voids and the effect would be particularly marked adjacent to the actual glass particles.

In the absence of contaminants in the water in the voids within the concrete the Sorptivity will be inversely related to the width of the pores through which water flows into the concrete. If all of the concrete mixes produce prisms with practically identical porosities but significantly different Sorptivities the implication is that there is a difference in the way that the voids are distributed within a hardened block. A possible explanation is that the conventional concrete contains numerous very fine voids whilst concrete containing glass contains fewer, but wider, voids. Such a difference in internal structure would account for the reduction of UPV values when normal fine aggregate is replaced by crushed glass - Section 5.2.2 and Figure 5.29. Furthermore, if the greater irregularity of the surface of the glass particles (as indicated by Percentage Concavity and Surface Texture Index values) promoted the presence of voidage adjacent to the particles (as proposed in Section 4.3) then this would also explain the reduction in compressive strength reported in Section 5.2.4. Park *et al*. (2004) previously claimed that the irregular shape of glass particles led to the entrapment of air. Nassar and Soroushian (2012) have shown that addition of milled waste glass, with a size of only 13µm, improved particle packing with filling effect and resulted in denser and hence less permeable microstructure. It could also be argued that the presence of voids next to the glass particles helped to mitigate any ASR volumetric expansion (reported in Section 5.2.3) by providing space into which the expansion products could more along the lines suggested by Suwito *et al.* (2002). As reported by Nassar and Soroushian (2012), unlike continuous pores, the presence of discontinuous pores in hydrated cement paste is not detrimental to the water absorption and thus durability of concrete. However, such as pores would results in reduced concrete strength.

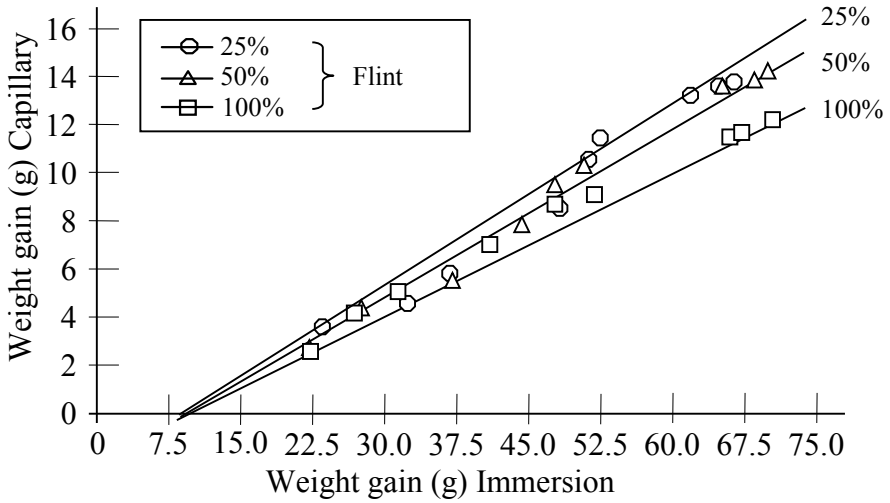

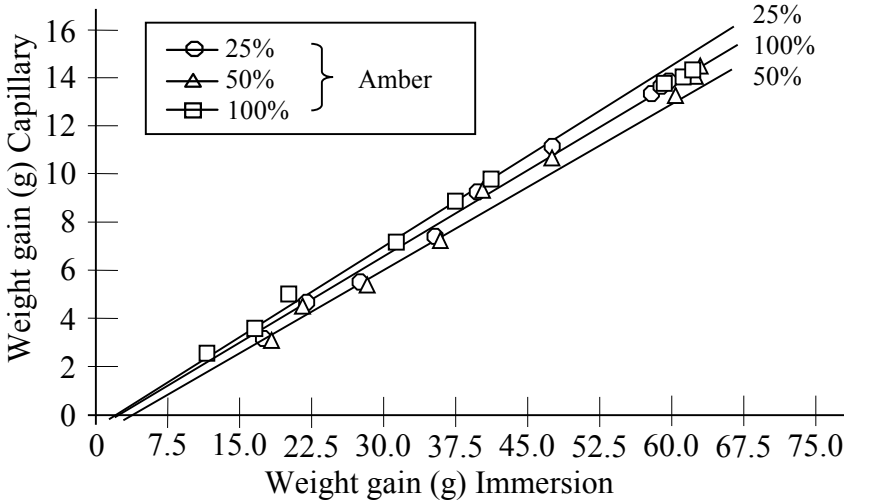

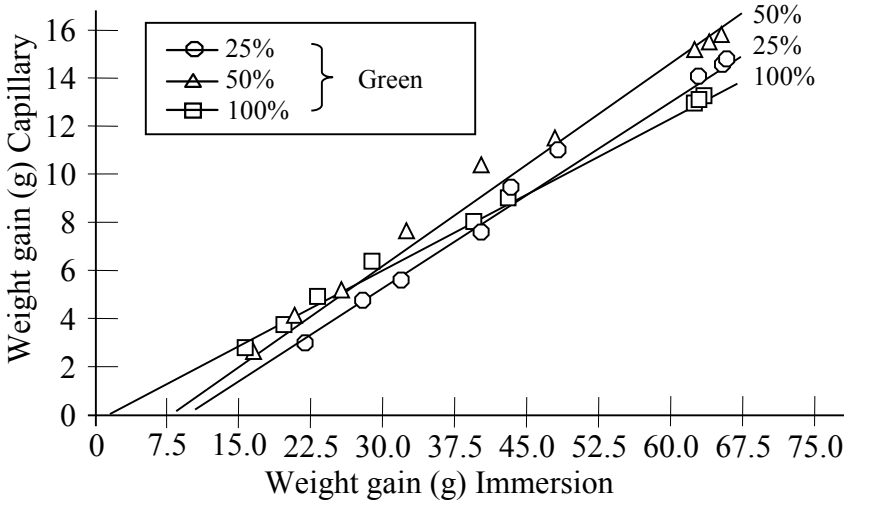

Fig. 5.31 Comparison of weight gain data for concrete containing glass

CHAPTER 6: CONCLUSIONS AND RECOMMENDATIONS FOR FURTHER WORK

6.1 Context of the research

The results presented and discussed in the foregoing chapters came from an experimental investigation of the effects, on a structural concrete, of replacing conventional fine aggregate (sand) by crushed waste glass. The glass was crushed to give a particle size distribution which was essentially the same as that of the conventional fine aggregate. Concrete mixes were produced with 25%, 50% and 100% of the sand replaced by different types of glass, i.e. flint (clear), green, amber (brown), mixed colours (washed), mixed colours (unwashed). In general the research work was focussed on the effects of glass fine aggregates the flow characteristics of fresh concrete and the engineering/ structural properties of hardened concrete and any time-related effects.

The glass particles used for most of this investigation were produced by manually crushing and sieving waste glass to produce a fine aggregate which had the same particle size distribution as the natural sand it replaced. However, this did not mean that the individual glass particles had the same shape and surface texture as the natural sand. Numerous measurements of the form of particles and statistical analysis of the distribution of particle forms within samples of fine aggregate were undertaken. The resultant data showed that there were quantifiable differences in shape and surface texture between the manually-produced glass aggregate and the sand that it replaced. There were also minor differences between the forms of different colours of glass aggregate and the laboratory-produced and commercially-supplied glass aggregates (Tables 4.26 and 4.27).

The British standard test BS EN 12620:2013 for particle size distribution only identify the proportion of sizes within a set of pre-defined range, it does not control or characterise particle shape or the distribution of particle shape in an aggregate. Therefore techniques developed was found that the crushed glass particles were more angular than the sand grains and this resulted in less fluidity as indicated by reduced slump and flow table value, which may suitable application for the low workability concrete.

Such concrete would be ideal for use in structures, precast concrete block work, and floor slab. The angularity may also have been responsible for some loss of bond between concrete paste and glass aggregate which led to a decrease in compressive strength in proportion to the amount of sand replaced by glass.

The conclusions reported in Section 6.2 and 6.3 must be viewed in the light that they relate to one specific concrete mix, i.e. components in a ratio of 1:2:4 with a water-cement ratio of 0.6. The concrete did not contain any admixtures such as plasticizes or ASR-suppressants. Furthermore there were quantifiable differences between the forms or the sand used in the conventional concrete which was used as a benchmark and the fine aggregate produced by crushing waste glass.

6.2 Characteristics of fresh concrete

The following conclusions have been drawn from the research work:

a) Slump values were decreased (Figure 4.12) by the use of fine glass aggregate and the greater the glass content the greater was the reduction. This trend had been previously reported by a number of researchers. It is believed that the sharp, angular nature of the glass particles (as quantified by aspect ratio and percentage concavity) resulted in more friction within the fresh concrete so that it had reduced fluidity. Previous researchers who had reported that the inclusion of fine glass aggregate caused an increase in slump value had not compared equivalent concrete mixes – in some cases the particle sizes of their conventional fine aggregate and glass aggregate were significantly different, in some investigations the concrete containing glass was made with a higher water content than the conventional concrete.

b) The aforementioned decrease in slump was observed for all colours of glass and it occurred regardless of whether the glass aggregate was in a washed or unwashed state (Figure 4.12). The same finding was reported by the very few researchers who had previously investigated this area and it had been suggested that a small amount of plasticiser admixture could be used to ensure that the slump was not detrimentally affected.

c) The flow table value (Figure 5.8) reduced with increasing waste glass content within the fine aggregate regardless of the colour of the glass. There is very little published data relating to this area of study. Whilst some publications have indicated that flow table value was reduced by the use of fine glass aggregate in other articles it has also been reported that inclusion of glass caused the flow value to increase. However, in these latter articles it was stated that super-plasticiser was added to the concrete mixes and this change in composition of the 'fluid' occupying the pores in the concrete skeleton could have promoted liquefaction failure of the concrete when it was subjected to shock loading (as occurs in the flow table test).

d) Notwithstanding the comments made above in items a, b and c it can be concluded that up to 25% of fine aggregate (sand) can be replaced by crushed glass before there is a significant change in the flow behaviour (quantified either as slump or flow table value) of the concrete. This finding is supported by virtually all published research relating to this topic.

e) Both initial and final setting time (Figure 4.23) were found to increase, more-or-less linearly, with the amount of conventional fine aggregate replaced by glass. The effect of not washing the glass prior to its use was to delay all setting times by a fixed amount, which was approximately 12% of the respective setting time for conventional concrete. Other researchers have previously reported the same general finding with regard to setting times of concrete containing crushed waste glass. The only previous investigation that reported a reduction of setting times due to the presence of glass aggregate had used the glass in the form of a very fine powder so that it acted as a pozzolan.

6.3 Properties of hardened concrete

The following conclusions have been drawn from the research work:

a) The bulk density of cured cubes containing glass fine aggregate was less, at all curing times, than the density of cubes made from conventional concrete. However, once account had been taken of the difference between the specific gravities of the sand and crushed glass particles and the amount of glass present in a specific concrete then the 'denseness' of cured cubes did not seem to be affected by the replacement of conventional fine aggregate. There was particularly good correspondence between measured densities and adjusted densities (values from conventional concrete amended to account for the different specific gravities of particles in the fine aggregate) for cubes after 1 year of curing. The aforementioned comparability of densities suggests that there was little difference between the internal structure of hardened conventional concrete and that made from mixes containing glass fine aggregate. Previous researches had also reported changes in the density of hardened concrete which could be accounted for by differences in the specific gravities of their sand and fine glass aggregate.

b) The Ultrasonic pulse velocity (UPV) of the hardened concrete decreased in proportion to the amount of conventional fine aggregate replaced by crushed glass for all curing times. A similar trend has been reported by other researchers who have tested concrete where the only difference between mixes was the amount of normal fine aggregate replaced by washed glass which had been crushed to the same grading curve as the sand it replaced. In one research the concrete was sliced in the direction of casting and the exposed surface was examined under a microscope. According to the researchers this examination revealed that the bonding achieved between cement paste and glass aggregate was different from the bonding with the flint aggregate that was used in the control concrete. Hence it would seem likely that the reduction in UPV values observed by the author was due to inferior bonding between the cement paste and the glass aggregate because bulk densities indicated general similarity of all concrete internal structures.

c) The use of crushed glass as fine aggregate caused a reduction in compressive strength, in comparison to the equivalent conventional concrete, at all curing times. However, all mixes exhibited very similar age factors during curing so that the proportional reduction of strength exhibited after 7 days was maintained as the concrete hardened further. Similar trends have been reported by researchers who have compared 'like-for-like' mixtures containing glass, i.e. where there has been no change in water content, fine aggregate grading, no addition of plasticiser, etc. It is believed that the observed reduction in compressive strength results from the bonding between glass aggregate and cement paste being inferior to that between sand and paste. This belief is supported by;

- the comparability of bulk densities, and hence voids contents, for mixes containing glass and only conventional fine aggregate;
- measurements of dimensional changes of cubes and prisms showed no major difference between expansion potential of the glass used in the investigation and the conventional fine aggregate;
- the reduction of UPV when glass was introduced into the concrete mix which was indicative of some barrier to transmission of the pulse within the concrete matrix;
- the significant difference between measured values of aspect ratio and percentage concavity for glass and sand particles;
- water absorption tests (immersion and capillarity) suggest that the voids in the concrete containing glass are larger and more widely-distributed than those in conventional concrete.

d) Despite the foregoing conclusion the research work indicates that up to 25% of fine aggregate could be replaced by crushed glass without any significant loss of functionality of the concrete. A similar finding has been previously reported by numerous researchers. Furthermore, it was found that if crushed washed green glass was used as the replacement material then there was essentially no difference between the performance of this mix and that of the equivalent conventional concrete. However particular attention should be paid to washing

waste glass thoroughly and removing any surface contaminants before it is used.

e) The potential presence of continuous micro-pores (between glass particles and cement paste) may be a cause for concern with regard to long-term durability of the concrete. Such passages could allow the ingress of salts or could promote damage due to freeze-thaw action. However, sorptivity measurements suggest that the depth to which moisture would penetrate by capillary action would be reduced by the use of glass aggregate. In addition, for the glasses used in this investigation there is no evidence that in the long-term Alkali Silica Reaction would cause significant or detrimental expansion.

6.4 Recommendations for further work

The research work has shown that some fine aggregate made from glass may be incorporated into a structural concrete without significant loss of functionality of the concrete. Nevertheless there was some reduction of workability and compressive strength with the reduction increasing with amount of glass present. However this loss might have been exacerbated, or even caused, by the combination of a 1:2:4 mix at a water-cement ratio of 0.6 with a glass aggregate made from bottles and which was measurably more angular (and consequently rougher) than the sand it replaced. Consequently it is proposed that further work should be undertaken as follows:

- Research the shape and surface texture of fine aggregates from other natural and waste glass sources. Then select 'pairs' of natural and glass aggregates with 'identical' particle forms for testing in various concrete mixes to compare directly their performance.

- Investigate the use of different water-cement ratios and the addition of plasticiser to concrete containing glass aggregate in order to achieve required consistency and workability.

- Conduct compression tests on concretes containing 'identical' shape forms of natural and glass aggregate to determine the effect of water-cement ratio, use of a plasticiser, amount of natural aggregate replaced by glass.

- Conduct further expansion tests using direct measurement of dimensional changes (in three dimensions) of concrete containing glass and undertake microscopic examination of sections to detect products of ASR.

- Undertake microscopic investigation of the quality of contact between fine glass particles and cement paste as a function of particle characteristics and state/ composition of the paste. (especially as affected by water-cement ratio)

REFERENCES

Ahmad, S., Azad, A. K.. and Loughlin, K. .F. (2005) A study of permeability and tortuosity of concrete, Our world in concrete and structures- 30th Conference.

Ai, S., Tang, L., Mao, Y., Pei, Y., Liu, Y. and Fang, D. (2013) Effect of aggregate distribution and shape on failure behavior of polyurethane polymer concrete under tension. Computational Materials Sciences 67, pp. 133–139.

Al-Otaibi, S. (2008) Durability of concrete incorporating GGBS activated by water-glass, Construction and Building Materials, 22(10), pp. 2059-2067.

Ali, E.E. and Al-Tersawy, S. H (2012) Recycled glass as a partial replacement for fine aggregate in self compacting concrete, Construction and Building Materials, v35, October 2012, pp. 785-791.

Bazant, Z. P., Zi, G. and Meyer, C. (2000) Fracture mechanics of ASR in concretes with waste glass particles of different sizes, Jour. eng. mechanics, 126(3),pp.226-232.

Bignozzi, M. C. and Sandrolini, F. (2004) Wastes by glass separated collection: A feasible use in cement mortar and concrete, International Conference on Sustainable Waste Management and Recycling: Glass Waste, Universita di Bologna, pp. 117-124.

Blott, S. J. and Pye, K. (2008) Particle shape: a review and new methods of characterization and classification. Sedimentology 55, pp. 31-63

Borhan, T. M. (2012) Properties of glass concrete reinforced with short basalt fibre. Materials and Design, 42, pp. 265-271

BRE (2004a) Alkali-silica reaction in concrete, detailed guidance for new construction, Digest 330 – Part 2, UK; BRE research project.

British Standards Institution (1975) BS 812-1:1975 Testing aggregates – Part 1: Methods for determination of particle size and shape, London; BSI.

British Standards Institute (1985) BS 812-105.1: Testing aggregates – Part 105.1. Methods for determination of particle shape – Flakiness index. London BSI.

British Standards Institute (1990) BS 812-105.2: Testing aggregates – Part 105.2. Methods for determination of particle shape – Elongation index of coarse aggregate. London BSI.

British Standards Institution (1989) BS 812-120:1989 Testing aggregates – Part 120: Method for testing and classifying drying shrinkage of aggregates in concrete, London; BSI.

British Standards Institution (1999) BS 812-123:1999 Testing aggregates – Part 123: Method of determination of alkali-silica reactivity - concrete prism method (incorporating corrigendum No.1), London; BSI.

British Standards Institution (1992) BS 882:1992 Specification for aggregates from natural sources for concrete, London; BSI.

British Standards Institution (1983) BS 1881-107:1983. Testing concrete – Part 107:. Method for determination of density of compacted fresh concrete, London: BSI.

British Standards Institution (2011) BS 1881-122:2011. Testing concrete – Part 122:. Method for determination of water absorption, London: BSI.

British Standards Institution (1988) BS 1881-124:1988 Testing concrete – Part 124: Methods for analysis of hardened concrete, London: BSI.

British Standards Institution (1997) BS 1881-128:1997 Testing concrete – Part 128: Methods for analysis of fresh concrete, London: BSI.

British Standards Institution (1985) BS 8110-1:1997 Structural use of concrete – Part 1: Code of practice for design and construction, London; BSI.

British Standards Institution (1985) BS 8110-2:1985 Structural use of concrete – Part 2: Code of practice for special circumstances, London; BSI.

British Standards Institution (2006) BS 8500-1:2006 Concrete - Complementary British Standard to BS EN 206-1 – Part 1: Method of specifying and guidance for the specifier, London: BSI.

British Standards Institution (2005) BS EN 196-3:2005 Methods of testing cement – Part 3: Determination of setting times and soundness, London: BSI.

British Standards Institution (2000) BS EN 933-4:2000 Tests for geometrical properties of aggregates – Part 4: Determination of particle shape. Shape index, London; BSI.

British Standards Institute (1998) BS EN 1097-3:1998: Tests for mechanical and physical properties of aggregates – Part 3: Determination of loose bulk density and voids. London BSI

British Standards Institution (2009) BS EN 12350-1:2009 Testing fresh concrete – Part 1: Sampling, London: BSI.

British Standards Institution (2009) BS EN 12350-2:2009 Testing fresh concrete – Part 2: Slump test, London: BSI.

British Standards Institution (2009) BS EN 12390-3:2009 Testing hardened concrete – Part 3: Compressive strength of test specimens, London: BSI.

British Standards Institution (2000) BS EN 12390-4:2000 Testing hardened concrete – Part 4: Compressive strength-Specification for testing machines, London: BSI.

British Standards Institution (2009) BS EN 12350-5:2009 Testing fresh concrete – Part 5: Flow table test, London: BSI.

British Standards Institution (2009) BS EN 12390-7:2009 Testing hardened concrete – Part 7: Density of hardened concrete, London: BSI.

British Standards Institution (2004) BS EN 12504-4:2004 Testing concrete – Part 4: Determination of ultrasonic pulse velocity, London: BSI.

British Standards Institution (2004) BS EN 12620:2013 Aggregates for concrete, London: BSI.

Buzzle (2010) Types of concrete, [online]. [Accessed 28 December 2010]. Available at: <http://www.buzzle.com/articles/types-of-concrete.html>.

Byars, E. A., Meyer, C., Zhu, H. (2003) Use of Waste Glass for Constructive Products: Legislative and Technical Issues, Proc., Int. Symp. on Recycling and Reuse of Waste Materials, University of Dundee

Byars, E. A., Belen, M. H. and Zhu, H. Y. (2004) Waste glass as concrete aggregate and pozzolan Laboratory and industrial projects, Concrete (London), Centre for cement and concrete, department of civil and engineering, University of Sheffield, 38(1), pp. 41-44.

Byars, E. A., Zhu, H. Y. and Morales, B. (2004a) Conglasscrete I, wrap final report, University of Sheffield.

Byars, E. A., Zhu, H. Y. and Morales, B. (2004b) Conglasscrete II, wrap final report, University of Sheffield.

Camilleri, J., Montesin, F. E. and Sammut, M. (2004) The use of waste glass and pulverized fuel asm in concrete construction, Proceedings of the international conference on sustainable waste management and recycling: glass waste, University of Malta, pp. 83-90.

Cassar, J. and Camilleri, J. (2012) Utilisation of imploded glass in structural concrete, Construction and Building Materials, 29, April 2012, pp. 299-307.

Castro, S. d and Brito, J. d (2013) Evaluation of the durability of concrete made with crushed glass aggregates, Journal of cleaner production, Vol.41, pp. 7-14

CCANZ (2011) Best practice guide for the use of recycled aggregates in new concrete, Cement and Concrete Association of New Zealand technical report. Wellington, New Zealand

Chen, C. H., Huang, R., Wu, J. K. and Yang, C. C. (2006) Waste E-glass particles used in cementitious mixtures, Cement and Concrete Research, 36(3), pp. 449-456.

Chen, S. H., Chang, C. S., Wang, H. Y. and Huang, W. L. (2011) Mixture design of high performance recycled liquid crystal glasses concrete (HPGC), Construction and Building Materials, 25(10), pp. 3886-3892.

Collins, R.J. and Bareham, P.D. (1987) Alkali silica reaction: suppression of expansion using porous aggregate. Cement and Concrete Research, 17 (1), pp. 89–96.

Concrete society (2010) Sampling and testing fresh concrete, Concrete on site, The concrete society, Surrey.

Corinaldesi, V. Gnappi, G., Moriconi, G. and Montenero, A. (2005) Reuse of ground waste glass as aggregate for mortars, Waste Management, 25(2) SPEC. ISS., pp. 197-201.

Correia, J. R., Branco, F. A. and Ferreira, J. G. (2007) Flexural behaviour of GFRP-concrete hybrid beams with interconnection slip, Composite Structures, 77(1), pp. 66-78.

Cox, E.A. (1927) A method for assigning numerical and percentage values to the degree of roundness of sand grains. Journal of Paleontology, (1), pp. 179–183.

Dhir, R. K., Dyer, T. D. and Tang, M. C (2003) Expansion due to alkali-silica reaction (ASR) of glass cullet used in concrete, Recycling and reuse of waste materials, proceedings of the international symposium, University of Dundee, pp. 751-760.

Dhir, R. K., Dyer, T. D, Tang, A., Cu, Y. J. and Wang, L. (2005) Towards maximising the use of glass cullet in concrete, Concrete technology unit, Concrete London, 39(8), University of Dundee, pp.32-34.

Din, Z. (1979) The physical chemistry of silicates (in Chinese) Chinese construction industry press, Beijing, China.

Ducman, V., Mladenovic, A. and Suput, J. S. (2002) Lightweight aggregate based on waste glass and its alkali-silica reactivity, Cement and Concrete Research, 32(2), pp. 223-226.

Dyer, T. D. and Dhir, R. K. (2001). Chemical reactions of glass cullet used as a cement component. Journal of Materials in Civil Engineering, 13(6), 412-417

Erdogan, S. T., Garboczi, E. J. and Fowler, D.W. (2007) Shape and size of microfine aggregates: X-ray microcomputed tomography vs. laser diffraction. Powder Technology, 177, pp. 53-63.

European Federation of Precast Concrete (2010) The Concrete Case - Workshop on the Management of C&D waste in the EU

Figg, J. W. (1981) Alkali aggregate reaction: Reaction between cement and artificial glass in concrete, Conference on alkali-aggregate reaction in concrete: Cape town South Africa.

HM Revenue & Customs (HMRC) (2011) A general guide to landfill tax, [online]. [Accessed 23 August 2011]. Available at: < http://customs.hmrc.gov.uk/ channelsPortalWebApp/channelsPortalWebApp.portal?_nfpb=true&_pageLabel=pag

eExcise_ShowContent&id=HMCE_CL_000509&propertyType=document&lang=_e#P143_15433>.

HM Revenue & Customs (HMRC) (2014) A general guide to landfill tax, [online]. [Accessed 17 September 2014]. Available at: < http://customs.hmrc.gov.uk/channelsPortalWebApp/channelsPortalWebApp.portal?_nfpb=true&_pageLabel=pageLibrary_ShowContent&id=HMCE_CL_000509&propertyType=document#downloadopt>.

HM Revenue & Customs (HMRC) (2011a) Aggregates levy - background, [online]. [Accessed 23 August 2011]. Available at: < http://customs.hmrc.gov.uk/channelsPortalWebApp/channelsPortalWebApp.portal?_nfpb=true&_pageLabel=pageLibrary&propertyType=document&id=HMCE_PROD_010290>.

IAEA The International Atomic Energy Agency (2002) Guidebook on non-destructive testing of concrete structure, Industrial applications and chemistry section, Austria.

ImageJ software. Freely available, Java based image processing software developed at the National Institutes of Health, USA by Wayne Rasband. (http://rsb.info.nih.gov//ij/)

Ismail, Z. Z. and Al-Hashmi, E. A. (2009) Recycling of waste glass as a partial replacement for fine aggregate in concrete, Waste Management, 29(2) pp. 655-659.

Jarque, C. M. and Bera, A. K. (1987) A test for normality of observations and regression residuals. International Statistical Review, 55, pp. 163–172.

Jin, W., Meyer, C., and Baxter, S (2000) 'Glascrete' Concrete with glass aggregate, ACI materials journal, 97(2), pp. 208-213.

Johnston, C. D. (1974) Waste glass as coarse aggregate for concrete, Journal of testing and evaluation, 2(5), pp. 344-350.

Jolicoeur, P. (1963) The multivariate generalization of the allometry equation. Biometrics, 19, pp. 497-499.

Khatik, J. M. and Wild, S. (1998) Sulphate resistance of metakaolin mortar, Cement and concrete research, 28(1), pp. 83-92.

Kou, S.C. and Poon, C. S. (2009) Properties of self-compacting concrete prepared with recycled glass aggregate, Cement and Concrete Composites, 31(2), pp. 107-113.

Kou, S.C. and Poon, C. S. (2013) A novel polymer concrete made with recycled glass aggregates, fly ash and metakaolin, Construction and Building Materials, v41, pp. 146–151.

Kowalewski, M., Dyreson, E., Marcot, J.D., Vargas, J.A., Flessa, K.W. and Hallmann, D.P. (1997) Phenetic discrimination of biometric simpletons: paleobiological implications of morphospecies in the lingulide brachiopod Glottidia. Paleobiology, 23(4), pp. 444-469 .

Krumbein, W. C. (1941) Measurement and geological significance of shape and roundness of sedimentary particles. Journal of Sedimentary Petrology, 11, pp. 64–72.

Lam, C. S., Poon, C. S. and Chan, D. (2007) Enhancing the performance of pre-cast concrete blocks by incorporating waste glass - ASR consideration, Cement and Concrete Composites, 29(8), pp. 616-625.

Landini, G. (2008) Particle8_Plus plugin in ImageJ. Available at: http://www.dentistry.bham.ac.uk/landini/software/software.html

Lees, G. (1964) A new method for determining the angularity of particles. Sedimentology, 3, pp. 2–21.

Lee, G., Poon, C.-S., Wong, Y.-L., Ling, T.-C. (2013) Effects of recycled fine glass aggregates on the properties of dry-mixed concrete blocks. Construction and Building Materials, 38, pp. 638-643

Limbachiya, M. C. (2009) Bulk engineering and durability properties of washed glass sand concrete, Construction and Building Materials, 23(2), pp. 1078-1083.

Limbachiya, M., Meddah, M. S. and Fotiadou, S. (2012) Performance of granulated foam glass concrete, Construction and Building Materials, 28(1) pp. 759-768.

Lin, K.L., Huang, W.J., Shie, J.L., Lee, T.C., Wang, K.S., Lee, C.H. (2009) The utilization of thin film transistor liquid crystal display waste glass as a pozzolanic material. Journal of Hazardous Materials. Vol. 163, pp. 916-921.

Ling, T. C. and Poon, C. S. (2012) Feasible use of recycled CRT funnel glass as heavyweight fine aggregate in barite concrete, Journal of Cleaner Production, V33, September 2012, pp. 42-49.

Liu, M. (2011) Incorporating ground glass in self-compacting concrete, Construction and Building Materials, 25(2) pp 919-925.

Malisch, W. R., Day, D. E. and Wixson, B. G. (1970) Use of domestic waste glass as aggregate in bituminous concrete, Highw Res Rec, University of Missouri-rolla. no 307, 1970, pp. 1-10.

Matos, A. and Sousa-Coutinho, J. (2012) Durability of mortar using waste glass powder as cement replacement. Construction and Building Materials, 36, pp. 205-215.

McCoy, W. J. and Caldwell, A. G. (1951) New approach to inhibiting alkali-aggregate expansion. Journal of the American concrete institute, n 47, pp. 693-706.

McLellan, G.W. and Shand, E. B. (1984) Glass engineering handbook, 3rd ed. New York: McGraw Hill

Meyer, C. and Baxter, S. (1997) Use of recycled glass for concrete masonry blocks, Columbia University final report to New York state energy research and development authority, Report no. 97-15, Albany, New York.

Meyer, C., Baxter, S. (1998) Use of recycled glass and fly ash for precast concrete. New York state energy research and development authority, Final report no 98-18, Albany, New York.

Moore, G. A. (1968) Automatic scanning and computer processes for the quantitative analysis of micrographs and equivalent subjects. In: Pictorial pattern recognition, Thompson Book Co, Washington, pp. 275-325.

Muller, U. and Rubner, K. (2006) The microstructure of concrete made with municipal waste incinerator bottom ash as an aggregate component, Cement and Concrete Research, 36(8), pp. 1434-1443.

Murdock, L. J., Brook, K. M. and Dewar, J. D. (1991) Concrete materials & practice. 6th ed. UK: Edward Arnold.

Nassar, R. U. D. and Soroushian, P. (2012) Strength and durability of recycled aggregate concrete containing milled glass as partial replacement for cement, Construction and Building Materials, V29, April 2012, pp. 368-377.

Nemes, R. and Jozsa, Z. (2006) Strength of lightweight glass aggregate concrete (Dept. of Construction Materials and Engineering Geology, Budapest Univ. of Technology and Economics), Journal of materials in civil engineering, 18(5), pp. 710-714.

Neville, A.M. (1995) Properties of concrete. 4th ed. England: Prentice Hall.

Nishikawa, T., Takatsu, M. and Daimon, M. (1995) Fracture behavior of hardened cement paste incorporating mineral additions. Cement and Concrete Research, 25(6), pp. 1218-24

Park, S. B. and Lee, B. C. (2004) Studies on expansion properties in mortar containing waste glass and fibers, Cement and Concrete Research, 34(7), pp. 1145-1152.

Park, S. B., Lee, B. C. and Kim, J. H. (2004) Studies on mechanical properties of concrete containing waste glass aggregate, Cement and Concrete Research, 34(12), pp. 2181-2189.

Pattengill, M. and Shutt, T.C (1973) Proceedings of a symposium on utilization of waste glass in secondary products, Colorado school of mines research institute, January 1973, pp 137-153

Pentland, A. (1927) A method of measuring the angularity of sands. Royal Society. Canada Proc. Trans. (Section 3), (21), pp. xciii.

Pereira-de-Oliveira, L.A., Castro-Gomes, J.P. and Santos, P.M.S (2012) The potential pozzolanic activity of glass and red-clay ceramic waste as cement mortars components, Construction and Building Materials, 31, pp. 197-203

Persson A. 1998. Image analysis of shape and size of fine aggregates. Engineering Geology, 50, pp. 177-186.

Phillips J. C. and Cahn D. S. and Keller, G. W. (1972) Refuse glass aggregate in Portland cement concrete. Proceedings, third mineral waste utilization symposium. Chicago, IL: US Bureau of Mines and IIT Research Institute, pp. 385-390.

Pike, R. G., Hubbard, D. and Newman, E. S. (1960) Binary silicate glasses in the study of alkali-aggregate reaction. Highway Research Board Bullettion, n 275, pp. 39-44.

Polley, C., Cramer, S. M. and Cruz, R. V. (1998) Potential for using waste glass in Portland cement concrete, Journal of materials in civil engineering, 10(4), pp 210-219.

Poutos, K. H., Alani, A. M., Walden, P. J. and Sangha, C. M. (2008) Relative temperature changes within concrete made with recycled glass aggregate, Construction and Building Materials, 22(4), pp. 557-565.

Press, W.H., Teukolsky, S.A., Vetterling, W.T. and Flannery, B.P. (1992) Numerical recipes in C: The art of scientific computing. Second Edition. Cambridge University Press.

Reynolds, C. E. and Steedman, J. C. and Threlfall, A. J. (2007) Reynolds's reinforced concrete designers handbook, 11th ed. London: Routledge.

Riley, N.A. (1941) Projection Sphericity. Journal of Sedimentary Petrology, 11, pp. 94–97.

Rittenhouse, G. (1943) A visual method of estimating two-dimensional sphericity. Journal of Sedimentary Petrology, 13(2), pp. 79–81.

Royston, P. 1995. A remark on AS 181: The W-test for normality. Applied Statistics 44:547-551.

Russell, R.D. and Taylor, R.E. (1937) Roundness and shape of Mississippi River sands. Journal of Geology, 45, pp. 225–267.

Sabir, B. B., Wild, S. and Bai, J. (2001) Metakaolin and calcined clays as pozzolans for concrete: a review, Cement and concrete composites, 23(6), Wales, pp 441-454.

Saccani, A. and Bignozzi, M. C. (2010) ASR expansion behavior of recycled glass fine aggregates in concrete, Cement and Concrete Research, 40(4), pp. 531-536.

Sagoe-Crentsil, K., Brown, T. and Taylor, A. (2001) Recycled glass as sand replacement in premix concrete, CSIRO building construction and engineering.

Sangha, C.M., Alani, A. M. and Walden, P. J. (2004) Relative strength of green glass cullet concrete (Department of Civil Engineering, University of Portsmouth, Lion State Building), Source: Magazine of Concrete Research, 56(5), June, 2004, pp 293-297.

Sarsby, R.W (2013) Environmental Geotechnics 2nd ed, ICE Publishing, London

Schmidt, A., Saia, W. H. F. (1963) Alkali-aggregate reaction tests on glass used for exposed aggregate wall panel work. Journal of American Concrete Institute, v60, pp1235-1236

Schwarz, N., Cam, H. and Neithalath, N. (2008) Influence of a fine glass powder on the durability characteristics of concrete and its comparison to fly ash, Cement and Concrete Composites, 30(6), pp. 486-496.

Shao, Y. X., Lefort, T., Moras, S. and Rodriguez, D. (2000) Studies on concrete containing ground waste glass, Cement and Concrete Research, 30(1), pp. 91-100.

Shapiro, S. S. and Wilk, M. B. (1965) An analysis of variance test for normality (complete samples). Biometrika, 52, pp. 591–611.

Shayan, A. and Xu, A. M. (2004) Value-added utilisation of waste glass in concrete, Cement and Concrete Research, 34(1), pp. 81-89.

Shayan, A. and Xu, A. M. (2006) Performance of glass powder as a pozzolanic material in concrete: A field trial on concrete slabs, Cement and Concrete Research, 36(3), pp. 457-468.

Shi, C. J. and Wu, Y. Z. (2005) Mixture proportioning and properties of self-consolidating lightweight concrete containing glass powder (State University of New York-Buffalo), ACI Materials Journal, 102(5), pp. 355-363.

Shi, C. J. and Zheng, K. (2007) A review on the use of waste glasses in the production of cement and concrete, Resources, Conservation and Recycling, 52(2), pp. 234-247.

Silverman, B.W. (1986) Density estimation for statistics and data analysis. Chapman and Hall.

Sneed, E.D. and Folk, R.L. (1958) Pebbles in the Lower Colorado River, Texas: a study in particle morphogenesis. Journal of Geology, 66, pp. 114–150.

Stanton, T. E. (1940) Expansion of concrete through reaction between cement and aggregate, Proceedings of the American society of civil engineers, 66(10), pp. 1781-1811.

Sukumaran, B. and Ashmawy, A.K. (2001) Quantitative characterisation of the geometry of discrete particles. Geotechnique, 51, pp. 619–627.

Suwito, A. and Jin, W. and Xi, Y. and Meyer, C. (2002) A mathematical model for the pessimum size effect of ASR in concrete. Concrete Science and Engineering (4), pp. 23-34.

Taha, B. and Nounu, G. (2008) Using lithium nitrate and pozzolanic glass powder in concrete as ASR suppressors, Cement and Concrete Composites, 30(6), pp. 497-505.

Taha, B. and Nounu, G. (2008a) Properties of concrete contains mixed colour waste recycled glass as sand and cement replacement, Construction and Building Materials, 22(5), pp. 713-720.

Tan, K. and Du, H. (2013) Use of waste glass as sand in mortar: Part I – Fresh, mechanical and durability properties. Cement and Concrete Composites, 35, pp. 109-117

Tang, M. C., Wang, L. and Dhir, R. K. (2005) Engineering and durability properties of concrete containing waste glass, Proceedings of the International Conference on Achieving Sustainability in Construction, University of Dundee, pp. 219-228.

ter Braak, C.J.F and van Dam, H. (1989) Inferring pH from diatoms: a comparison of old and new calibration methods. Hydrobiologia, 178, pp. 209-223.

Terro, M. J. (2006) Properties of concrete made with recycled crushed glass at elevated temperatures, Building and Environment, 41(5), pp. 633-639.

Tickell, F.G. (1931) The Examination of Fragmental Rocks. Stanford University Press, Stanford, pp. 129.

Topcu, I. B., Boga, A. R. and Bilir, T. (2008) Alkali-silica reactions of mortars produced by using waste glass as fine aggregate and admixtures such as fly ash and Li2CO3, Waste Management, 28(5), pp. 878-884.

Topcu, I. B. and Canbaz, M. (2004) Properties of concrete containing waste glass, Cement and Concrete Research, 34(2), pp. 267-274.

True, G. F. (2011) Development of image analysis techniques to assist evaluation of both air void structure and aggregate shape factors in concrete. Ph.D. Thesis, University of Wolverhampton

Tuan, B.L.A., Hwang, C. L., Lin, K. L., Chen, Y.Y., and Young, M.P. (2013) Development of lightweight aggregate from sewage sludge and waste glass powder for concrete, Construction and Building Materials, Vol. 47, pp. 334-339

Tuncan, M., Karasu, B. and Yalcin, M. (2001) The suitability for using glass and fly ash in portland cement concrete, Proceedings of the international offshore and polar engineering conference, Anadolu University, Vol. 4, pp. 146-152.

Tuncan, M., Karasu, B., Yalcin, M. and Tuncan, A. (2004) The effects of filler glasses on mechanical properties of concrete, Department of civil engineering, Key

engineering materials, 264-268(3), Euro Ceramics VIII, Anadolu University, pp 2169-2172.

Turanli, L., Bektas, F. and Monteiro, P. J. M. (2003) Use of ground clay brick as a pozzolanic material to reduce the alkali-silica reaction, Cement and Concrete Research, 33(10), pp. 1539-1542.

Wand, M.P. 1997. Data-based choice of histogram bin width. American Statistician 51. pp. 59-64.

Wadell, H. (1932) Volume, shape, and roundness of rock particles. Journal of Geology, 40, pp. 443–451.

Wadell, H. (1933) Sphericity and Roundness of Rock Particles. Journal of Geology. 41. pp. 310-331.

Wadell, H. (1935) - Volume, shape and roundness of quartz particles. Journal of Geology, 43, pp. 250-280.

Wang, H.Y. (2009) A study of the engineering properties of waste LCD glass applied to controlled low strength materials concrete, Construction and Building Materials, 23(6), pp. 2127-2131.

Wang, H. Y. and Chen, J. S. (2010) Mix proportions and properties of CLSC made from thin film transition liquid crystal display optical waste glass, Journal of Environmental Management, 91(3), pp. 638-645.

Wang, H. Y. and Huang, W. L. (2010) A study on the properties of fresh self-consolidating glass concrete (SCGC), Construction and Building Materials, 24(4), pp. 619-624.

Wang, H. Y. and Huang, W. L. (2010a) Durability of self-consolidating concrete using waste LCD glass, Construction and Building Materials, 24(6), pp. 1008-1013.

Wentworth, C.K. (1919) A laboratory and field study of cobble abrasion. Journal of Geology, (27), pp. 507–521.

Wrap (2011) Sustainable aggregates, [online]. [Accessed 23 August 2011]. Available at: < http://aggregain.wrap.org.uk/sustainable_2.html>.

Wrap (2013) GlassFlow 2012 Final report - Environmental compliance, recycling and sustainability solutions, Valpak Ltd , Warwickshire

Xu, G. J. Z., Watt, D. F. and Hudec, P. P. (1995) Effectiveness of mineral admixtures in reducing ASR expansion, Cement and Concrete Research, 25(6), pp. 1225-1236.

Zammit, L., Montesin, F. E. and Torpiano, A. (2004) The use of crushed glass waste as fines in concrete construction, Proceedings of the international conference on sustainable waste management and recycling: glass waste, University of Malta, pp. 125-131.

Zar, J.H. (1996) Biostatistical analysis. 3rd ed. Prentice Hall.

Zhao, H., Poon, C. S., and Ling, T. C. (2013) Utilizing recycled cathode ray tube funnel glass sand as river sand replacement in the high-density concrete. Journal of Cleaner Production, Volume 51, pp. 184-190

Zhu, H. Y. (2004) Alkali-silica reaction of glass aggregates in concrete. Proceedings of the national seminars on high value use of waste glass in concrete products. Doncaster and London.

Zhu, H. Y. and Byars, E. (2004) Post-consumer glass in concrete: Alkali-silica reaction and case studies, Proceedings of the international conference on sustainable waste management and recycling, University of Sheffield, pp.99-108.

Zingg, T. (1935) Beitrag zur schotteranalyse. Schweizer Mineralogie und Petermanns Mitteilungen, 15, pp. 39-140.

BIBLIOGRAPHY

Abukersh, S. A. (2009) High quality recycled aggregate concrete, PhD thesis, Edinburgh Napier University.

Al-Sibahy, A. and Edwards, R. (2012) Mechanical and thermal properties of novel lightweight concrete mixtures containing recycled glass and metakaolin, Construction and Building Materials, V31, June 2012 pp. 157-167.

Alvarez, J. L. and Vega, N. (1996) The use of volcanic glasses in cellular concrete Materials de Construction, no 244, p 39.

Aquino, W., Lange, D. A. and Olek, J. (2001) The influence of metakaolin and silica fume on the chemistry of alkali-silica reaction products, Cement and Concrete Composites, 23(6), pp. 485-493.

Arabani. M. (2011) Effect of glass cullet on the improvement of the dynamic behaviour of asphalt concrete, Construction and Building Materials, 25(3) pp. 1181-1185.

ASTM C 150-72 (1974) Waste glass as coarse aggregate for concrete, American Society of Testing and Materials.

ASTM C 1260 (2007) Standard test method for potential alkali reactivity of aggregates (mortar-bar method). American Society of Testing and Materials.

Bazant, Z. P. and Steffens, A. (2000) Mathematical model for kinetics of alkali-silica reaction in concrete, Cement and Concrete Research, 30(3), pp. 419-428.

Barber, J.H. (1977) Fibrous Concrete – Glass, Proceedings of the society of photo-optical instrumentation engineers, Concr Inst of Aust, Bienn Conf, 8th, Conf Pap, Brisbane, pp. 1-9.

Batalin, B. S. and Pravina, N. A. (1992) Use of waste sheet and bottle glass for making devitrified glass concrete (Permskij Politekhnicheskij Inst), Steklo i Keramika, 49(11-12), pp. 510-513.

Batayneh, M., Marie, I. and Asi, I. (2007) Use of selected waste materials in concrete mixes, Waste Management, 27(12), pp. 1870-1876.

Bernhard, F. (2004) Glass-concrete composite technology, Journal of the international association for bridge and structural engineering, Graz University of Technology, Austria, 14(2), pp. 111-117.

BRE (1991) Shrinkage of natural aggregates in concrete, Concise reviews of building technology, Digest 357 part 2, UK; BRE research project.

BRE (2004) Alkali-silica reaction in concrete, background to the guidance notes, Digest 330 part 1, UK; BRE research project.

BRE (2004b) Alkali-silica reaction in concrete, working examples, Digest 330 – Part 3, UK; BRE research project.

BRE (2004c) Alkali-silica reaction in concrete, simplified guidance for new construction using normal reactivity aggregates, Digest 330 – Part 4, UK; BRE research project.

British Standards Institution (2006) BS 8500-2:2006 Concrete - Complementary British Standard to BS EN 206-1 – Part 2: Specification for constituent materials and concrete, London: BSI.

British Standards Institution (2009) BS EN 12350-6:2009 Testing fresh concrete – Part 6: Density, London: BSI.

Brown, M. T. and Buranakan, V. (2003) Emergy indices and ratios for sustainable material cycles and recycle options, Resources, Conservation and Recycling, 38(1), pp 1-22.

CBDG Concrete Bridge Development Group (2002) Guide to testing and monitoring the durability of concrete structures, Technical Guide No. 2, Surrey

Chen, J. and Poon, C. S. (2009) Photocatalytic activity of titanium dioxide modified concrete materials, Journal of Environmental Management, 90(11) pp. 3436-3442.

Chidiac, S.E. and Mihaljevic, S. N. (2011) Performance of dry cast concrete blocks containing waste glass powder or polyethylene aggregates, Cement and Concrete Composites, 33(8), pp. 855-863.

Chu, W., Wu, L. and Karbhari, V.M. (2006) Comparative degradation of pultruded E-glass/vinylester in deionized water, alkaline solution, and concrete leachate solution, Journal of Applied Polymer Science, 99(4), University of California, pp. 1405-1414.

Dahl, P. A. (2002) Glass concrete-documentation and execution, Concrete precasting plant and technology, 68(8), pp. 18-22.

Du, H. and Tan, K. (2013) Use of waste glass as sand in mortar: Part II – Alkali–silica reaction and mitigation methods. Cement and Concrete Composites, 35, pp. 118-126.

Federico, L. M. and Chidiac, S. E. (2009) Waste glass as a supplementary cementitious material in concrete - Critical review of treatment methods, Cement and Concrete Composites, Sustainability of Civil Engineering Structures - Durability of Concrete, 31(8), pp. 606-610.

Gorreta, K. C., Burdt, M. L., Cuber, M. M., Perry, L. A., Singh, D., Wagh, A. S., Routbort, J. L. and Weber, W. J. (1999) Solid-particle erosion of Portland cement and concrete, Wear, 224(1), pp. 106-112.

Gu, H. and Zhonge, Z. (2005) Compressive behaviour of concrete cylinders reinforced by glass and polyester filaments, Materials and Design, 26(5), pp. 450-453.

Hansen, W.C. (1944) Studies relating to the mechanism by which the alkali-aggregate reaction proceeds in concrete. Journal of the American concrete Institute, 15(3), pp. 213-227.

Jain, J. J. and Neithalath, N. (2010) Chloride transport in fly ash and glass powder modified concretes - Influence of test methods on microstructure, Cement and Concrete Composites, 32(2), pp. 148-156.

Juenger, M. C. G. and Jennings, H. M. (2001) New insights into the effects of sugar on the hydration and microstructure of cement pastes, Cement and Concrete Research 32(3), pp. 393-399.

Karasik, V.L., Kuzmina, T.N., Kotkina, T.V., Shiron, A.V., Chechun, L.G., Glushchenko, T.A., Ivanova, N.D., Kosenko, V.R. and Dynkin, B.L. (1988) Corundum-silicon carbide-bearing concrete parts made using a liquid glass binder, L.I. Brezhnev Dnepropetrovsk Metallurgical Inst, Russia, 29(1-2), pp. 3-12.

Karbhari, V.M., Murphy, K and Zhang, S. (2002) Effect of concrete based alkali solutions on short-term durability of E-glass/vinylester composites, Journal of composite materials, University of California, 36(17), pp. 2101-2121.

Kim, D., Quinlan, M. and Yen, T. F. (2009) Encapsulation of lead from hazardous CRT glass wastes using biopolymer cross-linked concrete systems, Waste Management, 29(1) pp. 321-328.

King, P. and Cather, R. (1989) Civil engineer's reference book, 4th ed. Part 4 – Materials, Arup research and development, England: Elsevier Butterworth-Heinemann.

Kozlova, S., Millrath, K., Meyer, C. and Shimanovich, S. (2004) A suggested screening test for ASR in cement-bound composites containing glass aggregate based on autoclaving, Cement and Concrete Composites, 26(7), pp. 827-835.

Kralj, D. (2009) Experimental study of recycling lightweight concrete with aggregates containing expanded glass, Process Safety
and Environmental Protection, 87(4) pp. 267-273.

Kurudirek, M, Ozdemir, Y., Simsek, O. and Durak, R. (2010) Comparison of some lead and non-lead based glass systems, standard shielding concretes and commercial window glasses, Journal of Nuclear Materials, 407(2) pp. 110-115.

Laobi, K., EI-Salakawy, E. and Benmokrane, B. (2006) Creep and durability of sand-coated glass FRP bars in concrete elements under freeze/thaw cycling and sustained loads, Cement and Concrete Composites, 28(10), pp. 869-878.

Lee, G., Ling, T. C., Wong, Y. L. and Poon, C. S. (2011) Effects of crushed glass cullet sizes, casting methods and pozzolanic materials on ASR of concrete blocks, Construction and Building Materials, 25(5) pp. 2611-2618.

Liles, K.J. and Yyrrell, M. E. (1976) Lightweight structural concrete aggregate from municipal waste glass, Tuscaloosa Metallurgy research laboratory, Alabama, pp. 220-222.

Ling, T. C., Poon, C. S, and Kou, S. C. (2012) Influence of recycled glass content and curing conditions on the properties of selfcompacting concrete after exposure to elevated temperatures, cement and Concrete Composites, 34(2), pp. 265-272.

Lippiatt, B. C., and Ahmad, S. (2004) Measuring the life-cycle environmental and economic performance of concrete: the bees approach, Building and fire research laboratory, national institute of standards and technology, American concrete institute international, USA, pp. 213-230.

Liu, L. H., Hashida, T., Teramura, S. and Karino, K. (2003) Development of a method for CO2 solidification of glass and concrete waste composites, Nippon Seramikkusu Kyokai Gakujutsu Ronbunshi/Journal of the Ceramic Society of Japan, 111(1293), pp. 357-361.

Meyer, C., Baxter, S, and Jin, W. (1997) Alkali silica reaction in concrete with waste glass a aggregate, Proceedings of the materials engineering conference, Columbia University, New York

Meyer, C. (2001) Recycled Glass - From Waste Material to Valuable Resource, Int symposium on recycling and reuse of glass cullet, University of Dundee, Scotland

Mindess, S., Young, J. F. and Darwing, D. (2003) Concrete. 2nd ed. USA: Prentice Hall.

Mladenovic, A., Suput, J. S., Ducman, V., and Skapin, A. S. (2004) Alkali-silica reactivity of some frequently used lightweight aggregates, Cement and concrete research, 34(10) Slovenia.pp 1809-1816.

Morrison, C. (2004) Reuse of CRT glass as aggregate in concrete (Building research establishment) Proceedings of the International conference on sustainable waste management and recycling, pp. 91-98.

Mu, B. and Meyer, C. (2002) Flexural behavior of fiber mesh-reinforced concrete with glass aggregate (Ctr. for Adv. Cement-Based Materials, Northwestern University), ACI Materials Journal, 99(5), pp. 425-434.

Newman, J. and Choo, B. S. (2003) Advanced concrete technology of constituent materials, UK: Butterworth Heinemann.

Newman, J. and Choo, B. S. (2003) Advanced concrete technology of concrete properties, UK: Butterworth Heinemann.

Neville, A.M. and Brook, J. J. (1990) Concrete technology. England: Longman Scientific & Technical.

Palomo, A., Grutzeck, M. W. and Blanco, M. T. (1999) Alkali-activated fly ashes: A cement for the future, Cement and Concrete Research, 29(8), pp. 1323-1329.

Polley, C. (1996) The effects of waste glass aggregate on the strength and durability of portland cement concrete, Master of Science Thesis, University of Wisconsin.

Poon, C. S. (2007) NO removal efficiency of photocatalytic paving blocks prepared with recycled materials, Construction and Building Materials, 21(8), pp. 1746-1753

Poon, C. S. and Chan, D. (2007) Effects of contaminants on the properties of concrete paving blocks prepared with recycled concrete aggregates, Construction and Building Materials, 21(1), pp 164-175.

Rossikhina, G.S., Podkholyuzin, V.V., Doroganov, E.A., Doroganov, V.A. (2006) Corrosion resistance of refractories made from low-cement concretes for glass making (Semiluki Refractory Factory, OJSC), Source: Glass and Ceramics (English translation of Steklo i Keramika), 63(11-12), Russia, pp. 24-28

Said, A. A. M. B. (2005) The use of crushed waste glass as replacement for sand in concrete. Master of Science Thesis, University of Wolverhampton.

Soong, W. H., Raghavan, J. and Rizkalla, S. H. (2011) Fundamental mechanisms of bonding of glass fiber reinforced polymer reinforcement to concrete, Construction and Building Materials, 25(6) pp 2813-2821.

Sprygin, A. I., Khoroshavin, L.B., Ustyantsev, V. M., Purgin, A. K., Mar'evich, V. P., Yu, Filin, A., Ivanov, N. P. and Tikhomirov, A. V. (1982) Mechanism of hardening of refractory concrete composites containing water glass with CO/2 purging. Refractories, 23(1-2), pp. 30-33.

Sprygin, A.I., Khoroshavin, L.B., Perepelitsyn, V.A., Ust'yantsev, V.M., Boriskova, T.I., Tikhomorov, A.V., Yu, A. and Ivanov, N.P. (1983) Interaction of titanium-containing metals with magnesia refractory concretes using water glass, Source: Refractories (English translation of Ogneupory), 24(6), Jun 1983, pp. 300-303.

Su, N. and Chen, J. S. (2002) Engineering properties of asphalt concrete made with recycled glass, Resources, Conservation and Recycling, 35(4), pp. 259-274.

Tam, V. W. Y. and Tam, C. M. (2006) A review on the viable technology for construction waste recycling, Resources, Conservation and Recycling, 47(3), pp. 209-221.

Tang, M. S., Xu, Z. Z. and Han, S. F. (1987) Alkali reactivity of glass aggregate, Nanjing Inst of Chemical Technology, Nanjing, China, Durability of building materials, 4(4), pp. 377-385.

The Institution of Structural Engineers (1992) Structural effects of alkali-silica reaction, Technical guidance on the appraisal of existing structures, London; IStructE.

Wrap (2006) Colourite project - maximising cullet additions in the glass container industry, glass technology services final report, Sheffield.

Wrap (2006a) The ICE demolition protocol for the Wembley stadium access corridor [online]. [Accessed on 12 February 2006]. Available from: <http://www.wrap.org.uk/ downloads/WRAP_Case_Study_SAC_formatted_050307.a4024871.4649.pdf> [Accessed on 12 February 2006].

Zhu, H. Y. and Byars, E. (2005) Potential for use of waste glass in concrete, Department of civil engineering, University of Sheffield, concrete London, 39(2) pp.41-45.

Table A4.12 Volumetric strains of cubes containing amber and green glass

Waste glass content in concrete (%)	Cube expansion as volumetric strain ε_v (%)					
	14 days	28 days	56 days	112 days	252 days	365 days
Natural sand						
Cube 1	0.0321	0.0412	0.0519	0.0652	0.0826	0.1062
Cube 2	0.0308	0.0423	0.0553	0.0682	0.0878	0.1188
Cube 3	0.0328	0.0400	0.0481	0.0609	0.0787	0.0931
Mean	0.0319	0.0412	0.0518	0.0648	0.0830	0.1060
Amber 25%						
Cube 1	0.0288	0.0355	0.0451	0.0572	0.0727	0.0935
Cube 2	0.0248	0.0332	0.0391	0.0481	0.0632	0.0831
Cube 3	0.0218	0.0253	0.0304	0.0385	0.0495	0.0619
Mean	0.0251	0.0314	0.0382	0.0480	0.0618	0.0795
Amber 50%						
Cube 1	0.0478	0.0622	0.0785	0.0984	0.1232	0.1557
Cube 2	0.0458	0.0589	0.0791	0.0898	0.1147	0.1346
Cube 3	0.0442	0.0587	0.0715	0.0952	0.1320	0.1563
Mean	0.0460	0.0599	0.0764	0.0945	0.1233	0.1489
Amber 100%						
Cube 1	0.0992	0.1170	0.1368	0.1619	0.1896	0.2072
Cube 2	0.0658	0.0777	0.0840	0.0915	0.1106	0.1313
Cube 3	0.1013	0.1192	0.1337	0.1564	0.1898	0.2194
Mean	0.0888	0.1046	0.1181	0.1366	0.1634	0.1860
Green 25%						
Cube 1	0.0167	0.0215	0.0271	0.0347	0.0440	0.0579
Cube 2	0.0218	0.0294	0.0390	0.0482	0.0617	0.0794
Cube 3	0.0265	0.0340	0.0409	0.0519	0.0668	0.0813
Mean	0.0217	0.0283	0.0356	0.0449	0.0575	0.0729
Green 50%						
Cube 1	0.0458	0.0588	0.0744	0.0930	0.1179	0.1462
Cube 2	0.0381	0.0484	0.0572	0.0716	0.0940	0.1225
Cube 3	0.0352	0.0450	0.0551	0.0703	0.0902	0.1030
Mean	0.0397	0.0507	0.0622	0.0783	0.1007	0.1239
Green 100%						
Cube 1	0.0706	0.0882	0.0977	0.1202	0.1524	0.1868
Cube 2	0.0892	0.0969	0.1056	0.1225	0.1343	0.1480
Cube 3	0.0679	0.0791	0.0952	0.1062	0.1373	0.1624
Mean	0.0759	0.0880	0.0995	0.1163	0.1414	0.1658

Table A4.13 Volumetric strains of cubes containing flint and mixed glass

Waste glass content in concrete (%)	Cube expansion as volumetric strain ε_v (%)					
	14 days	28 days	56 days	112 days	252 days	365 days
Flint 25%						
Cube 1	0.0325	0.0418	0.0526	0.0660	0.0836	0.1073
Cube 2	0.0303	0.0421	0.0499	0.0614	0.0784	0.1059
Cube 3	0.0319	0.0399	0.0500	0.0614	0.0767	0.0933
Mean	0.0316	0.0413	0.0508	0.0629	0.0796	0.1022
Flint 50%						
Cube 1	0.0713	0.0773	0.0906	0.1133	0.1379	0.1674
Cube 2	0.0683	0.0752	0.0846	0.1045	0.1186	0.1306
Cube 3	0.0725	0.0883	0.1062	0.1225	0.1574	0.1869
Mean	0.0707	0.0803	0.0938	0.1134	0.1380	0.1616
Flint 100%						
Cube 1	0.0729	0.0936	0.1078	0.1233	0.1553	0.1888
Cube 2	0.1138	0.1328	0.1441	0.1685	0.1811	0.1981
Cube 3	0.0830	0.0990	0.1192	0.1396	0.1617	0.1915
Mean	0.0899	0.1085	0.1237	0.1438	0.1660	0.1928
Mixed washed 25%						
Cube 1	0.0325	0.0424	0.0534	0.0670	0.0848	0.1089
Cube 2	0.0382	0.0492	0.0652	0.0819	0.1081	0.1474
Cube 3	0.0353	0.0444	0.0535	0.0678	0.0869	0.1092
Mean	0.0353	0.0454	0.0574	0.0722	0.0933	0.1218
Mixed washed 50%						
Cube 1	0.0492	0.0631	0.0797	0.0998	0.1265	0.1626
Cube 2	0.0483	0.0611	0.0796	0.0981	0.1259	0.1534
Cube 3	0.0500	0.0635	0.0809	0.1049	0.1364	0.1685
Mean	0.0492	0.0626	0.0801	0.1010	0.1296	0.1615
Mixed washed 100%						
Cube 1	0.0809	0.0984	0.1215	0.1517	0.1919	0.2411
Cube 2	0.0654	0.0737	0.0863	0.1033	0.1297	0.1550
Cube 3	0.0663	0.0806	0.0970	0.1150	0.1425	0.1692
Mean	0.0709	0.0842	0.1016	0.1233	0.1547	0.1884
Mixed unwashed 25%						
Cube 1	0.0558	0.0717	0.0905	0.1134	0.1437	0.1846
Cube 2	0.0508	0.0663	0.0867	0.1068	0.1369	0.1846
Cube 3	0.0443	0.0542	0.0652	0.0825	0.1067	0.1263
Mean	0.0503	0.0640	0.0808	0.1009	0.1291	0.1652
Mixed unwashed 50%						
Cube 1	0.0525	0.0673	0.0852	0.1066	0.1350	0.1735
Cube 2	0.0696	0.0785	0.0921	0.1134	0.1258	0.1628
Cube 3	0.0804	0.0883	0.1063	0.1245	0.1474	0.1744
Mean	0.0675	0.0780	0.0945	0.1148	0.1361	0.1702
Mixed unwashed 100%						
Cube 1	0.0925	0.1069	0.1264	0.1529	0.1723	0.1983
Cube 2	0.0817	0.0928	0.1090	0.1367	0.1572	0.1736
Cube 3	0.0929	0.1141	0.1373	0.1559	0.1877	0.2246
Mean	0.0891	0.1046	0.1243	0.1485	0.1724	0.1988